

**Investigation of the gallbladder host environment and small RNAs in the pathobiology
of *Campylobacter jejuni* sheep abortion clone IA 3902**

by

Amanda Jo Kreuder

A dissertation submitted to the graduate faculty
in partial fulfillment of the requirements for the degree of

DOCTOR OF PHILOSOPHY

Major: Veterinary Microbiology

Program of Study Committee:
Paul J. Plummer, Co-Major Professor
Qijing Zhang, Co-Major Professor
F. Chris Minion
Eric Burrough
Micheal Yaeger

Iowa State University

Ames, Iowa

2016

Copyright © Amanda Jo Kreuder, 2016. All rights reserved.

TABLE OF CONTENTS

	Page
NOMENCLATURE	iv
ACKNOWLEDGMENTS	vi
ABSTRACT.....	vii
CHAPTER 1 LITERATURE REVIEW AND INTRODUCTION.....	1
Specific aims and significance	1
Organization of the dissertaton	2
Literature review	2
CHAPTER 2 HISTOPATHOLOGY AND SPATIAL DISTRIBUTION OF PUTATIVE GROWTH FACTORS IN THE OVINE GALLBLADDER FOLLOWING DIRECT INOCULATION WITH <i>CAMPYLOBACTER</i> <i>JEJUNI</i> SHEEP ABORTION CLONE IA 3902.....	21
Abstract	21
Introduction	22
Materials and methods	24
Results	34
Discussion	41
Figures and tables	49
CHAPTER 3 THE TRANSCRIPTOME OF <i>CAMPYLOBACTER JEJUNI</i> SHEEP ABORTION CLONE IA 3902 FOLLOWING <i>IN VIVO</i> EXPOSURE TO THE OVINE GALLBLADDER	58
Abstract	58
Introduction	59
Materials and methods	62
Results	72
Discussion	79
Figures and tables	99
CHAPTER 4 THE TRANSCRIPTOME OF MUTANTS Δ CjNC110, Δ LUXS, AND Δ CjNC110 Δ LUXS IN THE <i>CAMPYLOBACTER JEJUNI</i> SHEEP ABORTION CLONE IA 3902.....	146
Abstract	146
Introduction	147
Materials and methods	150
Results	157

Discussion	165
Figures and tables	178
CHAPTER 5 PHENOTYPIC CHANGES ASSOCIATED WITH INACTIVATION OF THE CjNC110 SMALL RNA IN <i>CAMPYLOBACTER JEJUNI</i> 1A 3902.....	
Abstract	205
Introduction	206
Materials and methods	208
Results	211
Discussion	214
Figures and tables	226
CHAPTER 6 SUMMARY AND FUTURE DIRECTIONS.....	
Summary	233
Future directions.....	240
REFERENCES.....	240

NOMENCLATURE

6-PPK	6-phosphofructokinase
YLD	years lived with disability
CDC	Centers for Disease Control
PFGE	Pulsed-field gel electrophoresis
MLST	Multi-locus sequence typing
SA	Sheep abortion
ST	Sequence type
RNA	Ribonucleic acid
DNA	Deoxyribonucleic acid
RNAseq	High-throughput RNA sequencing
TSS	Transcriptional start sites
mRNA	Messenger RNA
sRNA	Small non-coding RNA
ncRNA	Small non-coding RNA
asRNA	Antisense RNA
UTRs	5' or 3' untranslated regions
MH	Mueller-Hinton
BAP	Blood agar plates
MOMP	Major outer membrane protein
PAS	Periodic acid-Schiff reaction
MALDI-TOF	Matrix assisted laser desorption ionization-time of flight

IACUC	Institutional Animal Care and Use Committee
CFU	Colony forming unit
ANOVA	Analysis of variance
H & E	Hematoxylin and eosin
PBS	Phosphate buffered saline
RAP	RNA adapter plate
IGV	Integrated Genome Viewer
COG	Clusters of Orthologous Groups
MCP	Methyl-accepting chemotaxis protein
TAT	Twin arginine targeting secretion system
NO	Nitric oxide
LB	Luria-Bertani
SAM	S-adenosylmethionine
AB	Autoinducer broth
CFS	Cell-free supernatant
AI-2	Autoinducer-2
RLU	Relative light units
SNPs	Single nucleotide polymorphisms
AAG	Autoagglutination

ACKNOWLEDGMENTS

I would like to thank my co-mentors, Drs. Paul Plummer and Qijing Zhang, and my committee members, Drs. Eric Burrough, Mike Yaeger, and Chris Minion for their guidance and support throughout the course of this research.

Thank you to Dr. Jennifer Schleining and Dr. Mike Yaeger for their invaluable assistance in developing the sheep gallbladder inoculation model, as well as Dr. Victoria Lashley and Dr. Mike Yaeger for assistance with the histopathology related to that project. Thank you to Dr. Andrew Severin for his assistance with bioinformatics related to RNA sequencing. Thank you also to Kathy Mou and the members of the Zhang lab for invaluable assistance in working with *Campylobacter*. In addition, I would also like to thank my friends, colleagues, the VDPAM and VMPM department faculty and staff for making my doctoral studies at Iowa State University an enjoyable and educational experience.

ABSTRACT

Campylobacter jejuni is an important zoonotic agent that is the leading cause of both human foodborne bacterial gastroenteritis worldwide, as well as ovine abortion in the United States. In particular, a single *C. jejuni* sheep abortion clone, of which IA 3902 is a prototypical isolate, has recently emerged as the dominant causative agent of sheep abortion due to *Campylobacter* sp. in the U.S. and has been increasingly identified in human outbreaks of disease. Multi-omics approaches to studying this hypervirulent strain have shown that it is remarkably similar to other common strains of *C. jejuni* such as 11168 that do not show the same ability to cause systemic clinical disease. Further work to elucidate the molecular mechanisms that allow for small changes in genomic structure to lead to large changes in virulence ability in this important zoonotic agent is warranted. A number of studies have demonstrated that the gallbladder of ruminants, as well as other domestic animal species, is often positive on culture for *Campylobacter* sp. following oral exposure, suggesting that this environment may serve as a chronic nidus of infection for maintenance of disease within populations. By utilizing a unique *in vivo* model of gallbladder infection, the work conducted within this dissertation has allowed identification of the preferred location of *C. jejuni* IA 3902 within the gallbladder host environment as well as demonstrated putative host factors that may play a role in its localization to that site. In addition, by utilizing emerging RNA sequencing technology, we were able to determine numerous protein coding genes and non-coding RNAs that were differentially expressed following exposure to the *in vivo* gallbladder host environment. One of these identified non-coding RNAs, CjNC110, was selected for further study. Inactivation of the CjNC110 non-coding RNA in IA 3902 allowed

us for the first time to identify transcriptomic and phenotypic changes associated with loss of function of a small RNA in any species of *Campylobacter*. The collective results of these experiments provide additional evidence to begin to elucidate the role of gallbladder colonization and small RNAs in the pathobiology of the important zoonotic pathogen, *C. jejuni* IA 3902.

CHAPTER 1

LITERATURE REVIEW AND INTRODUCTION

Specific Aims and Significance

Colonization of the gallbladder by *Campylobacter jejuni*, as well as other enteric pathogens such as *Salmonella typhi*, *Listeria monocytogenes*, and *Helicobacter pylori*, is thought to play a key role in transmission and persistence of these important zoonotic agents, however, there is a fundamental knowledge gap in our understanding of the molecular mechanisms that these organisms utilize to establish infection in such a harsh environment. The long-term goal of our research is to improve the understanding of the pathogenic mechanisms utilized by enteric pathogens to colonize the mammalian gallbladder and to develop novel targets for prevention and control of these pathogens, particularly *C. jejuni*. To accomplish this goal, our objective for this dissertation was to begin to determine the molecular mechanisms responsible for *C. jejuni* colonization of the gallbladder as well as localize the site of colonization within the gallbladder. Our central hypothesis was that changes in expression of the *C. jejuni* transcriptome including both protein coding genes and non-coding RNAs allow it to adapt to the bile-rich environment and colonize the protective mucous lining of the gallbladder where it acts as a chronic nidus of pathogen shedding. The rationale for the proposed research is that once the genetic determinants of colonization of the bile-rich environment are known, novel vaccination or therapeutic strategies can be developed to prevent chronic carriage in ruminants, reduce shedding, and thereby decrease human and animal disease with *C. jejuni* and potentially other enteric pathogens. To accomplish these goals, the following specific aims were developed: 1) identify the location

of gallbladder colonization by *C. jejuni*, 2) identify specific bacterial elements responsible for adaptation of *C. jejuni* for survival in bile, and 3) select specific non-coding RNAs that are differentially expressed in the gallbladder environment for further study.

Organization of the Dissertation

This dissertation is presents four sets of studies designed to address the specific aims listed above. The first chapter (Chapter 1) consists of a general introduction and literature review. The four chapters that follow (Chapters 2 – 5) are comprised of four groups of experiments addressing the specific aims of interest and include all relevant tables and figures. The final chapter (Chapter 6) contains general conclusions and suggestions for future research. A single reference list appears at the end of the dissertation.

Literature Review

***Campylobacter jejuni*: general biology**

Campylobacter jejuni is a member of the Epsilon proteobacteria class and Campylobacterales family which includes the genera *Campylobacter*, *Helicobacter* and *Wolinella*. The primary habitat of these organisms is the gastrointestinal tract which requires special bacterial adaptations for survival. *C. jejuni* is a true microaerophile, which implies that while oxygen is required for growth, it is unable to grow at normal atmospheric oxygen levels (Kelly, 2001). Due to a lack of the 6-phosphofructokinase (6-PPK) enzyme, *C. jejuni* is not able to catabolize glucose and thus utilizes catabolism of amino acids, particularly serine, aspartate, glutamate and proline which are commonly found in the chicken gut, as its most important energy source (Stahl *et al.*, 2012). In addition to amino acids, recent studies

have shown that some strains do have the ability to utilize L-fucose for growth (Muraoka and Zhang, 2011; Stahl *et al.*, 2011). Other species of *Campylobacter*, including *C. coli* and *C. doylei*, have also recently been demonstrated to house a plasticity region between the 16S and 23S genes that allows for utilization of glucose in the absence of 6-PPK (Vorwerk *et al.*, 2015). *Campylobacter* spp. typically possess polar flagella at either one or both ends of the cell and are helical in shape which allows for corkscrew-like motility (Debruyne *et al.*, 2008).

***Campylobacter* species: broad host range and zoonotic risk**

The two thermophilic *Campylobacter* species, *C. jejuni* and *C. coli*, so named due to their optimal growth temperature being 42°C, are frequently found as commensals of the intestinal tract of both mammals and birds. The ability of *C. jejuni* and *C. coli* to survive in a variety of hosts and environments can be partly attributed to the wide variety of genetic variation observed both between and within strains; of the 37,351 isolates of *C. jejuni* that have been reported to the pubMLST database as of December 2015, there are 8084 distinct sequence type (ST) profiles (<http://pubMLST.org/campylobacter/>) (Jolley and Madden, 2010).

Worldwide, poultry are the most commonly colonized type of animals; the average reported prevalence of *Campylobacter*-positive poultry flocks ranges from 2 – 100% depending on the country, production system and time of year, with the majority of birds becoming colonized within a short period of time once it is introduced to a flock (Sahin *et al.*, 2015). Colonization in poultry has been classically thought to be as a commensal with minimal observation of disease. While not as common as in poultry, colonization of the

gastrointestinal tract of a wide variety of domestic mammals does occur. Prevalence of thermophilic *Campylobacter* found in the feces of domestic livestock has been reported to range from 21.9% to 66.7% in cattle (Oporto *et al.*, 2007; Ogden *et al.*, 2009), and from 26.7 to 82.6% in pigs (Ogden *et al.*, 2009; Burrough *et al.*, 2013). Prevalence in sheep has been reported to range from 8.8% to 24.9% (Oporto *et al.*, 2007; Ogden *et al.*, 2009). With the exception of ovine campylobacteriosis, which is one of the most common causes of infectious abortion in sheep worldwide, induction of disease by *Campylobacter* in other species of domestic livestock occurs sporadically despite frequent exposure and colonization.

Human exposure to *Campylobacter*, on the other hand, frequently leads to more serious consequences in the form of gastroenteritis. Of the approximately 600 million cases of foodborne illness in 2010, infectious agents that cause diarrheal disease accounted for 550 million of those cases, with *Campylobacter* spp. being the leading bacterial cause of foodborne illness (WHO 2015). While not typically fatal, *Campylobacter* is also the leading bacterial foodborne illness agent in years lived with disability (YLDs) due to post-infection complications related to Guillain-Barre syndrome and other immune mediated sequelae.

Poultry products are still considered the primary source of non-outbreak associated sporadic campylobacteriosis in humans, however, reports of outbreaks linked to ruminant exposure, particularly those associated with raw milk, occur on a fairly regular basis with 33 outbreaks reported to the CDC from 2000 to 2006 (Oliver *et al.*, 2009). This is not surprising given that the occurrence of *C. jejuni* in bulk tank milk in the United States has been reported to range from 2 to 9.2% (Jayarao *et al.*, 2001; Jayarao *et al.*, 2006). While the majority of outbreaks associated with ruminant exposure are related to raw milk, significant risks for sporadic infection due to carcass contamination, particularly in sheep, by thermophilic

Campylobacter exist as up to 91.7% of intestinal contents of lambs at slaughter have been shown to be positive on culture (Stanley *et al.*, 1998). Indeed, reports of isolation from retail meat indicate that while isolation rates were much lower than that of poultry (89.1%), 6.9% of lamb and 3.5% of beef was positive for *C. jejuni* (Wong *et al.*, 2007).

Campylobacteriosis in the ovine species

Historically, clinical campylobacteriosis in the ovine species has been predominantly caused by infection with *Campylobacter fetus* subsp. *fetus* (formerly classified as *Vibrio fetus*), and observation of abortion storms of close to 25% of a flock following exposure are not uncommon (Skirrow 1994). Occasionally, *C. jejuni* and *C. coli* were reported to account for a small percentage of diagnosed cases of abortion both in the U.S. and in other countries (Diker and Istanbuluoglu 1986; Diker *et al.*, 1988; Mannering *et al.*, 2006). Beginning in the late 1980's, however, a shift in the species of *Campylobacter* isolated from sheep abortion outbreaks in the United States began to occur. A report compiling the diagnosed causative agents of ovine abortion from the South Dakota Veterinary Diagnostic Laboratory from 1980 to 1989 revealed that while *C. fetus* subsp. *fetus* was the predominant cause of campylobacteriosis during the time period studied, beginning in 1983 the prevalence of *C. jejuni* associated abortions began to rise until it was the predominant cause of *Campylobacter* associated abortion by 1989 (Kirkbride 1993). Another report of abortion cases from the western U.S. (Idaho, Oregon, and Wyoming) also identified a similar shift in species as analysis from 15 abortion outbreaks associated with *Campylobacter* spp. revealed that 14 of the 15 were *C. jejuni*, represented by multiple strain types, and only one isolate was *C. fetus* subsp. *fetus* (DeLong *et al.*, 1996). Analysis of 46 isolates from the Iowa State Veterinary

Diagnostic Laboratory obtained from abortion outbreaks during 2003 to 2007 from 33 farms in Iowa indicated that 41 of the isolates were *C. jejuni*; pulsed-field gel electrophoresis (PFGE) fingerprinting of 33 of those isolates revealed that 32 were clonal (Sahin *et al.*, 2008). In addition, further analysis of *C. jejuni* isolates obtained from three other states revealed 18 of 19 Idaho isolates, 9 of 11 South Dakota isolates, and 7 of 8 California isolates to also exhibit the same PFGE type which was confirmed to match the ST-8 MLST type strain (Sahin *et al.*, 2008). This strain of *C. jejuni* has since been referred to as sheep abortion (SA) clone, with the type strain being clinical isolate IA 3902 which has been utilized extensively for further study of this emerging pathogen including full genome sequencing (Wu *et al.*, 2013).

Further work to better elucidate the emergence of clone SA has determined that representative isolates of ST-8 were present in the United States during the 1990s but that they generally lacked tetracycline resistance (19%) and while they represented the majority of isolates (68%), they were not completely dominant (Wu *et al.*, 2014). In contrast, isolates obtained after 2000 in the US consistently demonstrated tetracycline resistance (100%) and were the dominant isolate obtained from sheep abortions (91%) (Wu *et al.*, 2014). Historically, antibiotics of the tetracycline class were the only type of antibiotic approved for use in prevention and control of ovine abortions in the United States (Giguere *et al.*, 2013) and treatment or prevention of abortions storms related to *Campylobacter* species has relied heavily on the use of chlortetracycline or tetracycline in the feed, which is an approved non-prescription use at 80 mg/head/day (Sahin *et al.*, 2008). While use of tetracyclines, either oral or injectable, do not currently require a veterinary prescription in the United States, in contrast, all antimicrobials administered to food producing animals in the United Kingdom

require a veterinary prescription according to the Veterinary Medicines Regulations act of 2005 (RUMA, 2005). In comparison, analysis of sheep abortion isolates of *C. jejuni* from the U.K. from 2002-2008, where it accounted for only 16% of isolates from sheep abortions, revealed no evidence of the ST-8 strain type and exhibited normal genetic diversity comprising 19 different STs (Wu *et al.*, 2014). Therefore, it has been speculated that antibiotic selection pressure may have played a role in the emergence of the sheep abortion clone in the United States, however, it is likely that other factors associated with the ST-8 clone and husbandry practices in the United States have also played key roles in the rapid expansion of this clone (Wu *et al.*, 2014).

The ability of the SA clone to induce abortion was first confirmed using both oral and intravenous inoculation of pregnant guinea pigs; the results of this study demonstrated that clone (SA) IA 3902 was highly abortifacient compared to other *C. jejuni* strains such as 11168, indicating the evolution of increased virulence in this clone when compared to other closely related strains (Burrough *et al.*, 2009; Wu *et al.*, 2013). Further work utilizing additional clinical isolates that matched the ST-8 type strain but were not IA 3902 demonstrated the ability of ST-8 isolates to induce abortion in some but not all of the sheep inoculated either orally or intravenously, while no abortions were noted in the placebo or the common laboratory strain 81-176 inoculated groups (Sanad *et al.*, 2014). These results help to partially fulfill Koch's postulates to prove that the sheep abortion clone of *C. jejuni* is indeed the predominant causative agent of ovine campylobacteriosis in the United States today.

Pathogenesis of ovine campylobacteriosis

The pathogenesis of ovine campylobacteriosis regardless of strain is thought to involve oral ingestion of contaminated material leading to intestinal colonization, mucosal invasion, bacteremia, and tropism for the fetoplacental unit leading to subsequent fetal death and abortion (Skirrow 1994). One of the key steps in the pathogenesis of *Campylobacter*-associated abortion is invasion of the intestinal epithelium allowing access to the blood stream and systemic spread. For *C. fetus* subsp. *fetus*, systemic infection is dependent on the resistance to serum complement binding provided by the expression of high molecular weight proteins in the surface layer (S-layer) (Blaser *et al.*, 1988; Blaser 1993; Grogono-Thomas *et al.*, 2000); however, these proteins are not expressed by *C. jejuni*. Recent work evaluating invasive *C. jejuni* strains in humans has shown that the capsule locus (kpsM) is critical for serum resistance in humans and survival of invasive *C. jejuni* (Keo *et al.*, 2011). While the MLST typing of the strain utilized in that study does not match the sheep abortion clonal isolates, it does suggest that the capsular structure of various strains of *C. jejuni* may play a role in invasiveness.

Ovine campylobacteriosis typically manifests itself as a spectrum of clinical disease including late term abortions, still births, premature births, birth of weak lambs, and metritis (Hedstrom *et al.*, 1987), with abortions typically occurring 1-3 weeks following exposure (Mearns *et al.*, 2007). Infection of the fetoplacental unit is characterized by a placentitis focused on the placentomes and with infection of the fetus yielding variable non-specific lesions including edema, bronchopneumonia and necrotizing hepatitis with characteristic target lesions (Schlafer and Miller, 2007).

Gallbladder colonization has been reported to be a key feature following infection with both *C. fetus* subsp. *fetus* (Firehammer *et al.*, 1962; Storz *et al.*, 1964; Bryner *et al.*, 1971; Clark *et al.*, 1979) and *C. jejuni* (Ertas *et al.*, 2003; Acik and Cetinkaya, 2006; Milnes *et al.*, 2008; Sahin *et al.*, 2012) and may play a key role in maintenance of infection within populations of animals. Indeed, abattoir surveys of *C. jejuni* carriage in ruminants demonstrated that up to 34% of sheep gallbladders were positive for *C. jejuni* with 66% of sheep gallbladders positive for *Campylobacter* species (Ertas *et al.*, 2003). Recent studies have also demonstrated that while there remains a substantial level of genetic diversity in isolates of *C. jejuni* collected from sheep gallbladders, isolates belonging to the ST-8 sheep abortion clone can readily be found in otherwise healthy animals (Sahin *et al.*, 2012). This indicates that the gallbladder may serve as an important reservoir for the sheep abortion clone within populations in the United States.

Bacterial colonization of the gallbladder

Multiple instances of cholecystitis in humans due to *Campylobacter* species have been previously reported, indicating that colonization of the gallbladder by *C. jejuni* is not unique to ruminant species (Dakdouki *et al.*, 2003; Vaughan-Shaw *et al.*, 2010). Other intestinal pathogens such as *Salmonella typhi* and *Listeria monocytogenes* have also been shown to have the unique ability to colonize the gallbladder in both humans and animals where they can establish a chronic carrier state in their host (Dowd *et al.*, 2011; Gonzalez-Escobedo *et al.*, 2011). In addition, the DNA of the closely related *H. pylori* has also been demonstrated to be frequently present in the gallbladder of patients with cholelithiasis (Guraya *et al.*, 2015).

The gallbladder environment is typically thought of as “harsh” with few bacteria able to survive under the conditions present. Bile acids (salts) are the main component of bile, along with cholesterol, phospholipids and bilirubin. Their amphipathic nature allows them to act as a detergent which plays a key role in lipid solubilization and emulsification leading to digestion of fats within the intestinal tract (Baptissart *et al.*, 2013). Studies have demonstrated that sheep bile, along with ox and pig bile, has a relatively high percentage of bile salts which constitute 10% w/v of the total contents of bile and have been proven to be very damaging to cellular membranes (Coleman *et al.*, 1979). In particular, the detergent property of bile has been demonstrated to have potent antimicrobial activity (Begley *et al.*, 2005). Recent rapid expansion of the use of metagenomics and microbiome research has proven that many sites previously thought to be inhospitable to bacterial colonization, such as the monogastric stomach, are now known to be home to a unique ecological community of bacteria (Yang and Suerbaum 2013). Recently, the first report of the characterization of the microbiome of the gallbladder in any species was published investigating the microbiota of the swine gallbladder (Jimenez *et al.*, 2014). The diversity of bacterial species identified within the gallbladder was much lower than reported for most other locations in the mammalian body that have been studied to date, and considerably lower than the diversity observed in the gut microbiota of the same species (Lamendella *et al.*, 2011).

Bacterial factors associated with virulence and survival in bile

The highly motile nature of *C. jejuni* plays an important role in its ability to cause disease. Critical to this ability is the presence of polar flagella which allow it to migrate through viscous layers of mucus within the intestinal tract, undergo chemotaxis towards areas

more opportune for survival, and adhere to and invade epithelial cells (Guerry *et al.*, 2007). The flagella of *C. jejuni* have also been shown to secrete virulence proteins (Konkel *et al.*, 1999; Rivera-Amill *et al.*, 2001; Konkel *et al.*, 2004). The flagella of *Campylobacter* are also heavily glycosylated (Guerry *et al.*, 2006) which has been shown to mediate autoagglutination, an important preliminary step in the formation of biofilms and microcolonies (Misawa and Blaser 2000; Golden and Acheson 2002).

While flagella control the ability of *C. jejuni* to migrate towards certain substances, chemotaxis provides the signal to direct the migration and is critical for pathogenesis within the host. The CheA-CheY phosphor-relay pathway has previously been shown to act as the master switch to control taxis by altering the direction of flagellar rotation from a swimming phenotype (counter-clockwise rotation) to a tumbling phenotype (clockwise rotation) (Lertsethtakarn *et al.*, 2011). The *cheY* gene has also been shown to be required for adhesion and invasion as well as virulence, without which colonization can occur but disease cannot be induced (Yao *et al.*, 1997). Once *C. jejuni* reaches its target destination, several studies have demonstrated critical genes that are necessary for adherence and invasion to host cells to allow colonization. The fibrinectin-binding outer membrane protein CadF has been demonstrated to mediate cell adhesion by binding to the cell matrix protein fibrinectin (Konkel *et al.*, 1997). The periplasmic binding protein PEB1 has also been shown to act both as an aspartate/glutamate transporter as well as a major cell adherence molecule (Pei and Blaser, 1993).

The ability to survive exposure to bile salts within the host intestinal tract is another key virulence trait associated with *C. jejuni*. Despite the importance of adaptation to bile exposure for *Campylobacter* survival both within the intestinal tract as well as in the

gallbladder environment, very little published work has focused on the exact molecular mechanisms by which *Campylobacter* is able to survive exposure to bile. The studies that have been performed frequently focused on the concentrations of bile salts typically found in the intestinal tract of humans (< 1% bile salts w/v) and not within the gallbladder of animals such as sheep (10% bile salts w/v) proposed to chronically harbor these pathogenic organisms. The efflux pumps CmeABC and CmeDEF are probably the most important genes demonstrated to play an important role in resistance of *Campylobacter* to bile salts *in vitro* (Lin *et al.*, 2002; Akiba *et al.*, 2006). Bile salts (cholate and taurocholate) have previously been shown to induce expression of CmeABC *in vitro* in a time and dose dependent manner (Lin *et al.*, 2005a). Expression of CmeABC has been demonstrated to be under the control of the transcription repressor CmeR, with exposure to bile salts *in vitro* inhibiting binding of CmeR to the promoter of *cmeABC* and allowing for increased transcription of the *cmeABC* operon (Lin *et al.*, 2005b). The *cmeDEF* operon, on the other hand, has been shown to be unaffected by CmeR repression (Akiba *et al.*, 2006), however, the expression of *cmeDEF* has been noted to be intrinsically lower than *cmeABC*, and inactivation of *cmeF* has been demonstrated to increase expression levels of *cmeABC* (Akiba *et al.*, 2006).

The response regulator CbrR (*Campylobacter* bile response regulator) has been shown to be required for resistance to the effects of bile salts *in vitro* as mutants lacking it are unable to grow under sub-inhibitory concentrations of sodium deoxycholate (Raphael *et al.*, 2005). It is believed that CbrR is a response regulator that is part of a two-component regulatory system which typically also includes a sensor kinase; this cognate protein has yet to be identified in *Campylobacter*. The secretory protein CiaB (*Campylobacter* invasion antigen B) has also been suggested to play a role in bile tolerance and has been demonstrated

to be secreted upon co-cultivation of *C. jejuni* with intestinal cells and plays a role in the ability of *C. jejuni* to invade host cells (Konkel *et al.*, 1999). Synthesis and secretion of the CiaB protein have been demonstrated to be independent events, with increased expression demonstrated upon exposure to bile salts suggesting that they might serve as the trigger for increased transcription (Rivera-Amill *et al.*, 2001; Malik-Kale *et al.*, 2008). An additional gene of interest previously described as important to the response of *Campylobacter* to exposure to bile is *flaA* (Alm *et al.*, 1993), which is responsible for production of the FlaA protein, one of two protein subunits that form the flagellar filament. It has been previously demonstrated through the use of reporter fusions that the σ^{28} promoter of *flaA* is upregulated when exposed to bovine bile, bile salts (deoxycholate), and L-fucose (Allen and Griffiths, 2001).

Additional studies have attempted to assess the response of *Campylobacter* to bile on a more global scale. Microarray analysis of RNA extracted from *C. jejuni* strain F3011 cultured with 0.1% deoxycholate for 12 hours allowed observation of a total of 156 upregulated and 46 downregulated genes under these conditions (Malik-Kale *et al.*, 2008). In addition to increased expression of the known bile-associated virulence genes *ciaB* and *cmeABC*, this study also specifically identified increased expression of two additional virulence factors, *dccR*, which has been shown to be part of a two-component system regulatory system that may play a role in the *in vivo* colonization ability of *C. jejuni* (MacKichan *et al.*, 2004), and *tlyA*, a hemolysin that has been shown to be important for *Helicobacter in vivo* colonization ability (Martino *et al.*, 2001). In a separate study, Fox *et al.*, (2007) utilized protein expression following 18 hours of exposure to 2.5 to 5% oxbile added to rich media to identify 14 proteins with increased expression including the

previously identified FlaA, as well as proteins such as elongation factors, ferritin, chaperones, and ATP synthase components.

Intestinal colonization with *C. jejuni* has been demonstrated to be associated with the ability to colonize the mucin and L-fucose-containing mucous layer of the intestinal epithelium where it is protected from the mechanical and chemical milieu of the intestinal lumen (McSweegan and Walker 1986; Shigematsu *et al.*, 1998). Unlike many other enteric pathogens that become trapped in this layer, *C. jejuni* is able to move freely within the mucin layer to inhabit the deep intestinal crypts (Lee *et al.*, 1986) and from there potentially become internalized within eukaryotic cells (Babakhani and Joens 1993; Russell *et al.*, 1993; van Spreuwel *et al.*, 1985). This ability has also been demonstrated in the closely related *H. pylori* to allow colonization of the glands of the stomach (Yang and Suerbaum, 2013). Mucin, L-fucose, and bile have all been shown to be strong chemoattractants for *C. jejuni* (Hugdahl *et al.*, 1988) and it has been demonstrated that some virulent strains of *C. jejuni* such as IA 3902 can utilize L-fucose as a substrate for growth due to possession of a specific genetic island (Stahl *et al.*, 2011; Muraoka and Zhang, 2011).

Unique attributes of the sheep abortion (SA) clone IA 3902

As described above, *Campylobacter jejuni* SA (sheep abortion clone) IA 3902 was initially isolated from an outbreak of sheep abortion in Iowa during 2006 and has since been utilized as the prototypical isolate to study the current most common cause of sheep abortion due to *Campylobacter* species in the United States (Sahin *et al.*, 2008). The genome of *C. jejuni* IA 3902 is compact and consists of only 1.6 Mb, similar to other commonly studied strains of *C. jejuni* such as 11168 and 81-176, and possesses the pVir plasmid (Wu *et al.*,

2013). All of the isolates belonging to the SA clone type ST-8 that have been identified since 2000 have been found to harbor tetracycline resistance via acquisition of a chromosomally encoded *tetO* gene (Wu *et al.*, 2014). Although chromosomal insertion of *tetO* has been occasionally observed, *tetO* is usually located on conjugative plasmids such as pTet (Gibree *et al.*, 2004; Poly *et al.*, 2008). Recent analysis of IA 3902 via a multi-omics approach revealed that IA 3902 is remarkably syntenic with the genome of *C. jejuni* type-strain 11168, and it does not harbor any additional pathogenicity islands or virulence factors known to be associated with abortion induced by *C. fetus* subsp. *fetus* (Grogono-Thomas *et al.*, 2003; van Putten *et al.*, 2009). However, comparison of the genomes did identify a large number of SNPs and indels, particularly within the promoter regions of 128 genes, as well as 25 genes specific to IA 3902 only; transcriptomic comparisons utilizing microarrays also revealed 108 genes to be upregulated and 81 genes to be downregulated in IA 3902 when compared to 11168 (Wu *et al.*, 2013). Taken together, these data suggests that relative mild changes in genomic structure have led to significant changes in gene expression along with greatly enhanced ability to cause disease and warrants further investigation.

Emergence of the SA clone in recent *Campylobacter* associated food borne illness outbreaks, particularly those related to raw milk (Sahin *et al.*, 2012), heightens the importance of understanding the mechanisms that have allowed this clonal isolate to emerge and thrive particularly in ruminant species. Interestingly, humans are typically considered the only species to routinely become ill after oral ingestion of *C. jejuni* with the exception of abortion induced in sheep due to strains such as *C. jejuni* IA 3902 (Wagenaar *et al.*, 2013). The reason for clinical disease in one species and absence of disease in other species is

mostly still unknown, however, the propensity for clinical disease in sheep by IA 3902 make them a useful animal model in which to study this important disease.

Gene regulation in *Campylobacter* and the discovery of non-coding RNAs

The fact that relatively mild changes in genomic structure have led to significantly enhanced ability to cause disease by *Campylobacter jejuni* strains such as IA 3902 as described above suggests that differences in gene regulation may play a key role in regulation of virulence. *Campylobacter jejuni* has only three known sigma factors identified within its genome to regulate transcription: σ^{70} (encoded by *rpoD*), σ^{54} (encoded by *rpoN*) and σ^{28} (encoded by *fliA*) (Parkhill *et al.*, 2000); this 1.6mb, low G/C content (31%) genome is only known to encode a total of 34 additional transcriptional regulators (Parkhill *et al.*, 2000; Pearson *et al.*, 2007). Besides transcriptional regulation, gene expression can occur at multiple levels, including post-transcriptional control via regulation of mRNA translation, stability, and processing; the primary players in post-transcriptional regulation are small non-coding RNAs (sRNAs, ncRNAs) (Papenfert and Vogel, 2010; Storz *et al.*, 2011; Caldelari *et al.*, 2013). Prior to completion of the transcriptional start site map via high throughput RNA sequencing (RNAseq) of *H. pylori* (Sharma *et al.*, 2010), the ϵ -proteobacteria were thought not to be capable of using small and antisense RNA as a regulatory mechanism, partly due to a lack of the small RNA chaperone Hfq (Valentin-Hansen *et al.*, 2004). Indeed, attempts at computational approaches of identification of small RNAs in *Campylobacter* failed to identify any potential candidates, with only 3 potential loci being identified in *Helicobacter* (Livny *et al.*, 2008). However, using differential RNAseq technology, Sharma *et al.*, (2010) were able to discover for the first time an unexpectedly high number of small RNAs (~60)

including the ϵ -subdivision counterpart of the regulatory 6S RNA as well as potential *cis*- and *trans*-encoded regulators of target messenger RNAs in *H. pylori*.

Recently, clear evidence that *C. jejuni* also has the capability to produce these important regulators has been published detailing identification of a wealth of small RNAs present in strains 11168, 81-176, 81116, and RM1221 (Chaudhuri *et al.*, 2011; Dugar *et al.*, 2013; Porcelli *et al.*, 2013; Taveirne *et al.*, 2013; Butcher and Stintzi, 2013). Dugar *et al.*, (2013), when comparing the transcriptomes of 4 different *C. jejuni* isolates, observed a large variation in transcriptional start sites (TSS) as well as expression patterns of both mRNA and non-coding RNA between strains. This suggests that variation between the existence and expression of small RNAs even among closely related strains may play a key role in the differences observed in virulence. Conservation analysis of the identified small RNAs in *C. jejuni* revealed that many are restricted to the *Campylobacter* genus only, and even the identified housekeeping RNAs show poor sequence conservation with other bacterial genera (Dugar *et al.*, 2013). In closely related *H. pylori*, studies are just starting to emerge where ncRNAs have been shown to influence gene expression at the post-transcriptional level (Wen *et al.*, 2013; Pernitzsch *et al.*, 2014). The first report attempting to elucidate the role of non-coding RNA just recently published in *Campylobacter* suggests that two recently identified ncRNAs may play a role in flagellar biosynthesis; however, they were unable to demonstrate phenotypic changes following inactivation of these non-coding RNAs (Le *et al.*, 2015).

Small RNA mechanisms of action

Small non-coding RNAs are derived from transcription of regions of the genome that typically do not encode an open reading frame for protein translation, thus leading to small

regions of untranslated RNA that can function as regulators of gene expression. Much of the work to elucidate the mechanisms of action of small RNAs to date has been performed in model organisms such as *E. coli* and *Salmonella*. Small RNAs typically use their ability to base pair with other single stranded RNA to directly interact with mRNA transcripts, leading to either repression or activation of translation (Papenfort and Vogel, 2009). In addition, some small RNAs have recently been shown to directly bind to proteins to modulate their activities (Waters and Storz, 2009). Dual function mRNAs have also been reported that can both be translated into proteins as well as act as regulatory RNAs themselves (Vanderpool *et al.*, 2011; Mellin and Cossart, 2015). Not unlike the protein master regulators of transcription, small RNAs can act globally to regulate multiple genes or pathways involved in the pathogenesis of disease.

The majority of functional sRNAs that have been characterized to date interact with their target via direct base pairing interactions which can be divided into two primary categories based on the relationship of the small RNA to the target: *cis*-encoded or *trans*-encoded. Because *cis*-encoded RNAs are located directly opposite of the target region of the mRNA, they often exhibit extensive complementarity with their targets (Wagner *et al.*, 2002; Brantl, 2007). Additional regulatory elements such as riboswitches and RNA thermometers also fall under the category of *cis*-acting RNA elements (Roth and Breaker, 2009; Kortmann and Narberhaus, 2012). The originally identified *cis*-encoded RNAs were observed to be part of toxin-antitoxin systems whereby the antisense sRNA bases pairs with the mRNA of the toxin gene to prevent translation (Jahn and Brantl, 2013; Brantl and Jahn, 2015). Later, *cis*-encoded sRNAs were found antisense to the 5' or 3' untranslated regions (UTRs) of mRNAs, or antisense to the coding region itself (Thomason and Storz, 2010; Georg and Hess, 2011).

Most recently, a large reservoir of potential sources of *cis*-encoded sRNAs in the form of pervasive antisense RNA (asRNA) transcription has been identified in a variety of bacteria via global transcriptome studies (Wade and Grainger, 2014). For example, at least one antisense transcriptional start site was identified in 46% of ORFs in *H. pylori* (Sharma *et al.*, 2010); in *C. jejuni*, 45% of all TSSs were antisense (Dugar *et al.*, 2013). Potential mechanisms by which asRNAs could modulate gene expression include occlusion of the ribosomal binding site or targeting for RNase degradation (Wade and Grainger, 2014). Whether these are truly functional non-coding RNAs or just transcriptional noise remains to be determined.

In comparison to *cis*-encoded sRNAs, *trans*-sRNAs are transcribed at a location other than their target mRNAs, often, but not exclusively, within intergenic spaces. Due to a lack of exact complementarity, interaction regions of *trans*-sRNA with their targets are much more limited, often as short as only 6-8 nt and in multiple discontinuous stretches (Waters and Storz, 2009). This lack of exact complementarity is what often allows for more than one target mRNA to be regulated by the same sRNA. The majority of mRNA regulation controlled by known *trans*-encoded sRNAs is negative, meaning that base pairing often leads to repression of protein production either via inhibition of translation or increased degradation of the target mRNA (Gottesman *et al.*, 2005). In many of the model organism species such as *E. coli* and *Salmonella*, the RNA chaperone protein Hfq is required for RNA-RNA interactions between *trans*-encoded small RNAs and their target mRNAs (Aiba, 2007). As the ϵ -proteobacteria genomes do not encode for Hfq, it remains unclear whether another protein serves a similar role or if sRNAs function without a protein chaperone in these species of bacteria. While the prototypical *trans*-sRNA typically interacts with regions such

as the ribosomal binding site, interactions with target RNAs can occur at any location. Targeting of upstream sites such as ribosome stand-by sites or translational enhancer sites as been reported (Darfeuille *et al.*, 2007), as has binding to the coding sequence of the mRNA to recruit RNases (Pfeiffer *et al.*, 2009). Overall, non-coding RNAs have been demonstrated to exist in a wide variety of forms and perform an extensive array of bacterial functions, from controlling diverse aspects of bacterial physiology to mediating virulence.

CHAPTER 2

HISTOPATHOLOGY AND SPATIAL DISTRIBUTION OF PUTATIVE GROWTH
FACTORS IN THE OVINE GALLBLADDER FOLLOWING DIRECT INOCULATION
WITH *CAMPYLOBACTER JEJUNI* IA 3902

Abstract

Campylobacter jejuni is an important zoonotic pathogen that is the leading cause of both human foodborne bacterial gastroenteritis worldwide, as well as ovine abortion in the United States. A number of studies have demonstrated that the gallbladder of ruminants as well as other domestic animal species is often positive on culture for *Campylobacter* sp., suggesting that this environment may serve as a chronic nidus of infection for maintenance of disease within populations. Previous studies have demonstrated the location of putative growth factors for *C. jejuni* in both the intestinal tract as well as the placental unit which may play a role in localization of the organism within these important environments; however, to date, no studies have been performed to assess for the presence of similar factors within the gallbladder. In this chapter, histochemistry was utilized to localize putative growth factors including neutral and acid mucins, along with L-fucose, within the deep glands of the ovine gallbladder as well as in aggregates along the mucosal surface. Direct gallbladder inoculation with *C. jejuni* IA 3902 followed by immunohistochemistry analysis and scanning electron microscopy allowed for identification of rapid accumulation of the organism in direct contact with the gallbladder mucosa and located within the deep gallbladder mucosal glands, suggesting that this is the preferred location of *C. jejuni* IA 3902 within the gallbladder host environment. Failure to occlude the common bile duct following direct gallbladder

inoculation led to a rapid loss of inoculum into the intestinal tract which was prevented via ligation of the duct. Taken together, this data suggests that to survive with the harsh environment of the gallbladder, colonization of the deep mucosal glands occurs to allow avoidance of the constant flushing action of bile release and the detergent activities of bile salts in the lumen. Further work to determine the significance of gallbladder colonization in pathogenesis of disease by *C. jejuni* IA 3902 is warranted.

Introduction

Campylobacter jejuni is the leading cause of foodborne bacterial gastroenteritis worldwide (WHO, 2015). In the United States alone, infection with *Campylobacter* causes over 1.3 million infections annually (CDC, 2013) and costs the U.S. economy an estimated 1.9 billion dollars each year (ERS, 2014). Humans are typically considered the only species to routinely become ill after oral ingestion of *C. jejuni* with the exception of abortion in ruminants due to strains such as *C. jejuni* IA 3902 (Wagenaar *et al.*, 2013). The reason for clinical disease in one species and absence of disease in other species is mostly still unknown, however, the propensity for clinical disease in sheep make them a useful animal model in which to study this important disease.

Historically, the primary causative agent of ovine abortion due to *Campylobacter* was *C. fetus* subsp. *fetus*, with only sporadic cases of *C. jejuni* of varying strain types reported (Kirkbride, 1993; Skirrow, 1994). Since the late 1980's, however, there has been a steady increase in the percentage of ovine abortions attributed to *C. jejuni* in the U.S., and by the end of the 1990's, isolates of *C. jejuni* outnumbered *C. fetus* subsp. *fetus* (Kirkbride, 1993; Delong *et al.*, 1996). Between the end of the last century and the 2000's, a single clonal

isolate, *C. jejuni* sheep abortion (SA) clone, was observed to become the predominant cause of ovine abortion in the United States (Sahin *et al.*, 2008). Additionally, outbreaks of zoonotic transmission to humans of this hypervirulent strain, primarily related to raw milk consumption, have been reported (Sahin *et al.*, 2012), highlighting the need for greater understanding of the mechanisms utilized by this virulent strain of *C. jejuni* to both cause disease and persist in animal hosts.

Chronic colonization and shedding of organisms into the environment is thought to play a key role in maintenance of *C. jejuni* in the sheep population, but to date no one has determined the exact location of chronic colonization that allows it to be maintained within animal populations. The majority of the work done to detect chronic carriage of *C. jejuni* in other species such as chickens has been performed looking at chronic colonization of the intestinal environment (reviewed in Sahin *et al.*, 2015); however, a positive culture from feces or intestinal contents does not necessarily prove that the intestines themselves are the home for chronic colonization. Constant bile secretion from the gallbladder into the intestinal tract provides an alternative location for chronic *C. jejuni* carriage that could lead to a positive fecal culture result.

Abattoir studies of sheep and other ruminants have shown that the gallbladder is frequently positive for *C. jejuni* even in the absence of clinical disease (Ertas *et al.*, 2003; Acik and Cetinkaya, 2006; Sahin *et al.*, 2012). In order to decrease colonization and chronic shedding with *C. jejuni* in animal reservoirs, there is a critical need to understand the mechanisms utilized by this organism to colonize and survive in this harsh environment. While *Campylobacter* sp. can frequently be found within the gallbladder, it is unclear how the bacteria reach the gallbladder and whether they survive primarily as free-living in the bile or by colonizing the protective mucous layer as has been demonstrated to play an important

role in intestinal colonization in other species (Van Deun *et al.*, 2008). Survival within the gallbladder itself, particularly within the mucus or mucosal layers may serve as a critical nidus for infection or shedding of *C. jejuni* into the environment. Previous studies have shown that mucins, L-fucose, and iron all can serve as chemoattractants for *C. jejuni* in other locations within the ovine host such as the placenta (Burrough *et al.*, 2012). To date, no other studies have been published assessing other locations within the ovine host that may contain these chemoattractant compounds.

Based on this information, we hypothesized that the gallbladder serves as a natural reservoir for *C. jejuni* within the ruminant host, where the mucous layer of the gallbladder epithelium provides a protected niche for *C. jejuni* colonization. To test this hypothesis, we developed a unique *in vivo* model in the natural ovine host to determine if *Campylobacter* can survive when placed within the ovine gallbladder, as well as where within the gallbladder it prefers to survive. In addition, we utilized previously described histochemical methods to confirm that many of the compounds previously identified to be chemoattractive to *C. jejuni* are present within the mucosal lining and deep glands of the ovine gallbladder. Taken together, our findings suggest that the deep glands of the gallbladder mucosa may provide a protected niche where *Campylobacter* can survive and replicate to establish a chronic nidus of infection within the ruminant host.

Materials and Methods

Bacterial strains and preparation of animal inoculum

A clinical isolate of the *C. jejuni* SA (sheep abortion) clone, IA 3902, was utilized for the entirety of this study. This isolate was obtained from a sheep abortion outbreak in Iowa in

2006 (Sahin *et al.*, 2008) and clonal isolates of this strain have been identified from within the gallbladder of sheep in abattoir studies (Sahin *et al.*, 2012). *C. jejuni* IA 3902 was routinely grown in Mueller-Hinton (MH) broth or agar plates (Becton-Dickinson, Franklin Lakes, NJ) at 42°C under microaerophilic conditions with the use of compressed gas (55% O₂, 10% CO₂, 85% N₂). Specific culture conditions utilized for growth out of bile and the ovine gallbladder experiments are described below.

For preparation of *in vivo* animal inoculum, 10 plates each containing 16 hours of overnight lawn growth were washed with 1 mL MH broth and collected into single sterile 50 mL conical tubes (FisherScientific, Pittsburg, PA). The volume of broth in each vial was then standardized to 10 mL and gently mixed to ensure even distribution of bacteria within the solution. Following pooling and gentle mixing of the cultures, 500 µL of the collected culture was removed and processed immediately for RNA protection as described in Chapter 3. An additional 100 µL was then removed for a dilution series to accurately determine the amount of inoculum in CFU/mL. The remaining inoculum was then centrifuged at 3000 x g for 5 minutes to pellet the cells and all but 1 mL of supernatant was removed. The remaining 1 mL of broth was then used to resuspend the cell pellet in each vial for a total inoculation volume of 1.5 mL per animal. The prepared inoculum was then placed under microaerophilic conditions and used within 3 hours of preparation.

For preparation of the inoculum for the *in vitro* bile study, two sets of 6 plates each containing overnight lawn growth were washed and collected into sterile 50 mL conical tubes as described above and standardized to 5 mL rather than 10 mL. From this 5 mL of concentrated culture, 500 µL each was removed and processed immediately for RNA protection again as described in Chapter 3. The two sets of inoculum were then combined

and an additional 100 μ L was removed for a dilution series to accurately determine the amount of inoculum in CFU/mL. The approximately 9 mL of remaining concentrated culture was then divided equally into four aliquots of 2.2 mL each and used directly for inoculation of the *in vitro* bile samples as described below.

***In vivo* exposure of *C. jejuni* IA 3902 to the sheep gallbladder environment**

All animal experiments were approved by the Iowa State University Institutional Animal Care and Use Committee (IACUC) prior to initiation and followed all appropriate animal care guidelines. Preliminary experiments utilizing one or two mixed breed female sheep obtained from local farms were performed to determine the best method to inoculate the gallbladder of sheep with *C. jejuni* and subsequently harvest enough viable bacteria for RNA isolation. The various methods studied included transcutaneous ultrasound guided inoculation, inoculation via laparoscopy, and full laparotomy with direct visualization of the gallbladder for inoculation. Of the options attempted, full laparotomy with and without placement of a stainless steel medium-large Hemoclip® designed for vessels up to 10 mm (Weck, Research Triangle Park, NC) over the common bile duct were the only options to be successfully performed in a single animal each. Based on the results of this preliminary work, a final determination of the necessity of full laparotomy with placement of a Hemoclip® over the common bile duct was made, and thereafter all future inoculations were performed via this method.

For the primary study, eight adult female mixed breed sheep were obtained from two local farms with no known history of *C. jejuni* related abortions. Sheep were held off feed for 24 hours and off water for 12 hours prior to induction of anesthesia for inoculation of the

gallbladder. Assignment to either the 2 hour or 24 hour incubation group was randomly chosen via a random number generator (www.random.org). Immediately prior to induction of anesthesia, a jugular catheter was placed and patency maintained for the remainder of the study using heparinized saline flushes every 8 hours. General anesthesia was obtained using an intravenous triple drip solution consisting of 500 mL guaifenesin 5% + 500 mg ketamine + 50 mg xylazine. Anesthesia was induced in 5 to 10 minutes by the rapid administration of 0.5 to 2 mL/kg of this solution and maintained at a rate of 2 mL/kg/hour until the end of the procedure. Once fully anesthetized, the animals were placed in left lateral recumbency and the right paracostal region was clipped and aseptically prepared for surgery.

Entry into the abdomen was made via a right paracostal approach to allow for best visualization of and access to the gallbladder. Following visualization of the gallbladder, the common bile duct was located and a Hemoclip® was placed to prevent outflow of bile from the gallbladder following inoculation. Using a sterile 3 mL syringe and 20 gauge 1” needle, 1 mL of bile was removed from the gallbladder of all animals prior to inoculation of *C. jejuni* IA 3902. Following removal of the pre-inoculation bile sample, 1.5 mL of MH broth containing approximately 10^{11} CFU/mL *C. jejuni* IA 3902 inoculum was then injected into the lumen of the gallbladder using a separate 3 mL syringe and 20 gauge 1” needle. The body wall incision was closed and the animals recovered uneventfully from surgery. Food and water were provided following recovery from anesthesia and animals were monitored for signs of pain or septicemia following the procedure.

At either 2 hours or 24 hours post-inoculation as previously determined via random assignment, the sheep were humanely euthanized via intravenous injection of 1 mL/10 lb body weight pentobarbital (Fatal Plus®; Vortech, Dearborn, MI). Immediately following

euthanasia, a clean incision was made into the ventral midline of the abdomen to expose the liver and gallbladder. Using a 16 gauge 1” sterile needle and a 60 mL syringe, the entire amount of bile retained in the gallbladder was removed via gentle aspiration. The collected bile was immediately processed for RNA protection as described in Chapter 3 and 100 μ L was used for a serial dilution in MH broth to determine viable counts of *C. jejuni* (CFU/mL) following exposure to bile. Following removal of the bile contents, the gallbladder was then removed in its entirety and further samples collected for histopathology, immunohistochemistry and electron microscopy as described below. Following collection of these samples, approximately half of the gallbladder wall remained; this tissue was rinsed with sterile saline to remove loose droplets of bile and then the entire mucosal surface was scraped with a straight edge sterile blade to remove the mucous layer and mucosal lining. This material was then collected via rinsing with sterile saline into 15 mL conical tubes (FisherScientific). Following collection, the volume in the vials was standardized to 3 mL each, the collected material was vortexed vigorously for 1 minute and 100 μ l of this solution was used for a serial dilution in MH broth to provide a semi-quantitative estimate of the amount of *C. jejuni* contained within the mucus layer of the gallbladder. The amount estimated in CFU/mL was then multiplied by 3 mL based on the starting volume of the mucosal scraping solution; this value was again multiplied by 2 based on the fact that only half of the gallbladder wall was utilized for this purpose to determine an estimate of total bacterial numbers within the gallbladder mucosa.

***In vitro* bile inoculation and incubation**

To compare the effect of exposure to the *in vivo* ovine gallbladder environment versus *in vitro* ovine bile exposure only, fresh bile and gallbladder samples were collected at necropsy of an additional group of eight sheep obtained from one of the same farms as above that were being utilized for an unrelated study. Again using a 16 gauge 1” sterile needle and a 60 mL syringe, the entire amount of bile retained in the gallbladder at necropsy of each sheep was removed via gentle aspiration. Following removal of the bile contents, the gallbladder was then removed in its entirety and fixed in 10% neutral buffered formalin for histology and immunohistochemistry as non-inoculated controls; only samples confirmed to be free of culturable bacteria were used for this purpose. Following collection, the bile was cultured as described below to determine if it was free of culturable bacteria. While awaiting culture results, the bile was stored at 4°C in sterile 50 mL conical tubes. Following confirmation of culture-negative status, the entire collected amount of bile ranging in volume from 14 mL to 33 mL from four of the animals confirmed to be culture-negative was pre-warmed to ovine body temperature (39.5°C) in an incubator for 20 minutes and then inoculated with 10¹¹ *C. jejuni* IA 3902 suspended in 2.2 mL MH broth prepared as described above. Following inoculation, the bile was then incubated under microaerophilic conditions at 39.5°C in a static incubator. At 2 hours, half of the total amount of bile was removed and processed for CFU/mL using serial dilutions, as well as processed for RNA isolation as described in Chapter 3. The remaining bile was then incubated until 24 hours at which time it was also processed to determine CFU/mL and perform RNA isolation. To estimate the total number of bacteria remaining in the bile at each time point, the calculated CFU/mL value was multiplied by the total starting volume in mL.

Bacterial culture from bile and gallbladder mucosa

All samples of bile to be inoculated with *C. jejuni* IA 3902 (either *in vivo* or *in vitro*) were processed identically to determine if culturable bacteria were present prior to inoculation. As previously described, 1 mL of bile was removed from the gallbladder of all animals prior to inoculation of *C. jejuni* IA 3902 during the *in vivo* model using a sterile 3 mL syringe and 20 gauge 1” needle; this sample was stored at 4°C for less than 2 hours until processed. For the bile to be utilized for *in vitro* studies, the entire volume of collected bile was stored at 4°C for less than 2 hours until processed. To screen for growth, from all bile samples 100 µL was plated onto each of the following plates and incubated as described: MH plates – (1) straight bile and (1) 1:100 dilution plate, both incubated at 42°C microaerophilic; blood agar plates (BAP) - (2) plates straight bile, one each incubated at 37°C either aerobic or anaerobic using anaerobic packets and jars (GasPak EZ Anaerobe Pouch System; Becton-Dickinson). Of the *in vivo* inoculated animals, one animal did not have any appreciable bile in its gallbladder at the time of inoculation, therefore fecal culture on MH plates supplemented with Preston *Campylobacter* selective supplement (Oxoid, Hampshire, United Kingdom) and *Campylobacter* growth supplement (Oxoid, Hampshire, United Kingdom) according to the manufacturer's recommendations for isolation of *Campylobacter* from fecal sources was utilized instead to screen for intestinal carriage of *C. jejuni* as a proxy for gallbladder carriage.

Following inoculation and incubation of both *in vivo* and *in vitro* samples, 100 µL from each bile sample as well as 100 µl of mucosal scraping was set aside and used to determine the viable CFU/mL following exposure via serial dilution onto MH plates and incubation at 42°C microaerophilic using the drop-plate method as previously described

(Chen *et al.*, 2003). Statistical analysis of differences in the amount of bacteria cultured between the bile and mucosal scrapings as well as between 2 and 24 hours of incubation was performed via a two-way ANOVA (not repeated measures) with Sidak's multiple comparisons test (GraphPad, Prism).

Gallbladder histology and histochemistry

Following removal of bile from the gallbladders of the inoculated and non-inoculated control sheep, samples of the gallbladder wall were collected and placed in 10% neutral buffered formalin and submitted to the Iowa State University College of Veterinary Medicine Comparative Pathology Core Service for histology, histochemistry, and immunohistochemistry processing and evaluation.

To prepare the samples for evaluation, serial sections of each formalin fixed sample of gallbladder wall were embedded in paraffin and sections cut to 5 μm thickness. Cut sections were then stained with hematoxylin and eosin (H & E) for routine histological examination. An additional subset of slides were stained with Perl's iron stain, Alcian blue (pH 2.5), and the periodic acid-Schiff reaction with and without diastase pre-treatment to identify the presence or absence of material with staining characteristics consistent with iron, acid mucins, and neutral mucins, respectively.

Lectin histochemistry to identify L-fucose containing glycans was performed as previously described (Burrough *et al.*, 2012). In brief, serial sections of gallbladder were cut to 3 μm , placed on aminoalkylsilane-coated glass slides, and baked in a 56°C oven for 2 hours. Sections were routinely deparaffinized in xylene and rehydrated in graded alcohol and water baths. Endogenous peroxidase was inhibited by immersing sections (2 immersions, 10

minutes each) in 3% hydrogen peroxide in water. Antigen was unmasked by treating sections with Tris-EDTA (pH 9.0) in a stream bath for 20 minutes; slides were then cooled to room temperature and rinsed 3 times in phosphate buffered saline (PBS) prior to placement in an automated cell staining system (BioGenex, Fremont, CA). The lectins used consisted of commercially available biotinylated *Ulex europaeus* agglutinin I (UEA-I; Vector, Burlingame, CA) and biotinylated *Lotus tetragonolobus* lectin (LTA; Vector) applied to sections at 20 µg/ml and incubated at 22°C for 30 minutes, followed by rinsing in a bath of PBS solution for 5 minutes. Lectin binding was visualized using a commercial kit (Vectastain Elite ABC; Vector) and chromogen (NovaRED; Vector) per the manufacturer's instructions; the sections were then counterstained with hematoxylin and mounted routinely.

Gallbladder immunohistochemistry

To determine the location of *C. jejuni* bacteria within the sections of gallbladder, immunohistochemistry directed against the major outer membrane protein (MOMP) of *C. jejuni* was performed on a subset of randomly chosen gallbladder samples (two each from the 2 hour and 24 hour inoculated sheep, and one uninoculated control) as previously described (Burrough *et al.*, 2009). Sections of gallbladder were cut at 3 µm, mounted on aminoalkylsilane coated glass slides, and placed in an oven at 56°C for 2 hours and routinely deparaffinized in xylene and rehydrated in graded alcohol solutions and water baths. Endogenous peroxidase inhibition was achieved by immersion (2 immersions; 10 min/immersion) in baths of 3% H₂O₂ in water. Slides were incubated with 0.1% protease in a Tris buffer (pH, 7.6) at 37°C for 15 minutes and rinsed 3 times in PBS solution. To inhibit non-specific binding, sections were incubated in 10% neutral goat serum at 22°C for 20

minutes. The primary antibody, which was directed against the major outer membrane protein of *C. jejuni*, was prepared as previously described (Zhang *et al.*, 2000) and was used at a dilution of 1:300; slides were incubated at 22°C for 60 minutes followed by rinsing in a bath of PBS solution for 5 minutes. A commercially available biotinylated secondary antibody (MultiLink; Biogenex) was used at a dilution of 1:80; slides were incubated at 22°C for 15 minutes followed by rinsing in a bath of PBS solution for 5 minutes. Sections were then incubated with horse radish peroxidase–streptavidin (Zymed; Invitrogen, Grand Island, NY) conjugated at 22°C for 15 minutes followed by rinsing in a bath of PBS solution for 5 minutes. The final reaction was developed by use of a commercial chromogen (NovaRED; Vector). Sections were rinsed and routinely counterstained with Shandon Harris hematoxylin (ThermoScientific) and Scott's tap water. Sections were dehydrated through graded alcohol and xylene solutions prior to mounting.

Scanning electron microscopy of ovine gallbladder inoculated with *C. jejuni*

Additional sections of gallbladder wall were also collected separately at necropsy and fixed in 2% paraformaldehyde and 3% glutaraldehyde in 0.1M cacodylate buffer at 4°C for 24 hours then submitted to the Iowa State University Microscopy and NanoImaging Facility to be prepared for scanning electron microscopy (SEM). A single sample representative of each time point (2 hours and 24 hours) was selected for further processing based on evidence of normal mucosal architecture present in the histopathology examination. Fixed samples were rinsed in deionized water and post-fixed in 2% aqueous osmium tetroxide followed by dehydration in a graded ethanol series up to 100% ultra-pure ethanol and dried using a Denton DCP-2 critical point dryer (Denton Vacuum, Moorestown, NJ). When dried, the

samples were placed onto adhesive coated aluminum stubs, sputter coated (Denton Desk II sputter coater, Denton Vacuum) with palladium/gold alloy, and imaged using a JEOL 5800LV scanning electron microscope (Japan Electron Optics Laboratory, Peabody, MA) at 10kV.

Results

Preliminary animal studies

Preliminary experiments utilizing one or two mixed breed female sheep obtained from local farms were performed to determine the best method to inoculate the gallbladder of sheep with *C. jejuni* and subsequently harvest enough viable bacteria for RNA isolation. Of the options attempted, full laparotomy with and without placement of a Hemoclip® over the common bile duct was successfully performed in a single animal each. Transcutaneous ultrasound guided inoculation was unsuccessful as bile could not be aspirated to confirm needle placement within the gallbladder. Inoculation via laparoscopy was also attempted, however, visualization of the gallbladder was challenging due to its location deep to the liver, and the length of the laproscopic instruments was determined to be insufficient to reach the gallbladder from the paracostal incisions. A full laparotomy with direct visualization of the gallbladder was the only method that allowed for good visualization and direct inoculation of the gallbladder. Initial attempts at collecting sufficient viable bacteria for RNA isolation following incubation in the gallbladder without Hemoclip® placement were unsuccessful due to extremely rapid turnover of bile within the gallbladder (**Figure 1**). Full laparotomy with placement of a Hemoclip® over the common bile duct to prevent secretion of bile into the intestinal tract finally yielded adequate numbers of viable bacteria recovered for isolation of

RNA of sufficient quality for next generation sequencing. Based on the results of this preliminary work, a final determination of the necessity of full laparotomy with placement of a Hemoclip® over the common bile duct was made, and thereafter all inoculations were performed via this method.

Pre-screening of bile for carriage of *C. jejuni*

Prior to inoculation of the gallbladder during the *in vivo* experiment, 1 mL of bile was removed from all animals to screen for the presence of culturable bacteria already inhabiting the gallbladder. Of the 7 animals that had bile that could be harvested from the gallbladder pre-inoculation, only 1 animal displayed any growth under the conditions studied; the remaining cultures were free of any bacterial colonization as detectable by these methods. The single animal that exhibited bacterial growth displayed a pure growth of colonies on MH agar at 42°C microaerophilic that was confirmed to be *C. jejuni* utilizing a MALDI-TOF mass spectrometry biotyper (Bruker Daltonics, Billerica, MA) for identification. Further strain typing was not performed; however, an aliquot of the isolate was frozen at -80°C in 20% glycerol for future analysis if necessary. Screening of the feces from the single animal that did not have bile for collection pre-inoculation did not reveal the presence of *C. jejuni*.

The bile utilized for the *in vitro* inoculation was also screened for the presence of culturable organisms prior to use. Of the eight sheep initially screened, four exhibited no growth detectable via microaerophilic incubation at 42°C on MH plates or via aerobic and anaerobic incubation at 37°C on BAP. One of the sheep exhibited heavy pure growth of white non-hemolytic mucoid colonies confirmed to be *E. coli* via MALDI-TOF, while two of the sheep exhibited a pure growth on MH plates of colonies suspected to be *Campylobacter*

sp; these colonies did not grow on subculture for MALDI-TOF analysis, therefore further identification was not possible. Another bile sample displayed growth of one single white colony on BAP; although growth of a single colony may be considered a contaminant, this sample was also considered positive for growth of bacteria. Any bile that exhibited growth was discarded for future use; therefore, the four “clean” bile samples (labeled 2, 3, 7, and 8) were utilized for the *in vitro* bile inoculation study.

Recovery of viable *C. jejuni* from *in vivo* gallbladders and *in vitro* bile

Figure 2 demonstrates the inoculated amount of *C. jejuni* IA 3902 compared with the amount that was recovered from both the bile and mucosal scrapings following incubation within the sheep gallbladder *in vivo*. The average inoculum after translation to log₁₀ for ease of comparisons was 11.5 (6×10^{11} total bacteria). After 2 hours of incubation, an average of 10.1 log₁₀ bacteria were collected out of the bile, with an additional 6.9 log₁₀ bacteria present in the gallbladder wall scrapings. Following 24 hours of incubation, an average of 8.4 log₁₀ bacteria were present in the bile, with an additional 7.3 log₁₀ bacteria estimated to be located within the gallbladder wall scrapings. Interestingly, the amount of bacteria present within the gallbladder wall scrapings appears to have increased between the 2 hour and 24 hour time points, while during the same timeframe the amount of viable bacteria present in bile in the lumen of the gallbladder decreased; statistical analysis via two-way ANOVA did not demonstrate statistical significance (**Figure 3**).

In comparison, **Figure 4** demonstrates the inoculated amount of *C. jejuni* IA 3902 compared with the amount that was estimated to be present at 2 and 24 hours when samples were recovered from *in vitro* incubated bile. The inoculum after translation to log₁₀ for ease

of comparisons was again $11.5 (3.5 \times 10^{11})$ total bacteria); this same inoculum was used for all replicates. On average, the amount of bacteria present within the bile was estimated to decrease by 0.9 log₁₀ over the first 2 hours of incubation, with an overall decrease of 2.3 log₁₀ by the end of 24 hours of incubation.

Routine histology findings

A summary of the routine histology findings of the sheep gallbladder samples is presented in **Table 1** with representative images of 2 hour and 24 hour samples presented in **Figures 5A** and **5B**. Briefly, at 2 hours post inoculation, there was a mild, diffuse infiltrate of low numbers of neutrophils and occasional eosinophils and Mott cells in the majority of slides examined. Multifocally, glands were observed to be expanded by neutrophils, cellular debris and/or mucus, which was also present within the lumen of the gallbladder. There were rare lymphoid nodules noted within the lamina propria, and multifocally blood vessels were noted to be congested.

At 24 hours post inoculation, the severity of the observed histological lesions was observed to be substantially increased. The mucosa was noted to be diffusely necrotic and multifocally ulcerated with loss of cellular detail which was replaced by large amounts of eosinophilic cellular debris, moderate amounts of karyorrhectic and karyolytic nuclear material, moderate numbers of degenerate neutrophils, congested blood vessels and small amounts of hemorrhage. Glands were occasionally observed to be lined by flattened, attenuated epithelia and were dilated with basophilic to eosinophilic flocculent material, small amounts of necrotic cellular debris and a few degenerate neutrophils. Rarely, there were up to 4 cell layers (glandular hyperplasia) with the gland lumen not readily apparent

and interspersed by small amounts of pyknotic nuclear debris. The lamina propria was moderately expanded by clear space (edema), congested blood vessels, and moderate numbers of neutrophils, eosinophils and occasional Mott cells. The muscularis was markedly expanded and disrupted as previously described along with small amounts of hemorrhage. Many lymphatics were congested and prominently expanded by large numbers of neutrophils within the lumen and extravasating the vessel walls. The endothelium of many vessels was plump and reactive. The serosa and adjacent adipose were markedly expanded by large amounts of eosinophilic proteinaceous fluid, fibrin and congested blood vessels and multifocal areas were overlain by a thick mat of neutrophils and fibrin with hemorrhage.

For the uninoculated culture negative gallbladders, there were occasional Mott cells present and rare lymphoid nodules noted within the lamina propria. Multifocally, blood vessels were noted to be mildly congested. No neutrophils or eosinophils were noted in any of the slides examined.

Immunohistochemistry and SEM

To determine the preferred location of *C. jejuni* within the gallbladder environment, immunohistochemistry directed towards the major outer membrane protein (MOMP) of *C. jejuni* was performed on a portion of the sheep gallbladder samples. Immunohistochemistry of the selected samples identified dense accumulation of organisms deep within the glands of the gallbladder and as multifocal aggregates within clumps of luminal debris and mucus. By 2 hours after inoculation both samples examined were observed to have *C. jejuni* located deep within many of the glands (**Figure 6**). By 24 hours, as much of the mucosal surface exhibited severe inflammation and necrosis, the majority of the *C. jejuni* was observed to be

present in aggregates adhered to mucin and inflammatory debris on the surface of the mucosa (**Figure 7A**), however, where glands were still visible, *C. jejuni* could still be observed to be located within them (**Figure 7B**). For all slides of inoculated gallbladders examined, there was also staining observed at the serosal surface indicative of leakage of inoculated bile from the puncture site. In contrast, the single uninoculated gallbladder sample that was confirmed via culture to be negative for *C. jejuni* did not exhibit any staining indicative of *C. jejuni* presence.

In addition to immunohistochemistry, scanning electron microscopy of a subset of the inoculated gallbladder samples (one each from the 2 hour and 24 hour time points) was also utilized in an attempt to locate *C. jejuni* on the surface of the gallbladder mucosa. **Figure 8A** demonstrates an aggregate of *C. jejuni* organisms at 2 hours post-inoculation closely adherent to the apical aspect of the mucosal surface located near a small focus of microvilli loss. The adjacent material within which the *C. jejuni* is located is likely made up of cellular debris and mucus. **Figure 8B** also taken at 2 hours post-inoculation demonstrates two *C. jejuni* organisms adherent to a focally extensive area of ulceration, again with adjacent material that is likely to be made up of cellular debris and mucus. These images demonstrate that within a relatively short amount of time post-inoculation, *C. jejuni* is able to migrate through the mucous layer to become intimately associated with the gallbladder mucosa. Additional organisms were observed within the spaces between villi; however, the microscope could not be focused to those regions to capture images.

Histochemistry

To determine if any factors previously known to be tropic for *C. jejuni* were present in the same locations in the ovine gallbladder as *C. jejuni* identified via immunohistochemistry, an additional subset of slides were stained with Perl's iron stain, Alcian blue (pH 2.5), lectin staining, and the periodic acid-Schiff (PAS) reaction with and without diastase pre-treatment. Perl's iron stain did not reveal appreciable staining within mucosa, submucosa, muscularis or serosa of sections examined, indicating that iron accumulation is not a feature of the gallbladder wall.

Alcian blue staining was utilized to identify the presence of acid mucins within sections of gallbladder at both 2 hours and 24 hours. Both time points demonstrated marked stain uptake within the cells and lumen of the deep crypts, extending throughout the gland lumen space and multifocally dispersed among gallbladder debris (**Figures 9A, 9B, and 9C**). Staining via PAS was utilized to identify the presence of neutral mucins within sections of gallbladder at both 2 hours and 24 hours. Again, both timepoints displayed marked PAS staining multifocally at the deep aspect of glands and as aggregates and streaming bands within the gallbladder lumen (**Figures 10A, 10B, and 10C**).

Lectin staining was also utilized to determine if L-fucose containing glycans were present within the gallbladder mucosa. Both time points displayed multifocal areas of variable to strong lectin staining within glands and on the surface of the epithelium (**Figure 11A and 11B**). Based on the staining patterns for both acid and neutral mucins, as well as L-fucose, the observed areas of MOMP immunohistochemistry correspond well to the same locations particularly deep within the glands of the gallbladder.

Discussion

Previous work by our lab has demonstrated that *C. jejuni* IA 3902 can be isolated from the gallbladders of clinically normal sheep (Sahin *et al.*, 2012) and that this strain can achieve similar *in vitro* growth in sheep bile as to that of rich media under normal laboratory growth conditions (Zhang lab, unpublished data). Additional studies in both sheep and other species of ruminants have also suggested that up to 34% of sheep may carry pathogenic *C. jejuni* within otherwise healthy bile with up to 66% of gallbladders positive for some species of *Campylobacter* (Acik and Cetinkaya, 2006; Ertas *et al.*, 2003).

The gallbladder environment is typically thought of as “harsh” with few bacteria able to survive under the conditions present. Bile acids (salts) are the main component of bile, along with cholesterol, phospholipids and bilirubin. Their amphipathic nature allows them to act as a detergent which plays a key role in lipid solubilization and emulsification leading to digestion of fats within the intestinal tract (Baptissart *et al.*, 2013). Studies have demonstrated that sheep bile, along with ox and pig bile, has a relatively high percentage of bile salts which constitute 10% w/v of the total contents of bile. The presence of high concentrations of bile salts have been proven to be very damaging to cellular membranes (Coleman *et al.*, 1979), and the detergent properties of bile has been demonstrated to have potent antimicrobial activity (Begley *et al.*, 2005). For evidence of the inhospitable nature of the gallbladder environment, one need not look farther than the exit of the common bile duct into the duodenum; while one location is home to a wide array of culturable bacterial species, the other, directly connected and separated by only a short distance, more often than not remains free of culturable bacteria.

Recent rapid expansion of the use of metagenomics and microbiome research has proven that many sites previously thought to be inhospitable to bacterial colonization, such as the monogastric stomach, are now known to be home to a unique ecological community of bacteria (Yang and Suerbaum, 2013). Therefore, it is likely naïve to assume that the gallbladder is completely free of a resident population of bacteria. Recently, the first report of characterization of the microbiome of the gallbladder in any species was published investigating the microbiota of the swine gallbladder (Jimenez *et al.*, 2015). While the study was limited in that it only assessed the bacterial diversity of 4 adult animals from the same farm, some important conclusions could be drawn. The diversity of bacterial species identified within the gallbladder was much lower than reported for most other locations in the mammalian body that have been studied to date, and considerably lower than the diversity observed in the gut microbiota of the same species (Lamendella *et al.*, 2011). All of the samples exhibited growth of culturable bacteria in the range of 3 to 20 unique species per sample which were also identified via DNA sequencing (Jimenez *et al.*, 2015). The amount and variety of species cultured from the swine gallbladder appears to differ substantially for our data and from what has been reported in studies of ruminant gallbladders; it is unclear whether the gallbladders of swine are more frequently colonized by bacteria, or whether these animals represent a departure from the norm.

The frequent isolation of *C. jejuni* from bile samples of multiple ruminant species suggests that the gallbladder may in fact serve as a protected niche for chronic colonization by certain bacteria adapted to survive within its walls. This phenomenon may not be limited to ruminants as multiple instances of cholecystitis in humans due to *Campylobacter* species have been reported (Dakdouki *et al.*, 2003; Vaughan-Shaw *et al.*, 2010). Other intestinal

pathogens such as *Salmonella typhi* and *Listeria monocytogenes* have also been shown to have the unique ability to colonize the gallbladder in both humans and animals where they can establish a chronic carrier state in their host (Dowd *et al.*, 2011; Gonzalez-Escobedo *et al.*, 2011). In addition, the DNA of the closely related *H. pylori* has also been demonstrated to be frequently present in the gallbladder of patients with cholelithiasis although direct culture has proven more challenging (Guraya *et al.*, 2015).

In this study, 15 gallbladders of otherwise healthy sheep were screened for carriage of culturable bacteria. Of those 15, three demonstrated heavy pure growth consistent in appearance with *C. jejuni* which was confirmed via MALDI-TOF identification for one of the isolates. An additional animal demonstrated pure growth of *E. coli* also identified via MALDI-TOF. These findings are consistent with reports of 11% carriage of *C. jejuni* within the gallbladders of healthy sheep performed in the same geographical area (Sahin *et al.*, 2012). *In vivo* and *in vitro* inoculation of bile in our study proved that *C. jejuni* IA 3902 in particular has the ability to survive within pure ovine bile both with and without interaction with the gallbladder mucosa. The high bacterial load utilized for inoculation in this study was not ideal to assess whether *C. jejuni* could replicate in bile or within the gallbladder as even within defined media *C. jejuni* frequently ceases replication prior to reaching a concentration of 10.0 log10. While not mimicking either the natural route of infection of the gallbladder (which is currently unknown), nor the likely infectious dose, the methods utilized provided several advantages to initiate studies into this important field. As one of the primary goals of the model was to be able to collect high enough levels of quality RNA for next generation sequencing as discussed in Chapter 3, high levels of inoculum were necessary to ensure that enough viable bacteria were available at the end of the study to obtain adequate amounts of

RNA. Indeed, for most of the 24 hour samples, all of the RNA collected was necessary to generate adequate amounts of library to be sequenced. High levels of inoculum placed directly at the site of interest also ensured that a rapid timeline for data collection could be utilized and increased the chance that measurable bacteria could be found within their protected niche of choice within the gallbladder environment. It is likely that the severity of histologic lesions observed within the inoculated gallbladders, particularly those observed at 24 hours, is a direct result of the amount of bacteria inoculated along with concomitant levels of endotoxin release, and not solely due to the pathologic ability of the organism itself. In addition, perforation of the gallbladder wall using a 20 gauge needle to introduce the inoculum likely led to leakage of contaminated bile from the puncture site which was visible in the histologic sections as serositis. Minimal reports in the literature exist of the normal histologic description of the ovine gallbladder with which to compare our findings. The presence of Mott cells and lymphoid nodules in the uninoculated healthy control samples, however, indicates that even in the absence of known pathogenic bacteria, the ovine gallbladder wall appears to normally have a resident population of immune cells present which suggests a chronic state of low grade inflammation or immune stimulation.

Prior to this study, the location within the gallbladder *C. jejuni* that typically prefers to be located was unknown. Knowledge of this important fact is critical for improved understanding of the mechanisms of virulence of this important pathogen and will lead to a greater understanding of how *Campylobacter* is able to survive within the harsh gallbladder environment. The unique *in vivo* method developed within this study has allowed us an unprecedented means by which to attempt to answer these questions utilizing the gallbladder environment of the natural ovine host. The large decrease in the concentration of viable

bacteria able to be recovered from the inoculated gallbladder of sheep when a Hemoclip® was not placed over the common bile duct for the initial preliminary trial suggests that the regular flushing action of frequent bile secretion, particularly in species like sheep where biliary secretion is tied to rumination which occurs throughout the day rather than simply during ingestion of meals which occurs at set intervals, should make chronic colonization of the gallbladder difficult for bacteria free-living within the gallbladder lumen. These findings are consistent with published data suggesting that sheep secrete up to 40 µl of bile per kg per minute which is seven times higher than the endogenous rate of bile flow in monogastrics such as dogs (Barnhart and Upson, 1979). Not all of this bile is stored within the gallbladder prior to release; however, it is reasonable to suggest that long-term survival by *C. jejuni* within the ovine gallbladder requires a mechanism to counteract the constant flushing action of bile release.

Intestinal colonization with this organism is associated with the ability to colonize the mucin and L-fucose-containing mucous layer of the intestinal epithelium where it is protected from the mechanical and chemical milieu of the intestinal lumen (McSweegan and Walker, 1986; Shigematsu *et al.*, 1998). Unlike many other enteric pathogens that become trapped in this layer, *C. jejuni* is able to move freely within the mucin layer to inhabit the deep intestinal crypts (Lee *et al.*, 1986) and from there potentially become internalized within eukaryotic cells (van Spreeuwel *et al.*, 1985; Babakhani and Joens, 1993; Russell *et al.*, 1993). This ability has also been demonstrated in the closely related *H. pylori* to allow colonization of the glands of the stomach (Yang and Suerbaum, 2013). Mucin, L-fucose, and bile have all been shown to be strong chemoattractants for *C. jejuni* (Hugdahl *et al.*, 1988) and it has been demonstrated that some virulent strains of *C. jejuni* such as IA 3902 can

utilize L-fucose as a substrate for growth due to possession of a specific genetic island encoding a region for fucose metabolism (Stahl *et al.*, 2011; Muroaka and Zhang, 2011).

The studies of the growth and chemotaxis of *Campylobacter* spp described above, as well as additional studies evaluating tropism of *C. jejuni* IA 3902 within the guinea pig placenta (Burrough *et al.*, 2012), provided potential target compounds to evaluate within the sheep gallbladder including mucins, L-fucose, and iron. The data presented in our work clearly demonstrates that many of the same factors thought to be chemotropic to *C. jejuni* in the guinea pig placenta, such as neutral and acid mucins and L-fucose, are also present in the ovine gallbladder. In addition, the location of MOMP staining indicative of *C. jejuni* antigens within the same locations at the chemoattractive mucins and L-fucose strongly suggests that *C. jejuni* has an affinity for these locations due to their enhanced presence in the same regions. The location of *C. jejuni*, as detected by immunohistochemistry, within the deeper aspects of the glands of the gallbladder mucosa was consistent, even in severely inflamed gallbladder mucosa. The large aggregates of *C. jejuni* organisms present within the deep aspects of the glands also suggest that replication of organisms may be occurring in those locations. These protected areas of the gallbladder would likely provide the most defense against the harsh luminal environment and constant flushing action of bile release, which would allow bacterial resources to be dedicated to replication rather than purely survival. Scanning electron microscopy also allowed us an unprecedented view of *Campylobacter* organisms in direct contact with the microvilli on the surface of the gallbladder epithelium; their location in association with what appears to be extracellular debris is also suggestive of an affinity for mucins. The culture data presented in this study is supportive of the likelihood of migration of *C. jejuni* from free-living with the gallbladder lumen towards the more

protected niche of the mucous layer and glands of the gallbladder wall. While not statistically significant, the amount of bacteria recovered from the bile decreased between the 2 hour and 24 hour time points, and the estimated amount of bacteria collected from mucosal scrapings increased. This suggests that either migration of inoculated bacteria towards the mucosal surface is occurring, or that the protected niche of the glandular regions allow for replication of *C. jejuni* in those areas.

To our knowledge, factors that may lead to tropism of *C. jejuni* to the gallbladder have not been described in any species. The effect of bile itself as a chemoattractant for *Campylobacter* has been variable depending on the species studied. Interestingly, while *C. jejuni* can be cultured out of the guinea pig gallbladder, the bile from guinea pigs has been shown to be chemorepellent (Burrough *et al.*, 2009). In contrast, diluted bovine and chicken bile have been described as chemoattractive for certain *C. jejuni* strains isolated from chickens; when the mucin fraction of the bile was removed, however, the remaining bile salts were universally chemorepellent (Hugdahl *et al.*, 1988). This suggests that biliary mucins may act as the chemoattractive fraction in bile. Our data which demonstrated aggregates of mucin staining within the lumen and deep glands of the gallbladder in conjunction with MOMP staining of *C. jejuni* within the same regions are supportive of the theory that mucins in bile may play a role in chemoattraction.

The composition of bile salts varies greatly between species and may also play a role in observed differences in chemoattraction between bile from different species. Based on type of conjugation, the composition of bile salts between sheep, bovine and guinea pigs has previously been shown to be very different and this composition strongly affects the hydrophilicity of the solution. Within ovine bile, 100% of bile salts are tauroconjugated,

while only 16% of guinea pig bile is tauroconjugated with the rest being glycoconjugated; bovine bile is approximately a 50:50 split between the two (Alvaro *et al.*, 1986). It is possible, therefore, that the composition of the bile salts, rather than only the mucin fraction, may also play a role in the affinity of *C. jejuni* to the gallbladder environment.

In summary, the data presented herein has demonstrated that *C. jejuni* IA 3902 appears to have an affinity for neutral mucin, acid mucin and L-fucose in the ovine gallbladder based on observations that the organism localized in higher numbers to areas with increased staining for PAS, Alcian blue and lectin, including the deeper aspects of the mucosal glands of the gallbladder and in free-floating luminal debris composed of neutral and acid mucin aggregates. This data suggests that to survive with the harsh environment of the gallbladder, colonization of the deep mucosal glands occurs to allow avoidance of the constant flushing action of bile release and the detergent activities of bile salts in the lumen.

Future work in models utilizing natural methods of *C. jejuni* inoculation (i.e. – oral) is warranted to confirm the observed location of *C. jejuni* within the gallbladder environment as well as determine the route by which gallbladder colonization occurs. Investigation of histopathologic lesions and IHC staining for *C. jejuni* within the gallbladder of orally inoculated as well as naturally infected animals is warranted to confirm our observations that *C. jejuni* localizes to the deep glands of the gallbladder mucosa. In addition, future work combining oral inoculation with prior placement of a Hemoclip® over the common bile duct should also prove useful in determining whether the route of infection of the gallbladder is septicemia via the bloodstream, liver, and secretion into the bile, or retrograde through the common bile duct into the gallbladder directly from the intestinal tract.

Table 1. Summary of histologic changes associated with direct inoculation of the ovine gallbladder with *C. jejuni*.

	Sample	Mucosal changes		Eosinophils within the mucosa and lamina propria	Mott cells within the mucosa and lamina propria	Lymphoid nodules	Neutrophilic infiltration	Changes within the muscularis		Serosa
		Ulceration	Gland abscesses					Vascular congestion/ lymphatic dilation	Edema	Serositis
2 hours	2	0	3	2	1	1	2	1	3	1
	3 ^a	0	1	2	1	0	2	1	2	2
	6	0	3	0	3	1	1	3	2	0
	8 ^{a,b}	0	1	2	2	2	2	1	1	0
24 hours	1 ^a	1	2	1	0	1	3	3	2	3
	4 ^a	3	0	2	3	0	3	3	3	1
	5	2-3 cm of transmural necrosis, demarcated by a band of degenerate neutrophils and cellular debris								
	7 ^b	0	2	1	1	2	2	1	1	2
Control^c	bile 7	0	0	0	1	2	0	1	0	0
	bile 8 ^a	0	0	0	1	1	0	1	0	0

Legend: 0 = none/no lesion of that type present; 1 = mild lesion present; 2 = moderate lesion present; 3 = severe lesion present

^a = sample processed for immunohistochemistry

^b = sample processed for SEM

^c = gallbladder samples taken from uninoculated sheep

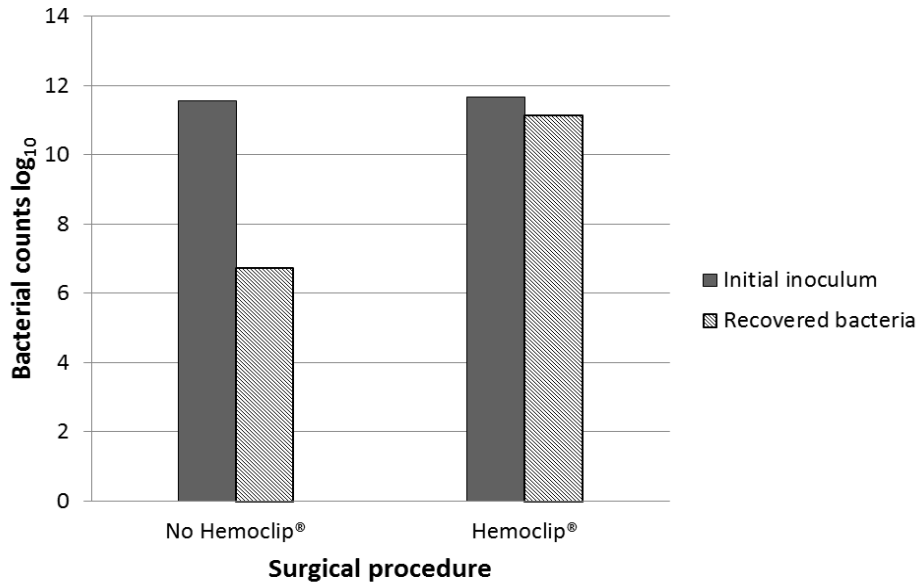


Figure 1. Comparison of recovery of bacteria with and without Hemoclip placement. Following direct inoculation of the ovine gallbladder, samples of bile were cultured to estimate total remaining bacterial (CFU/mL) using serial dilutions and the drop plate method of enumeration.

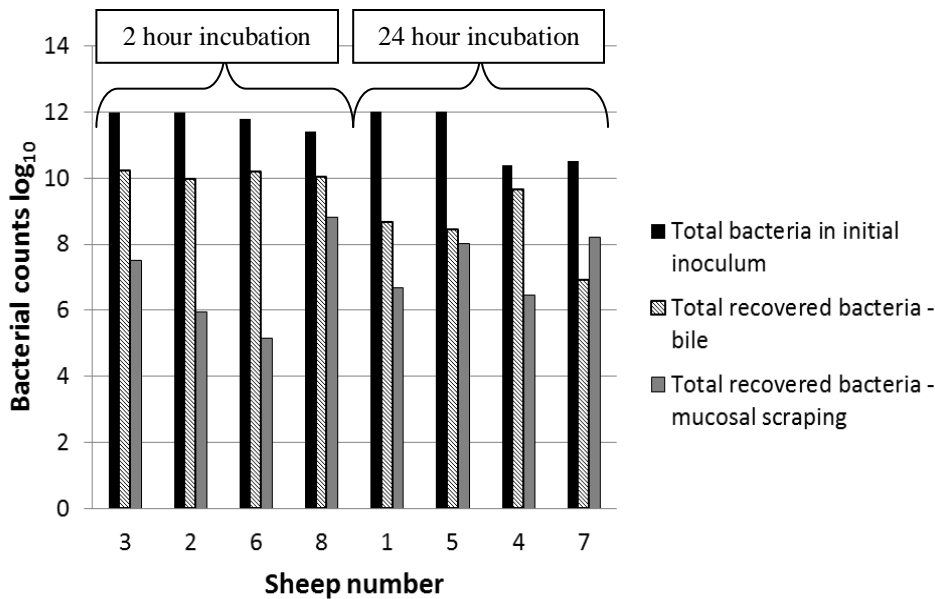


Figure 2. Recovery of *C. jejuni* in bile and mucosal scrapings from *in vivo* inoculation. Samples of bile and mucosal scrapings following 2 and 24 hour incubation of *C. jejuni* inoculated directly into the ovine gallbladder were cultured to estimate total remaining bacterial (CFU/mL) using serial dilutions and the drop plate method of enumeration.

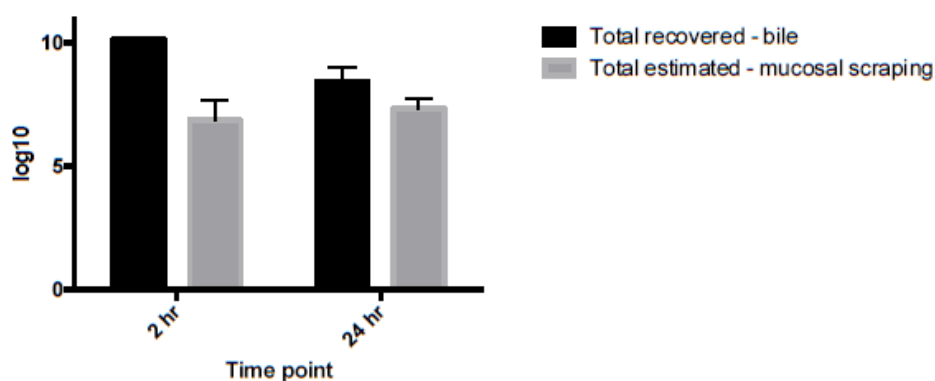


Figure 3. Average recovery of bacteria between bile and mucosal scrapings (mean \pm SEM). Samples of bile and mucosal scrapings following 2 and 24 hour incubation of *C. jejuni* inoculated directly into the ovine gallbladder were cultured to estimate total remaining bacteria (CFU/mL) using serial dilutions and the drop plate method of enumeration. The average of these results are presented to demonstrate that the number of bacteria within the gallbladder wall scrapings appears to have increased between the 2 hour and 24 hour timepoints while during the same timeframe the amount of viable bacteria present in bile in the lumen of the gallbladder decreased. No statistically significant difference was found.

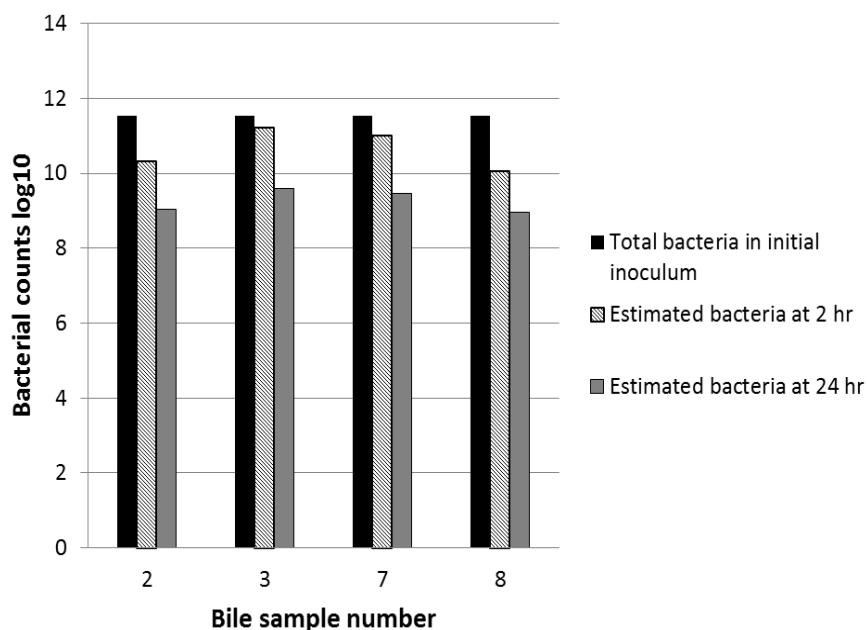
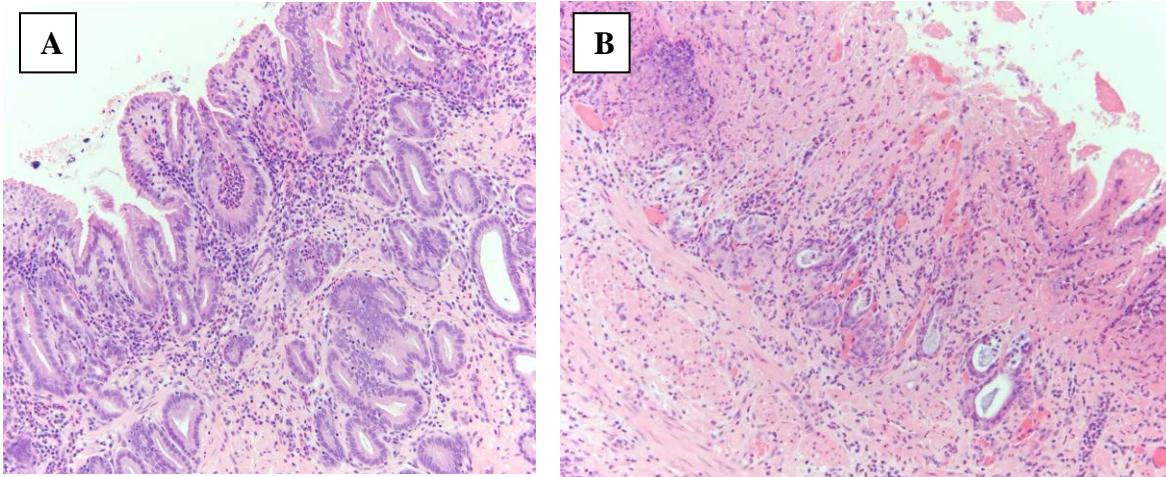


Figure 4. Recovery of *C. jejuni* from bile after 2 and 24 hours of incubation *in vitro*. Samples of bile following 2 and 24 hour incubation of *C. jejuni* inoculated *in vitro* were cultured to estimate total remaining bacteria (CFU/mL) using serial dilutions and the drop plate method of enumeration.



Figures 5A and 5B. Routine H & E staining of sheep gallbladders inoculated with *C. jejuni* IA 3902. At 2 hours post-inoculation (A), there is mild to moderate diffuse neutrophilic infiltration within the lamina propria mildly separating and surrounding glands. There is distension of the basal aspect of multifocal glands by neutrophils, cellular debris and/or mucus, which is also present within the lumen of the gallbladder. At 24 hours post-inoculation (B), mucosal architecture is diffusely disrupted, the apical aspect of gland mucosa are necrotic, moderate numbers of glands are lined by attenuated epithelium and are ectatic with mucus, degenerate neutrophils and pyknotic cellular debris. There is vascular congestion and hemorrhage, moderate transmural neutrophilic inflammation and moderate, multifocal, neutrophilic serositis. (Photos courtesy of Dr. Victoria Lashley)

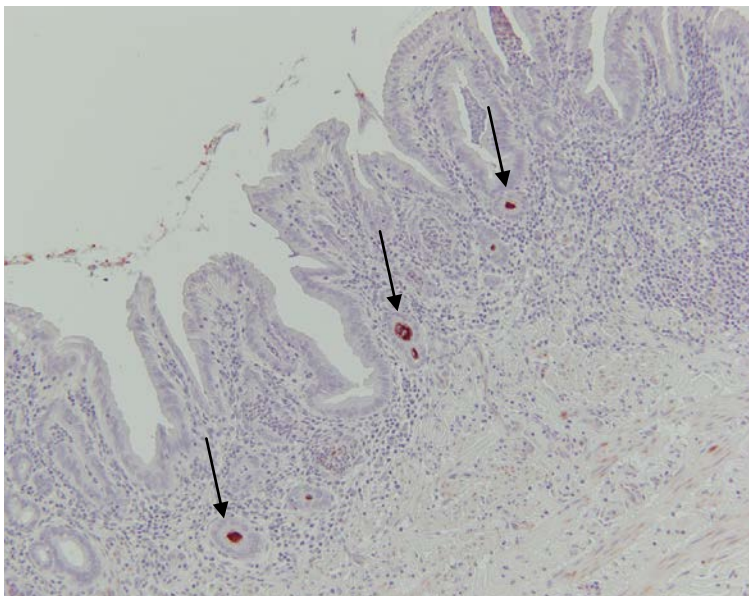
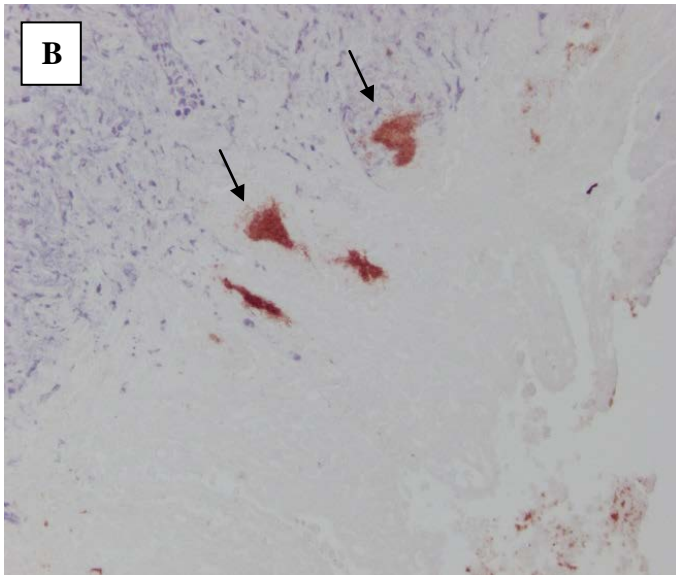
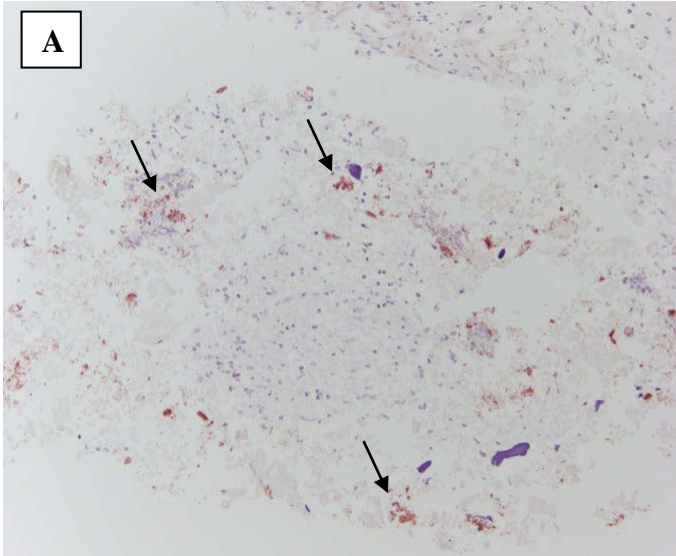
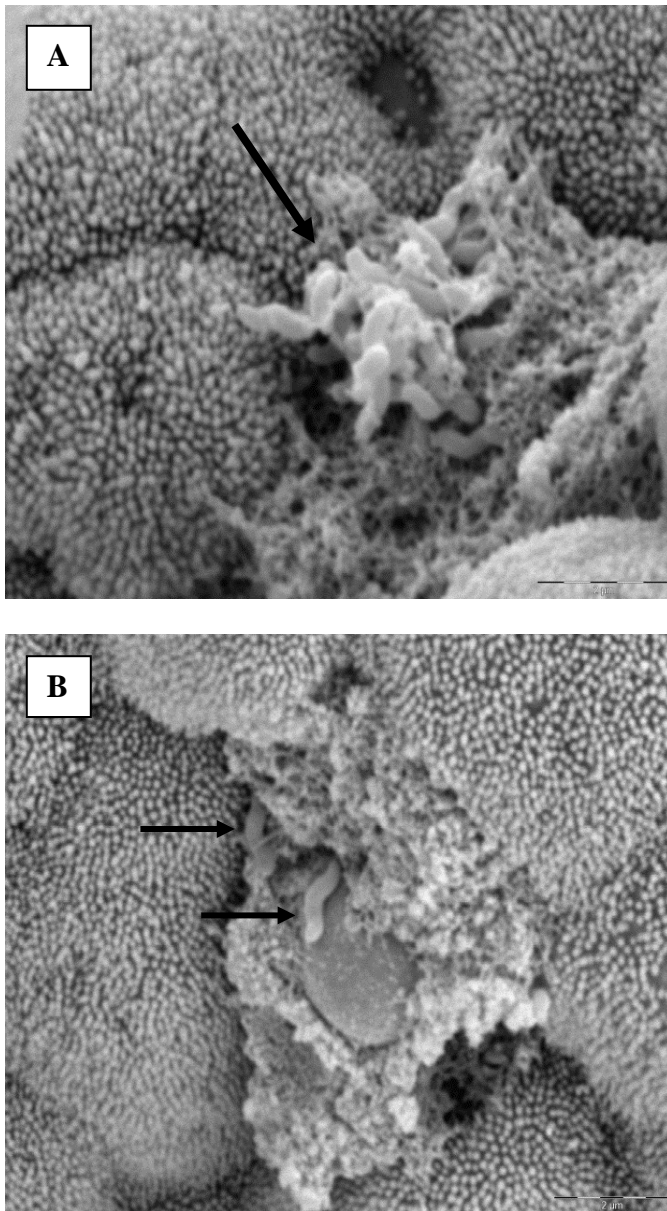


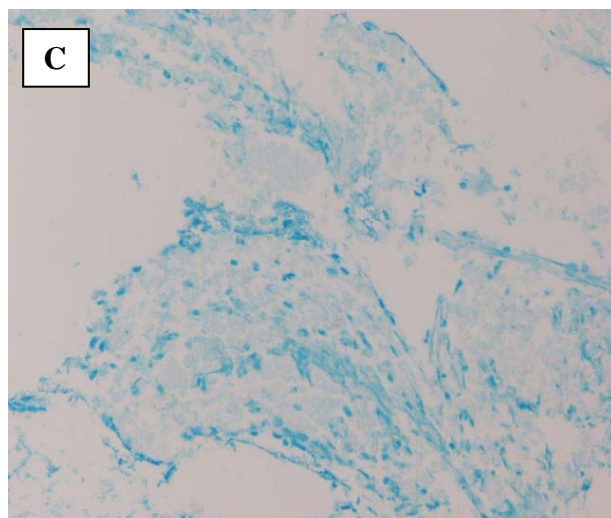
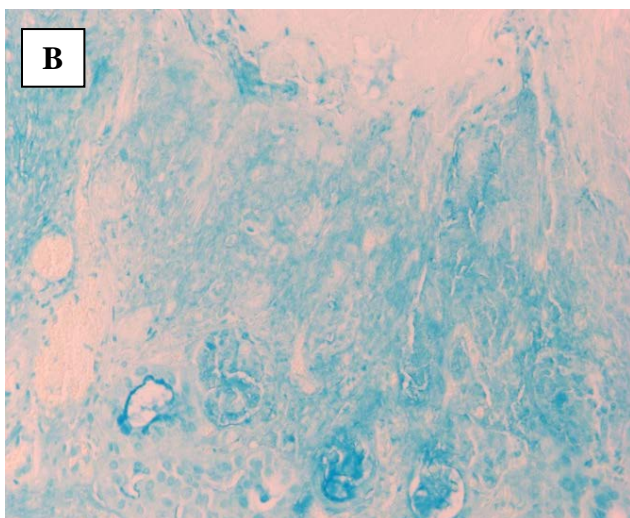
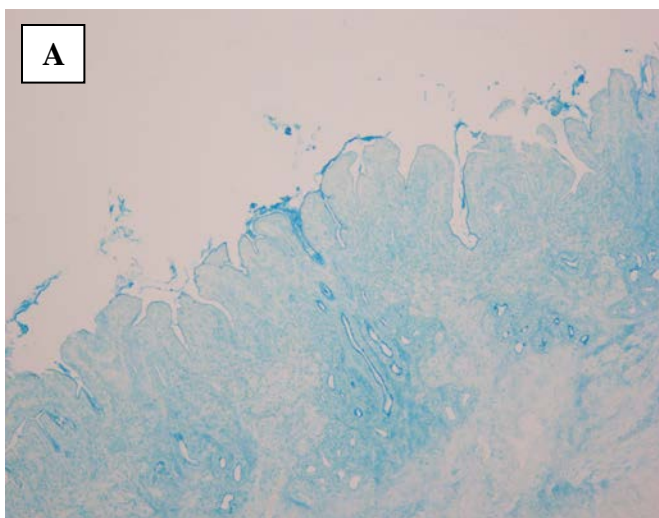
Figure 6. Gallbladder, 2 hours post-inoculation, major outer membrane protein (MOMP) immunohistochemistry. Photomicrograph of a section of ovine gallbladder tissue after immunohistochemical staining for *C. jejuni*. Notice the *C. jejuni* organisms (red stain) located deep within the luminal glands (arrows). (Photo courtesy of Dr. Victoria Lashley)



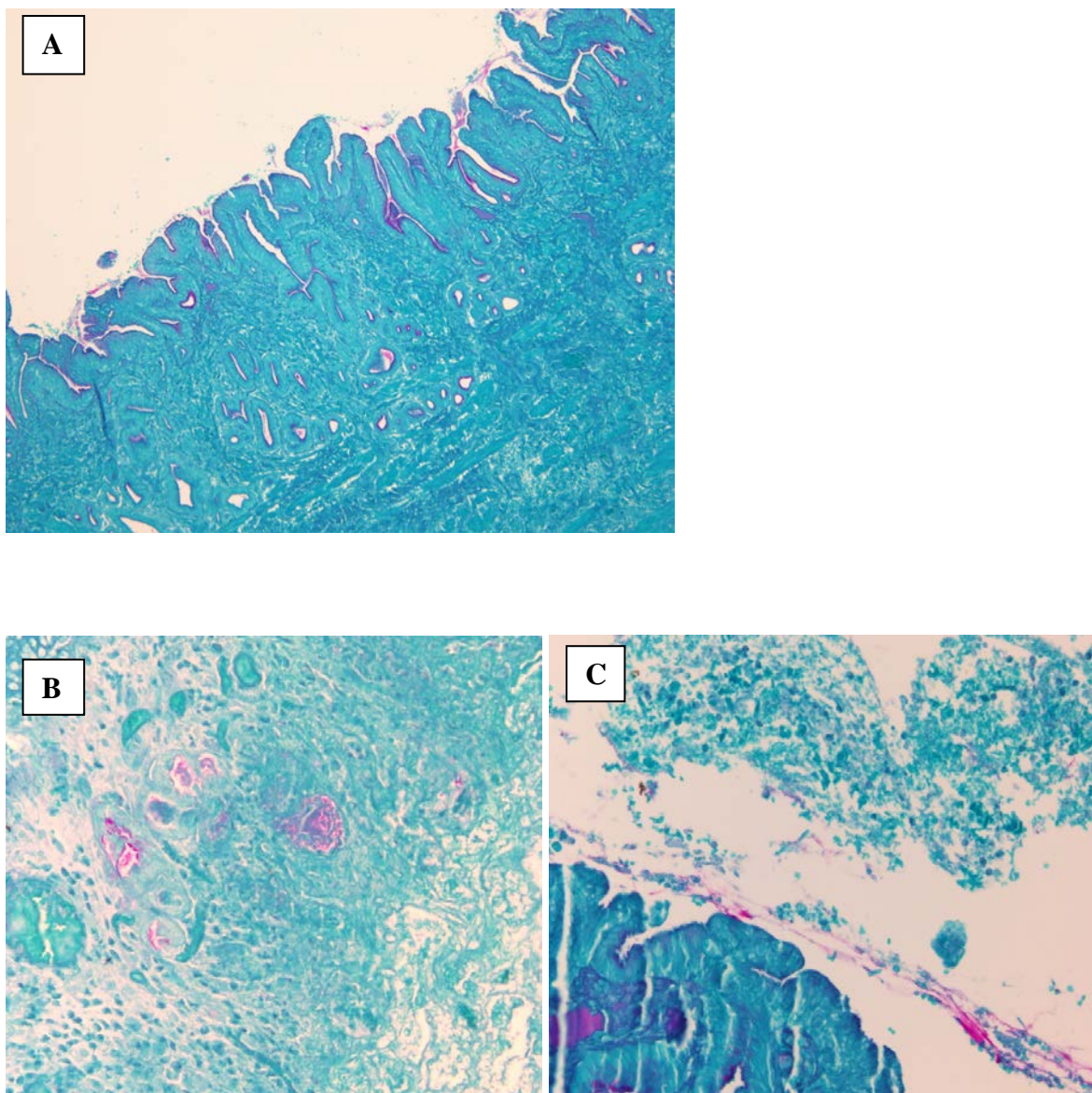
Figures 7A and 7B. Gallbladder, 24 hours post-inoculation, major outer membrane protein (MOMP) immunohistochemistry. Photomicrograph of a section of ovine gallbladder tissue after immunohistochemical staining for *C. jejuni*. Notice the *C. jejuni* organisms (red stain, arrows) located (A) as multifocal aggregates within clumps of luminal debris and as well as (B) deep within the remaining luminal glands. (Photos courtesy of Dr. Victoria Lashley)



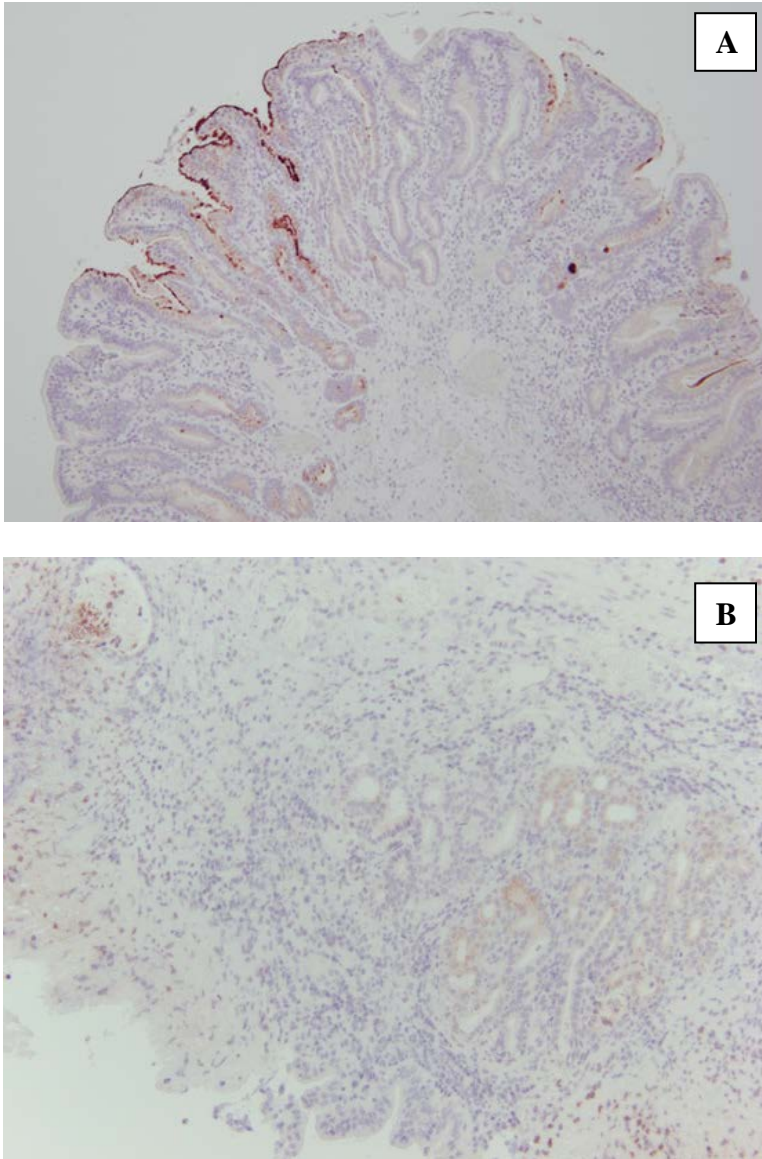
Figures 8A and 8B. Gallbladder, 2 hours post-inoculation, scanning electron micrographs (SEM) of the surface of the gallbladder mucosa. SEM image of (A) an aggregate of a number of *C. jejuni* organisms (arrow) adherent to the apical aspect of the mucosa with loss of, clumping and blunting/ shortening of the adjacent microvilli, and (B) an area of focally extensive ulceration, with two *C. jejuni* organisms (arrows).



Figures 9A, 9B and 9C. Gallbladder, 2 hours (A) and 24 hours (B, C) post-inoculation, Alcian blue (pH 2.5) staining for acid mucin. Photomicrographs of sections of ovine gallbladder tissue after Alcian blue staining (deep blue color) for acid mucin. (A) The mucosal surface and deep crypts are lined with moderate amounts of acid mucin at 2 hours post-inoculation. By 24 hours post-inoculation, acid mucin staining is still marked within the cells and lumen of the deep crypts (B), but is also seen to extend throughout the gland lumen space and is dispersed among gallbladder debris (C). (Photo courtesy of Dr. Victoria Lashley)



Figures 10A, 10B, and 10C. Gallbladder, 2 hours (A) and 24 hours (B, C) post-inoculation, PAS staining for neutral mucin. Photomicrographs of sections of ovine gallbladder tissue after PAS staining for neutral mucin (light purple color). (A) The mucosal surface and deep crypts are lined with marked amounts of neutral mucin at 2 hours post-inoculation. By 24 hours post-inoculation, neutral mucin staining is still marked within the cells and lumen of the deep crypts (B), but is also seen to extend throughout the gland lumen space and is dispersed among gallbladder debris (C). (Photo courtesy of Dr. Victoria Lashley)



Figures 11A and 11B. Gallbladder, 2 hours (A) and 24 hours (B) post-inoculation, lectin staining for L-fucose containing glycans. Photomicrographs of sections of ovine gallbladder tissue after lectin staining for L-fucose (deep brown color). (A) The mucosal surface and deep crypts are lined with marked amounts of L-fucose at 2 hours post-inoculation. By 24 hours post-inoculation (B), L-fucose staining is still present within glands and debris in remnant gallbladder mucosa. (Photos courtesy of Dr. Victoria Lashley)

CHAPTER 3

THE TRANSCRIPTOME OF *CAMPYLOBACTER JEJUNI* SHEEP ABORTION CLONE
IA 3902 FOLLOWING *IN VIVO* EXPOSURE TO THE OVINE GALLBLADDER**Abstract**

Colonization of the gallbladder by enteric pathogens such as *Salmonella typhi*, *Listeria monocytogenes*, and *Campylobacter jejuni* is thought to play a key role in transmission and persistence of these important zoonotic agents; however, little is known about the molecular mechanisms that allow for bacterial survival within this harsh environment. The recent emergence of a highly virulent *C. jejuni* sheep abortion clone, which is represented by the clinical isolate IA 3902, as the dominant cause for sheep abortion in the United States, combined with its ability to cause gastroenteritis in humans, make further understanding of the molecular mechanisms that allow for colonization and virulence of this particular strain especially important. To begin to understand the molecular mechanisms associated with survival in the host gallbladder, *C. jejuni* IA 3902 was exposed for up to 24 hours to both the natural ovine host *in vivo* gallbladder environment, as well as ovine bile *in vitro*. Following exposure, total RNA was isolated from the bile and high throughput deep sequencing of strand specific rRNA-depleted total RNA was used to characterize the transcriptome of IA 3902 under these conditions. Our results demonstrated for the first time the complete transcriptome of *C. jejuni* IA 3902 during exposure to an important host environment, the sheep gallbladder. Exposure to the host environment as compared to *in vitro* bile alone provided a more robust picture of the complexity of gene regulation required for survival in the host gallbladder. A subset of genes including a large number of protein

coding genes as well as seven previously identified non-coding RNAs were confirmed to be differentially expressed within our data, suggesting that they may play a key role in adaptation upon exposure to these conditions. This research provides valuable insights into the molecular mechanisms that may be utilized by *C. jejuni* IA 3902 to induce disease and develop a carrier state within the inhospitable gallbladder environment.

Introduction

Campylobacter jejuni is now the leading cause of ovine campylobacteriosis in the United States, recently surpassing *C. fetus* subsp. *fetus* as the primary causative agent of bacterial abortion (Kirkbride, 1993; DeLong, 1996). This change has been driven by the rapid emergence of a highly virulent sheep abortion (SA) clone that harbors chromosomally encoded tetracycline resistance (Sahin *et al.*, 2008). Outbreaks of zoonotic transmission to humans related to raw milk consumption have been reported (Sahin *et al.*, 2012), highlighting the need for greater understanding of the mechanisms utilized by this highly virulent strain of *C. jejuni* to both cause disease and persist in animal hosts.

Chronic colonization and shedding of organisms into the environment is thought to play a key role in maintenance of *C. jejuni* in the sheep population. Abattoir studies of sheep and other ruminants have shown that the gallbladder is frequently positive for *C. jejuni* even in the absence of clinical disease (Ertas *et al.*, 2003; Acik and Cetinkaya, 2006; Sahin *et al.*, 2012). In order to decrease colonization and chronic shedding with *C. jejuni* in animal reservoirs, there is a critical need to understand the mechanisms utilized by this organism to colonize and survive in this harsh environment. In Chapter 2, we demonstrated that survival within the gallbladder mucous layer and deep glands may serve as a critical nidus for chronic

infection or shedding of *C. jejuni* into the environment. Additional work is necessary to determine the molecular mechanisms that allow *C. jejuni* to survive exposure to bile and establish colonization of the gallbladder mucosa.

Although multiple *in vitro* studies have shown expression of key virulence factors in the presence of bile salts (Gaynor *et al.*, 2001; Lin *et al.*, 2003; Lin *et al.*, 2005a; Raphael *et al.*, 2005; Fox *et al.*, 2007; Malik-Kale *et al.*, 2008; Dzieciol *et al.*, 2011), the levels assessed in these studies were equivalent to intestinal not gallbladder conditions. Little is known about how *Campylobacter* adapts to the harsh environment of the gallbladder; however, the ability to survive in bile is likely critical to their survival and colonization of the rest of the gastrointestinal tract as well (Gunn, 2000). In addition to a basic lack of studies replicating gallbladder bile exposure *in vitro*, the use of *in vitro* studies alone does not fully capture the intricacies of the *in vivo* gallbladder environment, nor the ongoing interaction between host and bacteria that is likely to be encountered.

Only three studies to date have been published assessing the *in vivo* transcriptome of *C. jejuni* under exposure to any host environment; two of the three utilized microarray technology to assess transcriptional changes, and both determined that there are marked differences in gene expression profiles between *in vivo* and *in vitro* samples (Stintzi *et al.*, 2005; Woodall *et al.*, 2005). While microarray studies have been very useful in beginning to understand gene expression and regulation, they are limited in that they can only identify changes in known genes. The third *in vivo* *Campylobacter* transcriptome study published to date utilized the emerging technology of high throughput RNA sequencing (RNAseq) to assess the *in vivo* transcriptome of *C. jejuni* during colonization of the chick intestinal tract and was able to demonstrate differential expression of both protein coding genes as well as

identify numerous putative regulatory RNAs (Taveirne *et al.*, 2013). The rapid advancement of high throughput deep sequencing technologies along with the ability to assess the entire transcriptome without prior knowledge of genome structure has allowed RNAseq to become the new method of choice for studying global gene expression (Croucher and Thomson, 2010; van Vliet, 2010; van Opijnen and Camilli, 2013). The power of global transcriptome studies utilizing the RNAseq approach to rapidly increase the knowledge base related to a particular area of interest is immense, and also is currently the method of choice for identification of the novel class of gene expression regulators, small non-coding RNAs (ncRNA, sRNA) (Sharma and Vogel, 2009). Using RNAseq technology, a large number of previously unknown non-coding RNAs have already recently been identified in other strains of *C. jejuni* (Chaudhuri *et al.*, 2011; Butcher and Stintzi, 2013; Dugar *et al.*, 2013; Porcelli *et al.*, 2013; Taveirne *et al.*, 2013); thus far the small RNA repertoire of sheep abortion clone IA 3902 remains uncharacterized.

The overall goal of this study was to utilize RNA sequencing technology to study the transcriptome of *C. jejuni* IA 3902 following exposure to both the *in vivo* gallbladder of a natural host species (sheep) as well as ovine bile alone *in vitro*. We reasoned that assessing exposure to both bile *in vitro* and the sheep gallbladder *in vivo* would enable the most complete assessment of the complex gene expression and regulatory networks necessary for survival within the host gallbladder environment provided to date, however, we hypothesized that by utilizing the *in vivo* host environment we would be able to identify an increased number of candidate genes required for survival in the gallbladder environment when compared to utilization of an *in vitro* model of bile alone. In addition, we hypothesized that the newly identified class of regulators, non-coding RNAs, could be identified utilizing this

same approach and would be observed to play an important role in survival within the host gallbladder. By utilizing strand-specific total RNA sequencing on the Illumina HiSeq platform, we were able to identify 434 protein coding genes to be upregulated and as well as 102 downregulated in the *in vivo* host environment following 24 hours of exposure. In addition, 89 known and putative non-coding RNA genes were observed to be upregulated with 12 downregulated under the same conditions. The number of genes identified in the *in vivo* host environment was demonstrated to be almost twice the number identified at the same time points *in vitro*. Overall, we identified for the first time expression patterns and potential regulatory mechanisms utilized by a highly virulent strain of *C. jejuni*, IA 3902, to survive within the harsh gallbladder environment which potentially serves as a chronic nidus of infection for spread of disease between animals and humans.

Materials and Methods

Bacterial strains and culture conditions

A clinical isolate of the *C. jejuni* SA (sheep abortion) clone, IA 3902, was utilized for the entirety of this study. This isolate was obtained from a sheep abortion outbreak in Iowa in 2006 (Sahin *et al.*, 2008) and clonal isolates of this strain have been identified from within the gallbladder of sheep in abattoir studies (Sahin *et al.*, 2012). *C. jejuni* IA 3902 was routinely grown in Mueller-Hinton (MH) broth or agar plates (Becton-Dickinson, Franklin Lakes, NJ) at 42°C under microaerophilic conditions with the use of compressed gas (55% O₂, 10% CO₂, 85% N₂). Specific culture conditions utilized during individual experiments to prepare animal and bile inoculums are described below, while culture of *C. jejuni* from bile and gallbladder mucosal scrapings are described in Chapter 2.

For preparation of the *in vivo* animal inoculum, 10 plates each containing 16 hours of overnight lawn growth were washed with 1 mL MH broth and collected into single sterile 50 mL conical tubes (FisherScientific, Pittsburg, PA). The volume of broth in each vial was then standardized to 10 mL and gently mixed to ensure even distribution of bacteria within the solution. Following pooling and gentle mixing of the cultures, 500 μ L of the collected culture was removed and processed immediately for RNA protection as described below. An additional 100 μ L was then removed for a dilution series to accurately determine the amount of inoculum in CFU/mL. The remaining inoculum was then centrifuged at 3000 x g for 5 minutes to pellet the cells and all but 1 mL of supernatant was removed. The remaining 1 mL of broth was then used to resuspend the cell pellet in each vial for a total inoculation volume of 1.5 mL per animal. The prepared inoculum was then placed under microaerophilic conditions and used within 3 hours of preparation.

For preparation of the inoculum for the *in vitro* bile study, two sets of 6 plates each containing overnight lawn growth were washed and collected into sterile 50 mL conical tubes as described above and standardized to 5 mL rather than 10 mL. From this 5 mL of concentrated culture, 500 μ L each was removed and processed immediately for RNA protection again as described below. The two sets of inoculum were then combined and an additional 100 μ L was removed for a dilution series to accurately determine the amount of inoculum in CFU/mL. The approximately 9 mL of remaining concentrated culture was then divided equally into four aliquots of 2.2 mL each and used directly for inoculation of the *in vitro* bile samples as described below.

***In vivo* exposure of *C. jejuni* IA 3902 to the sheep gallbladder environment**

All animal experiments were approved by the Iowa State University Institutional Animal Care and Use Committee (IACUC) prior to initiation and followed all appropriate animal care guidelines. Preliminary experiments utilizing one or two mixed breed female sheep obtained from local farms were performed to determine the best method to inoculate the gallbladder of sheep with *C. jejuni* and subsequently harvest enough viable bacteria for RNA isolation. Based on the results of this preliminary work which are more fully described in Chapter 2, a final determination of the necessity of full laparotomy with placement of a Hemoclip® (Weck, Research Triangle Park, NC) over the common bile duct was made, and thereafter all inoculations were performed via this method.

For the primary study, eight adult female mixed breed sheep were obtained from two local farms with no known history of *C. jejuni* related abortions. The sheep were randomly divided into two groups, either 2 hour or 24 hour incubation, via a random number generator (www.random.org) and were inoculated via full laparotomy with placement of a Hemoclip® as described in Chapter 2. At either 2 hours or 24 hours post-inoculation as previously determined via random assignment, the sheep were humanely euthanized via intravenous injection of 1 mL/10 lb body weight barbituates (Fatal Plus®; Vortech, Dearborn, MI). Immediately following euthanasia, a clean incision was made into the ventral midline of the abdomen to expose the liver and gallbladder. Using a 16 gauge 1” sterile needle and a 60 mL syringe, the entire amount of bile retained in the gallbladder was removed via gentle aspiration. The collected bile was then immediately processed for RNA protection and isolation as described below.

***In vitro* bile inoculation and incubation**

To compare the *in vivo* gallbladder environment to only bile exposure *in vitro*, fresh bile was collected from an additional group of eight sheep obtained from one of the same farms as above that were being utilized for an unrelated study. Again using a 16 gauge 1” sterile needle and a 60 mL syringe, the entire amount of bile retained in the gallbladder was removed via gentle aspiration. Following collection, the bile was cultured as described in Chapter 2 to determine if it was free of culturable bacteria. While awaiting culture results, the bile was stored at 4°C in sterile 50 mL conical tubes. Following confirmation of culture negative status, the entire collected amount of bile ranging in volume from 14 mL to 33 mL from four of the animals confirmed to be culture-negative was pre-warmed to ovine body temperature (39.5°C) in an incubator for 20 minutes and then inoculated with 10^{11} *C. jejuni* IA 3902 suspended in 2.2mL MH broth prepared as described in Chapter 2. Following inoculation, the bile was then incubated under microaerophilic conditions at 39.5°C in a static incubator. At 2 hours, half of the total amount of bile was removed for RNA protection and isolation as described below. The remaining bile was then incubated until 24 hours at which time it was also processed for RNA protection and isolation.

RNA extraction and DNase treatment

The bacterial inoculum samples that were set aside during preparation of animal and bile inoculums were processed immediately for RNA protection to maintain integrity of the RNA transcripts present. To minimize the number of replicates necessary for sequencing yet maintain a representation of all of the inoculums utilized, the inoculums for the *in vivo* experiment were pooled in sets of two (total of four sets of samples) to yield 1 mL each of

bacterial culture for processing. The 500 μ L of inoculum for the two samples collected from the *in vitro* bile were processed individually. The inoculum samples were then centrifuged at 8000 x g for 2 minutes immediately following collection to rapidly pellet the cells while minimizing the time elapsed between collection and introduction of an RNA protection solution. Following pelleting of the cells, the supernatant was decanted and 1 mL QIAzol Lysis Reagent (QIAGEN, Germantown, MD) was added to the cultures to quench further RNA production and protect the RNA present from degradation. To resuspend the pellet, the mixture was then pipetted up and down and vortexed at high speed for 1 minute. Following vortexing, the QIAzol-culture mixture was incubated at room temperature for 5 minutes. QIAzol-protected cultures were then stored at -80°C for up to two months prior to proceeding with total RNA isolation.

For the bile samples inoculated with *C. jejuni* IA 3902, immediately following collection from either the *in vivo* gallbladder or from the samples incubating *in vitro*, the bile was transferred into 15 mL conical tubes (FisherScientific) with no more than 7 mL bile per tube. The tubes were then centrifuged at 8000 x g for 2 minutes to rapidly pellet the cells while minimizing the time elapsed between collection and introduction of an RNA protection solution. The bile supernatant was then decanted and the size of the pellet obtained used to determine the amount of QIAzol Lysis Reagent to add to the tube for RNA protection. For concentrated bile samples (less than 10 mL total recovered bile), 1 mL of QIAzol Lysis reagent was added to the cell pellet per 1.5 mL of the starting bile amount. For dilute bile samples (greater than 10 mL total recovered bile), 1 mL QIAzol was added per 3mL of the starting bile amount. The samples were then processed identically to the description above for the inoculums and stored at -80°C for up to two months prior to proceeding with total RNA isolation.

Total RNA isolation was performed using the miRNeasy Mini Kit (QIAGEN) according to the manufacturer's instructions to isolate total RNA >18 nt. One column was used per 1 mL of

QIAzol utilized for RNA stabilization. On-column DNase treatment was performed using the RNase-free DNase set (QIAGEN). 10µg of extracted RNA was further treated with the TURBO DNA-free kit (Life Technologies, Carlsbad, CA) following RNA isolation to remove any residual DNA contamination. The total RNA was then purified using the RNeasy MinElute Cleanup kit (QIAGEN) with the following modifications as recommended by QIAGEN Technical Services to retain total RNA, including RNA <200nt in length. No more than 50 µL of RNA sample was utilized to enter the RNeasy MinElute Cleanup protocol at a time; to the RNA sample, 350 µL of Buffer RLT was added, followed by 600 µL of 100% ethanol. The RNA-RLT-ethanol mixture then proceeded with the standard bind/wash/elute steps of the protocol as provided by the manufacturer.

RNA concentration was measured using the NanoDrop ND-1000 spectrophotometer (ThermoScientific, Wilmington, DE) and Qubit RNA BR Assay (ThermoFisher Scientific, Waltham, MA) and RNA quality was measured using the Agilent 2100 Bioanalyzer RNA 6000 Nano kit (Agilent Technologies, Santa Clara, CA). Verification of complete removal of any contaminating DNA was performed via PCR amplification of a portion of the CjSA_1356 gene, which is part of the capsule locus and has previously been determined via comparative genomics to only be present in *C. jejuni* IA 3902, using primers SA1356F and SA1356R (Luo *et al.*, 2012). A single 24 hour *in vivo* sample failed to isolate any RNA following extraction and purification; therefore, it did not continue with the rest of the library preparation.

RNAseq library preparation and sequencing

For the preliminary RNA sequencing, the total RNA isolation was performed as described above except the RNeasy MinElute Cleanup step was omitted. Depletion of rRNA was performed on 5 µg each of gallbladder exposed and plate growth RNA using the Ribo-

Zero rRNA Removal Kit for Gram Negative Bacteria (Epicentre, Madison, WI) according to the manufacturer's instructions. A portion of RNA from each of the same samples was reserved and was not treated for rRNA removal. Following rRNA removal, rRNA removal efficiency was analyzed via the Agilent 2100 Bioanalyzer RNA 6000 Pico kit (Agilent Technologies). RNA samples, both Ribo-Zero treated and non-Ribo-Zero treated, were then submitted to the Iowa State University DNA Facility for library preparation. Each of the samples submitted was then subjected to two separate library preparation methods. Strand-specific cDNA libraries of both Ribo-Zero treated and non-treated total RNA from the *in vivo* and plate grown samples were generated using the ScriptSeq mRNA-seq Library prep kit (Epicentre) according to manufacturer's instructions. In addition, non-strand specific cDNA libraries of both Ribo-Zero treated and non-treated total RNA from the *in vivo* and plate grown samples were generated using the TruSeq RNA Sample Preparation Kit (Illumina, San Diego, CA). All samples were barcoded using standard Illumina barcodes. The samples were then sequenced on a 100-cycle single lane of the Illumina HiSeq 2000.

For the full scale project, analysis of the *in vivo* collected RNA samples via the Agilent Bioanalyzer suggested that some samples likely contained host (ovine) RNA along with bacterial RNA; therefore, an rRNA removal kit suited to removal of both eukaryotic and prokaryotic rRNA was chosen for preparation of the RNAseq library. 2.5 µg of confirmed DNA-free total RNA was treated with Ribo-Zero Magnetic Gold rRNA Removal Kit (Epicentre) according to the manufacturer's instructions (Epicentre). Following rRNA removal, the rRNA depleted total RNA was again purified using the RNeasy MinElute Cleanup kit using the same modifications as described above. Following clean-up, the RNA was eluted into 12 µl of sterile RNase-free water; quality, quantity, and rRNA removal

efficiency was then analyzed via the Agilent 2100 Bioanalyzer RNA 6000 Pico kit (Agilent Technologies).

Library preparation for sequencing on the Illumina HiSeq platform was completed using the TruSeq stranded mRNA HT library preparation kit (Illumina) with some modifications. As this kit was designed for use with eukaryotic RNA with poly-A tails, the initial poly-A RNA purification step was omitted. To enter the protocol, 5 μ l of the rRNA-depleted RNA totaling approximately 200 ng was added to 13 μ l of the “Fragment, Prime, Finish” mix. The remainder of the library preparation was carried out according to the manufacturer’s instructions and all 24 samples were barcoded using the high-throughput (HT) 96-well RNA Adapter Plate (RAP) as supplied by the manufacturer. Following enrichment of the cDNA fragments, the quality of the cDNA was validated using the Agilent 2100 Bioanalyzer DNA 1000 kit (Agilent Technologies) and quantity was determined via the Qubit dsDNA BR Assay (ThermoFisher Scientific). Following library validation, the indexed cDNA samples were submitted to the Iowa State University DNA Facility where they were normalized and pooled according to the manufacturer’s instructions. The pooled library was then sequenced on an Illumina HiSeq 2500 machine in high-output single read mode with 100 cycles.

Differential gene expression analysis of RNAseq data

For the preliminary RNAseq experiment only, data analysis was performed by Dr. Andrew Severin of the Iowa State University Genome Informatics Facility. Differential gene expression between the *in vivo* gallbladder exposed and plate grown control samples was initially assessed via QuasiSeq using upper quartile normalization (Lund *et al.*, 2012; Smyth,

2004). Following analysis, a change in gene expression was deemed significant when the Q-value (false discovery rate) was below 5% and a >1.5 fold change in expression levels was present. Once the Rockhopper method of differential gene expression described below was available, this original data was also reanalyzed using the newer method as well.

For the primary study, to analyze the differences in gene expression between the plate grown inoculum, *in vivo* gallbladder, and *in vitro* bile exposed strains *C. jejuni* IA 3902 at various time points, Rockhopper (<http://cs.wellesley.edu/~btjaden/Rockhopper/>), a freely available RNAseq analysis platform, was utilized as previously described using the standard settings of the program (McClure *et al.*, 2013). Using this program, results of gene expression are normalized and reported by the program as expression of genes using reads per kilobase per million reads (RPKM), except that instead of dividing by the total number of reads, Rockhopper divides by the upper quartile of gene expression.

Following computational analysis via Rockhopper, a change in gene expression was deemed significant when the Q-value (false discovery rate) was below 5% and a >1.5 fold change in expression levels was present. If in any condition being compared the expression level (RPKM) was “0”, it was changed to “1” to allow for statistical analysis to be performed. Any significant changes in 16S or 23S rRNA genes were ignored as these were determined to be due to differences in efficiency of rRNA removal by Ribo-Zero and not inherent differences between strains and conditions. Read count data was visually assessed using the Integrated Genome Viewer (IGV) (<https://www.broadinstitute.org/igv/>) (Robinson *et al.*, 2011; Thorvaldsdóttir *et al.*, 2013). Differentially expressed genes were then assessed for function using the Clusters of Orthologous Groups (COG) (Galperin *et al.*, 2015) as previously described in IA 3902 (Wu *et al.*, 2013). Venn diagrams depicting overlap of genes

differentially regulated in multiple conditions were generated using the Venny website (<http://bioinfogp.cnb.csic.es/tools/venny/index.html>) (Oliveros, 2007-2105). Metabolic pathway analysis was performed using the Kegg Pathways when appropriate (<http://www.genome.jp/kegg/pathway.html>) (Kanehisa *et al.*, 2015).

Validation of gene expression observed in RNAseq data with NanoString

To validate the results of the gene expression and antisense expression data generated in the preliminary RNAseq experiment, NanoString nCounter technology (Fortina and Surrey, 2008; Geiss *et al.*, 2008) was utilized similar to previous reports in bacteria to validate sense and antisense transcription following RNAseq experiments (Passalacqua *et al.*, 2012). Briefly, a portion of the same RNA samples that were utilized for the preliminary Illumina sequencing along with other samples of interest previously generated within our lab were sent to NanoString at a concentration of 100 ng/μl. Strand specific probes of 100 bp in length were designed by NanoString to target genes, putative small RNAs, and areas of antisense transcription of interest identified in the RNAseq study, as well as known housekeeping genes (*gyrA*, *lpxC*, *rrsA/rrsB/rrsC*, and *thiC*) for normalization control. Twelve genes were selected to have probes designed to detect both sense and antisense transcripts; nine of these were observed to have high levels of antisense transcription in the RNAseq experiment, while three were observed to have minimal antisense transcription observed via RNAseq. Two intergenic regions that demonstrated reads suggestive of the presence of a non-coding RNA were selected to have probes designed for those regions. Three technical replicates were run on each sample submitted. To analyze the results, raw counts were adjusted using the geometric mean of the reference genes present in the codeset; the positive

control probe normalization factors for all assays were within the range of 0.3-3, indicating minimal inter-assay technical variation. Reference gene normalization factors were also within the recommended range of 0.1-10, indicating very reproducible mRNA input between samples. The average background signal was then calculated for each sample, and this was subtracted from the experimental data to remove background noise. Following background normalization, the average of the three technical replicates was taken to result in an average signal for each area of interest.

Results

Preliminary animal studies, RNA sequencing, and NanoString validation

Preliminary experiments utilizing one or two mixed breed female sheep obtained from local farms were performed to determine the best method to inoculate the gallbladder of sheep with *C. jejuni* and subsequently harvest enough viable bacteria for RNA isolation. A full laparotomy with placement of a Hemoclip[®] over the common bile duct to prevent secretion of bile into the intestinal tract finally yielded adequate numbers of viable bacteria recovered for isolation of RNA of sufficient quality for next generation sequencing. Based on the results of this preliminary work, a final determination of the necessity of full laparotomy with placement of a Hemoclip[®] over the common bile duct was made, and thereafter all inoculations were performed via this method.

A preliminary Illumina sequencing run was made based on the RNA collected from this first animal to validate that quality data could be achieved using the proposed RNA isolation methods and to assess for the necessity of Ribo-Zero rRNA removal and strand specific libraries. **Table 1a** and **1b** shows the results of this preliminary RNAseq run which

confirmed that Ribo-Zero depletion with strand specific library preparation yielded high quality data for further analysis. Early analysis using QuasiSeq to determine differentially expressed genes predicted 361 upregulated and 108 downregulated genes following 2 hour incubation in the gallbladder (data not shown). Included in the list of upregulated genes were *cmeB* and *cmeDEF*, all of which have been previously identified as being important in bile tolerance (Lin *et al.*, 2003; Lin *et al.*, 2005a). Additional analysis for non-coding RNAs and antisense RNA revealed multiple areas of interest for putative non-coding RNAs, as well as significant amounts of antisense transcription genome-wide (data not shown). Reanalysis of the same data using Rockhopper yielded minimal identification of differentially expressed genes (12 protein coding genes and 7 non-coding RNAs predicted downregulated; 3 protein coding genes and 1 non-coding RNA predicted upregulated) likely due to a lack of replicate data. Of particular interest, however, a previously identified small RNA, CjNC110 (Dugar *et al.*, 2013), was noted to exhibit a substantial difference in expression between the bile and control condition when analyzed via both QuasiSeq and Rockhopper (**Figure 1**).

NanoString nCounter technology was utilized to valid the gene expression data observed in the preliminary experiment for a select number of genes either demonstrated as differentially expressed in the preliminary data or previously suggested to play a role in survival in exposure to bile. **Table 2** demonstrates a comparison of the calculated fold change for these genes using both the NanoString and RNAseq data. While the exact levels of expression are not identical, the NanoString data confirms the direction of change present following exposure of *C. jejuni* to the host gallbladder environment in six of the seven genes assessed.

As a number of genes were observed to demonstrate significant antisense transcription in the dataset, NanoString probes designed to target antisense regions of the coding ORF as well as the coding strand itself were designed for 12 genes in an effort to determine if the antisense transcripts were real or an artificial byproduct of the library preparation process (**Table 3**). For six of the nine genes observed to have high antisense transcription in the RNAseq data, some level of antisense transcription was also observed via NanoString in the plate grown sample. Interestingly, for five of those six genes, antisense transcription was observed to be negligible in the gallbladder exposed sample; for the other gene, the presence of antisense transcription was noted to increase in the gallbladder environment. For the remaining three genes observed to have high levels of antisense transcription via RNAseq, no transcripts could be detected in the same region using NanoString under either condition. Interestingly, the *rnpB* gene was noted to exhibit extremely high levels of transcription only antisense to the annotated gene. Further analysis of this region of the genome for IA 3902 when compared to other annotated strains of *C. jejuni* indicated that the *rnpB* gene was annotated on the opposite (incorrect) strand for IA 3902 as compared to all other sequenced strains of this species (Dugar *et al.*, 2013) which explains the observed flipped levels of transcription. For the three genes observed to have low levels of antisense transcripts present in the RNAseq data, all three were noted to have negligible antisense transcripts present for the plate grown samples, however, some level of antisense transcripts were noted in two of the three the gallbladder exposed samples.

Summary of Illumina RNAseq results from primary study

Overall, 21 barcoded libraries were sequenced in a single lane on the Illumina HiSeq 2500 yielding over 74 million reads, with close to 67 million high quality reads aligning to either the genome or pVir plasmid of *C. jejuni* IA 3902 and averaging 3,176,824 reads per library (**Tables 4A** and **4B**). The majority of reads (average of 72% of total reads), mapped to protein coding genes of the chromosome, with an average of 20% of reads mapping to ribosomal RNA following rRNA depletion with Ribo-Zero (median of 15%). Only four of the 21 libraries contained less than or equal to 5% ribosomal RNA reads, which would be consistent with the manufacturer's predicted rRNA removal efficiency. The majority of the libraries (14 of 21) did not exhibit efficient rRNA removal (>10% rRNA reads) with one library completely failing to exhibit rRNA removal at all (93% of reads mapped to rRNA genes); the reason for this is unclear. An average of 1% of reads mapped to antisense regions of the annotated protein coding genome on both the chromosome and pVir plasmid. On the pVir plasmid, 91% of reads mapped to protein coding genes, while an average of 8% of reads were to unannotated regions.

Differential gene expression analysis of RNAseq data

Rockhopper was utilized for analysis of differential gene expression between the *in vivo* and *in vitro* bile samples, IA 3902 plate growth for inoculum, and 2 and 24 hour time points. A summary of the differences in numbers of genes with increased and decreased expression under either *in vivo* or *in vitro* bile exposure when compared to unexposed IA 3902 is given in **Table 5**. Overall, the *in vivo* samples consistently identified a larger number of genes when compared to the same time point *in vitro*. In addition, a larger number of

genes were identified at the 24 hour time point when compared to 2 hours both *in vivo* and *in vitro*. The *in vivo* sheep gallbladder exposed samples at 24 hours yielded the most differentially expressed genes of all the conditions and time points, therefore, **Table 6A** (down regulated) and **6B** (up regulated) lists all of the genes differentially expressed with annotation to indicate which genes are part of multi-gene operons. Overall, 86 operons of the 363 predicted by Rockhopper to exist on both the IA 3902 chromosome (350) and pVir plasmid (13) demonstrated at least 2 consecutive genes differentially upregulated, with 21 of those exhibiting changes in all of the genes predicted in the operon. Conversely, 21 of the 363 predicted operons (19 chromosome, 3 pVir) were demonstrated to have at least 2 consecutive genes downregulated, with 9 of those exhibiting changes in all of the genes predicted in that operon. **Supplementary Tables S1, S2, and S3** list all of the genes that were determined to be differentially expressed when compared to the unexposed IA 3902 inoculum for each of the other *in vivo* and *in vitro* conditions and time points.

To estimate the functional categories of genes affected by each condition and time point, the COG function for each gene was mapped and the totals compiled for each condition and time point; these totals were then compared to the total number of possible genes within each category in *C. jejuni* IA 3902 and the percentage of possible genes differentially expressed was then utilized to assessed for trends in the data (**Figures 2A, 2B, 2C, and 2D**). For all conditions and time points studied, the “cell motility” category demonstrated either the highest or second highest percentage of total genes upregulated. “Secondary metabolites biosynthesis, transport and catabolism” was also one of the highest categories consistently upregulated under all conditions, and “intracellular trafficking and secretion” was also highly upregulated on a percentage basis. While not noted to be within

the top categories on a percentage basis, “cell wall/membrane biogenesis” was consistently noted to be the top category represented in all conditions and time points based on total number of genes upregulated rather than percentage. In contrast, the categories observed to have the highest percentage decreased in all comparisons and time points were “signal transduction mechanisms” and “amino acid transport and metabolism.” In the *in vivo* conditions only, “energy production and conversion” was observed to be one of the top categories decreased at both time points. Based on total number of genes downregulated rather than percentage, “energy production and conversion” was again the highest category for both *in vivo* conditions, while “amino acid transport and metabolism” was consistently the highest category decreased for both *in vitro* conditions.

To compare the upregulated annotated genes that were identified for all four conditions with the unexposed IA 3902 inoculum, a Venn diagram was constructed to allow for visual comparisons (**Figure 3**). A total of 67 known genes were found to be upregulated in all 4 conditions, suggesting that these genes are required for survival following exposure to bile (**Table 7**). An additional 125 genes were identified that were upregulated in 3 of the 4 conditions; the likelihood that these genes are also important to the response to bile is high. **Table 8** demonstrates the 77 genes that were identified to be only upregulated in both *in vivo* conditions, suggestive of a role related to sensing of and interaction with the host environment unique from just exposure to bile. Conversely, a total of 10 genes (**Table 9**) were observed to be downregulated in all 4 conditions when compared to unexposed IA 3902 again utilizing a Venn diagram for visual comparison (**Figure 4**), with an additional 23 genes observed to be downregulated in 3 of the 4 conditions.

Table 10 demonstrates a summary of the number of genes found to be differentially expressed when the 2 hour and 24 hour time points for each condition were compared. Again, a greater number of genes were observed to be increased at the 24 hour time point as opposed to the 2 hour time point *in vivo*, suggesting continued evolution of the response to changes in the host environment over time. In contrast, very few genes were observed to be substantially different between the 2 and 24 hour time points *in vitro*. As the *in vitro* environment was static between the time points, it appears reasonable to suggest that little further adaptation was necessary between 2 and 24 hours for survival within bile alone.

Identification of differentially expressed putative non-coding RNAs

The Rockhopper program was utilized to parse the data from the primary experiment and construct a list of predicted novel non-coding RNAs that may play a role in survival of *C. jejuni* within the sheep gallbladder. A total of 91 potential non-coding RNA were predicted by the program, with 27 of the predictions indicating an antisense RNA, and the other 64 predictions being small RNAs primarily located within intergenic regions. Differential expression of these predicted non-coding RNAs was performed identically to the known annotated genes by the Rockhopper program and the results are included in the previously described supplementary tables (S1-S3) as well as Table 6. **Figures 5A and 5B** demonstrates a Venn diagram which allows visual comparison of all of the putative non-coding RNAs that were identified for all four conditions when compared to unexposed IA 3902. A total of 26 predicted non-coding RNAs were found to be upregulated in all 4 conditions, as well as 3 noted to be downregulated in all conditions. These lists were then manually curated and the reads viewed via IGV and compared with the list of known genes

highly up and down regulated in the dataset. Many of these non-coding RNAs appear to be located in either the 5' UTR or within intergenic regions of operons that were already determined to be either up or downregulated with the exception of one intergenic region, thus it is unlikely that the majority of them are truly unique non-coding RNAs (**Supplemental Table S4**).

Manual examination of the entire list of non-coding RNAs did identify several previously validated non-coding RNAs (Dugar *et al.*, 2013) as present and differentially regulated in our dataset; these are listed in **Table 11A** along with their differential expression between conditions in **Table 11B**. The CjNC110 small RNA previously identified within the preliminary dataset as differentially expressed in the gallbladder at 2 hours was not identified by Rockhopper in this study; therefore, a comparison of differential expression levels could not be made. Manual examination of the region via IGV did demonstrate reads aligning to this region, however, the level of expression was low in all conditions which likely explains why Rockhopper failed to identify it in this dataset. Additionally, the locations of the previously identified CjNC10, CjNC170, CjNC190, CjNC200 and tracrRNA, as well as reads antisense to CjSA_0158 (CJas_0168c), CjSA_0336 (CJas_0363c), CjSA_0668 (CJas_0704) (Dugar *et al.*, 2013), which were predicted to exist in IA 3902, all appeared to have expression in the same or similar location as these small RNAs, however, Rockhopper failed to identify them as well, also likely due to lower levels of expression.

Discussion

The rapid advancement of high throughput deep sequencing technologies along with the ability to assess the entire transcriptome without prior knowledge of genome structure

have allowed RNA sequencing (RNAseq) to become the new method of choice for studying gene expression (Croucher *et al.*, 2010; van Vliet, 2010; van Opijnen and Camilli, 2013). With the rapid increase in the quality of RNASeq data over the past several years and the use of replicates, this next-generation sequencing approach will likely soon be thought of to have the same reliability as RT-PCR experiments, the current gold standard for gene expression evaluation (de Sa *et al.*, 2015). While RT-PCR can only be utilized to assess gene expression one gene at a time, the power of global transcriptome studies utilizing the RNAseq approach to rapidly increase the knowledge base related to a particular area of interest is immense, and also is currently the method of choice for identification of the novel class of gene expression regulators, small non-coding RNAs (ncRNA, sRNA) (Sharma and Vogel, 2009). Using RNAseq technology, a large number of previously unknown non-coding RNAs have already recently been identified in other strains of *C. jejuni* (Chaudhuri *et al.*, 2011; Butcher and Stintzi, 2013; Dugar *et al.*, 2013; Porcelli *et al.*, 2013; Taveirne *et al.*, 2013;). The data generated in our study represents the first report of the small RNA repertoire of the emergent and highly virulent *C. jejuni* sheep abortion clone IA 3902.

Overall, the dataset that was generated from this study provides a very robust assessment of the global transcriptome of *C. jejuni* within an important host environment. The method of RNA isolation utilized was able to maintain high quality total RNA despite the challenges associated with RNA extraction from bile. The use of strand-specific RNA sequencing on the Illumina HiSeq platform following rRNA depletion using Ribo-Zero yielded adequate numbers of high quality reads that successfully aligned to the genome of IA 3902 albeit with a higher than anticipated number of reads mapping to the rRNA genes. The rRNA depletion kit utilized, Ribo-Zero Magnetic Gold rRNA Removal Kit (Epidemiology),

is specifically designed for use with eukaryotic (human/mouse/rat) and prokaryotic (gram positive and negative bacteria) mixed samples as would be encountered during *in vivo* experiments. This kit was chosen due to visual evidence of potential eukaryotic RNA presence observed in the RNA samples post-isolation, however, the drawback to utilizing a mixed population epidemiology kit is that a decreased number of probes were likely present to target gram negative rRNA. As the majority of the rRNA was still likely gram negative bacterial in this case, it is likely that the binding capacity of those probes was exceeded and thus increased the amount of bacterial rRNA that remained in the sample despite the visual appearance of removal of all 16S and 23S rRNA via the Agilent Bioanalyzer. The overall percentage of reads that mapped to the *C. jejuni* genome was quite high, indicating that very little eukaryotic or other types of prokaryotic RNA were present in the samples. Only one sample failed to rRNA deplete, while an additional sample was observed to have a lower percentage of reads mapping to *C. jejuni* IA 3902. Analysis of differential gene expression via Rockhopper with and without the inclusion of these samples yielded minimal alterations in results; therefore it was elected to maintain the samples within the dataset. Despite the minor difficulties related to less than ideal rRNA depletion, the samples averaged over 3 million high quality mapped reads per sample. Previous studies undertaken to assess the necessary amount of reads per prokaryotic sample to generate statistically significant data indicate that when data from well-correlated biological replicates are utilized, 2-3 million reads per sample enables a significant number of genes differentially expressed to be identified with high statistical significance (Haas *et al.*, 2012).

While our differential expression dataset cannot be utilized to necessarily measure genes associated with growth of *C. jejuni* IA 3902 in bile or in the gallbladder as the amount

of bacteria inoculated into each condition was already higher than the concentration typically observed during *in vitro* growth under laboratory conditions, it did allow for identification of genes associated with survival in both bile and within the *in vivo* gallbladder of the natural ovine host. A requirement of a false discovery rate (Q value) of less than 0.05 along with a fold change of greater than 1.5 was utilized to narrow the list of proposed differentially regulated genes to a complete yet hopefully biologically relevant list. The fact that a large number of operons were observed to be differentially regulated in our data adds increased confidence that the results obtained are likely to be statistically sound and biologically relevant.

The presence of antisense transcripts within datasets such as this has garnered great debate and discussion over the past few years (Sharma *et al.*, 2010; Dugar *et al.*, 2013; Conway *et al.*, 2014). To determine if the antisense expression present in our preliminary data was real, we utilized the NanoString nCounter technology as previously described to validate antisense transcription data (Passalacqua *et al.*, 2012). Our results suggests that in some cases transcription antisense to annotated genes may be real and warrants further study, however, a portion of the observed antisense transcripts may be a spurious artifact of RNA library preparation. The observation that the overall number of reads mapping antisense to protein coding regions of the genome in the plate grown IA 3902 condition decreased from 4% in the preliminary dataset to an average of less than 1% in the primary study with all other methods held the same supports this claim and would suggest that it is highly likely that strand specificity of library preparation technology has improved over the 3 year span between the preparation of the separate libraries. In addition, the use of NanoString technology to demonstrate that antisense transcripts could only be validated in a portion of

the genes where expression was observed via RNAseq supports this claim. Further work to continue improve detection of true versus spurious antisense transcripts within bacterial transcriptomes is warranted.

To broadly assess the gene expression adaptations necessary for survival within both the *in vivo* and *in vitro* conditions, the COG function for each differentially expressed gene was mapped and the totals compiled for each condition and time point; these totals were then compared to the total number of possible genes within each COG category in *C. jejuni* IA 3902 and the percentage of possible genes differentially expressed was then utilized to assessed for trends in the data. For all conditions and time points studied, the “cell motility” category demonstrated either the highest or second highest percentage of total genes upregulated. As motility has previously been demonstrated to be a requirement for *in vivo* colonization and virulence (Guerry *et al.*, 2008), it seems reasonable that an increased production of genes associated with motility would be an important part of the response to the bile and gallbladder environments by *C. jejuni*. In addition, and as demonstrated in Chapter 2, it is highly likely that *C.jejuni* would seek out a location within the gallbladder such as the mucous layer and mucosal lining for chronic colonization. This behavior has already been described for *C. jejuni* in the small intestine (McSweegan and Walker, 1986; Shigematsu *et al.*, 1998), and to be able to achieve this requires effective motility. “Secondary metabolites biosynthesis, transport and catabolism” was also one of the highest categories consistently upregulated under all conditions, however, a closer look reveals that while on a percentage basis this category is highly represented, only a very small number of genes are listed under this COG code for *C. jejuni*, therefore they represent a small percentage of the actual genes differentially expressed; the same can also be said about the

“intracellular trafficking and secretion” category. While not noted to be within the top categories on a percentage basis, “cell wall/membrane biogenesis” was consistently noted to be the top category represented in all conditions and time points based on total number of genes upregulated rather than percentage. Based on the strong detergent properties of bile salts that have been shown to be highly antibacterial as well as able to induce cellular lysis (Coleman *et al.*, 1979; Begley *et al.*, 2005), rapid repair and turnover of cell wall and membrane components is likely to be a key part of survival by *C. jejuni* when exposed to high concentrations of bile salts such as in bile or in the gallbladder.

In contrast, the categories observed to have the highest percentage decreased in all comparisons and time points were “signal transduction mechanisms” and “amino acid transport and metabolism.” In the *in vivo* conditions only, “energy production and conversion” was observed to be one of the top categories decreased at both time points. On the surface, it appears counterintuitive that expression for these categories of genes be down regulated as it would be expected that there would be increased need for transmission of extracellular signals into the cell and increased amino acid turnover to provide for increased protein production. When assessed more closely, in all cases there were a similar number of genes also upregulated within the same categories, which suggests a shift in the specific pathways utilized for these cellular processes rather than an overall decrease in these processes. Based on total number of genes downregulated rather than percentage, “energy production and conversion” was the highest category for both *in vivo* conditions; again, closer examination revealed that a large number of genes within this category were also upregulated, suggesting a shift in pathways and not an overall decline in energy production.

Despite the importance of adaptation to bile exposure for all bacteria surviving within the gastrointestinal tract, very little published work has focused on the exact molecular mechanisms by which *Campylobacter* survives exposure to bile. Even those studies that have been performed frequently focused on the concentrations of bile salts typically found in the intestinal tract (i.e. – 1% w/v), not within the gallbladder itself (i.e. – 10% w/v). As presented in **Table 12**, only 14 genes have been specifically reported to be involved in the bile tolerance response in *Campylobacter*, 2 of which are not present in strain IA 3902. The efflux pumps *cmeABC* and *cmeDEF* are probably the most important genes to have previously been shown to play an important role in resistance of *Campylobacter* to bile salts *in vitro* (Lin *et al.*, 2002; Akiba *et al.*, 2006). The observation of universally increased expression of *cmeAB* and *cmeE* in all conditions exposed to bile in our study when compared to plate growth confirms that these genes, while not expressed at high levels, are likely critical to survival when exposed to bile. As *cmeC* and *cmeF* are the last genes transcribed in each of the operons, it is reasonable to suggest that some decrease in the amount of full length transcript produced may occur as transcription moves across the operon, thus the reason that the fold change for those genes was always observed to be less than the corresponding gene at the start of the operon and significance was not reached in all conditions. Bile salts (cholate and taurocholate) have previously been shown to induce expression of *cmeABC* *in vitro* in a time and dose dependent manner ranging from 6- to 16-fold increases in expression (Lin *et al.*, 2005a). A much lower magnitude of increase was observed when exposed to pure bile both *in vivo* and *in vitro* in our study. This suggests that the complexities of complete bile may blunt the response observed when only certain components such as bile salts are utilized under controlled settings. The expression of

cmeDEF has previously been noted to be intrinsically lower than *cmeABC*, and inactivation of *cmeF* has been demonstrated to increase expression levels of *cmeABC* (Akiba *et al.*, 2006). While overall expression levels for both operons were similar in our study, this suggests that the efflux pumps encoded by *cmeABC* and *cmeDEF* may work together to ensure the viability of *Campylobacter* under conditions of exposure to toxic substances such as bile.

Expression of *cmeABC* has also been previously shown to be under the control of the transcription repressor CmeR, with exposure to bile salts *in vitro* inhibiting binding of CmeR to the promoter of *cmeABC* and allowing for increased transcription of the *cmeABC* operon (Lin *et al.*, 2005b). Exposure to cholate *in vitro* in that same study did not demonstrate an increase in expression of the *cmeR* gene. In our study, mild increases in *cmeR* expression were observed that were only found to be statistically significant *in vitro* at 24 hours. Based on the previously described interaction of CmeR with bile salts, it is likely that these mild increases in expression have minimal biological effect on *cmeABC* expression as CmeR-mediated repression is likely to be inhibited under these conditions. The *cmeDEF* operon has been shown to be unaffected by CmeR repression (Akiba *et al.*, 2006).

The response regulator CbrR (*C*ampylobacter bile response regulator) has also been shown to be required for resistance to the effects of bile salts as mutants lacking it are unable to grow under sub-inhibitory concentrations of sodium deoxycholate (Raphael *et al.*, 2005). It is believed that CbrR is a response regulator that is part of a two-component regulatory system which typically also includes a sensor kinase. Minimal changes in expression of this gene were noted in our data, with only the *in vivo* 24 hour condition found to have a statistically significant increase in expression. Because of the proposed role as a response

regulator, it seems reasonable that while its presence is necessary for survival when exposed to bile, its expression level may not need to change for its function to be fulfilled. The signal mediated by this system is likely to lead to downstream changes in the expression of multiple genes, however, that may affect the ability of *Campylobacter* to respond to exposure to bile.

The secretory protein CiaB (*Campylobacter* invasion antigen B) has also been suggested to play a role in bile tolerance and has been demonstrated to be secreted upon co-cultivation of *C. jejuni* with intestinal cells and plays a role in the ability of *C. jejuni* to invade host cells (Konkel *et al.*, 1999). As synthesis and secretion of the CiaB protein have been demonstrated to be independent events, Rivera-Amill *et al.*, (2001) proposed that *C. jejuni* normally begins to synthesize the Cia proteins upon passage into the small intestine, accumulates them within the cell, and then secretes them upon contact with the host cells lining the gastrointestinal tract as a concentrated release may be necessary to evoke an effect on the host cells. Increased expression when exposed to the bile salt sodium deoxycholate *in vitro* was demonstrated via RT-PCR, which suggests that exposure to bile salts in the intestinal tract might normally be the trigger for increased expression (Rivera-Amill *et al.*, 2001). Interestingly, expression of *ciaB* was not demonstrated to be significantly altered in any of the conditions in our study. A tendency towards decreased expression was noted at 2 hours both *in vivo* and *in vitro*, with levels above non-exposed controls slightly increased at 24 hours in both conditions. There are several possibilities to explain these findings. It is possible that the response to the bile environment was rapid and thus not present by the time samples were taken at 2 hours, or occurred during the time between the 2 hour and 24 hour samples. Additional studies have shown that *ciaB* expression when exposed to deoxycholate was maximal at 12 hours and began to decline again by 15 hours (Malik-Kale *et al.*, 2008). It

is also possible that the higher levels of bile salts encountered in the gallbladder do not have the same effect as low concentrations such as what would be found in the intestinal tract. Finally, as these RNA samples were taken from bacteria free within the lumen of the gallbladder, and not intimately in contact with host cells, it is conceivable that direct contact with host cells may play a role in expression *in vivo*.

The last gene of interest to be previously described as important in the response of *Campylobacter* to exposure to bile is *flaA* (Alm *et al.*, 1993), which is responsible for production of the FlaA protein, one of two protein subunits that form the flagellar filament. It has been previously demonstrated through the use of reporter fusions that the σ^{28} promoter of *flaA* is upregulated when exposed to bovine bile, bile salts (deoxycholate), and L-fucose (Allen and Griffiths, 2001). In our study, expression of *flaA* was not shown to be statistically different under any of the conditions studied. This was an unexpected finding given the previous work done *in vitro*; however, as the *in vitro* work looked at very specific conditions and did not actually measure gene transcripts, only promoter activity, it is possible that exposure to a complex host environment renders a different response, or again, that the increased expression response was missed in the time points studied.

A few additional works have attempted to assess the response of *Campylobacter* to bile on a more global scale. Microarray analysis of RNA extracted from *C. jejuni* strain F3011 cultured with 0.1% deoxycholate for 12 hours allowed observation of a total of 156 upregulated and 46 downregulated genes under these conditions (Malik-Kale *et al.*, 2008). In addition to increased expression of the known bile-associated virulence genes *ciaB* and *cmeABC*, they also specifically identified increased expression of two additional virulence factors: *dccR*, which has been shown to be part of a two-component system regulatory

system that may play a role in the *in vivo* colonization ability of *C. jejuni* (MacKichan *et al.*, 2004), and *tlyA*, a hemolysin that has been shown to be important for *Helicobacter in vivo* colonization ability (Martino *et al.*, 2001). Expression levels of *tlyA* were minimal to non-existent in all conditions examined in our work; this may be related to differences between strains of *C. jejuni*. Expression of *dccR* was observed to be increased 1.4 fold at 24 hours under both *in vivo* and *in vitro* conditions; therefore it is possible that during the time period between 2 and 24 hours significantly increased expression may have occurred. In a separate study, Fox *et al.*, (2007) utilized protein expression following 18 hours of exposure to 2.5 to 5% oxbile added to rich media to identify 14 proteins with increased expression. Comparison of the proteins found to be increased to our work demonstrated no correlation with increased expression of the mRNA transcripts of those same exact proteins; however, some of the basic categories of upregulated genes were the same. While this previous work represents important information regarding exposure to differing levels of bile *in vitro*, it is possible that differences between the simplified *in vitro* environment and the complex *in vivo* environment presented in our study allowed for differing results. In addition, altered translation efficiency in the absence of increased presence of the mRNAs of the respective proteins may also play a role and lead to difficulty in comparing protein expression to transcriptomic data.

One of the biggest advantages and disadvantages of generating RNAseq transcriptomic data under multiple *in vivo* and *in vitro* conditions as we have demonstrated here is the sheer amount of data that is generated. Many other comparisons and conclusions can likely be drawn from this data and hopefully will be in the future; however, for the work presented here we have limited our analysis of the data to answering the original hypotheses of the study. As our focus was on what could be identified by utilizing a natural host *in vivo*

model, the gallbladder *in vivo* 24 hour time point was utilized for further data analysis to demonstrate important cellular pathways that are affected by exposure to the host environment.

Multiple genes responsible for chemotaxis were observed to be upregulated in the gallbladder condition only (**Figure 6**), including *cheY*, *cheR*, and a putative methyl-accepting chemotaxis protein (MCP) CjSA_0897. The CheA-CheY phosphor-relay pathway has previously been shown to act as the master switch to control taxis by altering the direction of flagellar rotation from a swimming phenotype (counter-clockwise rotation) to a tumbling phenotype (clockwise rotation) (Lertsethtakarn *et al.*, 2011). The *cheY* gene has also been shown to be required for adhesion and invasion (Yao *et al.*, 1997). CjSA_0897 is a putative methyl-accepting chemotaxis protein (MCP); MCPs have been shown to play an important role in sensing the environmental signals to activate the CheA-CheY system (Lacal *et al.*, 2010). As there would be minimal signals present in the *in vitro* environment from the host to direct chemotaxis nor host cells to adhere to or invade, it seems reasonable that these important genes would only be upregulated in the host environment where seeking out other host locations would be advantageous. Related to chemotaxis in the host environment, and based on our data presented in Chapter 2, we were surprised to find that the L-fucose permease, *fucP*, was not upregulated under any of the conditions in our data. As L-fucose staining was concentrated in areas intimately associated with the mucosal layer, and as the RNA for this study was collected from bacteria free within the gallbladder lumen or in bile alone, it is possible that the bacteria sampled had not yet encountered L-fucose in sufficient quantities to warrant upregulation of the genes related to its use as an energy source. The ability to seek out new environments relies heavily on cell motility, which was demonstrated

to be an overall area of increased gene expression in our data. **Figure 7** demonstrates genes upregulated in the Kegg pathway for flagellar assembly at 24 hours in the *in vivo* gallbladder environment. While *flaA* was not observed to be upregulated in our data, the increased expression of these additional flagella-associated genes suggests that increased flagellar assembly is occurring.

An additional finding of interest within the dataset is the upregulation of the twin arginine targeting (TAT) secretion system. Upregulation of *tatC* was demonstrated at 24 hours both in *in vivo* and *in vitro*, and *tatB* was upregulated in all but the *in vitro* 2 hour condition. The TAT secretion system is widely distributed across bacteria genera and has been demonstrated to consist of a cytoplasmic pore that uses proton motive force to transport folded proteins across the cytoplasmic membrane (Berks *et al.*, 2000). This system has been characterized in *C. jejuni* and is thought to play an important role in stress response and colonization (Rajashekara *et al.*, 2009). As the primary role for this system is to secrete proteins across the cytoplasmic membrane, we compared our dataset to the list of 14 predicted conserved proteins in *C. jejuni* generated by Rajashekara *et al.* (2009) with TAT targeting motifs; 6 of the 14 demonstrated increased expression under at least one condition, with 2 (NrfH and SdhA) exhibiting increased expression under all 4 conditions. The majority of the proteins predicted to contain a TAT motif are thought to be involved in cellular respiration, indicating an important role in generation of cellular energy.

The *sdhA* (CjSA_0409) and *sdhB* (CjSA_0410 and CjSA_0411) genes were originally annotated as part of a succinate dehydrogenase complex (Sdh), however, further work in *C. jejuni* determined that this was a misannotation and that the correct annotation of this operon was Mfr as it was demonstrated to actually encode a methylmenaquinol:fumarate

reductase (MfrABE) (Guccione *et al.*, 2010). Both MfrA and MfrB were demonstrated in that paper to be localized to the periplasm and upregulated under oxygen limiting conditions as would be experienced *in vivo*. Further work by Hitchcock *et al.* (2010) conclusively determined that the TAT secretion system is required for MfrA and MfrB localization to the periplasm, with MfrB being co-localized as it does not contain a TAT motif. Interestingly, *sdhB* (*mrfB*), was also demonstrated to be upregulated in all conditions examined within our study, suggesting that the function of the methylmenaquinol:fumarate reductase is critical to survival of *C. jejuni* within the bile environment.

The other potential TAT-secreted protein identified upregulated in all conditions was NrfH, a membrane bound cytochrome-c type protein which is the sole electron donor to the periplasmic nitrite reductase NrfA; the two proteins are believed to form a tight complex within the periplasmic space (Pittman *et al.*, 2007). Interestingly, *nrfA* was also demonstrated to be upregulated under all conditions examined in our study. NrfA has been shown to be the terminal enzyme in the reduction of nitrite to ammonia (Pittman and Kelly, 2005) and was demonstrated to play a key role in the resistance to reactive nitrogen species and nitric oxide (NO) in *C. jejuni* (Pittman *et al.*, 2007). Resistance to nitric oxide is thought to be a key feature of *C. jejuni* pathogenesis as NO production within the intestinal tract has been shown to be increased in human patients with *C. jejuni*-induced diarrhea (Enocksson *et al.*, 2004). While additional work by Hitchcock *et al.* (2010) suggests that NrfH is not in fact a TAT secreted protein, this does not lessen the fact that *nrfH* and *nrfA* appear to play an important role in survival following exposure to bile by *C. jejuni*.

An additional pathway in the area of energy generation that also appears upregulated in the majority of conditions examined in our study is the F-type bacterial ATPase, of which

four components were identified as upregulated (*atpF* - all conditions; *atpF'* and *atpB* – 3 of 4 conditions; *atpH* –*in vivo* 24 hour only). The F-type ATP synthase has previously been shown to play a key role in the bile tolerance of other types of intestinal bacteria (Sanchez *et al.*, 2006). In addition, some components of ATP synthase were also identified in *C. jejuni* by Fox *et al.* (2007) as increased proteins produced when exposed to bile. Based on the large number of other cellular processes that are upregulated during exposure to bile, it seems reasonable to suggest that the upregulation of the ATP synthase may aid in compensation for the increased energy needs of cellular processes such as increased efflux pump activity and chemotaxis, among others.

Of particular interest within the observed genes to be upregulated under all conditions examined, two hypothetical proteins (CjSA_0040 and CjSA_0528) exhibited extreme upregulation when compared to plate grown control samples; this response was particularly robust in the host environment for both genes. CjSA_0040 is predicted to be a 107 amino acid protein that appears to be well conserved across the *Campylobacter* genus but is not found in other genera of bacteria. Assessment for conserved structural domains was performed using NCBI Protein BLAST and yielded no predictions of conserved structure for CjSA_0040. CjSA_0528 is predicted to be a 309 amino acid protein that also appears to be well conserved across the *Campylobacter* genus but again the sequence does not appear to be conserved in other genera of bacteria. Assessment for conserved structural protein domains was performed using NCBI Protein BLAST and in this case did yield a prediction of conserved structure within the outer membrane channel domain for CjSA_0528. Proteins within this family are considered to be part of the porin superfamily and may be related to gram negative porins or ligand gated channels (Marchler-Bauer *et al.*, 2015). Both

CjSA_0040 and CjSA_0538 were also noted to be increased in expression levels in our preliminary experiment, with CjSA_0538 one of only 14 protein coding genes that were considered significant by Rockhopper on reanalysis. The combination of data presented here provides strong evidence to support an important role for both of these genes in bile tolerance and suggests that, in particular, further work to determine the structure and function of CjSA_0538 may lead to important new insights in the mechanisms utilized by *C. jejuni* to survive in the bile rich gallbladder environment. In addition, if further analysis confirms that the location of CjSA_0538 is indeed in the outer membrane, it may prove to be immunogenic and a valuable target for vaccine research.

One of the primary goals in generating this data was to validate the hypothesis that small non-coding RNAs play a role in the adaptation to survival within bile and the gallbladder environment. Non-coding RNAs can be rapidly produced as they do not require translation to be active, and once produced in the cell they can rapidly be recycled if necessary (Papenfort and Vogel, 2010). Non-coding RNAs can also regulate multiple different targets within a cell in a variety of ways to coordinate rapid responses to changing environments (Waters and Storz, 2009). Based on the demonstrated ability of small RNAs to rapidly respond to changing environments and thus rapidly mediate altered translation of genes, it seemed reasonable that small RNAs should play a key role in adaptation to exposure to bile and the *in vivo* gallbladder. Analysis of expression data by Rockhopper and prediction of non-coding RNAs demonstrated expression of a number of previously identified non-coding RNAs (7 identified by Rockhopper, with 9 additionally identified by manual curation) that were validated to exist in the closely related 11168 and predicted to exist in IA 3902 based on sequence homology (Dugar *et al.*, 2013). In contrast, of the predicted small RNAs

to have >80% nucleotide identity to regions within the IA 3902 genome in Dugar *et al.*, (2013), 9 were not observed to have any transcription in the region of homology. This is consistent with observations in both *Campylobacter* as well as other species of bacteria such as *Listeria* where expression of conserved ncRNAs has been shown to be very divergent even among closely related strains (Wurtzel *et al.*, 2012; Dugar *et al.*, 2013). Differences in growth temperatures, library construction protocols, and prediction algorithms have also been shown to play a role in the ability to detect non-coding RNAs between separate experiments even within the same strain (Taveirne *et al.*, 2013), thus these nuances also likely played a role in this case.

Of the seven ncRNAs confirmed to be observed in IA 3902 by Rockhopper in our data, all exhibited differential gene expression, with six of the seven demonstrating increased expression in at least one of the conditions studied. CjNC140 and CjNC180 demonstrated differential expression in the majority of conditions and time points studied (three of four, and all four, respectively) and were observed to be consistently more increased in the *in vivo* rather than *in vitro* conditions. This suggests that these non-coding RNAs may play a key role in the ability of *C. jejuni* to sense the changing host environment and respond quickly to those changes. The exact mechanism by which these small RNAs exert their regulatory control cannot be determined at this time as it is quite possible that each could, for example, serve to both stabilize some mRNA transcripts for increased protein expression while at the same time targeting other mRNA transcripts for degradation and decreased protein expression. Interestingly, expression in the region of CjNC190, a small RNA reported antisense to CjNC180 was also observed but again, not at high enough levels to be identified by the Rockhopper program. No reads were observed in the region of CjNC190 in the plate

grown samples, with increased expression subjectively visible in all exposed conditions and time points, suggesting that both CjNC180 and CjNC190 may play a role either together or separately in adaptation to the bile environment. No additional publications describing the function of any of these small RNAs in *Campylobacter* have been published at this time; therefore, future work to elucidate the targets and mechanisms of action of these potent regulators is warranted.

Of the identified non-coding RNAs, the only one to be observed to be downregulated, particularly within the *in vivo* host conditions, was CjNC130, which has been proven to be a 6S RNA homologue. The 6S RNA has been shown in other model organisms to play an important role in regulating transcription on a global scale by competing with DNA promoters for binding to RNA polymerase (Wassarman and Storz, 2000). The coding sequence of 6S is not conserved across bacterial genera, however, computational searches based on secondary structure have allowed for its identification across much of the prokaryotic kingdom (Wehner *et al.*, 2014). The formation of a secondary structure consisting of a large double stranded hairpin with a central bulge is essential as it resembles an open promoter complex that allows for binding to RNA polymerase (Barrick *et al.*, 2005). It seems reasonable given the evidence of upregulation of expression of a large number of genes in our data at both time points *in vivo* that decreased expression of the 6S RNA may allow for an overall increase in gene expression due to decreased interference by the 6S RNA with RNA polymerase binding. While this change is likely to globally affect gene transcription due to a direct effect on RNA polymerase rather than individual gene transcription, the evidence presented here demonstrates that overall transcription regulation within the host is likely important for establishing colonization and induction of disease.

While we were unable to validate the differential expression of the CjNC110 small RNA as was observed in the preliminary experiment, visual observation of expression in that region suggests that a decrease in expression was observed in all conditions when compared to the plate grown *C. jejuni* as was shown in the preliminary experiment. The likely reason for a lack of recognition by Rockhopper was again the generally low expression levels overall, including in the plate grown samples. In the preliminary experiment, there was a very high level of expression of CjNC110 in the plate grown samples as well as the neighboring *luxS* gene, which allowed for obvious recognition by the program. The plate grown samples were prepared identically for each set of experiments, so it is unclear what led to the large difference in expression under normal growth conditions and this finding warrants further study.

In summary, this is the first report of the complete transcriptome of *C. jejuni* IA 3902 during exposure to an important host environment, the sheep gallbladder. We have demonstrated that the transcriptional environment during direct interaction within the host, as displayed by utilizing *in vivo* inoculation of and RNA recovery from the sheep gallbladder environment, provides a more robust picture of the complexity of gene regulation required for survival when compared to *in vitro* exposure to ovine bile alone. A subset of genes were identified that are believed to play important role in survival within bile, as well as survival in the host environment, including two highly expressed hypothetical proteins that warrant further study. In addition to identification of important protein coding genes, seven previously identified non-coding RNAs were confirmed to be differentially expressed within our data, suggesting that they may also play a key role in rapid regulation of gene expression upon exposure to bile and the host environment. Additional work to validate the differential

expression of a subset of the genes and non-coding RNAs identified in this study, such as via the NanoString nCounter or RT-PCR, is warranted.

Table 1A. Summary of RNAseq results of the preliminary samples that were rRNA depleted and utilized strand specific library preparation.

Library	Total reads	Number of successfully aligned reads			Percent mapped reads
		Chromosome	pVir	Total	
IA 3902 plate growth 16hr preliminary run	10925096	7557580	50312	7607892	69.6%
IA 3902 sheep gallbladder 2 hr preliminary run	11480013	6450502	5728	6456230	56.2%
AVERAGE	11202555	7004041	28020	7032061	62.9%
TOTAL	22405109			14064122	

69

Table 1B. Summary of RNAseq mapping results of the preliminary samples presented in Table 1A.

Library	Percent mapped reads									
	Chromosome							pVir		
	Protein coding genes		Ribosomal RNA		Other known RNA		Unannotated Regions	Protein coding genes		Unannotated regions
	Sense	Antisense	Sense	Antisense	Sense	Antisense		Sense	Antisense	
IA 3902 plate growth 16hr preliminary run	86	4	1	0	4	2	2	89	4	7
IA 3902 gallbladder 2hr preliminary run	16	0	82	1	0	0	1	90	2	8
AVERAGE	51	2	42	1	2	1	2	90	3	8

Table 2. Comparison of the calculated fold change for genes known to be important in the response of *C.jejuni* to bile using both the NanoString and RNAseq data in the preliminary dataset.

	Fold Change	
	<i>In vivo</i> vs plate grown	
	Nanostring	RNAseq
CjNC110	-5.9	-13.1
<i>cbrR</i>	-1.7	-1.4
<i>cmeR</i>	-1.7	-1.1
<i>cmeA</i>	1.4	1.7
<i>cmeB</i>	1.3	1.7
<i>flaA</i>	-1.5	1.6

Table 3. Comparison of the average normalized signal for sense and antisense expression of genes observed to have either high or low antisense expression in the preliminaryRNAseq dataset as assessed by NanoString nCounter technology.

Target Gene	Plate growth 16 hours NanoString target		<i>In vivo</i> gallbladder 2 hour NanoString target	
	Sense (coding)	Antisense	Sense (coding)	Antisense
HIGH ANTISENSE EXPRESSION LEVELS on RNAseq				
<i>cbrR</i>	861	15	506	1
<i>cmeA</i>	1419	156	1948	1
<i>cmeB</i>	1347	283	1697	1891
<i>flaA</i>	42803	24	29487	1
<i>peb1</i>	28424	122	5619	1
<i>ssrA</i>	196652	55	81034	1
<i>rnpB</i>	1	36592	1325	17693
<i>porA</i>	166538	1	45806	1
<i>purD</i>	7630	1	2770	1
LOW ANTISENSE EXPRESION LEVELS on RNAseq				
<i>cftA</i>	1	1	1	1
<i>chuA</i>	1	1	1	227
<i>nrfH</i>	193	1	1904	201

All counts reported as reference gene normalized background subtracted

1 = signifies no expression present

Table 4A. Summary of RNAseq results from the primary study including 21 rRNA depleted strand specific libraries generated on a single lane of the Illumina HiSeq 2500.

Library	Total reads	Number of successfully aligned reads			Percent mapped reads
		Chromosome	pVir	Total	
IA 3902 gallbladder 2 hr – 1	3213364	2405222	12658	2417880	75.2%
IA 3902 gallbladder 2 hr – 2	2802472	1989859	7305	1997164	71.3%
IA 3902 gallbladder 2 hr – 3	3977312	3843651	23073	3866724	97.2%
IA 3902 gallbladder 2 hr – 4	3452608	3352807	7167	3359974	97.3%
IA 3902 gallbladder 24 hr – 1	3625410	2859526	18047	2877573	79.4%
IA 3902 gallbladder 24 hr – 2	4342702	4066527	14730	4081257	94.0%
IA 3902 gallbladder 24 hr – 3	3016425	494901	3088	497989	16.5%
IA 3902 bile <i>in vitro</i> 2 hrs – 1	3794841	3666255	22332	3688587	97.2%
IA 3902 bile <i>in vitro</i> 2 hrs – 2	5389416	5195381	10339	5205720	96.6%
IA 3902 bile <i>in vitro</i> 2 hrs – 3	3610288	3465827	7170	3472997	96.2%
IA 3902 bile <i>in vitro</i> 2 hrs – 4	2654785	2577672	1094	2578766	97.1%
IA 3902 bile <i>in vitro</i> 24 hrs – 1	3299251	3190727	22126	3212853	97.4%
IA 3902 bile <i>in vitro</i> 24 hrs – 2	2753010	2670812	15853	2686665	97.6%
IA 3902 bile <i>in vitro</i> 24 hrs – 3	3461969	3330945	16918	3347863	96.7%
IA 3902 bile <i>in vitro</i> 24 hrs – 4	3362952	3233165	9087	3242252	96.4%
IA 3902 plate growth 16hr – 1	3663245	3430105	15841	3445946	94.1%
IA 3902 plate growth 16hr – 2	3241200	3123409	13195	3136604	96.8%
IA 3902 plate growth 16hr – 3	3636647	3463128	18606	3481734	95.7%
IA 3902 plate growth 16hr – 4	2753937	2653828	21870	2675698	97.2%
IA 3902 plate growth 16hr – 5	3311668	3198827	25085	3223912	97.4%
IA 3902 plate growth 16hr – 6	4319642	4184757	30393	4215150	97.6%
AVERAGE	3508721	3161778	15047	3176824	89.8%
MINIMUM	2654785	494901	1094	497989	16.5%
MAXIMUM	5389416	5195381	30393	5205720	97.6%
TOTAL	73683144			66713308	90.5%

Table 4B. Summary of RNAseq mapping results of the 21 samples from the primary experiment presented in Table 1A.

Library	Percent mapped reads									
	Chromosome							pVir		
	Protein coding genes		Ribosomal RNA		Other known RNA		Unannotated regions	Protein coding genes		Unannotated regions
	Sense	Antisense	Sense	Antisense	Sense	Antisense		Sense	Antisense	
IA 3902 gallbladder 2 hr - 1	72	1	21	0	2	1	3	90	1	9
IA 3902 gallbladder 2 hr - 2	87	1	5	0	3	1	2	90	2	9
IA 3902 gallbladder 2 hr - 3	85	1	7	0	3	2	3	91	1	8
IA 3902 gallbladder 2 hr - 4	79	1	12	0	5	1	2	92	1	7
IA 3902 gallbladder 24 hr - 1	90	2	2	0	2	1	4	81	2	17
IA 3902 gallbladder 24 hr - 2	86	1	8	0	2	1	3	85	2	13
IA 3902 gallbladder 24 hr - 3	79	1	12	0	2	2	4	89	2	9
IA 3902 bile <i>in vitro</i> 2 hrs - 1	67	0	27	0	2	1	2	92	0	7
IA 3902 bile <i>in vitro</i> 2 hrs - 2	58	0	33	0	4	2	3	94	1	5
IA 3902 bile <i>in vitro</i> 2 hrs - 3	59	0	33	0	3	2	2	95	0	4
IA 3902 bile <i>in vitro</i> 2 hrs - 4	6	0	93	0	0	0	0	91	1	9
IA 3902 bile <i>in vitro</i> 24 hrs - 1	84	1	3	0	6	2	3	89	1	10
IA 3902 bile <i>in vitro</i> 24 hrs - 2	89	1	3	0	2	2	3	92	1	7
IA 3902 bile <i>in vitro</i> 24 hrs - 3	78	0	15	0	2	2	3	93	0	7
IA 3902 bile <i>in vitro</i> 24 hrs - 4	55	0	35	0	5	1	3	91	1	8
IA 3902 plate growth 16hr - 1	64	1	27	0	4	1	3	91	1	9
IA 3902 plate growth 16hr - 2	65	0	26	0	5	1	2	94	1	6
IA 3902 plate growth 16hr - 3	71	1	20	0	5	1	2	92	1	7
IA 3902 plate growth 16hr - 4	85	1	6	0	5	1	2	92	0	7
IA 3902 plate growth 16hr - 5	76	1	15	0	4	2	3	93	0	6
IA 3902 plate growth 16hr - 6	76	0	14	0	4	2	3	93	0	6
AVERAGE	72	1	20	0	3	1	3	91	1	8

Table 5. Summary of the differences in numbers of genes with increased and decreased expression under either *in vivo* or *in vitro* bile exposure when compared to unexposed IA 3902 at both 2 hours and 24 hours.

	Condition							
	<i>In vivo</i> gallbladder				<i>In vitro</i> bile			
	2 hours		24 hours		2 hours		24 hours	
	Chromosome	pVir	Chromosome	pVir	Chromosome	pVir	Chromosome	pVir
Protein-coding genes								
Number downregulated	105	7	96	6	10	4	54	7
Number upregulated	283	10	420	14	102	7	248	11
Non-coding RNA genes								
Number downregulated	[15]	[1]	[12]	[0]	[7]	[0]	[16]	[1]
Number upregulated	[62]	[1]	[87]	[2]	[44]	[1]	[53]	[1]

[] = signifies that this is a putative list generated by Rockhopper of predicted non-coding RNA as well as known non-coding RNA genes

Table 6A. Genes with decreased differential expression in the *in vivo* sheep gallbladder exposed samples at 24 hours with annotation to indicate which genes are a part of multi-gene operons.

Name	Synonym	COG Code	Product	Expression (RPKM)		Significance	
				Plate 16hr	GB <i>in vivo</i> 24 hr	Q Value	Fold change
DECREASED EXPRESSION AT 24 HOURS EXPOSURE TO GALLBLADDER							
-	CJSA_0004 ^a		hypothetical protein	45	17	2.9E-04	-2.6
-	CJSA_0005 ^a	R	molybdopterin oxidoreductase family protein	45	21	8.9E-03	-2.1
<i>gltD</i>	CJSA_0009	ER	glutamate synthase subunit beta	114	31	1.6E-08	-3.7
-	CJSA_0016	R	ExsB protein	55	23	6.0E-03	-2.4
-	CJSA_0025	R	sodium/dicarboxylate symporter	151	50	2.7E-05	-3.0
-	CJSA_0037	C	cytochrome c family protein	239	69	5.9E-07	-3.5
-	CJSA_0063	HJ	hypothetical protein	627	181	3.0E-04	-3.5
-	CJSA_0066 ^b	S	hypothetical protein	409	98	2.0E-11	-4.2
-	CJSA_0067 ^b	C	iron-sulfur cluster binding protein	1024	210	3.4E-06	-4.9
-	CJSA_0068 ^b	C	putative oxidoreductase iron-sulfur subunit	991	168	3.4E-15	-5.9
<i>lctP</i>	CJSA_0069	C	L-lactate permease	1674	464	3.0E-02	-3.6
-	CJSA_0082 ^c	R	putative lipoprotein	213	82	2.2E-03	-2.6
-	CJSA_0083 ^c		hypothetical protein	108	44	5.8E-03	-2.5
-	CJSA_0084 ^c	M	hypothetical protein	85	30	7.4E-05	-2.8
<i>atpC</i>	CJSA_0099	C	F0F1 ATP synthase subunit epsilon	278	119	1.2E-02	-2.3
-	CJSA_0158		hypothetical protein	1356	338	1.4E-10	-4.0
-	CJSA_0216	C	NifU family protein	790	233	6.7E-04	-3.4
<i>cheW</i>	CJSA_0259	NT	purine-binding chemotaxis protein CheW	516	218	3.8E-02	-2.4
<i>peb3</i>	CJSA_0265	R	major antigenic peptide PEB3	560	236	3.4E-02	-2.4

Table 6A continued

<i>panD</i>	CJSA_0270	H	aspartate alpha-decarboxylase	116	54	1.3E-02	-2.1
<i>modA</i>	CJSA_0277	P	molybdate transport system substrate-binding protein	207	54	1.1E-09	-3.8
-	CJSA_0301	J	endoribonuclease L-PSP family protein	98	44	1.4E-02	-2.2
-	CJSA_0335	S	hypothetical protein	55	24	2.1E-02	-2.3
-	CJSA_0388	E	putative GMC oxidoreductase subunit	248	72	7.9E-05	-3.4
-	CJSA_0399		hypothetical protein	721	243	1.8E-04	-3.0
<i>uxaA</i>	CJSA_0452 ^d	G	putative altronate hydrolase N-terminus	79	34	1.3E-02	-2.3
<i>uxaA</i>	CJSA_0453 ^d	G	putative altronate hydrolase C-terminus	79	20	2.1E-11	-4.0
-	CJSA_0459	S	hypothetical protein	24	8	1.7E-05	-3.0
<i>purQ</i>	CJSA_0484	F	phosphoribosylformylglycinamide synthase I	130	54	4.8E-03	-2.4
<i>mdh</i>	CJSA_0499	C	malate dehydrogenase	413	157	1.3E-02	-2.6
<i>sucD</i>	CJSA_0501	C	succinyl-coA synthetase alpha chain	824	265	2.9E-03	-3.1
<i>oorB</i>	CJSA_0504 ^e	C	2-oxoglutarate-acceptor oxidoreductase subunit OorB	985	320	6.8E-03	-3.1
<i>oorC</i>	CJSA_0505 ^e	C	2-oxoglutarate-acceptor oxidoreductase subunit OorC	966	227	3.2E-07	-4.3
-	CJSA_0520 ^f	S	hypothetical protein	95	33	4.4E-05	-2.9
-	CJSA_0521 ^f		hypothetical protein	140	22	2.7E-36	-6.4
<i>Fba</i>	CJSA_0565	G	fructose-bisphosphate aldolase	831	293	3.1E-02	-2.8
<i>hypE</i>	CJSA_0594	O	hydrogenase expression/formation protein HypE	53	26	2.5E-02	-2.0
-	CJSA_0620 ^g	E	M24 family peptidase	410	107	3.5E-05	-3.8
-	CJSA_0621 ^g	E	MFS di-/tripeptide transporter	183	44	6.0E-11	-4.2
<i>Pta</i>	CJSA_0652 ^h	C	phosphate acetyltransferase	314	94	6.1E-04	-3.3
<i>ackA</i>	CJSA_0653 ^h	C	acetate kinase	386	95	3.2E-07	-4.1
<i>glnA</i>	CJSA_0663	E	glutamine synthetase, type I	463	116	2.6E-05	-4.0
<i>rpsP</i>	CJSA_0674	J	30S ribosomal protein S16	452	203	2.7E-02	-2.2
-	CJSA_0685		hypothetical protein	109	48	4.6E-03	-2.3
-	CJSA_0787 ⁱ	C	Na ⁺ /H ⁺ antiporter family protein	64	23	2.8E-04	-2.8
-	CJSA_0788 ⁱ	R	putative oxidoreductase	128	40	5.8E-07	-3.2
-	CJSA_0849	E	putative amino-acid transport protein	461	137	5.0E-04	-3.4
<i>hupB</i>	CJSA_0858	L	DNA-binding protein HU-like protein	5807	1691	4.4E-02	-3.4

Table 6A continued

-	CJSA_0861 ^j	S	hypothetical protein	147	38	2.6E-10	-3.9
<i>cstA</i>	CJSA_0862 ^j	T	carbon starvation protein A	293	60	2.2E-09	-4.9
-	CJSA_0864 ^k	E	amino acid ABC transporter permease	136	50	1.3E-04	-2.7
-	CJSA_0865 ^k	E	amino acid ABC transporter permease	594	127	2.8E-10	-4.7
<i>peb1A</i>	CJSA_0866 ^k	ET	bifunctional adhesin/ABC transporter aspartate/glutamate	3087	689	4.0E-03	-4.5
<i>pebC</i>	CJSA_0867 ^k	E	amino acid ABC transporter ATP-binding protein	584	175	2.2E-04	-3.3
<i>argH</i>	CJSA_0876 ^l	E	argininosuccinate lyase	134	59	2.6E-02	-2.3
<i>pckA</i>	CJSA_0877 ^l	C	phosphoenolpyruvate carboxykinase	292	125	3.5E-02	-2.3
-	CJSA_0880	R	putative sodium:amino-acid symporter family protein	22	8	3.2E-04	-2.8
<i>purH</i>	CJSA_0898	F	bifunctional formyltransferase/IMP cyclohydrolase	40	16	4.5E-04	-2.5
<i>purL</i>	CJSA_0900	F	phosphoribosylformylglycinamide synthase II	42	18	1.5E-02	-2.3
<i>cjaA</i>	CJSA_0925	ET	putative amino-acid transporter periplasmic solute-binding protein	1299	311	2.9E-05	-4.2
<i>hipO</i>	CJSA_0928	R	hippurate hydrolase	90	22	4.4E-13	-4.1
-	CJSA_0930	P	putative MFS (Major Facilitator Superfamily) transport protein	75	18	8.3E-12	-4.2
-	CJSA_0948	O	putative membrane bound ATPase	31	15	1.8E-02	-2.1
-	CJSA_0955 ^m		hypothetical protein	38	12	1.1E-06	-3.2
-	CJSA_0956 ^m	O	putative cytochrome C biogenesis protein	45	20	2.0E-02	-2.3
<i>livM</i>	CJSA_0959 ^{m'}	E	high affinity branched-chain amino acid ABC transporter permease	37	19	5.1E-02	-1.9
<i>livH</i>	CJSA_0960 ^m	E	high affinity branched-chain amino acid ABC transporter permease	91	40	1.1E-02	-2.3
-	CJSA_1093	C	cytochrome c553	2759	880	5.0E-03	-3.1
-	CJSA_1102	S	hypothetical protein	279	109	3.2E-04	-2.6
<i>metF</i>	CJSA_1140	E	5,10-methylenetetrahydrofolate reductase	38	17	1.5E-02	-2.2
<i>htrA</i>	CJSA_1166	O	serine protease (protease DO)	319	118	1.3E-02	-2.7
<i>hydD</i>	CJSA_1203 ⁿ	C	putative hydrogenase maturation protease	259	116	2.4E-02	-2.2
<i>hydC</i>	CJSA_1204 ⁿ	C	Ni/Fe-hydrogenase B-type cytochrome subunit	635	223	7.3E-03	-2.8
<i>acpP3</i>	CJSA_1242		putative acyl carrier protein	69	32	3.0E-02	-2.2
<i>fldA</i>	CJSA_1316	C	lavodoxin FldA	1818	428	2.3E-06	-4.2
-	CJSA_1322	J	putative endoribonuclease L-PSP	477	131	1.6E-08	-3.6
-	CJSA_1408 ^o		hypothetical protein	211	69	8.9E-06	-3.1

Table 6A continued

-	CJSA_1409 ^o		hypothetical protein	506	218	1.5E-02	-2.3
<i>putP</i>	CJSA_1424 ^p	ER	putative sodium/proline permease	451	50	1.6E-63	-9.0
<i>putA</i>	CJSA_1425 ^p	C	putative proline dehydrogenase/carboxylate dehydrogenase	399	95	5.2E-04	-4.2
<i>moaE</i>	CJSA_1439	H	putative molybdopterin converting factor,subunit 2	196	79	2.4E-03	-2.5
<i>Acs</i>	CJSA_1453	I	acetyl-coenzyme A synthetase	406	87	2.2E-07	-4.7
-	CJSA_1456	H	putative tungsten ABC-transport/periplasmic substrate binding protein	450	129	2.0E-05	-3.5
-	CJSA_1457	R	hypothetical protein	115	38	4.3E-06	-3.0
-	CJSA_1459	E	putative allophanate hydrolase subunit 2	50	23	1.1E-02	-2.2
<i>nuoI</i>	CJSA_1483 ^q	C	NADH dehydrogenase I subunit I	133	58	1.1E-02	-2.3
<i>nuoH</i>	CJSA_1484 ^q	C	NADH dehydrogenase I subunit H	83	36	1.4E-02	-2.3
<i>hisA</i>	CJSA_1513	E	phosphoribosylformimino-5-aminoimidazole carboxamide isomerase	52	24	2.1E-02	-2.2
<i>kgpP</i>	CJSA_1531	G	alpha-ketoglutarate permease	364	108	3.9E-04	-3.4
<i>sdaA</i>	CJSA_1536 ^r	E	L-serine dehydratase	533	151	2.1E-04	-3.5
<i>sdaC</i>	CJSA_1537 ^r	E	amino acid transporter	397	173	4.7E-02	-2.3
<i>p19</i>	CJSA_1570 ^s	P	periplasmic protein p19	1423	546	4.6E-02	-2.6
-	CJSA_1572 ^s	M	ABC transporter permease	54	24	8.1E-03	-2.3
-	CJSA_1573 ^s	M	ABC transporter permease	35	18	4.8E-02	-1.9
<i>gltA</i>	CJSA_1592	C	citrate synthase	1082	284	5.6E-03	-3.8
<i>leuC</i>	CJSA_1626	E	3-isopropylmalate dehydratase large subunit	52	21	8.2E-04	-2.5
<i>virB9</i>	CJSA_pVir0002 ^t		VirB9	37	7	1.4E-19	-5.3
<i>virB10</i>	CJSA_pVir0003 ^t		VirB10	23	5	1.2E-19	-4.6
-	CJSA_pVir0008 ^u		hypothetical protein	644	55	5.9E-145	-11.7
-	CJSA_pVir0009 ^u		hypothetical protein	1372	130	9.8E-63	-10.6
-	CJSA_pVir0050 ^v		hypothetical protein	128	17	1.2E-56	-7.5
-	CJSA_pVir0051 ^v		hypothetical protein	40	8	1.4E-17	-5.0
-	CJSA_CjSRP1	-		18640	1476	3.0E-74	-12.6
-	CJSA_t0030		Ser tRNA	436	105	3.0E-12	-4.2
-	predicted RNA		antisense: CJSA_1568; 87nt length, 1577262 to 1577349 positive strand	216	30	2.1E-51	-7.2
-	predicted RNA		176nt length; 1331258 to 1331434 positive strand	198	37	2.0E-24	-5.4

Table 6A continued

-	predicted RNA	10nt length; 443535 to 443545 positive strand	147	39	3.7E-07	-3.8
-	predicted RNA	255nt length; 1457504 to 1457759 positive strand	277	77	6.0E-09	-3.6
-	predicted RNA	13nt length; 1183928 to 1183941 positive strand	961	278	6.8E-09	-3.5
-	predicted RNA	antisense: glnQ; 86nt length, 845047 to 844961 negative strand	179	52	2.4E-08	-3.4
-	predicted RNA	106nt length; 1331076 to 1331182 positive strand	233	100	1.4E-02	-2.3
-	predicted RNA	32nt length; 577201 to 577169 negative strand	312	136	6.8E-03	-2.3
-	predicted RNA	antisense: CJSa_0192; 299nt length, 198809 to 199108 positive strand	1528	667	4.0E-02	-2.3
-	predicted RNA	antisense: CJSa_0215; 50nt length; 226428 to 226378 negative strand	136	69	4.4E-02	-2.0

a, b, aa, bb, ect = matching superscript signifies expression within the same operon

Table 6B. Genes with increased differential expression in the *in vivo* sheep gallbladder exposed samples at 24 hours with annotation to indicate which genes are a part of multi-gene operons.

Name	Synonym	COG Code	Product	Expression (RPKM)		Significance	
				Plate 16hr	GB <i>in vivo</i> 24 hr	Q Value	Fold change
INCREASED EXPRESSION AT 24 HOURS EXPOSURE TO GALLBLADDER							
<i>dnaA</i>	CJSA_0001	L	chromosomal replication initiator protein DnaA	21	50	2.2E-06	2.4
<i>dnaN</i>	CJSA_0002	L	DNA polymerase III subunit beta	32	106	7.2E-13	3.3
<i>dsbI</i>	CJSA_0017 ^a	O	DsbB family disulfide bond formation protein	78	210	1.0E-09	2.7
<i>Dba</i>	CJSA_0018 ^a		disulfide bond formation protein	46	301	3.8E-84	6.5
-	CJSA_0030 ^b		hypothetical protein	2	70	0.0E+00	35.0

Table 6B continued

-	CJSA_0031 ^b		hypothetical protein	1	35	0.0E+00	35.0
-	CJSA_0035	G	MFS family drug resistance transporter	15	49	5.9E-17	3.3
-	CJSA_0040 ^c		hypothetical protein	15	783	0.0E+00	52.2
-	CJSA_0041 ^c		hypothetical protein	62	379	6.3E-65	6.1
<i>flgD</i>	CJSA_0042 ^c	N	flagellar basal body rod modification protein	309	824	5.0E-05	2.7
<i>flgE</i>	CJSA_0043 ^c	N	flagellar hook protein	160	534	6.8E-08	3.3
-	CJSA_0045	P	putative iron-binding protein	39	208	4.2E-40	5.3
-	CJSA_0049		hypothetical protein	53	207	3.7E-19	3.9
<i>fliM</i>	CJSA_0054 ^d	N	flagellar motor switch protein FliM	61	158	1.3E-08	2.6
<i>fliA</i>	CJSA_0055 ^d	K	flagellar biosynthesis sigma factor	77	336	3.1E-25	4.4
-	CJSA_0056 ^d		hypothetical protein	34	361	7.6E-290	10.6
<i>folk</i>	CJSA_0059	H	hydroxymethyldihydropteridine pyrophosphokinase	21	70	3.5E-18	3.3
-	CJSA_0061	FR	Chlorohydrolase	13	27	5.0E-05	2.1
-	CJSA_0065	P	hemerythrin family non-heme iron protein	7	33	2.0E-24	4.7
<i>cdtC</i>	CJSA_0070		cytolethal distending toxin C	19	29	1.0E-02	1.5
<i>cydA</i>	CJSA_0074	C	cytochrome d ubiquinol oxidase, subunit I	10	31	1.3E-13	3.1
-	CJSA_0080	S	putative lipoprotein	36	82	9.2E-06	2.3
<i>obgE</i>	CJSA_0087	R	GTPase ObgE	40	135	1.9E-14	3.4
<i>proB</i>	CJSA_0088 ^e	E	gamma-glutamyl kinase	23	69	8.7E-14	3.0
<i>Fmt</i>	CJSA_0089 ^e	J	methionyl-tRNA formyltransferase	11	27	8.9E-09	2.5
<i>birA</i>	CJSA_0090 ^e	H	biotin--protein ligase	20	44	1.4E-06	2.2
-	CJSA_0091 ^e	D	ParA family chromosome partitioning ATPase	73	153	4.4E-05	2.1
-	CJSA_0092 ^e	K	ParB family chromosome partitioning protein	29	62	2.9E-05	2.1
<i>atpF'</i>	CJSA_0093 ^e	C	F0F1 ATP synthase subunit B	67	276	1.3E-22	4.1
<i>atpF</i>	CJSA_0094 ^e	C	F0F1 ATP synthase subunit B	37	147	1.1E-26	4.0
<i>atpH</i>	CJSA_0095 ^e	C	F0F1 ATP synthase subunit delta	2	39	0.0E+00	19.5
-	CJSA_0102 ^{e'}		TonB domain-containing protein	17	48	4.3E-12	2.8
<i>tolB</i>	CJSA_0103 ^{e'}	U	translocation protein TolB	73	146	1.3E-05	2.0
-	CJSA_0105	S	hypothetical protein	147	263	8.9E-04	1.8

Table 6B continued

-	CJSA_0110 ^f	Q	putative pyrazinamidase/nicotinamidase	18	52	2.5E-13	2.9
-	CJSA_0111 ^f		putative recombination protein RecO	5	28	5.8E-31	5.6
-	CJSA_0112 ^f	R	putative metalloprotease	17	33	1.2E-04	1.9
-	CJSA_0113 ^f		hypothetical protein	115	338	6.8E-12	2.9
-	CJSA_0119	G	inositol monophosphatase family protein	16	25	4.6E-03	1.6
-	CJSA_0124 ^g	O	putative glycoprotease family protein	10	39	1.4E-19	3.9
<i>thrB</i>	CJSA_0125 ^g	E	homoserine kinase	23	46	2.9E-05	2.0
-	CJSA_0126 ^g	K	hypothetical protein	19	83	1.1E-25	4.4
-	CJSA_0142 ^h		hypothetical protein	5	28	3.5E-43	5.6
-	CJSA_0143 ^h		hypothetical protein	56	136	5.9E-07	2.4
-	CJSA_0144 ^h	J	RNA methyltransferase	134	255	4.3E-05	1.9
-	CJSA_0145 ^h	R	tetrapyrrole methylase family protein	28	47	6.6E-03	1.7
-	CJSA_0149 ⁱ	C	cytochrome c family protein	31	50	5.5E-03	1.6
-	CJSA_0150 ⁱ	H	putative 6-pyruvoyl tetrahydropterin synthase	53	102	7.5E-04	1.9
-	CJSA_0154		hypothetical protein	7	35	1.3E-28	5.0
-	CJSA_0161	QR	hypothetical protein	38	93	2.5E-08	2.4
-	CJSA_0166		putative lipoprotein	14	173	2.2E-219	12.4
-	CJSA_0167	S	TonB-dependent colicin lipoprotein, putative	2	35	3.1E-296	17.5
-	CJSA_0172	I	putative transporter	21	51	1.4E-06	2.4
<i>argC</i>	CJSA_0201	E	N-acetyl-gamma-glutamyl-phosphate reductase	55	92	4.0E-03	1.7
-	CJSA_0207 ^j	H	nicotinate phosphoribosyltransferase	20	38	1.0E-03	1.9
-	CJSA_0209 ^j	S	hypothetical protein	17	62	1.4E-19	3.6
<i>pyrE</i>	CJSA_0210 ^j	F	orotate phosphoribosyltransferase	272	407	3.2E-02	1.5
<i>Frr</i>	CJSA_0211 ^j	J	ribosome recycling factor	238	351	1.1E-02	1.5
<i>secG</i>	CJSA_0212 ^j	U	preprotein translocase subunit SecG	237	394	8.2E-04	1.7
<i>cynT</i>	CJSA_0214 ^k	P	carbonic anhydrase	41	75	1.7E-03	1.8
-	CJSA_0215 ^k	M	mechanosensitive ion channel family protein	16	29	4.9E-03	1.8
-	CJSA_0219		hypothetical protein	1	37	0.0E+00	37.0
-	CJSA_0228		hypothetical protein	65	113	5.5E-04	1.7

Table 6B continued

-	CJSA_0233 ^l	R	Sulfatase	14	35	7.8E-09	2.5
<i>dgkA</i>	CJSA_0234 ^l	M	diacylglycerol kinase	10	49	3.9E-32	4.9
<i>pyrC</i>	CJSA_0236 ^l	F	Dihydroorotase	13	36	2.8E-11	2.8
-	CJSA_0238	H	putative SAM-dependent methyltransferase	11	35	2.3E-15	3.2
-	CJSA_0240	P	zinc transporter ZupT	12	25	6.2E-06	2.1
<i>mreC</i>	CJSA_0254	M	rod shape-determining protein MreC	35	55	1.5E-02	1.6
-	CJSA_0262	S	hypothetical protein	17	37	3.2E-06	2.2
<i>lpxB</i>	CJSA_0264	M	lipid-A-disaccharide synthase	34	57	9.9E-03	1.7
<i>surE</i>	CJSA_0267	R	stationary phase survival protein SurE	27	42	9.3E-03	1.6
-	CJSA_0283 ^m	P	SMR family multidrug efflux pump	22	32	2.6E-02	1.5
-	CJSA_0284 ^m	P	SMR family multidrug efflux pump	13	39	2.5E-10	3.0
<i>Pth</i>	CJSA_0286 ⁿ	J	peptidyl-tRNA hydrolase	85	168	2.6E-04	2.0
-	CJSA_0287 ⁿ	R	hypothetical protein	2	28	3.5E-244	14.0
<i>perR</i>	CJSA_0296	P	FUR family transcriptional regulator	47	168	1.2E-20	3.6
<i>ubiE</i>	CJSA_0298	H	ubiquinone/menaquinone biosynthesis methyltransferase	15	30	3.4E-05	2.0
<i>fabH</i>	CJSA_0302 ^o	I	3-oxoacyl-ACP synthase	39	115	2.5E-10	2.9
<i>plsX</i>	CJSA_0303 ^o	I	putative glycerol-3-phosphate acyltransferase PlsX	116	253	2.4E-06	2.2
-	CJSA_0305 ^o		hypothetical protein	124	603	7.8E-33	4.9
<i>Ndk</i>	CJSA_0306 ^o	F	nucleoside diphosphate kinase	455	849	8.0E-03	1.9
<i>flhB</i>	CJSA_0309	NU	flagellar biosynthesis protein FlhB	85	202	3.5E-08	2.4
<i>trpE</i>	CJSA_0319	EH	anthranilate synthase component I	41	66	1.0E-02	1.6
<i>trpF</i>	CJSA_0321	E	N-(5phosphoribosyl)anthranilate isomerase	23	37	4.7E-03	1.6
-	CJSA_0326		putative transmembrane protein	11	35	4.8E-14	3.2
-	CJSA_0327 ^p	FP	Ppx/GppA family phosphatase	24	41	6.8E-03	1.7
<i>fdxB</i>	CJSA_0328 ^p	C	ferredoxin, 4Fe-4S	102	194	5.0E-04	1.9
-	CJSA_0337		hypothetical protein	2	36	5.3E-255	18.0
<i>cmeC</i>	CJSA_0338 ^q	MU	RND efflux system, outer membrane lipoprotein CmeC	62	92	4.6E-03	1.5
<i>cmeB</i>	CJSA_0339 ^q	V	RND efflux system, inner membrane transporter CmeB	82	138	3.1E-02	1.7
<i>cmeA</i>	CJSA_0340 ^q	M	RND efflux system, membrane fusion protein CmeA	102	269	1.7E-09	2.6

Table 6B continued

-	CJSA_0344		hypothetical protein	151	233	2.6E-03	1.5
-	CJSA_0348 ^r		putative lipoprotein	9	28	2.2E-10	3.1
-	CJSA_0349 ^r		hypothetical protein	5	27	2.9E-42	5.4
-	CJSA_0358	S	integral membrane protein	16	26	4.8E-03	1.6
-	CJSA_0370		hypothetical protein	9	59	5.8E-69	6.6
-	CJSA_0372	R	colicin V production protein-like protein	93	140	3.2E-02	1.5
-	CJSA_0384	R	GTP-binding protein	10	26	3.3E-07	2.6
-	CJSA_0389		hypothetical protein	178	669	4.2E-19	3.8
-	CJSA_0390		hypothetical protein	30	62	1.2E-05	2.1
-	CJSA_0394		putative H-T-H containing protein	20	54	3.7E-08	2.7
-	CJSA_0395		hypothetical protein	14	25	1.4E-02	1.8
<i>mraY</i>	CJSA_0405	M	phospho-N-acetylmuramoyl-pentapeptide-transferase	13	34	3.4E-09	2.6
<i>sdhA</i>	CJSA_0409 ^s	C	succinate dehydrogenase, flavoprotein subunit	35	85	2.8E-07	2.4
<i>sdhB</i>	CJSA_0410 ^s	C	succinate dehydrogenase, iron-sulfur protein subunit	37	74	2.6E-04	2.0
-	CJSA_0417		NUDIX domain-containing protein	21	50	1.3E-07	2.4
<i>Rpe</i>	CJSA_0421	G	ribulose-phosphate 3-epimerase	33	73	4.1E-06	2.2
-	CJSA_0424 ^t		hypothetical protein	10	27	8.5E-09	2.7
-	CJSA_0425 ^t		hypothetical protein	10	33	5.4E-13	3.3
-	CJSA_0426 ^t		hypothetical protein	12	125	7.3E-275	10.4
-	CJSA_0427 ^t	S	hypothetical protein	56	178	3.0E-12	3.2
-	CJSA_0429 ^t		hypothetical protein	94	216	3.5E-06	2.3
<i>nusA</i>	CJSA_0430	K	transcription elongation factor NusA	63	129	3.0E-05	2.0
<i>Ctb</i>	CJSA_0435	R	group III truncated hemoglobin	29	49	7.0E-04	1.7
<i>paqP</i>	CJSA_0437	E	amino-acid ABC transporter integral membrane protein	24	35	2.0E-02	1.5
<i>rpmG</i>	CJSA_0441	J	50S ribosomal protein L33	367	857	1.5E-06	2.3
<i>secE</i>	CJSA_0442	U	preprotein translocase subunit SecE	583	947	1.4E-03	1.6
-	CJSA_0465 ^u		hypothetical protein	21	68	2.6E-12	3.2
-	CJSA_0466 ^u	R	putative methyltransferase domain protein	4	27	4.5E-54	6.8
-	CJSA_0467 ^u	R	hypothetical protein	53	92	1.1E-03	1.7

Table 6B continued

-	CJSA_0474 ^v	R	Gfo/Idh/MocA family oxidoreductase	11	25	2.0E-07	2.3
-	CJSA_0475 ^v	M	DegT/DnrJ/EryC1/StrS aminotransferase family protein	41	76	1.5E-03	1.9
<i>pbpB</i>	CJSA_0492 ^w	M	penicillin-binding protein	15	77	1.7E-34	5.1
<i>fliE</i>	CJSA_0493 ^w	NU	flagellar hook-basal body protein FlIE	287	885	7.9E-14	3.1
<i>flgC</i>	CJSA_0494 ^w	N	flagellar basal-body rod protein FlgC	461	1258	3.4E-05	2.7
<i>flgB</i>	CJSA_0495 ^w	N	flagellar basal-body rod protein FlgB	362	1355	7.7E-15	3.7
-	CJSA_0506 ^x		hypothetical protein	23	100	1.8E-26	4.3
-	CJSA_0507 ^x		hypothetical protein	23	74	9.8E-17	3.2
-	CJSA_0508 ^x	H	polyprenyl synthetase family protein	18	49	3.3E-10	2.7
-	CJSA_0517		hypothetical protein	172	299	3.5E-03	1.7
-	CJSA_0528		hypothetical protein	55	1172	0.0E+00	21.3
<i>rib</i>	CJSA_0540	H	bifunctional phosphate synthase/GTP cyclohydrolase II protein	82	132	1.9E-03	1.6
<i>tatC</i>	CJSA_0546 ^y	U	Sec-independent protein translocase TatC	17	46	8.6E-11	2.7
<i>tatB</i>	CJSA_0547 ^y	U	sec-independent translocase	36	114	5.7E-16	3.2
<i>nidH</i>	CJSA_0549	LR	dinucleoside polyphosphate hydrolase	68	162	3.5E-06	2.4
<i>Nth</i>	CJSA_0563	L	endonuclease III	11	43	2.6E-21	3.9
-	CJSA_0572	S	putative polyphosphate kinase	23	41	8.6E-04	1.8
-	CJSA_0574 ^z	M	putative secretion protein HlyD	34	73	4.3E-05	2.1
-	CJSA_0575 ^z	V	ABC-type transmembrane transport protein	15	30	3.5E-04	2.0
<i>pstS</i>	CJSA_0581	P	phosphate transport system substrate-binding protein	22	44	7.5E-05	2.0
-	CJSA_0585		hypothetical protein	29	54	1.2E-04	1.9
-	CJSA_0596	L	prophage Lp2 protein 6	72	171	2.5E-07	2.4
-	CJSA_0600	S	hypothetical protein	17	43	1.6E-08	2.5
<i>Pnk</i>	CJSA_0608 ^{aa}	G	inorganic polyphosphate/ATP-NAD kinase	20	51	7.9E-09	2.6
<i>recN</i>	CJSA_0609 ^{aa}	L	DNA repair protein RecN	15	26	1.8E-03	1.7
<i>cbrR</i>	CJSA_0610 ^{bb}	T	response regulator/GGDEF domain-containing protein	70	136	3.3E-05	1.9
-	CJSA_0611 ^{bb}	L	TatD family hydrolase	53	78	4.6E-02	1.5
-	CJSA_0616 ^{bb'}	S	OstA family protein	16	39	4.9E-08	2.4
-	CJSA_0623	E	MFS di-/tripeptide transporter	34	51	4.2E-02	1.5

Table 6B continued

-	CJSA_0632	R	putative ATP/GTP-binding protein	21	39	1.9E-04	1.9
<i>rpoN</i>	CJSA_0634	K	RNA polymerase factor sigma-54	14	29	1.5E-05	2.1
-	CJSA_0636		hypothetical protein	26	73	1.2E-08	2.8
-	CJSA_0646 ^{cc}		hypothetical protein	109	215	2.7E-04	2.0
-	CJSA_0647 ^{cc}		hypothetical protein	10	44	8.2E-27	4.4
<i>priA</i>	CJSA_0648 ^{cc}	L	primosome assembly protein PriA	6	28	2.7E-37	4.7
<i>flgH</i>	CJSA_0651	N	flagellar basal body L-ring protein	197	864	1.2E-25	4.4
-	CJSA_0655		hypothetical protein	16	79	7.6E-44	4.9
<i>mraW</i>	CJSA_0657	M	S-adenosyl-methyltransferase MraW	9	31	5.6E-19	3.4
-	CJSA_0658	O	hypothetical protein	44	140	1.4E-13	3.2
<i>flgG2</i>	CJSA_0661 ^{dd}	N	flagellar basal-body rod protein	359	1124	3.3E-07	3.1
<i>flgG</i>	CJSA_0662 ^{dd}	N	flagellar basal-body rod protein FlgG	368	1069	3.7E-06	2.9
-	CJSA_0664 ^{ee}		hypothetical protein	100	164	3.0E-03	1.6
-	CJSA_0665 ^{ee}	O	peptidase, U32 family	72	107	5.3E-03	1.5
-	CJSA_0667 ^{ee}		hypothetical protein	47	76	1.4E-02	1.6
-	CJSA_0669 ^{ee}	S	hypothetical protein	13	27	3.6E-06	2.1
-	CJSA_0670 ^{ee}	R	hypothetical protein	72	202	2.4E-09	2.8
<i>kdtA</i>	CJSA_0671 ^{ee}	M	3-deoxy-D-manno-octulosonic-acid transferase	4	27	7.1E-50	6.8
-	CJSA_0672 ^{ee}	J	putative ribosomal pseudouridine synthase	22	42	1.2E-04	1.9
<i>Ffh</i>	CJSA_0673 ^{ee}	U	signal recognition particle protein	87	141	2.2E-03	1.6
<i>rimM</i>	CJSA_0676 ^{ff}	J	16S rRNA processing protein RimM	83	160	5.8E-04	1.9
<i>trmD</i>	CJSA_0677 ^{ff}	J	tRNA (guanine-N(1)-)-methyltransferase	22	88	1.9E-27	4.0
<i>rpIS</i>	CJSA_0678 ^{ff}	J	50S ribosomal protein L19	307	546	3.7E-04	1.8
-	CJSA_0681	P	putative ArsC family protein	81	185	5.9E-06	2.3
-	CJSA_0688		hypothetical protein	96	144	1.6E-02	1.5
<i>corA</i>	CJSA_0690	P	magnesium and cobalt transport protein	88	162	1.2E-04	1.8
-	CJSA_0699		hypothetical protein	9	44	1.0E-35	4.9
-	CJSA_0708		hypothetical protein	3	126	0.0E+00	42.0
<i>tonB3</i>	CJSA_0710	M	TonB transport protein	23	73	7.2E-16	3.2

Table 6B continued

<i>cfrA</i>	CJSA_0712	P	ferric enterobactin uptake receptor	22	95	3.4E-23	4.3
<i>hcrA</i>	CJSA_0713 ^{gg}	K	heat-inducible transcription repressor	265	1056	9.3E-12	4.0
<i>grpE</i>	CJSA_0714 ^{gg}	O	heat shock protein GrpE	346	885	4.0E-05	2.6
-	CJSA_0716 ^{hh}	R	hypothetical protein	64	177	5.9E-10	2.8
-	CJSA_0717 ^{hh}	S	hypothetical protein	40	114	2.5E-12	2.9
<i>flgA</i>	CJSA_0725 ⁱⁱ	NO	flagellar basal body P-ring biosynthesis protein FlgA	10	40	7.5E-23	4.0
-	CJSA_0726 ⁱⁱ	P	NLPA family lipoprotein	52	118	6.5E-06	2.3
-	CJSA_0727 ⁱⁱ	P	NLPA family lipoprotein	97	259	1.8E-09	2.7
-	CJSA_0732		hypothetical protein	43	92	4.0E-05	2.1
<i>napL</i>	CJSA_0740 ^{ij}		hypothetical protein	11	31	1.7E-13	2.8
<i>napD</i>	CJSA_0741 ^{ij}	P	NapD protein-like protein	7	46	1.1E-51	6.6
-	CJSA_0743 ^{ij'}		hypothetical protein	31	89	6.4E-12	2.9
-	CJSA_0744 ^{ij}		hypothetical protein	33	96	1.9E-12	2.9
-	CJSA_0745 ^{ij}	J	polyA polymerase family protein	18	45	5.8E-08	2.5
<i>purU</i>	CJSA_0746 ^{ij}	F	formyltetrahydrofolate deformylase	22	48	4.5E-06	2.2
<i>flgS</i>	CJSA_0749	T	sensor histidine kinase	11	35	1.3E-15	3.2
<i>murF</i>	CJSA_0751	M	Mur ligase family protein	8	29	2.1E-18	3.6
-	CJSA_0753		prevent-host-death family protein	6	29	1.2E-22	4.8
-	CJSA_0765	R	metallo-beta-lactamase family protein	21	34	3.3E-03	1.6
-	CJSA_0770		hypothetical protein	3	30	1.5E-147	10.0
-	CJSA_0773 ^{kk}		putative lipoprotein	47	185	1.7E-27	3.9
-	CJSA_0774 ^{kk}		small hydrophobic protein	10	57	3.1E-36	5.7
-	CJSA_0785	S	hypothetical protein	11	107	2.4E-167	9.7
-	CJSA_0794		hypothetical protein	22	34	3.7E-02	1.5
<i>mobB</i>	CJSA_0796	H	molybdopterin-guanine dinucleotide biosynthesis protein MobB	5	43	9.4E-89	8.6
-	CJSA_0801 ^{ll}	R	Ser/Thr protein phosphatase family protein	22	51	2.6E-06	2.3
<i>Psd</i>	CJSA_0802 ^{ll}	I	phosphatidylserine decarboxylase	30	59	1.7E-04	2.0
-	CJSA_0805		putative MFS (Major Facilitator Superfamily) transport protein	12	53	2.5E-32	4.4
-	CJSA_0809		hypothetical protein	45	78	1.5E-03	1.7

Table 6B continued

<i>fspA2</i>	CJSA_0814		FspA2	114	381	9.0E-14	3.3
-	CJSA_0818 ^{mm}		hypothetical protein	109	175	1.6E-02	1.6
<i>dsbB</i>	CJSA_0819 ^{mm}	O	putative disulfide oxidoreductase	54	97	2.5E-03	1.8
-	CJSA_0822 ⁿⁿ	C	hypothetical protein	19	53	1.7E-08	2.8
-	CJSA_0823 ⁿⁿ	C	putative cytochrome C	90	166	9.8E-04	1.8
-	CJSA_0825		hypothetical protein	3	73	0.0E+00	24.3
<i>flhA</i>	CJSA_0829 ^{oo}	NU	flagellar biosynthesis protein FlhA	19	38	3.7E-04	2.0
-	CJSA_0830 ^{oo}	K	RrF2 family protein, putative	35	159	5.9E-36	4.5
<i>rspO</i>	CJSA_0831	J	30S ribosomal protein S15	212	480	4.5E-06	2.3
<i>ftsK</i>	CJSA_0832	D	putative cell division protein	22	62	2.8E-10	2.8
<i>flgL</i>	CJSA_0833	N	flagellar hook-associated protein FlgL	155	817	3.4E-20	5.3
-	CJSA_0846		small hydrophobic protein	10	31	4.0E-08	3.1
<i>Alr</i>	CJSA_0851	M	alanine racemase	8	35	2.0E-32	4.4
-	CJSA_0852	S	hypothetical protein	30	126	1.8E-23	4.2
<i>cheR</i>	CJSA_0868	NT	putative MCP protein methyltransferase	25	66	2.4E-10	2.6
<i>rpiB</i>	CJSA_0870 ^{pp}	G	ribose 5-phosphate isomerase B	54	143	3.5E-09	2.6
-	CJSA_0871 ^{pp}		hypothetical protein	25	81	3.2E-16	3.2
<i>Apt</i>	CJSA_0872 ^{pp}	F	adenine phosphoribosyltransferase	39	65	3.4E-03	1.7
<i>Aas</i>	CJSA_0883 ^{qq}	IQ	2-acylglycerophosphoethanolamine acyltransferase	14	29	1.0E-04	2.1
-	CJSA_0884 ^{qq}		hypothetical protein	1	60	0.0E+00	60.0
-	CJSA_0894	E	peptidyl-arginine deiminase family protein	24	41	4.8E-03	1.7
-	CJSA_0897		putative HAMP containing membrane protein	22	45	1.6E-05	2.0
-	CJSA_0904 ^{rr}	S	hypothetical protein	84	155	1.6E-03	1.8
<i>rnpA</i>	CJSA_0905 ^{rr}	J	ribonuclease P protein component	312	463	5.0E-03	1.5
-	CJSA_0910	R	putative acyl-CoA thioester hydrolase	31	85	2.3E-11	2.7
-	CJSA_0920	Q	hypothetical protein	521	1943	1.3E-10	3.7
<i>rpoD</i>	CJSA_0944	K	RNA polymerase sigma factor RpoD	83	239	3.1E-08	2.9
-	CJSA_0952	S	TrkA domain-containing protein	17	35	1.4E-04	2.1
<i>Tgt</i>	CJSA_0953	J	queuine tRNA-ribosyltransferase	15	28	1.7E-04	1.9

Table 6B continued

-	CJSA_0964		porin domain-containing protein	16	81	3.1E-36	5.1
<i>flgR</i>	CJSA_0967 ^{ss}	T	sigma-54 associated transcriptional activator	34	178	3.8E-37	5.2
-	CJSA_0968 ^{ss}		hypothetical protein	82	438	1.1E-40	5.3
-	CJSA_0971 ^{ss'}	R	putative purine/pyrimidine phosphoribosyltransferase	28	49	1.4E-03	1.8
<i>cmeD</i>	CJSA_0974 ^{tt}	MU	outer membrane component multidrug efflux system CmeDEF	19	73	6.9E-22	3.8
<i>cmeE</i>	CJSA_0975 ^{tt}	M	membrane fusion component multidrug efflux system CmeDEF	23	45	3.1E-05	2.0
-	CJSA_0977	O	adenylosuccinate lyase	37	191	3.5E-38	5.2
-	CJSA_0983 ^{uu}	P	putative MFS (Major Facilitator Superfamily) transport protein	5	33	1.9E-57	6.6
-	CJSA_0984 ^{uu}		putative periplasmic ATP/GTP-binding protein	20	32	9.6E-03	1.6
<i>this</i>	CJSA_0990	H	thiamine biosynthesis protein ThiS	29	43	4.2E-02	1.5
<i>murC</i>	CJSA_0997	M	UDP-N-acetylmuramate--L-alanine ligase	34	54	2.1E-02	1.6
<i>rpsF</i>	CJSA_1012 ^{vv}	J	30S ribosomal protein S6	557	945	2.7E-02	1.7
<i>Ssb</i>	CJSA_1013 ^{vv}	L	single-stranded DNA-binding protein	392	700	1.8E-02	1.8
-	CJSA_1016	R	putative lipoprotein	70	126	2.2E-03	1.8
-	CJSA_1017	S	flagellar assembly factor FlhW	137	372	8.4E-09	2.7
<i>mfd</i>	CJSA_1027	LK	transcription-repair coupling factor	23	44	2.0E-04	1.9
-	CJSA_1029 ^{ww}	M	M24/M37 family peptidase	60	142	2.0E-06	2.4
<i>folC</i>	CJSA_1030 ^{ww}	H	olylpolyglutamate synthase/dihydrofolate synthase	7	45	7.9E-71	6.4
-	CJSA_1039 ^{xx}	E	serine/threonine transporter SstT	14	35	1.7E-09	2.5
<i>pyrB</i>	CJSA_1040 ^{xx}	F	aspartate carbamoyltransferase catalytic subunit	19	33	1.2E-03	1.7
<i>csrA</i>	CJSA_1045 ^{xx'}	T	carbon storage regulator	89	162	3.3E-04	1.8
-	CJSA_1046 ^{xx}	I	4-diphosphocytidyl-2-C-methyl-D-erythritol kinase	13	35	3.2E-10	2.7
<i>prmA</i>	CJSA_1059 ^{yy}	J	50S ribosomal protein L11 methyltransferase	82	201	9.8E-08	2.5
<i>cheY</i>	CJSA_1060 ^{yy}	T	chemotaxis protein CheY	470	791	1.7E-02	1.7
-	CJSA_1086		hypothetical protein	7	37	1.0E-35	5.3
<i>gmhB</i>	CJSA_1092	E	D,D-heptose 1,7-bisphosphate phosphatase	10	32	2.2E-12	3.2
-	CJSA_1094	P	putative cytochrome oxidase maturation protein, cbb3-type	6	28	7.2E-25	4.7
<i>Rho</i>	CJSA_1096 ^{zz}	K	transcription termination factor Rho	59	114	8.2E-05	1.9
<i>dnaX</i>	CJSA_1097 ^{zz}	L	DNA polymerase III subunits gamma and tau	17	39	4.0E-06	2.3

Table 6B continued

-	CJSA_1100 ^{aaa}		putative heavy-metal-associated domain protein	14	50	1.5E-14	3.6
-	CJSA_1101 ^{aaa}	P	cation efflux family protein	41	77	1.2E-03	1.9
-	CJSA_1104	S	hypothetical protein	8	25	4.2E-11	3.1
<i>omp50</i>	CJSA_1108		50 kda outer membrane protein precursor	112	172	2.0E-02	1.5
-	CJSA_1111 ^{bbb}	P	SMR family multidrug efflux pump	5	25	1.3E-21	5.0
-	CJSA_1112 ^{bbb}	P	SMR family multidrug efflux pump	5	34	7.4E-41	6.8
-	CJSA_1116 ^{ccc}		hypothetical protein	59	99	6.1E-04	1.7
<i>fliR</i>	CJSA_1117 ^{ccc}	NU	flagellar biosynthesis protein FliR	3	47	0.0E+00	15.7
-	CJSA_1118 ^{ccc}	V	ABC transporter ATP-binding protein	33	128	5.4E-24	3.9
<i>rpsB</i>	CJSA_1120 ^{ccc'}	J	30S ribosomal protein S2	374	750	4.7E-03	2.0
<i>Cfa</i>	CJSA_1121	M	cyclopropane-fatty-acyl-phospholipid synthase	57	135	4.5E-07	2.4
<i>gidA</i>	CJSA_1126	D	tRNA uridine 5-carboxymethylaminomethyl modification protein GidA	34	52	1.1E-02	1.5
-	CJSA_1129	T	putative PAS domain containing signal-transduction sensor protein	24	137	2.1E-68	5.7
-	CJSA_1131		hypothetical protein	5	26	4.6E-35	5.2
<i>pyrC2</i>	CJSA_1133	F	Dihydroorotase	21	33	1.4E-02	1.6
<i>atpB</i>	CJSA_1142	C	F0F1 ATP synthase subunit A	67	176	5.5E-08	2.6
-	CJSA_1146 ^{ddd}	H	putative 5-formyltetrahydrofolate cyclo-ligase family protein	14	57	4.1E-30	4.1
-	CJSA_1147 ^{ddd}	R	Phosphodiesterase	54	103	7.2E-05	1.9
-	CJSA_1148 ^{ddd}	S	DedA family protein	18	37	6.7E-06	2.1
-	CJSA_1153	M	peptidase, M23/M37 family	37	56	4.1E-02	1.5
-	CJSA_1162	P	hemerythrin family non-heme iron protein	63	93	5.0E-02	1.5
<i>cbpA</i>	CJSA_1167 ^{eee}	O	co-chaperone protein DnaJ	107	344	1.2E-15	3.2
<i>hspR</i>	CJSA_1168 ^{eee}	K	heat shock transcriptional regulator	176	322	4.8E-04	1.8
<i>kefB</i>	CJSA_1169 ^{eee}	P	putative glutathione-regulated potassium-efflux system protein	24	59	4.4E-07	2.5
-	CJSA_1180		hypothetical protein	470	3330	2.1E-69	7.1
<i>hemE</i>	CJSA_1181	H	uroporphyrinogen decarboxylase	116	188	2.1E-03	1.6
<i>uvrC</i>	CJSA_1184 ^{fff}	L	excinuclease ABC subunit C	7	31	6.1E-27	4.4
-	CJSA_1185 ^{fff}		hypothetical protein	1	29	0.0E+00	29.0
-	CJSA_1186		hypothetical protein	26	102	2.5E-19	3.9

Table 6B continued

-	CJSA_1188	D	hypothetical protein	16	25	2.0E-02	1.6
<i>purD</i>	CJSA_1189 ^{egg}	F	phosphoribosylamine--glycine ligase	268	451	2.4E-02	1.7
-	CJSA_1190 ^{egg}	S	hypothetical protein	78	161	1.6E-04	2.1
-	CJSA_1191 ^{egg}	M	hypothetical protein	26	77	2.0E-10	3.0
-	CJSA_1194	R	putative isomerase	13	56	1.9E-22	4.3
<i>racS</i>	CJSA_1201	T	two-component sensor (histidine kinase)	42	83	2.2E-04	2.0
-	CJSA_1215		hypothetical protein	4	25	2.5E-55	6.3
-	CJSA_1219	J	putative ribosomal pseudouridine synthase	34	78	1.4E-05	2.3
<i>ktrB</i>	CJSA_1221 ^{hhh}	P	putative K ⁺ uptake protein	5	29	8.6E-54	5.8
<i>ktrA</i>	CJSA_1222 ^{hhh}	P	putative K ⁺ uptake protein	15	25	1.6E-03	1.7
<i>pseB</i>	CJSA_1231 ⁱⁱⁱ	MG	UDP-GlcNAc-specific C4,6 dehydratase/C5 epimerase	301	729	2.4E-04	2.4
<i>pseC</i>	CJSA_1232 ⁱⁱⁱ	M	C4 aminotransferase specific for PseB product	102	318	1.4E-13	3.1
-	CJSA_1233 ⁱⁱⁱ	R	hypothetical protein	22	85	4.4E-19	3.9
<i>acpP2</i>	CJSA_1237 ^{iii'}	IQ	putative acyl carrier protein	48	83	6.9E-04	1.7
-	CJSA_1245	Q	putative amino acid activating enzyme	22	34	3.5E-02	1.5
-	CJSA_1248		hypothetical protein	36	60	8.2E-03	1.7
<i>hisF</i>	CJSA_1252	E	imidazole glycerol phosphate synthase subunit HisF	78	117	2.1E-02	1.5
<i>maf1</i>	CJSA_1256	S	motility accessory factor	19	63	1.9E-13	3.3
-	CJSA_1262 ^{jjj}	J	putative methyltransferase	24	69	8.6E-13	2.9
<i>neuB2</i>	CJSA_1263 ^{jjj}	M	N-acetylneuraminate synthase	95	403	6.6E-29	4.2
<i>neuC2</i>	CJSA_1264 ^{jjj}	M	putative UDP-N-acetylglucosamine 2-epimerase	13	78	1.1E-64	6.0
-	CJSA_1265 ^{jjj}	MJ	putative sugar-phosphate nucleotide transferase	12	40	5.5E-19	3.3
-	CJSA_1266 ^{jjj}	R	hypothetical protein	24	99	5.4E-26	4.1
<i>ptmB</i>	CJSA_1267 ^{jjj}	M	cylneuraminate cytidyltransferase (flagellin modification)	122	316	1.5E-09	2.6
<i>ptmA</i>	CJSA_1268 ^{jjj}	IQ	flagellin modification protein A	94	178	1.5E-04	1.9
<i>maf3</i>	CJSA_1270 ^{jjj'}	S	motility accessory factor	15	25	1.2E-02	1.7
<i>maf4</i>	CJSA_1271 ^{jjj}	S	motility accessory factor	18	63	3.0E-15	3.5
<i>Dxr</i>	CJSA_1281 ^{kkk}	I	1-deoxy-D-xylulose 5-phosphate reductoisomerase	41	79	5.0E-04	1.9
<i>cdsA</i>	CJSA_1282 ^{kkk}	I	phosphatidate cytidyltransferase	55	110	1.9E-04	2.0

Table 6B continued

-	CJSA_1283 ^{kkk}		putative coiled-coil protein	104	262	2.9E-07	2.5
-	CJSA_1291		hypothetical protein	46	101	1.3E-05	2.2
<i>nrfA</i>	CJSA_1292 ^{lll}	P	putative periplasmic cytochrome C	37	140	6.9E-20	3.8
<i>nrfH</i>	CJSA_1293 ^{lll}	C	putative periplasmic cytochrome C	16	177	6.6E-294	11.1
<i>ruvB</i>	CJSA_1296	L	Holliday junction DNA helicase RuvB	19	42	7.6E-07	2.2
-	CJSA_1301	O	putative nucleotidyltransferase	13	27	8.5E-05	2.1
-	CJSA_1302	HR	hypothetical protein	69	102	1.4E-02	1.5
-	CJSA_1304 ^{mmm}	R	putative nucleotide phosphoribosyltransferase	26	39	9.6E-03	1.5
-	CJSA_1305 ^{mmm}	M	putative periplasmic protein (VacJ-like protein)	24	37	1.1E-02	1.5
-	CJSA_1306 ^{mmm}	Q	putative periplasmic toluene tolerance protein	10	25	2.3E-07	2.5
-	CJSA_1308	F	RdgB/HAM1 family non-canonical purine NTP pyrophosphatase	9	40	3.0E-23	4.4
<i>selA</i>	CJSA_1312	E	selenocysteine synthase	16	25	1.0E-02	1.6
-	CJSA_1317 ⁿⁿⁿ		hypothetical protein	4	46	1.4E-216	11.5
-	CJSA_1318 ⁿⁿⁿ	S	hypothetical protein	41	169	9.6E-30	4.1
<i>kata</i>	CJSA_1319 ^{ooo}	P	Catalase	76	405	3.1E-46	5.3
-	CJSA_1320 ^{ooo}	R	ankyrin repeat-containing protein	10	92	4.0E-144	9.2
-	CJSA_1321	S	helix-turn-helix containing protein	17	39	2.6E-07	2.3
-	CJSA_1328	P	putative ferrous iron transport protein	15	52	2.2E-15	3.5
-	CJSA_1343 ^{ppp}		hypothetical protein	9	57	2.2E-70	6.3
<i>kpsS</i>	CJSA_1344 ^{ppp}	M	capsule polysaccharide export protein KpsS	11	48	4.8E-32	4.4
-	CJSA_1348	R	putative amidotransferase	17	43	1.5E-09	2.5
-	CJSA_1354 ^{qqq}		capsular polysaccharide biosynthesis protein	9	42	1.1E-32	4.7
-	CJSA_1355 ^{qqq}		capsule biosynthesis phosphatase	85	145	6.8E-03	1.7
-	CJSA_1361 ^{qqq'}	R	HAD superfamily hydrolase	8	46	3.4E-49	5.8
-	CJSA_1362 ^{qqq}	C	hypothetical protein	12	48	2.2E-25	4.0
<i>kpsT</i>	CJSA_1371 ^{rrr}	GM	capsular polysaccharide ABC transporter ATP-binding protein	49	143	7.0E-10	2.9
<i>kpsM</i>	CJSA_1372 ^{rrr}	GM	capsular polysaccharide ABC transporter permease	47	80	6.3E-03	1.7
-	CJSA_1374		putative ATP/GTP-binding protein	478	941	7.3E-03	2.0
-	CJSA_1376		hypothetical protein	6	28	9.5E-22	4.7

Table 6B continued

<i>prfB</i>	CJSA_1379	J	peptide chain release factor 2	30	56	1.9E-03	1.9
<i>thiL</i>	CJSA_1382	H	thiamine monophosphate kinase	7	27	3.8E-20	3.9
-	CJSA_1383		hypothetical protein	27	48	4.9E-03	1.8
<i>flgI</i>	CJSA_1386 ^{sss}	N	lagellar basal body P-ring protein	218	627	8.8E-06	2.9
-	CJSA_1387 ^{sss}		hypothetical protein	89	441	4.4E-34	5.0
-	CJSA_1389 ^{sss'}		hypothetical protein	572	2299	8.0E-12	4.0
<i>flgK</i>	CJSA_1390 ^{sss}	N	flagellar hook-associated protein FlgK	127	571	3.8E-15	4.5
-	CJSA_1391 ^{sss}		hypothetical protein	8	36	1.8E-28	4.5
-	CJSA_1392 ^{sss}	R	hypothetical protein	12	28	3.1E-08	2.3
<i>ctsR</i>	CJSA_1398		hypothetical protein	18	38	4.5E-05	2.1
-	CJSA_1406		putative lipoprotein	20	43	2.7E-06	2.2
-	CJSA_1415 ^{ttt}	T	putative two-component sensor	47	101	3.1E-05	2.1
-	CJSA_1416 ^{ttt}	S	hypothetical protein	14	33	7.0E-08	2.4
<i>carA</i>	CJSA_1417 ^{ttt}	EF	carbamoyl phosphate synthase small subunit	103	191	2.0E-04	1.9
-	CJSA_1418 ^{ttt}	S	hypothetical protein	77	235	1.5E-11	3.1
-	CJSA_1419 ^{ttt}	S	hypothetical protein	56	87	2.9E-02	1.6
-	CJSA_1422 ^{uuu}	R	putative inner membrane protein	16	27	3.5E-03	1.7
-	CJSA_1423 ^{uuu}	O	hypothetical protein	16	37	1.4E-05	2.3
<i>selD</i>	CJSA_1426	E	putative selenide,water dikinase	27	51	6.5E-04	1.9
-	CJSA_1427	O	putative two-component response regulator (SirA-like protein)	31	87	1.1E-11	2.8
-	CJSA_1434 ^{vvv}		Tat pathway signal sequence domain-containing protein	185	402	3.9E-05	2.2
-	CJSA_1435 ^{vvv}	R	hypothetical protein	56	291	5.2E-38	5.2
<i>dapF</i>	CJSA_1447 ^{www}	E	diaminopimelate epimerase	39	86	4.1E-05	2.2
-	CJSA_1448 ^{www}	R	hypothetical protein	12	31	9.4E-10	2.6
-	CJSA_1449	R	putative helix-turn-helix containing protein	30	165	7.6E-42	5.5
-	CJSA_1462 ^{xxx}	K	putative transcriptional regulator	6	29	5.6E-21	4.8
-	CJSA_1463 ^{xxx}	M	Blc protein-like protein	7	25	6.7E-14	3.6
-	CJSA_1471	K	putative transcriptional regulator	6	57	1.1E-100	9.5
<i>pflA</i>	CJSA_1477		paralysed flagellum protein	8	27	5.9E-16	3.4

Table 6B continued

-	CJSA_1486		hypothetical protein	25	37	2.0E-02	1.5
<i>nuoA</i>	CJSA_1491	C	NADH dehydrogenase I subunit A	36	90	3.3E-09	2.5
-	CJSA_1496	E	putative peptide ABC-transport periplasmic peptide-binding protein	13	32	1.3E-08	2.5
<i>infA</i>	CJSA_1502	J	translation initiation factor IF-1	32	94	5.0E-12	2.9
<i>rpmJ</i>	CJSA_1503 ^{yyy}		50S ribosomal protein L36	466	1058	6.4E-06	2.3
<i>rpsM</i>	CJSA_1504 ^{yyy}	J	30S ribosomal protein S13	448	775	5.8E-03	1.7
<i>rpsK</i>	CJSA_1505 ^{yyy}	J	30S ribosomal protein S11	461	862	5.7E-03	1.9
-	CJSA_1525	P	putative pyridoxamine 5-phosphate oxidase	201	350	2.9E-03	1.7
<i>chuA</i>	CJSA_1526 ^{zzz}	P	hemin uptake system outer membrane receptor	32	74	1.3E-06	2.3
<i>chuB</i>	CJSA_1527 ^{zzz}	P	putative hemin uptake system permease protein	14	39	3.3E-12	2.8
<i>chuD</i>	CJSA_1529 ^{zzz'}	P	putative hemin uptake system periplasmic hemin-binding protein	10	28	3.4E-11	2.8
-	CJSA_1533		hypothetical protein	14	31	7.0E-07	2.2
<i>ribD</i>	CJSA_1534 [^]	H	riboflavin-specific deaminase/reductase	3	100	0.0E+00	33.3
-	CJSA_1535 [^]		hypothetical protein	2	29	8.4E-229	14.5
<i>exbB2</i>	CJSA_1540*	U	exbB/tolQ family transport protein	59	112	5.7E-04	1.9
<i>exbD2</i>	CJSA_1541*	U	exbB/tolQ family transport protein	20	52	1.6E-09	2.6
-	CJSA_1544		hypothetical protein	26	174	1.2E-70	6.7
<i>rnhA</i>	CJSA_1548 [#]	L	ribonuclease H	24	35	1.8E-02	1.5
-	CJSA_1549 [#]	G	hypothetical protein	5	46	4.2E-119	9.2
<i>dnaG</i>	CJSA_1550	L	DNA primase	17	37	2.7E-05	2.2
-	CJSA_1552		hypothetical protein	18	60	6.2E-19	3.3
-	CJSA_1554	S	hypothetical protein	44	102	2.9E-07	2.3
-	CJSA_1560	Q	putative ABC transport system periplasmic substrate-binding protein	8	26	7.9E-14	3.3
-	CJSA_1562		hypothetical protein	77	343	3.1E-27	4.5
<i>murl</i>	CJSA_1564^^	M	glutamate racemase	11	28	2.1E-08	2.5
<i>nlpC</i>	CJSA_1565^^	M	putative lipoprotein nlpC	33	60	5.5E-04	1.8
<i>nhaA2</i>	CJSA_1566^^	P	Na ⁺ /H ⁺ antiporter	32	98	1.7E-11	3.1
<i>nhaA1</i>	CJSA_1567^^	P	Na ⁺ /H ⁺ antiporter	25	251	9.6E-182	10.0
-	CJSA_1579		hypothetical protein	26	165	1.0E-83	6.3

Table 6B continued

-	CJSA_1590		hypothetical protein	11	25	1.5E-06	2.3
-	CJSA_1596	G	putative MSF family efflux protein	23	93	1.2E-21	4.0
<i>rpIW</i>	CJSA_1614**	J	50S ribosomal protein L23	259	487	1.7E-04	1.9
<i>rpIC</i>	CJSA_1616**'	J	50S ribosomal protein L3	279	477	6.0E-03	1.7
<i>rpsJ</i>	CJSA_1617**	J	30S ribosomal protein S10	293	576	2.0E-05	2.0
<i>ksgA</i>	CJSA_1620	J	dimethyladenosine transferase	44	130	3.6E-10	3.0
-	CJSA_1621	F	hypothetical protein	8	27	2.6E-12	3.4
-	CJSA_1624	R	GNAT family acetyltransferase	15	110	6.6E-112	7.3
-	CJSA_1631	R	putative GTP cyclohydrolase I	12	167	0.0E+00	13.9
-	CJSA_pVir0013		hypothetical protein	6	55	2.5E-103	9.2
-	CJSA_pVir0016		hypothetical protein	12	31	2.4E-08	2.6
-	CJSA_pVir0020		hypothetical protein	14	25	2.9E-03	1.8
-	CJSA_pVir0024 ^{##}		putative plasmid partitioning ParA protein	33	135	1.9E-26	4.1
-	CJSA_pVir0025 ^{##}		hypothetical protein	19	103	1.7E-55	5.4
<i>repE</i>	CJSA_pVir0026		putative replication protein RepE	26	283	1.0E-263	10.9
-	CJSA_pVir0032		hypothetical protein	18	33	3.1E-04	1.8
-	CJSA_pVir0034		hypothetical protein	1	47	0.0E+00	47.0
-	CJSA_pVir0040^^		hypothetical protein	11	89	1.0E-82	8.1
-	CJSA_pVir0041^^		hypothetical protein	27	138	3.2E-35	5.1
-	CJSA_pVir0042		hypothetical protein	8	124	0.0E+00	15.5
-	CJSA_pVir0044		hypothetical protein	5	112	0.0E+00	22.4
-	CJSA_pVir0045***		hypothetical protein	66	178	1.1E-10	2.7
-	CJSA_pVir0046***		putative RelE/StbE family addiction module toxin	16	55	1.7E-13	3.4
<i>rnpB</i>	CJSA_CjrnpB1	-		22	166	3.4E-110	7.5
-	CJSA_t0001		Ala tRNA	27	217	3.0E-85	8.0
-	CJSA_t0002		Ile tRNA	49	463	9.1E-155	9.4
-	CJSA_t0004		Ala tRNA	35	206	8.2E-48	5.9
-	CJSA_t0005		Ile tRNA	49	461	9.0E-153	9.4
-	CJSA_t0006		Thr tRNA	97	306	3.0E-14	3.2

Table 6B continued

-	CJSA_t0008	Gly tRNA	1429	2162	4.7E-03	1.5
-	CJSA_t0009	Thr tRNA	590	1716	3.4E-10	2.9
-	CJSA_t0011	Arg tRNA	92	248	6.7E-10	2.7
-	CJSA_t0012	Met tRNA	25	111	3.3E-21	4.4
-	CJSA_t0014	Ala tRNA	34	213	2.7E-53	6.3
-	CJSA_t0015	Ile tRNA	51	422	2.7E-115	8.3
-	CJSA_t0018	Leu tRNA	43	69	2.7E-02	1.6
-	CJSA_t0019	Asp tRNA	25	172	5.0E-56	6.9
-	CJSA_t0020	Val tRNA	46	167	4.0E-16	3.6
-	CJSA_t0021	Arg tRNA	243	529	1.5E-06	2.2
-	CJSA_t0022	Lys tRNA	223	589	2.4E-10	2.6
-	CJSA_t0023	Val tRNA	64	301	1.8E-29	4.7
-	CJSA_t0024	Lys tRNA	29	125	9.1E-20	4.3
-	CJSA_t0032	Gly tRNA	144	210	1.3E-02	1.5
-	CJSA_t0033	Leu tRNA	418	745	3.0E-03	1.8
-	CJSA_t0034	Cys tRNA	255	865	1.2E-18	3.4
-	CJSA_t0035	Ser tRNA	81	343	3.2E-28	4.2
-	CJSA_t0037	Arg tRNA	318	610	3.3E-04	1.9
-	CJSA_t0038	Arg tRNA	583	1123	5.0E-04	1.9
-	CJSA_t0040	Pro tRNA	81	139	2.7E-03	1.7
-	CJSA_t0041	Met tRNA	2	41	0.0E+00	20.5
-	CJSA_t0043	Ala tRNA	19	73	8.7E-18	3.8
-	CJSA_t0044	Val tRNA	53	260	1.0E-33	4.9
-	predicted RNA	99nt length; 250059 to 249960 negative strand	94	139	1.1E-02	1.5
-	predicted RNA	109nt length; 815016 to 815125 positive strand	52	77	4.6E-02	1.5
-	predicted RNA	825nt length; 1047424 to 1046599 negative strand	276	437	4.6E-02	1.6
-	predicted RNA	antisense: CJSA_0417; 44nt length, 419785 to 419741 negative strand	99	160	2.1E-02	1.6
-	predicted RNA	266nt length; 1630649 to 1630383 negative strand	187	310	7.3E-03	1.7
-	predicted RNA	54nt length; 388170 to 388224 positive strand	112	209	6.1E-04	1.9

Table 6B continued

-	predicted RNA	antisense: prfA; 96nt length, 1537068 to 1536972 negative strand	86	163	1.1E-04	1.9
-	predicted RNA	109nt length; 1630884 to 1630775 negative strand	117	237	2.1E-05	2.0
-	predicted RNA	antisense: CJSa_0136; 16nt length, 150574 to 150558 negative strand	65	140	7.0E-05	2.2
-	predicted RNA	34nt length; 1522668 to 1522702 positive strand	44	98	9.2E-05	2.2
-	predicted RNA	42nt length; 735002 to 735044 positive strand	26	60	2.0E-05	2.3
-	predicted RNA	39nt length; 1113972 to 1113933 negative strand	216	520	2.0E-08	2.4
-	predicted RNA	283nt length; 1046498 to 1046215 negative strand	80	212	1.4E-09	2.7
-	predicted RNA	61nt length; 809228 to 809167 negative strand	59	197	9.2E-14	3.3
-	predicted RNA	269nt length; 1555790 to 1555521 negative strand	95	326	1.3E-15	3.4
-	predicted RNA	101nt length; 726401 to 726300 negative strand	179	637	5.2E-21	3.6
-	predicted RNA	18nt length; 1463578 to 1463560 negative strand	22	80	8.4E-14	3.6
-	predicted RNA	antisense: CJSa_0921; 93nt length, 915128 to 915221 positive strand	45	164	1.9E-16	3.6
-	predicted RNA	13nt length; 1153787 to 1153800 positive strand	1007	3802	5.1E-24	3.8
-	predicted RNA	antisense: dccS; 116nt length, 1155464 to 1155580 positive strand	76	290	4.6E-25	3.8
-	predicted RNA	antisense: CJSa_0401; 61nt length, 395623 to 395684 positive strand	149	569	1.8E-25	3.8
-	predicted RNA	11nt length; 914526 to 914537 positive strand	61	234	5.2E-16	3.8
-	predicted RNA	16nt length; 71942 to 71926 negative strand	77	311	7.6E-21	4.0
-	predicted RNA	31nt length; 1386282 to 1386313 positive strand	119	533	1.8E-27	4.5
-	predicted RNA	22nt length; 1053999 to 1053977 negative strand	46	219	9.1E-31	4.8
-	predicted RNA	711nt length; 197103 to 197814 positive strand	41	199	8.7E-33	4.9
-	predicted RNA	10nt length; 1163099 to 1163109 positive strand	55	296	5.4E-34	5.4
-	predicted RNA	antisense: CJSa_0390; 81nt length, 388537 to 388618 positive strand	41	233	5.2E-46	5.7
-	predicted RNA	antisense: CJSa_0363; 359nt length, 362675 to 362316 negative strand	72	412	2.7E-51	5.7
-	predicted RNA	antisense: CJSa_0223; 161nt length, 231589 to 231750	58	386	5.3E-96	6.7
-	predicted RNA	9nt length; 198494 to 198503 positive strand	18	121	5.5E-56	6.7
-	predicted RNA	70nt length; 1175070 to 1175140 positive strand	106	766	4.6E-105	7.2
-	predicted RNA	23nt length; 197874 to 197897 positive strand	13	102	3.6E-66	7.8
-	predicted RNA	antisense: flpP; 78nt length, 771731 to 771809 positive strand	15	119	1.3E-96	7.9
-	predicted RNA	69nt length; 210449 to 210518 positive strand	17	143	4.6E-105	8.4

Table 6B continued

-	predicted RNA	antisense: ispG; 155nt length, 644706 to 644551 negative strand	32	272	2.4E-118	8.5
-	predicted RNA	37nt length; 198556 to 198593 positive strand	16	144	3.6E-110	9.0
-	predicted RNA	55nt length; 417148 to 417203 positive strand	20	185	3.5E-145	9.3
-	predicted RNA	antisense: pbpA; 61nt length, 479304 to 479243 negative strand	14	131	5.9E-132	9.4
-	predicted RNA	129nt length; 1193304 to 1193433 positive strand	23	227	6.1E-162	9.9
-	predicted RNA	antisense: CJSa_0390; 14nt length, 388983 to 388997 positive strand	8	102	1.5E-190	12.8
-	predicted RNA	antisense: CJSa_0826; 174nt length; 818541 to 818715 positive strand	13	166	1.7E-273	12.8
-	predicted RNA	20nt length; 409962 to 409982 positive strand	12	157	2.4E-230	13.1
-	predicted RNA	23nt length; 198048 to 198071 positive strand	10	135	1.7E-253	13.5
-	predicted RNA	34nt length; 1555303 to 1555269 negative strand	11	149	6.0E-282	13.5
-	predicted RNA	35nt length; 1259305 to 1259340 positive strand	37	601	0.0E+00	16.2
-	predicted RNA	52nt length; 959493 to 959441 negative strand	9	168	0.0E+00	18.7
-	predicted RNA	94nt length; 1572367 to 1572461 positive strand	13	258	0.0E+00	19.8
-	predicted RNA	antisense: CJSa_0401; 33nt length, 395896 to 395929 positive strand	6	120	0.0E+00	20.0
-	predicted RNA	10nt length; 1175229 to 1175929 positive strand	7	150	0.0E+00	21.4
-	predicted RNA	antisense: pseE; 274nt length, 1272527 to 1272253 negative strand	8	182	0.0E+00	22.8
-	predicted RNA	antisense: glnA; 123nt length, 660916 to 661039 positive strand	8	185	0.0E+00	23.1
-	predicted RNA	17nt length; 1465 to 1482 positive strand	6	140	0.0E+00	23.3
-	predicted RNA	19nt length; 59713 to 59732 positive strand	8	413	0.0E+00	51.6
-	predicted RNA	18nt length; 706803 to 706821 positive strand	2	162	0.0E+00	81.0
-	predicted RNA	13nt length; 645467 to 645454 negative strand	1	122	0.0E+00	122.0
-	predicted RNA	24nt length; 828765 to 828741 negative strand	2	245	0.0E+00	122.5
-	predicted RNA	antisense: pseE; 69nt length, 1271969 to 1271900 negative strand	0	110	0.0E+00	110.0
-	predicted RNA	25nt length; 31479 to 31504 positive strand pVir	47	108	2.3E-05	2.3
-	predicted RNA	antisense: CJSa_pVir0033; 168 length, 25244 to 25412 positive strand	208	542	7.1E-08	2.6

a, b, aa, bb, ect = matching superscript signifies expression within the same operon

Table 7. List of annotated genes identified to be upregulated under all four conditions when compared with the unexposed IA 3902 inoculum with a comparison of fold change under each category.

Name	Synonym	COG Code	Product	Fold Change			
				GB <i>in vivo</i> 2 hr	GB <i>in vivo</i> 24 hr	Bile <i>in vitro</i> 2 hr	Bile <i>in vitro</i> 24 hr
-	CJSA_0035	G	MFS family drug resistance transporter	3.5	3.3	2.0	3.7
-	CJSA_0040		hypothetical protein	21.4	52.2	10.9	15.1
-	CJSA_0041		hypothetical protein	3.1	6.1	1.6	2.2
-	CJSA_0045	P	putative iron-binding protein	2.8	5.3	3.8	4.2
-	CJSA_0049		hypothetical protein	1.9	3.9	1.5	1.6
-	CJSA_0056		hypothetical protein	3.0	10.6	1.6	3.2
<i>folk</i>	CJSA_0059	H	2-amino-4-hydroxy-6-hydroxymethyldihydropteridine pyrophosphokinase	2.7	3.3	2.9	3.1
<i>atpF'</i>	CJSA_0093	C	FOF1 ATP synthase subunit B	2.7	4.1	1.9	2.5
-	CJSA_0126	K	hypothetical protein	2.5	4.4	2.3	2.9
-	CJSA_0166		putative lipoprotein	4.8	12.4	2.2	3.5
-	CJSA_0305		hypothetical protein	2.8	4.9	1.5	2.8
<i>cmeB</i>	CJSA_0339	V	RND efflux system, inner membrane transporter CmeB	3.7	1.7	1.7	1.9
<i>cmeA</i>	CJSA_0340	M	RND efflux system, membrane fusion protein CmeA	3.8	2.6	2.3	2.1
-	CJSA_0370		hypothetical protein	3.2	6.6	2.6	5.0
<i>sdhA</i>	CJSA_0409	C	succinate dehydrogenase, flavoprotein subunit	6.5	2.4	2.5	1.5
<i>sdhB</i>	CJSA_0410	C	succinate dehydrogenase, iron-sulfur protein subunit	5.0	2.0	2.5	1.5
-	CJSA_0426		hypothetical protein	3.5	10.4	1.8	3.8
-	CJSA_0528		hypothetical protein	29.3	21.3	17.3	15.8
<i>Nth</i>	CJSA_0563	L	endonuclease III	2.2	3.9	2.3	4.2
-	CJSA_0596	L	prophage Lp2 protein 6	1.5	2.4	1.5	2.1
-	CJSA_0636		hypothetical protein	2.2	2.8	1.5	2.3
<i>flgH</i>	CJSA_0651	N	flagellar basal body L-ring protein	1.6	4.4	2.0	1.7
-	CJSA_0655		hypothetical protein	2.4	4.9	1.6	3.9

Table 7 continued

-	CJSA_0716	R	hypothetical protein	2.9	2.8	1.7	1.7
-	CJSA_0785	S	hypothetical protein	2.8	9.7	2.3	6.2
-	CJSA_0818		hypothetical protein	2.7	1.6	2.7	2.2
<i>dsbB</i>	CJSA_0819	O	putative disulfide oxidoreductase	3.5	1.8	2.6	2.2
<i>flgL</i>	CJSA_0833	N	flagellar hook-associated protein FlgL	2.2	5.3	1.9	1.9
-	CJSA_0852	S	hypothetical protein	1.9	4.2	1.5	2.0
-	CJSA_0920	Q	hypothetical protein	2.0	3.7	2.3	1.5
<i>rpoD</i>	CJSA_0944	K	RNA polymerase sigma factor RpoD	1.7	2.9	1.7	1.9
<i>cmeE</i>	CJSA_0975	M	membrane fusion component multidrug efflux system CmeDEF	1.9	2.0	1.5	1.5
-	CJSA_0977	O	adenylosuccinate lyase	2.5	5.2	2.4	3.4
<i>Rho</i>	CJSA_1096	K	transcription termination factor Rho	1.8	1.9	1.6	1.7
-	CJSA_1129	T	putative PAS domain containing signal-transduction sensor protein	4.8	5.7	1.8	2.1
-	CJSA_1146	H	putative 5-formyltetrahydrofolate cyclo-ligase family protein	1.6	4.1	1.6	2.3
-	CJSA_1180		hypothetical protein	2.1	7.1	1.9	2.1
<i>pseC</i>	CJSA_1232	M	C4 aminotransferase specific for PseB product	2.0	3.1	1.7	1.5
-	CJSA_1233	R	hypothetical protein	2.7	3.9	1.6	1.7
<i>maf1</i>	CJSA_1256	S	motility accessory factor	2.3	3.3	2.4	2.2
<i>neuC2</i>	CJSA_1264	M	putative UDP-N-acetylglucosamine 2-epimerase	4.4	6.0	1.8	2.5
-	CJSA_1266	R	hypothetical protein	1.6	4.1	1.6	2.3
<i>maf4</i>	CJSA_1271	S	motility accessory factor	2.5	3.5	2.3	2.3
<i>nrfA</i>	CJSA_1292	P	putative periplasmic cytochrome C	3.4	3.8	3.2	3.3
<i>nrfH</i>	CJSA_1293	C	putative periplasmic cytochrome C	6.1	11.1	7.8	6.3
-	CJSA_1304	R	putative nucleotide phosphoribosyltransferase	1.8	1.5	1.5	2.1
-	CJSA_1387		hypothetical protein	2.1	5.0	1.7	1.8
<i>infA</i>	CJSA_1502	J	translation initiation factor IF-1	2.9	2.9	1.7	2.3
-	CJSA_1533		hypothetical protein	1.8	2.2	1.9	2.2
-	CJSA_1544		hypothetical protein	2.9	6.7	3.1	3.8
-	CJSA_1554	S	hypothetical protein	1.8	2.3	1.5	2.2
-	CJSA_1562		hypothetical protein	2.6	4.5	1.5	2.1

Table 7 continued

-	CJSA_1596	G	putative MSF family efflux protein	3.9	4.0	3.1	4.0
-	CJSA_1624	R	GNAT family acetyltransferase	3.0	7.3	1.7	2.5
-	CJSA_pVir0024		putative plasmid partitioning ParA protein	1.7	4.1	4.2	4.5
-	CJSA_pVir0025		hypothetical protein	4.6	5.4	4.2	5.3
<i>repE</i>	CJSA_pVir0026		putative replication protein RepE	3.4	10.9	4.3	6.5
-	CJSA_pVir0040		hypothetical protein	3.5	8.1	2.5	3.9
-	CJSA_pVir0044		hypothetical protein	5.4	22.4	6.0	13.8
-	CJSA_t0001		Ala tRNA	6.1	8.0	2.2	3.4
-	CJSA_t0002		Ile tRNA	8.1	9.4	1.9	3.2
-	CJSA_t0004		Ala tRNA	5.0	5.9	1.5	2.1
-	CJSA_t0014		Ala tRNA	4.6	6.3	2.0	2.5
-	CJSA_t0015		Ile tRNA	7.7	8.3	1.7	3.0
-	CJSA_t0023		Val tRNA	2.2	4.7	1.7	1.5
-	CJSA_t0043		Ala tRNA	1.9	3.8	1.6	1.9
-	CJSA_t0044		Val tRNA	2.3	4.9	1.8	2.0

Table 8. List of annotated genes identified to be upregulated only in both *in vivo* conditions when compared with the unexposed IA 3902 inoculum with a comparison of fold change under each category.

Name	Synonym	COG Code	Product	Fold Change	
				GB <i>in vivo</i> 2 hr	GB <i>in vivo</i> 24 hr
<i>dsbI</i>	CJSA_0017	O	DsbB family disulfide bond formation protein	2.1	2.7
<i>Dba</i>	CJSA_0018		disulfide bond formation protein	3.0	6.5
<i>fliM</i>	CJSA_0054	N	flagellar motor switch protein FliM	1.9	2.6
<i>fliA</i>	CJSA_0055	K	flagellar biosynthesis sigma factor	2.0	4.4
<i>cydA</i>	CJSA_0074	C	cytochrome d ubiquinol oxidase, subunit I	2.4	3.1
-	CJSA_0080	S	putative lipoprotein	1.8	2.3
<i>obgE</i>	CJSA_0087	R	GTPase ObgE	1.5	3.4
-	CJSA_0111		putative recombination protein RecO	5.4	5.6
-	CJSA_0112	R	putative metalloprotease	3.1	1.9
<i>thrB</i>	CJSA_0125	E	homoserine kinase	2.2	2.0
-	CJSA_0149	C	cytochrome c family protein	1.5	1.6
-	CJSA_0150	H	putative 6-pyruvoyl tetrahydropterin synthase	1.8	1.9
-	CJSA_0228		hypothetical protein	1.6	1.7
-	CJSA_0233	R	Sulfatase	2.9	2.5
<i>dgkA</i>	CJSA_0234	M	diacylglycerol kinase	3.6	4.9
<i>pyrC</i>	CJSA_0236	F	Dihydroorotase	2.3	2.8
-	CJSA_0240	P	zinc transporter ZupT	2.5	2.1
<i>mreC</i>	CJSA_0254	M	rod shape-determining protein MreC	1.8	1.6
<i>lpxB</i>	CJSA_0264	M	lipid-A-disaccharide synthase	1.6	1.7
<i>Ndk</i>	CJSA_0306	F	nucleoside diphosphate kinase	1.8	1.9
<i>flhB</i>	CJSA_0309	NU	flagellar biosynthesis protein FlhB	1.9	2.4
-	CJSA_0327	FP	Ppx/GppA family phosphatase	1.8	1.7
<i>fdxB</i>	CJSA_0328	C	ferredoxin, 4Fe-4S	1.6	1.9

Table 8 continued

-	CJSA_0358	S	integral membrane protein	1.5	1.6
-	CJSA_0384	R	GTP-binding protein	2.7	2.6
-	CJSA_0424		hypothetical protein	3.1	2.7
-	CJSA_0425		hypothetical protein	2.5	3.3
<i>rpmG</i>	CJSA_0441	J	50S ribosomal protein L33	1.5	2.3
-	CJSA_0467	R	hypothetical protein	1.8	1.7
-	CJSA_0474	R	Gfo/Idh/MocA family oxidoreductase	2.2	2.3
-	CJSA_0517		hypothetical protein	2.1	1.7
-	CJSA_0572	S	putative polyphosphate kinase	1.7	1.8
-	CJSA_0575	V	ABC-type transmembrane transport protein	1.9	2.0
<i>recN</i>	CJSA_0609	L	DNA repair protein RecN	1.5	1.7
-	CJSA_0699		hypothetical protein	3.1	4.9
-	CJSA_0717	S	hypothetical protein	2.6	2.9
<i>purU</i>	CJSA_0746	F	formyltetrahydrofolate deformylase	1.5	2.2
<i>ftsK</i>	CJSA_0832	D	putative cell division protein	2.1	2.8
-	CJSA_0894	E	peptidyl-arginine deiminase family protein	2.1	1.7
-	CJSA_0897		putative HAMP containing membrane protein	2.0	2.0
-	CJSA_0910	R	putative acyl-CoA thioester hydrolase	2.2	2.7
<i>flgR</i>	CJSA_0967	T	sigma-54 associated transcriptional activator	1.7	5.2
-	CJSA_0968		hypothetical protein	2.1	5.3
<i>Ssb</i>	CJSA_1013	L	single-stranded DNA-binding protein	1.6	1.8
<i>mfd</i>	CJSA_1027	LK	transcription-repair coupling factor	1.9	1.9
-	CJSA_1086		hypothetical protein	3.1	5.3
-	CJSA_1118	V	ABC transporter ATP-binding protein	2.2	3.9
-	CJSA_1153	M	peptidase, M23/M37 family	1.8	1.5
<i>kefB</i>	CJSA_1169	P	putative glutathione-regulated potassium-efflux system protein	1.5	2.5
<i>uvrC</i>	CJSA_1184	L	excinuclease ABC subunit C	3.3	4.4
-	CJSA_1190	S	hypothetical protein	1.6	2.1
<i>racS</i>	CJSA_1201	T	two-component sensor (histidine kinase)	1.5	2.0

Table 8 continued

<i>ktrA</i>	CJSA_1222	P	putative K ⁺ uptake protein	1.9	1.7
<i>hisF</i>	CJSA_1252	E	imidazole glycerol phosphate synthase subunit HisF	2.3	1.5
<i>maf3</i>	CJSA_1270	S	motility accessory factor	2.1	1.7
-	CJSA_1305	M	putative periplasmic protein (VacJ-like protein)	1.6	1.5
-	CJSA_1416	S	hypothetical protein	1.9	2.4
<i>seld</i>	CJSA_1426	E	putative selenide,water dikinase	1.7	1.9
-	CJSA_1448	R	hypothetical protein	1.8	2.6
<i>rpsM</i>	CJSA_1504	J	30S ribosomal protein S13	1.7	1.7
<i>rnhA</i>	CJSA_1548	L	ribonuclease H	1.7	1.7
<i>murL</i>	CJSA_1564	M	glutamate racemase	2.5	2.5
<i>nlpC</i>	CJSA_1565	M	putative lipoprotein nlpC	1.7	1.8
<i>nhaA2</i>	CJSA_1566	P	Na ⁺ /H ⁺ antiporter	1.7	3.1
-	CJSA_1631	R	putative GTP cyclohydrolase I	2.6	13.9
-	CJSA_pVir0016		hypothetical protein	2.9	2.6
-	CJSA_pVir0020		hypothetical protein	2.0	1.8
-	CJSA_t0009		Thr tRNA	1.7	2.9
-	CJSA_t0011		Arg tRNA	2.3	2.7
-	CJSA_t0012		Met tRNA	1.6	4.4
-	CJSA_t0020		Val tRNA	1.8	3.6
-	CJSA_t0033		Leu tRNA	1.8	1.8
-	CJSA_t0034		Cys tRNA	1.7	3.4
-	CJSA_t0035		Ser tRNA	2.3	4.2
-	CJSA_t0037		Arg tRNA	1.9	1.9
-	CJSA_t0038		Arg tRNA	2.1	1.9
-	CJSA_t0040		Pro tRNA	1.5	1.7

Table 9. List of annotated genes identified to be downregulated in all conditions when compared with the unexposed IA 3902 inoculum with a comparison of fold change under each category.

Name	Synonym	COG Code	Product	Fold Change			
				GB <i>in vivo</i> 2 hr	GB <i>in vivo</i> 24 hr	Bile <i>in vitro</i> 2 hr	Bile <i>in vitro</i> 24 hr
-	CJSA_0025	R	sodium/dicarboxylate symporter	-7.2	-3	-2.4	-7.6
<i>cjaA</i>	CJSA_0925	ET	putative amino-acid transporter periplasmic solute-binding protein	-5.3	-4.2	-3.5	-3.7
<i>metF</i>	CJSA_1140	E	5,10-methylenetetrahydrofolate reductase	-2.7	-2.2	-4.2	-6.3
<i>putP</i>	CJSA_1424	ER	putative sodium/proline permease	-4.7	-9	-2.0	-2.9
-	CJSA_1573	M	ABC transporter permease	-2.1	-1.9	-2.9	-7
-	CJSA_pVir0008		hypothetical protein	-4.2	-11.7	-2.5	-2.7
-	CJSA_pVir0009		hypothetical protein	-3.8	-10.6	-2.4	-2.7
-	CJSA_pVir0050		hypothetical protein	-6.7	-7.5	-4.1	-5.3
-	CJSA_pVir0051		hypothetical protein	-5	-5	-4.4	-5
	CJSA_t0030		Ser tRNA	-7.4	-4.2	-3.6	-6.9

Table 10. Summary of the number of genes found to be differentially expressed when the 2 hour and 24 hour time points for each condition were compared.

	Condition	
	2 hours vs 24 hours	
	GB <i>in vivo</i>	Bile <i>in vitro</i>
Protein-coding genes		
Increased at 2 vs 24 hours	38	16
Increased at 24 vs 2 hours	136	9
Non-coding RNA genes		
Increased at 2 vs 24 hours	[4]	[8]
Increased at 24 vs 2 hours	[57]	[3]

[] = signifies that this is a putative list generated by Rockhopper of predicted non-coding RNA as well as known non-coding RNA genes

Table 11A. List of previously validated non-coding RNAs (Dugar *et al.*, 2013) expressed and differentially regulated in our dataset with location, length, and orientation.

Transcription Start	Transcription Stop	Length	Strand	Product	LFG	RFG	Orientation	Location
INCREASED EXPRESSION								
250059	249960	99	-	CjNC20	CjSA_0232	CjSA_0233	<<<	intergenic
675392	675240	152	-	CjNC60	CjSA_0681	<i>dnaE</i>	><>	intergenic
1155464	1155580	116	+	CjNC120	<i>groEL</i>	<i>dccS</i>	>><	intergenic/antisense <i>dccS</i>
1193304	1193433	129	+	CjNC140	CjSA_1197	<i>porA</i>	>>>	intergenic
1572367	1572461	94	+	CjNC180	CjSA_1562	<i>map</i>	>><	intergenic
25244	25412	168	+	Cjpv2	CjSA_pVir0032	CjSA_pVir0032	>><	intergenic
DECREASED EXPRESSION								
1183928	1183941	13	+	CjNC130/6S	CjSA_1188	CjSA_1188	>>>	intergenic

Table 11B. Differential expression between conditions of previously validated non-coding RNAs (Dugar *et al.*, 2013).

Product	Fold change			
	GB <i>in vivo</i> 2 hr	GB <i>in vivo</i> 24 hr	Bile <i>in vitro</i> 2 hr	Bile <i>in vitro</i> 24 hr
INCREASED EXPRESSION				
CjNC20	1.1	1.5	2.8	1.7
CjNC60	0.8	1	1.3	1.7
CjNC120	1.3 ^a	3.8	1.1 ^a	1.2 ^a
CjNC140	3.1	9.9	1.4 ^a	4.6
CjNC180	6	19.8	1.8	4.8
Cjpv2	-1.4	2.6	-1.2	-1.1
DECREASED EXPRESSION				
CjNC130/6S	-5.7	-3.5	-1.8 ^b	-1.8 ^b

^a = Q value >0.05 but fold change <1.5^b = fold change >1.5 but Q value <0.05**Bold** indicates significant differential expression

Table 12. Fold change expression data for the 14 genes previously reported to be involved in the bile tolerance response in *Campylobacter*, 2 of which are not present in strain IA 3902.

	Present in IA 3902	Fold Change				Expected change	Reference
		Gallbladder		Bile			
		2 hours	24 hours	2 hours	24 hours		
<i>cmeA</i>	Yes	3.8	2.6	2.3	2.1	Increase	Lin <i>et al.</i> , 2002, 2005
<i>cmeB</i>	Yes	3.7	1.7	1.7	1.9	Increase	Lin <i>et al.</i> , 2002, 2005
<i>cmeC</i>	Yes	2.6	1.5	1.2	1.8	Increase	Lin <i>et al.</i> , 2002, 2005
<i>cmeD</i>	Yes	1.9	3.8	1.4 ^a	2.6	Increase	Akiba <i>et al.</i> , 2005
<i>cmeE</i>	Yes	1.9	2	1.5	1.5	Increase	Akiba <i>et al.</i> , 2005
<i>cmeF</i>	Yes	1.9	1.5	1.1	1.3	Increase	Akiba <i>et al.</i> , 2005
<i>cmeR</i>	Yes	1.3 ^a	1.1	1.2 ^a	1.7	None	Lin <i>et al.</i> , 2005
<i>cbrR</i>	Yes	1.1	1.9	1.0	1.4 ^a	None	Raphael <i>et al.</i> , 2005
<i>ciaB</i>	Yes	0.8	1	0.9	1.4 ^a	Increase	Rivera-Amill <i>et al.</i> , 2001
<i>flaA</i>	Yes	0.9	1	1.3	0.7	Increase	Allen and Griffiths, 2001
<i>tlyA</i>	Yes	NE	NE	NE	NE	Increase	Malik-Kale <i>et al.</i> , 2008
<i>dccR</i>	Yes	1.2	1.4 ^a	1.0	1.4 ^a	Increase	Malik-Kale <i>et al.</i> , 2008
<i>hcp1</i>	No	-	-	-	-	-	Lertpiriyapong <i>et al.</i> , 2012
<i>icmF1</i>	No	-	-	-	-	-	Lertpiriyapong <i>et al.</i> , 2012

NE = not expressed under any conditions studied (<5 RMPK)

^a = Q value >0.05 but fold change <1.5

Bold indicates significant differential expression

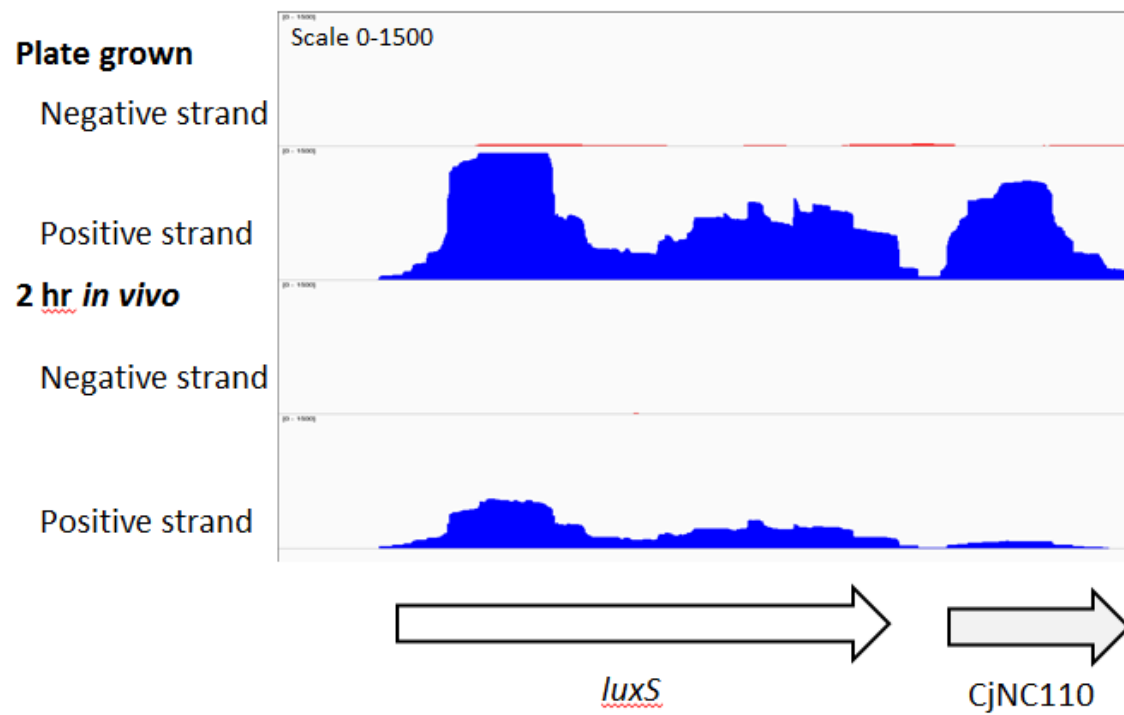
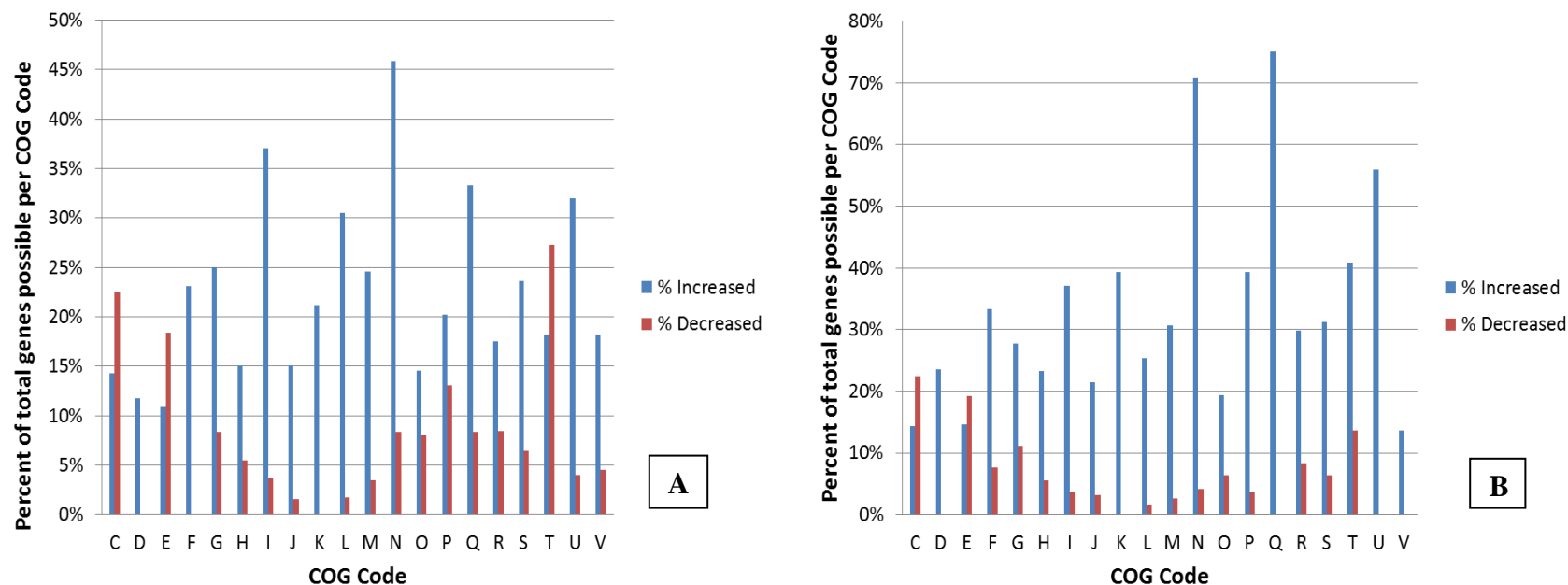
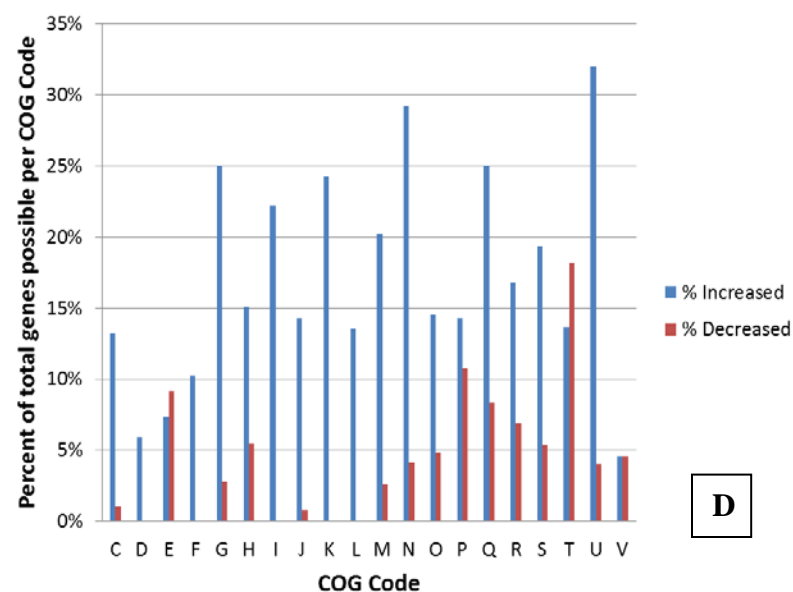
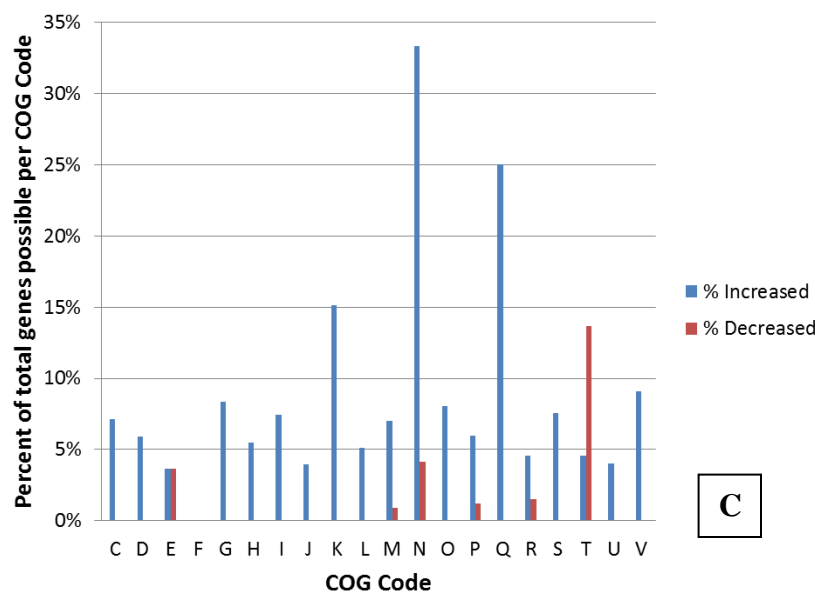


Figure 1. IGV screen capture from preliminary RNAseq experiment, *luxS* and CjNC110 region. Screen capture image of the expression levels of the *luxS* gene and the predicted CjNC110 small RNA observed during the preliminary RNAseq experiment, with significantly increased expression present in the *in vitro* plate grown inoculum when compared to the 2 hour *in vivo* gallbladder sample.



Figures 2A and 2B. Analysis of the differentially expressed genes based on COG function detected by RNAseq, gallbladder *in vivo* samples at 2 hours (A) and 24 hours (B). Clusters of Orthologous Groups (COG) categories are indicated on the x-axis, with the percentage of genes enriched shown on the y-axis; blue bars indicate increased expression, red bars indicate decreased expression. COG category codes: C - Energy production and conversion; D - Cell cycle control, mitosis and meiosis; E - Amino acid transport and metabolism; F - Nucleotide transport and metabolism; G - Carbohydrate transport and metabolism; H - Coenzyme transport and metabolism; I - Lipid transport and metabolism; J - Translation; K - Transcription; L - Replication, recombination and repair; M - Cell wall/membrane biogenesis; N - Cell motility; O - Posttranslational modification, protein turnover, chaperones; P - Inorganic ion transport and metabolism; Q - Secondary metabolites biosynthesis, transport and catabolism; R - General function prediction only; S - Function unknown; T - Signal transduction mechanisms; U - Intracellular trafficking and secretion; V - Defense mechanisms; W - Extracellular structures.



Figures 2C and 2D: Analysis of the differentially expressed genes based on COG function detected by RNAseq, bile *in vitro* samples at 2 hours (C) and 24 hours (D). Clusters of Orthologous Groups (COG) categories are indicated on the x-axis, with the percentage of genes enriched shown on the y-axis; blue bars indicate increased expression, red bars indicate decreased expression. COG category codes: C - Energy production and conversion; D - Cell cycle control, mitosis and meiosis; E - Amino acid transport and metabolism; F - Nucleotide transport and metabolism; G - Carbohydrate transport and metabolism; H - Coenzyme transport and metabolism; I - Lipid transport and metabolism; J - Translation; K - Transcription; L - Replication, recombination and repair; M - Cell wall/membrane biogenesis; N - Cell motility; O - Posttranslational modification, protein turnover, chaperones; P - Inorganic ion transport and metabolism; Q - Secondary metabolites biosynthesis, transport and catabolism; R - General function prediction only; S - Function unknown; T - Signal transduction mechanisms; U - Intracellular trafficking and secretion; V - Defense mechanisms; W - Extracellular structures.

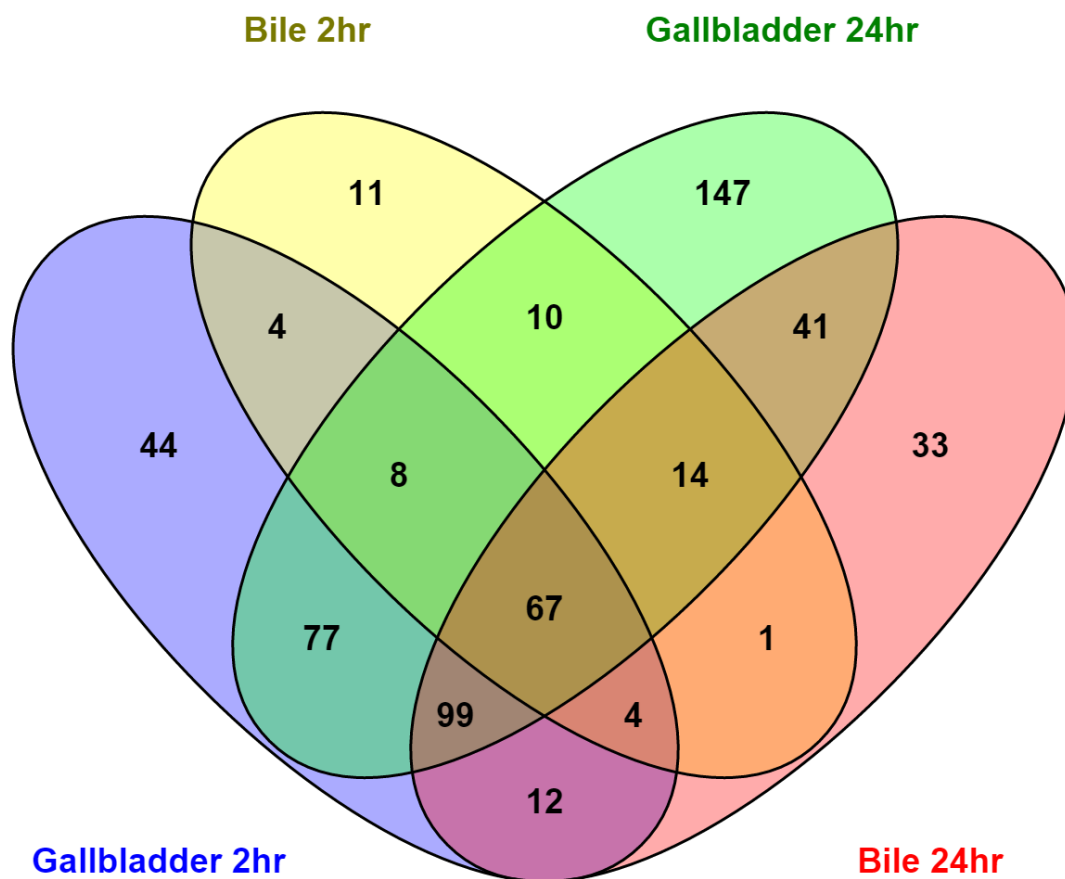


Figure 3. Venn diagram depicting the overlap of upregulated annotated genes in all conditions compared to the unexposed IA 3902 inoculum. All known annotated genes including both protein coding and previously validated ncRNA were compared to each other utilizing the Venny program.

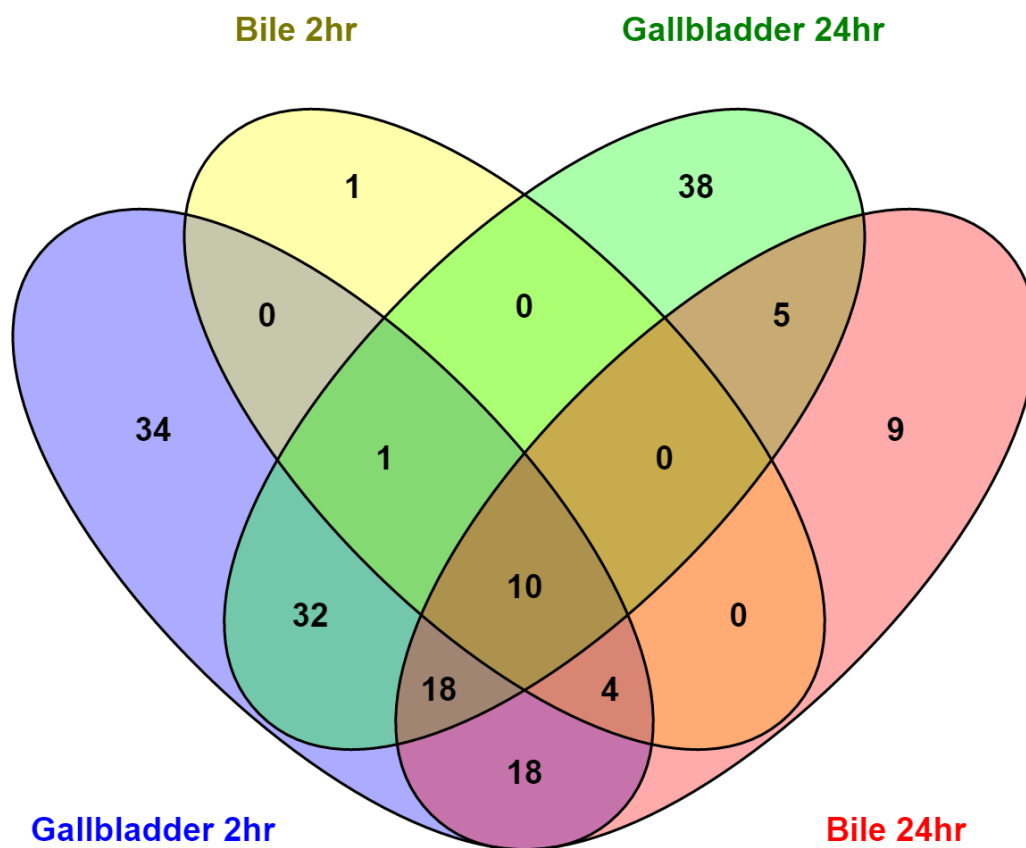
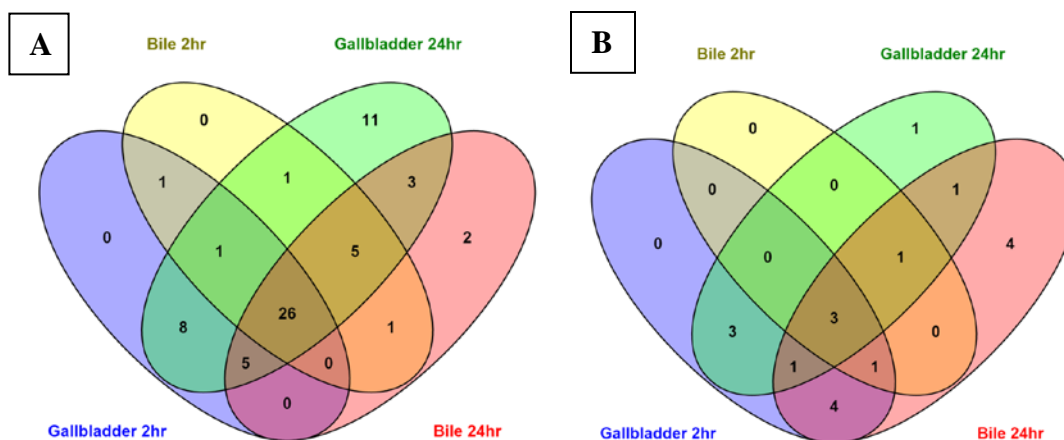


Figure 4. Venn diagram depicting the overlap of downregulated annotated genes in all conditions compared to the unexposed IA 3902 inoculum. All known annotated genes including both protein coding and previously validated ncRNA were compared to each other utilizing the Venny program.



Figures 5A and 5B. Venn diagrams depicting the overlap of upregulated (A) and downregulated (B) predicted non-coding RNA unannotated genes in all conditions compared to the unexposed IA 3902 inoculum. All putative ncRNA predicted by Rockhopper as differentially expressed under each condition were compared to each other utilizing the Venny program.

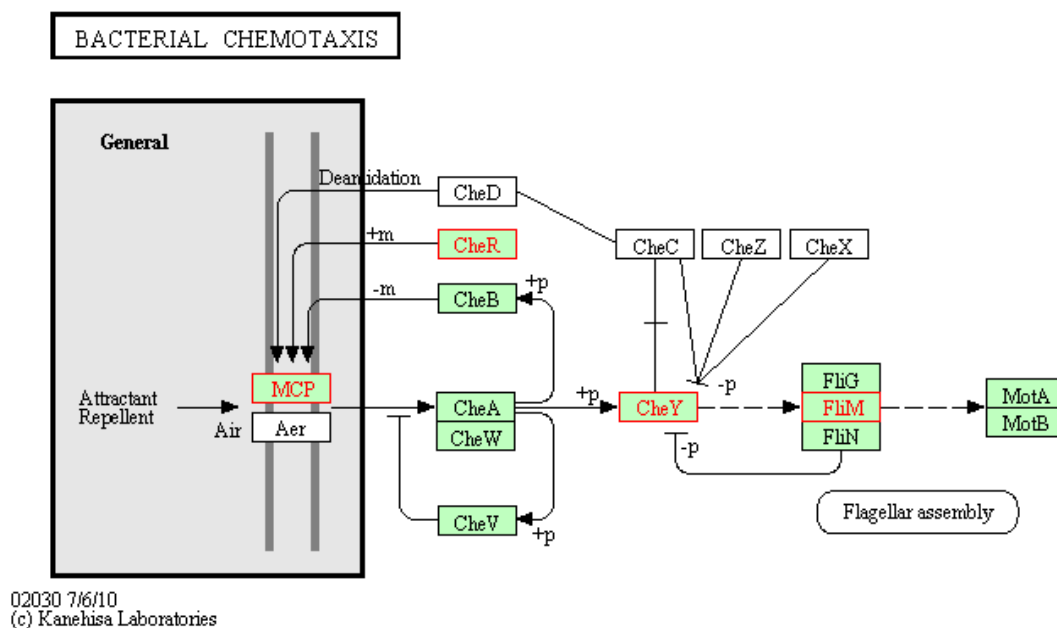
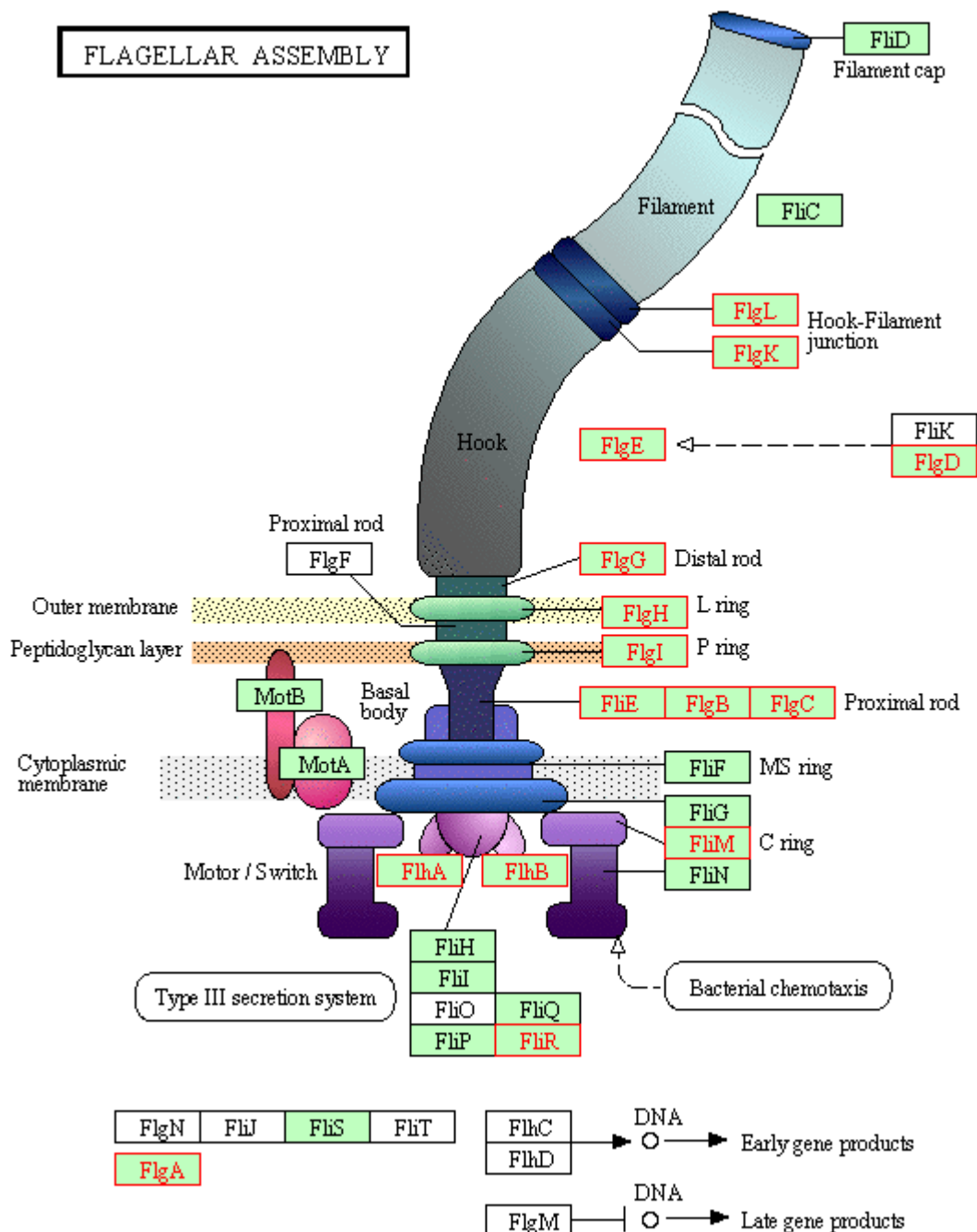


Figure 6. KEGG Pathway for chemotaxis in *C. jejuni*. Multiple genes responsible for chemotaxis were observed to be upregulated in the gallbladder condition only, including cheY, cheR, and a putative MCP CjSA_0897 (increased differential expression denoted by red highlight).



02040 6/23/10
(c) Kanehisa Laboratories

Figure 7. KEGG Pathway for flagellar assembly in *C. jejuni*. Multiple genes responsible for flagellar assembly were observed to be upregulated in the gallbladder condition only; image depicts 24 hours in the *in vivo* gallbladder environment (increased differential expression denoted by red highlight).

CHAPTER 4

THE TRANSCRIPTOME OF MUTANTS Δ CjNC110, Δ LUXS, AND Δ CjNC110 Δ LUXS IN
THE *CAMPYLOBACTER JEJUNI* SHEEP ABORTION CLONE IA 3902**Abstract**

Recent advances in the use of high throughput deep sequencing of RNA (RNAseq) have revolutionized the study of gene expression and identification of small non-coding RNAs in pathogenic microorganisms. Previous studies in *Campylobacter jejuni* have identified the presence of this important class of post-transcriptional gene regulators in the transcriptome of various strains of *C. jejuni*, however, few studies have been published to date that have attempted to elucidate the function of this emerging class of regulatory molecules. In the previous chapter, we demonstrated for the first time small RNAs differentially expressed in the zoonotic pathogen *C. jejuni* sheep abortion clone IA 3902 under *in vivo* host conditions. One of these small RNAs, CjNC110, was selected for further study based on its location immediately downstream of the *luxS* gene which has been previously demonstrated to play an important role in the virulence of *C. jejuni*. Deletional mutagenesis was performed to create Δ CjNC110 in *C. jejuni* IA 3902, and this mutation was then transferred into the previously constructed IA 3902 Δ luxS mutant to create the double knockout mutant IA 3902 Δ CjNC110 Δ luxS. Evaluation of the complete transcriptome of the Δ CjNC110, Δ luxS, and Δ CjNC110 Δ luxS mutants compared to wild type IA 3902 during both exponential and stationary growth utilizing strand specific RNAseq was observed to result in distinctly different transcriptomes in each mutant during both growth stages. This data was then utilized to generate a list of potential regulatory targets of the CjNC110 small

RNA in IA 3902 which was then compared to computational methods of mRNA target identification via TargetRNA2. Further evaluation of the transcriptome of the Δ CjNC110 Δ luxS mutant suggests that previous studies describing the transcriptome of *luxS* only mutants may have unknowingly caused polar effects in the expression of CjNC110. This work provides for the first time valuable insights into the potential regulatory targets of the CjNC110 small RNA in the zoonotic pathogen *C. jejuni*.

Introduction

Campylobacter jejuni sheep abortion (SA) clone IA 3902 has recently emerged as an important pathogen of both ovine abortion and human gastroenteritis (Sahin *et al.*, 2008; Sahin *et al.*, 2012). Recent analysis of IA 3902 via a multi-omics approach revealed that IA 3902 is remarkably syntenic with the genome of *C. jejuni* type-strain 11168 (Wu *et al.*, 2013) and it does not harbor any additional pathogenicity islands or virulence factors known to be associated with abortion induced by *C. fetus* subsp. *fetus* (Grogono-Thomas *et al.*, 2003; van Putten *et al.*, 2009). The fact that relatively mild changes in genomic structure have led to significantly enhanced ability to cause disease by *C. jejuni* sheep abortion clone IA 3902 as described above suggests that differences in gene regulation may play a key role in the enhanced virulence of this strain.

C. jejuni has only three known sigma factors identified within its genome to regulate transcription: σ^{70} (encoded by *rpoD*), σ^{54} (encoded by *rpoN*) and σ^{28} (encoded by *fliA*) (Parkhill *et al.*, 2000). Besides control at the transcriptional level, regulation of gene expression can occur by post-transcriptional control via regulation of mRNA translation, stability and processing; the primary players in post-transcriptional regulation are small

RNAs (Papenfort and Vogel, 2010; Storz *et al.*, 2011; Caldelari *et al.*, 2013). Prior to completion of the transcriptional start site map via high throughput RNA sequencing (RNAseq) of *H. pylori* (Sharma *et al.*, 2010), the ϵ -proteobacteria were thought not to be capable of using small and antisense RNA as a regulatory mechanism, partly due to a lack of the small RNA chaperone protein Hfq (Valentin-Hansen *et al.*, 2004). Indeed, attempts at computational approaches of identification of small RNAs in *Campylobacter* failed to identify any potential candidates, with only 3 potential loci being identified in *Helicobacter* (Livny *et al.*, 2008). Recently, clear evidence that *C. jejuni* also has the capability to produce these important regulators has been published detailing identification of a wealth of small RNAs present in strains 11168, 81-176, 81116, and RM1221 (Chaudhuri *et al.*, 2011; Butcher and Stintzi, 2013; Dugar *et al.*, 2013; Porcelli *et al.*, 2013; Taveirne *et al.*, 2013). Dugar *et al.* (2013), when comparing the transcriptomes of 4 different *C. jejuni* isolates, observed a large variation in transcriptional start sites (TSS) as well as expression patterns of both mRNA and non-coding RNA between strains. This suggests that variation between the existence and expression of small RNAs even among closely related strains may play a role in the differences observed in virulence.

In closely related *Helicobacter pylori*, studies are just starting to emerge where ncRNAs have been shown to influence gene expression at the post-transcriptional level (Wen *et al.*, 2013; Pernitzsch *et al.*, 2014). The first report attempting to elucidate the role of two recently identified non-coding RNAs just recently published in *C. jejuni* suggests these ncRNAs may play a role in flagellar biosynthesis; however, they were unable to demonstrate phenotypic changes following inactivation of either non-coding RNA (Le *et al.*, 2015). Beyond simply establishing the existence of non-coding RNA transcripts in *Campylobacter*,

there is strong need to begin to determine the functional role of these potential regulators in this important zoonotic pathogen.

In Chapter 3, we demonstrated for the first time the expression of previously identified non-coding RNAs in *C. jejuni* sheep abortion clone IA 3902, including a number that were differentially expressed in the *in vivo* host environment. In particular, the conserved small RNA CjNC110 (Dugar *et al.*, 2013) was strongly differentially expressed during our preliminary experiments, warranting further investigation. The location of this ncRNA in the intergenic region immediately downstream of the *luxS* gene was of particular interest to our group as previous work in our lab has already highlighted the importance of the *luxS* gene in the virulence of *C. jejuni* (Plummer *et al.*, 2012), and experiments to improve understanding of the regulation of quorum sensing in *C. jejuni* related to *luxS* are ongoing in our lab. In addition, a recent article assessing the effect of various methods of mutation of the *luxS* gene in *Campylobacter* has suggested that certain methods of *luxS* mutation may have polar effects on this newly described ncRNA that have led to differences in the various reports of phenotypic and gene expression changes due to *luxS* mutation in *Campylobacter* (Adler *et al.*, 2014). Based on these observations, we chose CjNC110 as our first attempt at characterizing the role a non-coding RNA might play in the virulence of *C. jejuni* IA 3902.

In this study, we investigated the effect of deletional mutagenesis of CjNC110, insertional mutagenesis of *luxS*, and combined mutation of both genes on the transcriptional landscape during exponential and stationary stages of growth of *C. jejuni* IA 3902. We hypothesized that inactivation of the CjNC110 small RNA would lead to changes in the abundance of mRNAs of genes whose expression is regulated by CjNC110. Inactivation of CjNC110 and *luxS*, both independently and when combined, was observed to result in

distinctly different transcriptomes during both exponential and stationary growth. This information will help direct future studies focused on elucidating the role of both *luxS* and CjNC110 in the pathobiology and virulence of *C. jejuni*.

Materials and Methods

Bacterial strains, plasmids and culture conditions

C. jejuni SA (sheep abortion) clone IA 3902 was initially isolated from an outbreak of sheep abortion in Iowa during 2006 and has been utilized by our laboratory as the prototypical isolate of a set of clonal isolates now identified as the most common cause of sheep abortion due to *Campylobacter* species in the United States (Sahin *et al.*, 2008). W7 is a highly motile variant of the commonly utilized laboratory strain *C. jejuni* 11168 (Plummer *et al.*, 2012). *C. jejuni* strains and their isogenic mutants were routinely grown in Mueller-Hinton (MH) broth or agar plates (Becton-Dickinson, Franklin Lakes, NJ) at 42°C under microaerophilic conditions with the use of compressed gas (55% O₂, 10% CO₂, 85% N₂). For strains containing a chloramphenicol resistance cassette, 5 µg/mL chloramphenicol was added to either the broth or agar plates when appropriate. For strains containing a kanamycin resistance cassette, 30 µg/mL kanamycin was added to either the broth or agar plates when appropriate.

For genetic manipulations, *Escherichia coli* competent cells were grown at 37°C on Luria-Bertani (LB) agar plates or broth (Becton-Dickinson, Franklin Lakes, NJ) with shaking at 125 rpm. When appropriate, 50 µg/mL kanamycin, 20 µg/mL chloramphenicol or 100 µg/mL ampicillin was added to the broth or agar plates for selection of colonies. All strains used in this study are described in **Table 1**, with all relevant plasmids listed in **Table 2** and

primer sequences in **Table 3**. All strains were maintained in 20% glycerol stocks at -80C and passaged from those stocks as needed for experimental procedures.

Creation of *C. jejuni* Δ Cjnc110 and Δ Cjnc110 Δ luxS mutants in IA 3902

An isogenic CjNC110 mutant of *C. jejuni* IA 3902 was constructed via deletional mutagenesis utilizing a combination of synthetic double-stranded DNA (dsDNA) fragments and traditional cloning methods. Based on previously published data depicting the proposed transcriptional start site for CjNC110 (Dugar *et al.*, 2013), the coding region of CjNC110 in IA 3902 and the prototypical *C. jejuni* strain 11168 were first confirmed to be identical. Then, a 200 bp section of the IA 3902 genome starting 20 bp upstream and including the entire 137 nt transcript of the CjNC110 sequence as predicted in Dugar *et al.* (2013) was replaced with 820 bp of the promoter and coding sequence of the chloramphenicol acetyltransferase (*cat*) gene of *Campylobacter coli* plasmid C-589 (Wang and Taylor, 1990a). Synthetic dsDNA including approximately 500 bp upstream and 500 bp downstream of the region replaced with the *cat* cassette was then synthesized in 4 fragments of 500 bp each with overlapping homologous ends (Integrated DNA Technologies, Coralville, IA). The Gibson Assembly method was then utilized to assemble the synthetic dsDNA fragments (Gibson *et al.*, 2009) using the Gibson Assembly Master Mix (New England Biolabs, Ipswich, MA). Following assembly, primers (CJnc110F2 and CJnc110R2) were designed to amplify a 1785 bp product of the assembled dsDNA; PCR amplification was achieved using TaKaRa Ex Taq DNA Polymerase (ClonTech, Mountain View, CA). This amplified PCR product was then cloned into the pGEM-T Easy Vector using T4 ligase (Promega, Madison, WI) resulting in the construction of pNC110::cat which was then transformed into chemically

competent *E. coli* DH5 α (New England Biolabs, Ipswich, MA). Transformants were then selected on LB agar plates containing chloramphenicol (20 μ g/ml), ampicillin (100 μ g/ml), and ChromoMax IPTG/X-Gal Solution (Fisher Scientific, Pittsburgh, PA). pNC110::cat was purified from the transformed *E. coli* using the QIAprep Miniprep kit (QIAGEN, Germantown, MD) and confirmed by PCR to contain the construct again using the CJnc110F2 and CJnc110R2 primers.

The pNC110::cat plasmid DNA was then introduced to *C. jejuni* W7 as a suicide vector and the deletion transferred into the genome of *C. jejuni* W7 via homologous recombination. Transformants were selected on MH agar plates containing chloramphenicol (5 μ g/ml) and deletional mutagenesis was again confirmed via PCR analysis and Sanger sequencing to create *C. jejuni* W7 Δ CjNC110. Following confirmation, natural transformation was used to move the gene deletion into *C. jejuni* IA 3902 as previously described (Wang and Taylor, 1990b) to create *C. jejuni* IA 3902 Δ CjNC110. Natural transformation was again used to move the CjNC110 gene deletion into the previously created *luxS* insertional mutant *C. jejuni* IA 3902 Δ luxS (Plummer *et al.*, 2012) to create the double mutant *C. jejuni* IA 3902 Δ CjNC110 Δ luxS. Transformants were selected on MH agar plates containing chloramphenicol (5 μ g/mL) and kanamycin (30 μ g/mL) and confirmed via PCR analysis and Sanger sequencing of the CjNC110 region along with the entire upstream (*luxS*) and downstream (CjSA_1137) genes. All colonies were screened for presence/absence of motility as described in Chapter 5, and only colonies with verified motility were used for future studies.

Growth curve

The A_{600} of overnight cultures were adjusted to 0.5 using sterile MH broth on a Genesys 10S VIS spectrophotometer (ThermoScientific, Waltham, MA). Cultures were then diluted 1:10 for a final targeted starting A_{600} of 0.05 in 90 mL sterile MH broth and placed in a sterile 250 mL Erlenmeyer glass flask. Cultures were incubated at 42°C under microaerophilic conditions with shaking at 125 rpm for 30 hours. Samples were removed from the flasks at designated time points (3, 6, 9, 12, 24, and 30 hours) and processed as described below for RNA isolation as well as assessed for A_{600} and actual colony counts using the drop-plate method as previously described (Chen *et al.*, 2003). All strains were assessed for growth via four independent experiments. The averages of the A_{600} of the four experiments over time were statistically analyzed using a two-way ANOVA (GraphPad Prism).

RNA extraction and DNase treatment

Culture samples collected from time points 3 and 6 hours (10 mL), and 9 and 12 hours (6 mL), of the growth curve described above were centrifuged at 8000 x *g* for 2 minutes immediately following collection to rapidly pellet the cells while minimizing the time elapsed between collection and introduction of an RNA protection solution. Following pelleting of the cells, the supernatant was decanted and 1 mL QIAzol Lysis Reagent (QIAGEN, Germantown, MD) was added to the cultures to quench further RNA production and protect the RNA present from degradation. To resuspend the pellet, the mixture was then pipetted up and down and vortexed at high speed for 1 minute. Following vortexing, the QIAzol-culture mixture was incubated at room temperature for 5 minutes. QIAzol-protected

cultures were then stored at -80°C for up to two months prior to proceeding with total RNA isolation.

Total RNA isolation was performed using the miRNeasy Mini Kit (QIAGEN, Germantown, MD) according to the manufacturer's instructions to isolate total RNA >18 nt. On-column DNase treatment was performed using the RNase-free DNase set (QIAGEN, Germantown, MD). 10 µg of extracted RNA was further treated with the TURBO DNA-free kit (Life Technologies, Carlsbad, CA) following RNA isolation to remove any residual DNA contamination. The total RNA was then purified using the RNeasy MinElute Cleanup kit (QIAGEN, Germantown, MD) with the following modifications as recommended by QIAGEN Technical Services to retain total RNA, including RNA <200nt in length. No more than 50 µL of RNA sample at a time was utilized to enter the RNeasy MinElute Cleanup protocol; to the RNA sample, 350 µl of Buffer RLT was added, followed by 600 µl of 100% ethanol. The RNA:RLT:ethanol mixture then proceeded with the standard bind/wash/elute steps of the protocol as provided by the manufacturer.

RNA concentration was measured using the NanoDrop ND-1000 spectrophotometer (ThermoScientific) and Qubit RNA BR Assay (Thermo Fisher Scientific, Waltham, MA) and RNA quality was measured using the Agilent 2100 Bioanalyzer RNA 6000 Nano kit (Agilent Technologies, Santa Clara, CA). All RNA samples utilized for downstream library preparation had a RNA integrity number (RIN) of >9.0, indicating high quality RNA. Verification of complete removal of any contaminating DNA was performed via PCR amplification of a portion of the CjSA_1356 gene, which is part of the capsule locus and has previously been determined via comparative genomics to only be present in *C. jejuni* IA 3902, using primers SA1356F and SA1356R (Luo *et al.*, 2012).

RNAseq library preparation and sequencing

Based on analysis of the growth curve, the 3 hour (exponential phase) and 12 hour (stationary phase) timepoints were selected for RNAseq analysis (**Figure 1**). 2.5 µg of confirmed DNA-free total RNA was treated with Ribo-Zero rRNA Removal Kit for Bacteria according to the manufacturer's instructions (Illumina, San Diego, CA). Following rRNA removal, the ribosomal depleted total RNA was again purified using the RNeasy MinElute Cleanup kit (QIAGEN) using the same modifications as described above. Following clean-up, the RNA was eluted into 12 µL of sterile RNase-free water; quality, quantity, and rRNA removal efficiency was then analyzed via the Agilent 2100 Bioanalyzer RNA 6000 Pico kit (Agilent Technologies).

Library preparation for sequencing on the Illumina HiSeq platform was completed using the TruSeq stranded mRNA HT library preparation kit (Illumina) with some modifications. As this kit was designed for use with eukaryotic RNA with poly-A tails, the initial poly-A RNA purification step was omitted. To enter the protocol, 5 µL of the rRNA-depleted RNA totaling approximately 200 ng was added to 13 µL of the "Fragment, Prime, Finish" mix. The remainder of the library preparation was carried out according to the manufacturer's instructions and all 24 samples were barcoded using the high throughput (HT) 96-well RNA adapter plate (RAP) as supplied by the manufacturer. Following enrichment of the cDNA fragments, the quality of the cDNA was validated using the Agilent 2100 Bioanalyzer DNA 1000 kit (Agilent Technologies) and quantity was determined via the Qubit dsDNA BR Assay (Thermo Fisher Scientific). The indexed cDNA samples were then submitted to the Iowa State University DNA Facility where they were normalized and pooled

according to the manufacturer's instructions. The pooled library was then sequenced on an Illumina HiSeq 2500 machine in high-output single read mode with 100 cycles.

Differential gene expression analysis of RNAseq data

To analyze the differences in gene expression between strains and timepoints, Rockhopper (<http://cs.wellesley.edu/~btjaden/Rockhopper/>), a freely available RNAseq analysis platform, was utilized as previously described using the standard settings of the program (McClure *et al.*, 2013). Using this program, results of gene expression are normalized and reported by the program as expression of genes using reads per kilobase per million reads (RPKM), except that instead of dividing by the total number of reads, Rockhopper divides by the upper quartile of gene expression.

Following computational analysis via Rockhopper, a change in gene expression was deemed significant when the Q-value (false discovery rate) was below 5% and a >1.5 fold change in expression levels was present. Any significant changes in 16S or 23S rRNA genes were ignored as these were determined to be due to differences in efficiency of rRNA removal by Ribo-Zero and not inherent differences between strains and conditions. Read count data was visually assessed using the Integrated Genome Viewer (IGV) (<https://www.broadinstitute.org/igv/>) (Robinson *et al.*, 2011; Thorvaldsdóttir *et al.*, 2013). Differentially expressed genes were then assessed for function using the Clusters of Orthologous Groups (COG) (Galperin *et al.*, 2015) as previously described in IA 3902 (Wu *et al.*, 2013). Venn diagrams depicting overlap of genes differentially regulated in multiple mutant strains were generated using BioVenn (Hulson *et al.*, 2008).

(<http://www.cmbi.ru.nl/cdd/biovenn/index.php>). Metabolic pathway analysis was performed using Kegg Pathways (Kanehisa *et al.*, 2015) (<http://www.genome.jp/kegg/pathway.html>).

TargetRNA2 and RNAFold

To attempt to computationally determine potential targets for regulation by CjNC110 for comparison to the RNAseq data, the freely available TargetRNA2 program (<http://cs.wellesley.edu/~btjaden/TargetRNA2/>) was utilized to predict potential targets of interest *a priori* (Kery *et al.*, 2014). The standard program settings were utilized, which included searching the region 80 nt upstream and 20 nt downstream of the predicted translational start site of all genes in the IA 3902 genome. Both the 137 nt read length predicted from Dugar *et al.*, (2013) and the 226 nt read length predicted from our data were analyzed via this method.

To attempt to determine the secondary structure of the CjNC110 non-coding RNA, the standard settings of the RNAFold webserver was used for prediction analysis (<http://rna.tbi.univie.ac.at/cgi-bin/RNAfold.cgi>) (Gruber *et al.*, 2008; Lorenz *et al.*, 2011). Again, both the 137 nt read length predicted from Dugar *et al.*, (2013) and the 226 nt read length predicted from our data were analyzed via this method.

Results

RNAseq data confirms mutant construction

The RNAseq data that was compiled for each of the mutants allowed visualization of the unique read signature related to the mutated regions via the Integrated Genome Viewer as presented in **Figure 2A** and as compared to the anticipated mutated gene structure (**Figure**

2B). In all timepoints and replicates sequenced for the Δ CjNC110 and Δ CjNC110 Δ luxS mutants, no reads mapped to the reported location of the CjNC110 small RNA; this was anticipated based on the method of mutant construction which removed that entire region of the genome en bloc and replaced it with an antibiotic resistance marker. Interestingly, in the Δ CjNC110 mutant only and not in the Δ CjNC110 Δ luxS, an obvious region of increased expression of the 3' end of the upstream *luxS* gene was noted; in fact, the Rockhopper program assigned this region putative small RNA status. Expression for this region is present in the 3902 wild-type sequencing at lower levels than the rest of the *luxS* gene, suggesting that it is potentially a part of the *luxS* transcript that may under normal conditions be truncated. Rockhopper did fail to identify CjNC110 as a small RNA candidate in this dataset which was somewhat unexpected. Further analysis of the data revealed that expression levels of this transcript were relatively low in the wild type at both stages of growth, which may explain why it was not recognized by Rockhopper as a unique non-coding RNA.

Downstream of the Δ CjNC110 deletion, additional reads above the wild-type values were also present immediately adjacent to the altered region but still within the intergenic region. This is likely due to read-through of the chloramphenicol resistance cassette due to lack of a strong transcription terminator related to insertion of the cassette; a similar phenomenon can also be seen immediately downstream of the insertion of the kanamycin resistance cassette in the Δ luxS and Δ CjNC110 Δ luxS mutants. Analysis of reads mapping to the annotated downstream gene, CjSA_1137, reveals no obvious changes in location of the transcriptional start site when comparing wild type to the mutant strains. Significantly different changes were present in the gene expression of CjSA_1137 in the Δ CjNC110 mutant during both exponential and stationary phase, as well as in the Δ CjNC110 Δ luxS

mutant during stationary phase; additional analysis via computational methods suggests that CjSA_1137 may be a potential target of CjNC110.

For the $\Delta luxS$ and $\Delta CjNC110\Delta luxS$ mutants, the location of the insertion of the kanamycin resistance cassette into the coding sequence of the *luxS* gene can be directly observed as a sudden decrease in the amount of reads downstream of the location of the insert. In the $\Delta luxS$ mutant, reads mapping to CjNC110 can also be seen which indicates that the mutation does not interfere with ability of the downstream small RNA to be transcribed. In the $\Delta CjNC110\Delta luxS$ mutant, no reads are present that map to the CjNC110 coding region, confirming that both genes are inactivated in that strain.

Summary of Illumina RNAseq results

Overall, 24 barcoded libraries were sequenced yielding over 109 million reads, with close to 100 million high quality reads aligning to either the genome or pVir plasmid of *C. jejuni* IA 3902 and averaging 4,553,847 reads per library (**Tables 4A** and **4B**). The vast majority of reads (average of 83% of total reads), mapped to protein coding genes of the chromosome, with only 7% of reads mapping to ribosomal RNA on average following rRNA depletion with Ribo-Zero (median of 3%). Over half of the libraries contained less than or equal to 3% ribosomal RNA reads, which is consistent with the manufacturer's predicted rRNA removal efficiency. One third of the libraries did not exhibit efficient rRNA removal (>10% rRNA reads); the reason for this is unclear. Interestingly, less than 1% of reads mapped to antisense regions of the annotated protein coding genome. This is in comparison to 2-7% of reads in a recent study completed in *H. pylori*, a closely related member of the epsilon-proteobacter family (Bischler *et al.*, 2015). An average of 2% of reads mapped

antisense to known non-coding RNAs, however, the majority of this is due to an error in the IA 3902 genome that incorrectly annotates the *mnpB* (ribonuclease P) gene in the wrong direction, thus attributing all of the sense strand reads as antisense (see Chapter 4 for further discussion).

Differential gene expression analysis of RNAseq data

Rockhopper was utilized for analysis of differential gene expression between timepoints and strains. A summary of the differences in numbers of genes with increased and decreased expression in the various strains and timepoints is given in **Table 5**. In the Δ CjNC110 mutant strain, six genes were found to be downregulated and four genes were found to be upregulated when compared to the IA 3902 wild type strain during exponential growth (**Table 6**). In addition, a previously described non-coding RNA, CjNC140 (Dugar *et al.*, 2013) was found to be upregulated in the mutant condition, as was a putative RNA predicted by Rockhopper to be present at the 3' end of *luxS*. During the stationary phase, 16 genes were found to be downregulated and seven genes were found to be upregulated in the mutant strain when compared to wild type. Of the regulated genes, three genes (*neuB2*, *hisF*, *ptmA*) were downregulated in the Δ CjNC110 mutant during both the exponential and stationary phases, and one hypothetical protein coding gene (CjSA_1261) was found to be upregulated in both conditions. Of the differentially expressed genes, five separate operons predicted by Rockhopper demonstrated multiple genes within the operon affected by the mutant condition (three operons upregulated, two operons downregulated). Analysis of functionality via the COG database revealed that multiple upregulated genes (*luxS*, *cetA*, *cetB*) were present in the “Signal transduction mechanisms” functional category; multiple

downregulated genes were also included in the “Cell wall/membrane biogenesis” (*neuB2*, *ptmB*, CjSA_1352) functional category and “Posttranslational modification, protein turnover, chaperones” (*tpx*, CjSA_0687) functional category.

In the Δ luxS mutant strain, one gene was found to be downregulated and 14 genes were found to be upregulated when compared to the IA 3902 wild type strain during exponential growth (**Table 7**). Similar to the Δ CjNC110 mutant, the previously described non-coding RNA CjNC140 (Dugar *et al.*, 2013) was also found to be upregulated in the mutant condition during exponential growth only. At 12 hours, six genes were found to be downregulated and six upregulated in the Δ luxS mutant strain when compared to wild type. Of the regulated genes, only one gene, CjSA_1350, a putative methyltransferase, was found to be downregulated in the Δ luxS mutant during both exponential and stationary phases, as was the putative ncRNA at the 3' end of *luxS* identified by Rockhopper. Three separate operons predicted by Rockhopper demonstrated multiple genes within the operon affected by the mutant condition (two operons upregulated, one operon downregulated). Analysis of functionality via the COG database revealed that multiple both up- (*trpF*, *trpB*) and down- (CjSA_0620, *leuC*) regulated genes were present in the “Amino acid transport and metabolism” functional category; multiple upregulated genes were also included in the “Cell motility” (*flgE*, *flgG2*, *flgG*) functional category. Only two genes were differentially expressed in both the Δ CjNC110 and Δ luxS mutants, CjSA_0008 (upregulated during exponential growth hours) and CjSA_1107 (upregulated during stationary phase); both of these genes are annotated as hypothetical proteins at this time.

In the Δ CjNC110 Δ luxS double knockout mutant, a large increase in both downregulated and upregulated genes when compared to wild type was observed at both

timepoints (**Table 8**). Sixty-one protein coding genes, seventeen tRNA genes, three known RNA genes (tmRNA, SRP, 6S) and seven newly predicted ncRNAs were downregulated during exponential phase compared to wild-type. In addition, 47 protein coding genes were upregulated in exponential phase, along with the previously described non-coding RNA, CjNC140 (Dugar *et al.*, 2013), which was also observed to be upregulated in the Δ CjNC110 and Δ luxS single knockout mutants. During stationary phase, 32 genes and two newly predicted non-coding RNAs were found to be downregulated, while 29 genes were upregulated in the mutant strain when compared to wild type. Of the observed genes with differential expression, many were observed to show altered expression during both exponential and stationary phase when compared to wild type; however, most were differentially expressed in the opposite direction between the two timepoints. This result was highly unexpected; however, considering that the majority of the genes involved fall under three main COG categories and three operons, it is plausible that during different stages of cell growth that the mutations present affect the regulation of certain genes in different ways. Only two genes (*motB*, CjSA_1350) were downregulated in both conditions, while no genes were observed to be upregulated at both timepoints. Many of the differentially upregulated genes demonstrated in both background mutants, Δ CjNC110 and Δ luxS, were observed in the double knockout (**Figures 3A** and **3B**), while fewer of the downregulated genes were shared (**Figures 4A** and **4B**).

Of the differentially expressed genes affected by the Δ CjNC110 Δ luxS double mutation, 20 separate operons predicted by Rockhopper demonstrated multiple genes within the operon affected by the mutant condition (eight operons upregulated, four operons downregulated, and eight operons that showed opposing regulation at the different

timepoints). **Figure 5** shows the number of genes in each COG category that were differentially expressed in the double mutant condition during either exponential or stationary growth. The categories most affected by these mutations were “Energy production and conversion,” “Amino acid transport and metabolism,” “Translation,” “Cell wall/membrane biogenesis,” “Cell motility,” and “Signal transduction mechanisms.”

KEGG Pathways was used to determine the effect of the mutations on important pathways in *C. jejuni* pathobiology. **Figures 6A** and **6B** compare the genes involved in flagellar assembly observed to be differentially expressed in the single knockout mutants during stationary phase. In contrast, **Figures 7A** and **7B** compare the genes observed to be differentially expressed in the double knockout mutant during both exponential and stationary phases for flagellar assembly. A much larger number of genes associated with flagellar assembly were noted to be differentially regulated in the double knockout mutant as compared to the single knockout mutants alone.

TargetRNA2 and RNAFold predictions

The TargetRNA2 program predicted 21 regulatory targets of CjNC110 in IA 3902 based on the standard input parameters of the program and a 137 nt length of the non-coding RNA (**Table 9**). Of those 21, only a single gene (CjSA_1137) was found to show significantly altered transcription in the CjNC110 mutant as compared to wild type; this significant decrease was observed during both exponential and stationary growth. When the 226 nt transcript was used as the input, the TargetRNA2 program predicted 23 regulatory targets of CjNC110 in IA 3902, again using the standard input parameters of the program. Of those 23, two genes (CjSA_1137, *tpx*) were found to show significantly decreased

transcription in the CjNC110 mutant as compared to wild type; CjSA_1137 during both exponential and stationary growth, and *txp* during stationary growth only. Interestingly, when the lists of predicted genes from the 137nt and 226nt lengths were compared, only 13 were shared between the lists. It was anticipated that all of the 21 genes identified within the original 137 nt transcript would also be identified in the 226 nt list as the primary structure of the 137 nt was still present in the 226 nt transcript, however, this was not the case. This suggests based on the prediction algorithms of the program that by altering the length of the transcript, the secondary structure of the RNA will be altered which may affect the binding ability for certain targets.

To assess secondary structure of the CjNC110, RNAFold was used to calculate the structure of CjNC110 which yielded a prediction of a Y-shaped stem-loop structure (**Figure 8**). When comparing the Target2RNA data of the 136 nt transcript to the RNAFold prediction for that same length, all of the predicted interaction areas of the non-coding RNA were grouped into the 3 unpaired loop regions of the RNA structure. In contrast, when the RNA transcript length was extended to 226 nt, no prediction of RNA secondary structure could be made by RNAFold. This suggests that the addition of 89nt to the length of CjNC110 is either a spurious finding in our data, or may completely alter the secondary structure and thus the targets of this small RNA between strains of *C. jejuni*. For example, of the nine targets predicted to interact with the first stem-loop structure of the 137 nt RNA by TargetRNA2, only one was also predicted to interact with the 226 nt RNA even though the base pair structure of that region is identical between the two lengths.

Identification of additional non-coding RNAs in IA 3902

In addition to determining differential gene expression between the mutant and wild-type strains of IA 3902, Rockhopper has the capability to predict non-coding RNAs present within the data. Prior to further manual analysis, Rockhopper predicted a total of 59 ncRNAs present in the data (57 chromosomal, 2 pVir). Of those 59, five align with previously identified ncRNAs (CjNC20, CjNC60, CjNC120, CjNC140, CJpv2), all of which were predicted to be conserved in IA 3902 by Dugar *et al.* (2013). Manual curation of the list decreased the number of predicted ncRNA candidates to 40 (**Table 10**). Candidate non-coding RNAs were discarded if they were related to the 16S or 23S genes as these were thought to be spuriously identified due to Ribo-Zero depletion differences between replicates; in addition, an antisense RNA was discarded due to incorrect annotation of the *rnpB* gene to the wrong strand in IA 3902. Of those remaining, 6 were demonstrated transcripts in the region of genes annotated as pseudogenes in IA 3902 (CjSA 1052, CjSA 1323, CjSA 1444, CjSA 1543 and CjSA 1630 – 2 separate ncRNA predictions). Two of the 40 remaining ncRNA candidates could potentially be classified as *cis* as they are transcribed opposite of transcribed regions of other genes; 25 would likely be considered *trans* ncRNAs as they are primarily located within intergenic regions; and seven are classified as anti-sense RNAs.

Discussion

Despite its relative importance in both human medicine as the leading cause of bacterial gastroenteritis, and in veterinary medicine as an emerging cause of bacterial abortion in small ruminants, very little is known about the regulation of genes in *C. jejuni*.

The absence of traditional regulatory systems that are present in model organisms like *E. coli* and *Salmonella* initially led to the suggestion that *Campylobacter* may have a lower level of complexity than other bacteria and may not possess non-coding RNAs as a regulatory feature (Livny *et al.*, 2008). Recent studies have proven that this is not the case as many putative non-coding RNA candidates have been identified in multiple strains of *C. jejuni* (Dugar *et al.*, 2013; Porcelli *et al.*, 2013; Taveirne *et al.*, 2013). Identification of the functional role of small RNAs has been slow to follow, however, and minimal further analyses of the role of non-coding RNAs in *Campylobacter* have been published. In closely related *H. pylori*, studies are just starting to emerge where ncRNAs have been shown to influence gene expression at the post-transcriptional level (Wen *et al.*, 2013; Pernitzsch *et al.*, 2014). The first report attempting to elucidate the role of non-coding RNA just recently published in *Campylobacter* suggests that two recently identified ncRNAs may play a role in flagellar biosynthesis; however, the authors were unable to demonstrate phenotypic changes following inactivation of these non-coding RNAs (Le *et al.*, 2015). Regulation of cellular processes by non-coding RNAs such as CjNC110 as described in our study provides a number of advantages to the bacteria when compared to the traditional model of protein-mediated regulation (Beisel and Storz, 2010). Non-coding RNAs can be rapidly produced as they do not require translation to be active, and once produced in the cell they can rapidly be recycled if necessary. Non-coding RNAs can also regulate multiple different targets within a cell in a variety of ways to coordinate rapid responses to changing environments.

The recent development of high throughput deep sequencing of RNA (RNAseq) has made this the current method of choice to analyze the transcriptome of bacteria under various conditions (Croucher *et al.*, 2010; van Vliet, 2010; van Opijnen and Camilli 2013) as it

allows evaluation of the entire transcriptome rather than only previously annotated regions as with older technology such as microarrays. Recent work in *Campylobacter* has demonstrated that RNAseq can be useful for analyzing transcriptomic differences between wild type and mutant strains of protein coding genes to better understand the effect of inactivation of certain genes on a global scale (Butcher *et al.*, 2015; Chandrashekhara *et al.*, 2015). In theory, RNAseq should also be able to be utilized for the same purpose of discovering the global effects of inactivation of non-coding RNAs. Non-coding RNAs have the ability to affect the abundance of mRNA transcripts through multiple mechanisms, some of which should then manifest as measurable changes in transcript levels. Small RNAs have been shown to be able to stabilize mRNA transcripts by multiple mechanisms (Waters and Storz, 2009), which should lead to increased levels of transcript availability and identification in RNAseq experiments. In contrast, interactions with small RNAs have also been shown to increase transcript turnover by targeting transcripts for RNase degradation or exposing RNase cleavage sites (Waters and Storz, 2009), which should lead to decreased levels of transcripts available for identification via RNAseq. Assessment of differential gene expression via RNAseq should then be useful for uncovering those interactions of small RNAs with their targets that directly leads to altered levels of mRNA transcripts in the cell. Of added benefit in the case of *luxS* and CjNC110, where the potential exists for polar effects of inactivation of *luxS* to inadvertently affect the expression of CjNC110, is that transcriptomic changes in both mutants can be measured individually as well as in combination. A limitation of the use of RNA sequencing data for discovery of targets of small RNAs is that some target interactions may not lead to direct changes in mRNA transcript levels, perhaps only leading to changes in the translation efficiency of the mRNA; these types of interactions cannot be

determined via this approach. Therefore, use of multiple additional methods such as computational approaches to determine potential targets of small RNAs is also warranted.

In other species of bacteria such as *Vibrio cholerae*, small RNAs have been shown to be involved in the regulation of quorum sensing (Shao and Bassler, 2012; Shao and Bassler, 2014). While there have been conflicting reports of the ability of *Campylobacter* to participate in quorum sensing (Holmes *et al.*, 2009), research in our lab has shown that the inactivation of *luxS*, a gene known to play an important role in quorum sensing in other species of bacteria, leads to attenuation of virulence and decreased colonization ability (Plummer *et al.*, 2012). Due to the proximity of CjNC110 to *luxS*, we were interested in evaluating the relationship between the two genes. In addition, a recent article assessing the effect of various methods of mutation of the *luxS* gene in *Campylobacter* suggested that certain methods of *luxS* mutation may have polar effects on this newly described ncRNA that have led to differences in the various reports of phenotypic and gene expression changes attributed to *luxS* mutation in *Campylobacter* (Adler *et al.*, 2014). While the TargetRNA2 computational algorithm did not predict an interaction between CjNC110 and the *luxS* gene, one of the goals in assessing the differential gene expression of these mutants via RNAseq was also to determine if an interaction exists between these genes. During stationary growth in the Δ CjNC110 mutant, the entire transcript of the *luxS* gene was determined to be statistically significantly upregulated when compared to wild-type; during exponential growth, increased expression was also present but did not reach statistical significance. This suggests that when present CjNC110 may normally interact with the *luxS* transcript to increase degradation of the mRNA in the cell and thus impact AI-2 expression and quorum sensing. No additional genes known to be involved in quorum sensing or the S-

adenosylmethionine (SAM) recycling pathway were differentially expressed in the Δ CjNC110 mutant; however, these same genes were not found to be differentially expressed in the Δ luxS mutant either. This is likely due to an overall low level of expression present in these genes in all strains examined under these conditions, which likely led to a decreased ability to detect differences in expression.

One additional mechanism for alteration of *luxS* transcript expression in the CjNC110 mutant that must be considered as well is the mutation process used to create Δ CjNC110. Because CjNC110 is adjacent to *luxS*, mutation of CjNC110 may have inadvertently caused changes in the expression of *luxS* that are not related to a direct regulatory role of the small RNA with the *luxS* gene. Sequencing of the Δ CjNC110 mutant construct confirmed that the annotated coding sequence of the *luxS* gene was identical to the reference strain for all nucleotides except for a single mismatch near the 3' end. This mismatch is at position 1132244 and exchanges a G for a T nucleotide. This substitution does not lead to a truncation of the protein; however, it does exchange arginine for leucine (L161R) in the primary structure at amino acid 161. The predicted length of LuxS is 165 amino acids, therefore, this mutation occurs at the far 3' end of the protein. Previous comparisons of the LuxS protein across various species of bacteria have shown that while the leucine residue is frequently conserved at that location, it is not always conserved and in fact often the LuxS protein is truncated prior to residue 161 (Plummer *et al.*, 2011). As this residue is not always present, it cannot be considered an essential residue for which a mutation will lead to a loss of function of the gene. If the effect of the substitution at this site were to render the LuxS protein non-functional, it would be anticipated that the transcriptomic changes observed in the Δ CjNC110

mutant would be identical to that of the $\Delta luxS$ mutant; this was not observed and in fact was frequently opposite.

In addition to overall increased expression of the *luxS* gene in the $\Delta CjNC110$ mutant, an obvious region of increased transcription of the 3' UTR of the *luxS* gene was identified by the Rockhopper program and assigned putative small RNA status. Expression for this region is present in the 3902 wild-type sequencing at lower levels than the rest of the gene, suggesting that mutation of $CjNC110$ is not solely responsible for the presence of transcripts in this region. One potential explanation for this difference is that the terminator of the *luxS* gene may normally be weak and allow for some extended transcription in this region. It is possible that the nucleotide change at the 3' end of the protein in the $\Delta CjNC110$ mutant may interfere with normal termination and lead to increased read-through in that region. It is also possible that another small RNA does exist in this area, however, our data does not allow for that determination to be made definitively. Additional work to determine if a unique transcriptional start site is present for this predicted ncRNA is warranted.

In this study we identified a number of additional genes and operons of importance that were differentially expressed in the $\Delta CjNC110$ mutant as opposed to wild type during both exponential and stationary growth. The *cetAB* operon which was upregulated during exponential growth is known to be important in energy taxis responses in *C. jejuni* and has been shown previously to be required for normal motility (Hendrixson *et al.*, 2001). The significant increase in expression observed in both genes of the operon in the $\Delta CjNC110$ mutant suggests that the mutant may exhibit differences in motility and energy taxis when compared to the wild type IA 3902. When examining the genes that were downregulated in both exponential and stationary growth phases, *ptmA* and *neuB2* are of interest as they have

been shown to be required for normal flagellar glycosylation in *C. jejuni* (McNally *et al.*, 2007; Logan *et al.*, 2002). Normal flagellar glycosylation has been proven to play an important role in the autoagglutination ability of *C. jejuni* strains (Guerry *et al.*, 2006); downregulation of these genes in the mutant suggest that autoagglutination ability could be decreased in the Δ CjNC110 mutant when compared to wild type IA 3902. The *tpx* gene, which has been shown to be involved in the stress response to peroxide exposure in *C. jejuni*, was also downregulated during stationary growth in the Δ CjNC110 mutant. Inactivation of the *tpx* gene has been shown to lead to a decreased ability to respond to peroxides (Atack *et al.*, 2008); therefore, increased sensitivity to peroxides may also be present in the Δ CjNC110 mutant. Also of interest, during stationary phase, expression of the *ciaB* was noted to be decreased; CiaB is a secreted protein that has been demonstrated to be required for *in vitro* invasion of epithelial cells (Konkel *et al.*, 1999). Studies have indicated that expression of the *ciaB* gene and secretion of the protein product are not coupled, with secretion requiring a stimulatory signal from the host environment (Rivera-Amill *et al.*, 2001). Inactivation of the *ciaB* gene has also been proven to impair the ability of *C. jejuni* to colonize the chicken cecum *in vivo* (Ziprin *et al.*, 2001); therefore, it is reasonable to suspect that decreased expression of *ciaB* in the Δ CjNC110 mutant could lead to defects in the colonization ability.

Interestingly, analysis of transcriptome changes in the Δ luxS mutant were not as enlightening as was expected. The list of genes identified does not overlap with the list of differentially expressed genes generated via microarray in *C. jejuni* strain 11168 which utilized the exact same mutant construct that was moved via homologous recombination into IA 3902 (Plummer, 2009); however, differences in the strain of *C. jejuni* utilized and culture conditions may explain why there was no overlap of differentially expressed genes. No genes

associated with the SAM recycling pathway were identified in our RNAseq data as have been previously reported via microarray in other strains of *C. jejuni* (He *et al.*, 2008), however, there was very minimal expression of many of the genes associated with the SAM pathway in our data (*metE*, *metF*, *pfs*) which may have led to an inability to detect a difference. Decreased transcription of *flaA* has previously been associated with *luxS* mutation in strain 11168 (Jeon *et al.*, 2003); expression of *flaA* during exponential growth was decreased 1.4 fold compared to wild-type, however, this change was not found to be statistically significant; no difference was present in *flaA* levels during stationary growth. A single gene, CjSA_1350, which is annotated as a putative methyltransferase, was found to be down-regulated during both exponential and stationary growth in the $\Delta luxS$ mutant of IA 3902. The LuxS enzyme is critical for the formation of S-adenosylmethionine (SAM), which is a major methyl donor necessary for methylation of DNA, proteins, carbohydrates and other molecules important to the physiology of prokaryotes (Parveen and Cornell, 2011). It is plausible that expression of this methyltransferase is sensitive to decreased availability of products from the activated methyl cycle due to *luxS* mutation; however, recent data generated within our lab group suggests that this gene does not encode an active methyltransferase (Mou, 2015).

In distinct contrast to the lack of similar findings to previous studies exhibited by the IA 3902 $\Delta luxS$ mutant, when the $\Delta CjNC110$ and $\Delta luxS$ mutations were combined into $\Delta CjNC110\Delta luxS$, many of the previously noted transcriptional changes attributed to mutation of the *luxS* gene alone became apparent (He *et al.*, 2008). The He *et al.* (2008) study was performed in a different strain of *C. jejuni*, 81-176, which also encodes and expresses CjNC110 (Dugar *et al.*, 2013). After attempting to compare various strains and

methods of mutation of the *luxS* gene and finding wide variation in phenotypical and transcriptional changes, Adler *et al.* (2014) suggested that some of the differences reported between *luxS* mutants in various studies may be due to unknown polar affects caused by alteration of expression of CjNC110 based on the mutation strategy used for the *luxS* mutation. It seems highly likely based on the data generated in our study that some of the changes attributed to *luxS* mutation alone in the He *et al.* (2008) study may in fact be due to inactivation of the CjNC110 transcript as well. To construct the $\Delta luxS$ mutant in that report, the entire coding region of the *luxS* gene was removed via overlap extension PCR, and a 1.2 kb flanking sequence upstream and downstream with a chloramphenicol cassette inserted in the middle was reintroduced to inactivate the gene. As this involved deletion of an entire region of the genome, and the exact start and stop location of the deletion is not reported in the publication, it is entirely possible that the CjNC110 coding region or its promoter were affected. Of the 57 genes listed as differentially expressed by the *luxS* mutant in He *et al.* (2008), 21 were also found to be differentially expressed in our $\Delta CjNC110\Delta luxS$ RNAseq data; again, none were found to be differentially expressed only in the $\Delta luxS$ mutant, while in contrast, three genes (*tpx*, *ptmB*, *ptmA*) were differentially expressed only in the $\Delta CjNC110$ mutant. Only the flagellar genes *flgE*, *flgG2*, and *flgG* were also differentially expressed in both the $\Delta luxS$ only mutant and the $\Delta CjNC110\Delta luxS$ mutant. These findings strongly suggest that in the previous study the main driver for the transcriptional changes seen was an inadvertent inactivation of both CjNC110 and *luxS*, and not *luxS* alone. Of the genes identified in both our study and He *et al.* (2008), a large number of the hook-basal body associated proteins (FlgD, FlgE, FlgG, FlgG2, FlgH, FlgI, and FlgK) that are under the control of σ^{54} (RpoN) promoters (Wosten *et al.*, 2004; Malik-Kale *et al.*, 2007) were

identified. Expression from σ^{54} promoters has been shown to require activation of the FlgRS two-component regulatory system (Wosten *et al.*, 2004; Joslin *et al.*, 2009). Many of these showed opposite differences based on growth phase (decreased exponential, increased stationary), and it has been previously demonstrated that regulation by these sigma-factors is growth cycle dependent, with σ^{54} genes typically expressed between σ^{70} and σ^{28} genes, which may help explain the differences seen here (Wosten *et al.*, 2004). Also of note is the fact that *flgS* was also observed to be upregulated in the Δ CjNC110 Δ luxS mutant. It has been previously suggested that an additional unknown factor may control the temporal regulation of σ^{54} dependent flagellar genes (Hendrixson *et al.*, 2003); therefore it is reasonable to consider that *luxS* or CjNC110 may play a role in this regulation. Two additional studies that have attempted to elucidate the role of *luxS* in *C. jejuni* also utilized a method that involved deletion of either all or some of the *luxS* coding sequence, however, neither of these studies attempted to determine transcriptional changes in the mutant (Elvers and Park 2002; Corcionivoschi *et al.*, 2009).

In addition to evaluation of transcriptional changes present in the mutant strains, the Rockhopper program identified additional putative small RNAs which allowed for confirmation of expression of five non-coding RNAs conserved among *Campylobacter* species that were previously predicted to be present in IA 3902. The majority of the other identified putative non-coding RNAs that were predicted by the program have not been previously reported in *C. jejuni*. Based on the data presented in Dugar *et al.* (2013) that suggests that many small RNAs in *Campylobacter* are strain-specific, the fact that the predicted RNAs were not previously discovered does not mean that they are not real. That being said, there are limitations to the identification of non-coding RNAs by Rockhopper.

One-third of the initially predicted ncRNAs were manually discarded as they mapped to the region of the 16S or 23S genes and were likely identified due to differences between replicates in Ribo-Zero rRNA depletion efficiency. Another subset of the identified non-coding RNAs were recognized by the program because the genome file utilized by Rockhopper does not include pseudogenes, therefore, reads that mapped to areas of putative pseudogenes were classified as non-coding RNA. While it is possible that these transcripts no longer serve as functional mRNA transcripts and now instead the transcribed RNA acts as functional non-coding RNA, it is probably more likely that these transcripts either do form functional proteins or are simply a non-functional remnant of what once was a functional protein coding message.

Due to the nature of the type of RNAseq data that was generated (i.e. – not enriched for primary transcripts), the majority of transcripts that were identified by Rockhopper as putative non-coding RNAs were found within intergenic regions. Confirmation of the predictions generated by Rockhopper utilizing either transcriptional start site detection or Northern blot analysis would be necessary to confirm the existence of the predicted ncRNAs that were not previously confirmed in other strains of *C. jejuni*; visual analysis via the IGV of the areas of interest indicate that some of the predictions are likely correct while others may simply be read-through of operons into the intergenic space.

One particular area of interest in the genome that was identified by Rockhopper and appears to have transcripts unrelated to annotated genes exists in the area of *tetO* insertion into the chromosome; this area is unique to IA 3902 when compared to the closely related 11168 (Wu *et al.*, 2013). Two non-coding RNAs were predicted in this region; these transcripts appear to be real, therefore, additional acquisition of active non-coding RNAs

along with the *tetO* gene may potentially be an area of differentiation between the two genomes of 11168 and IA 3902 that are otherwise highly syntenic and that may have helped enable the altered virulence phenotypes observed between the two strains.

An additional area of interest that warrants further investigation based on our data is the two non-coding RNAs that were identified as being differential expressed in these mutants that were also previously identified and confirmed to be transcribed in multiple other *Campylobacter* species, CjNC140 and CjNC130/6S (Dugar *et al.*, 2013). Of particularly interest is the CjNC140 non-coding RNA. Predicted to be transcribed in the intergenic region upstream of *porA*, this non-coding RNA was upregulated during exponential growth in all three of the mutant strains when compared to wild type (**Figure 9**). As increased expression was not observed during stationary growth, this suggests that CjNC140 may serve as a regulator involved in mediating changes during different stages of bacterial growth. The fact that its expression is similarly altered under all 3 mutant conditions also suggests that the three genes, *luxS*, CjNC110 and CjNC140, may normally interact within the cell in some way to facilitate these changes.

The other newly identified non-coding RNA that was also observed to be differentially expressed in our data is the CjNC130, which has been shown to be a 6S RNA homologue. The function of the 6S RNA has been elucidated in other model bacterial species and is considered to be very important in regulating transcription on a global scale by competing with DNA promoters for binding to RNA polymerase (Wassarman and Storz, 2000). The coding sequence of 6S is not conserved across bacterial genera, however, computational searches based on secondary structure have allowed for its identification across much of the prokaryotic kingdom (Wehner *et al.*, 2014). The formation of a secondary

structure consisting of a large double stranded hairpin with a central bulge is essential as it resembles an open promoter complex that allows for binding to RNA polymerase (Barrick *et al.*, 2005). CjNC130 was demonstrated to have decreased expression during exponential phase in the Δ CjNC110 Δ luxS mutant only, which suggests that increased overall RNA transcription would be allowed to occur in that mutant during exponential phase. Further investigation into the role this additional non-coding RNA may play in the physiology of *C. jejuni* is warranted.

In summary, by utilizing RNAseq technology, we were able to perform transcriptional analysis following inactivation of the CjNC110 and *luxS* genes in *C. jejuni* IA 3902 which has allowed us to identify for the first time potential regulatory roles for the CjNC110 non-coding RNA. The results reported here establish that differential RNAseq can be used to help determine functional roles of non-coding RNAs within bacteria to help direct future studies of phenotypic changes. In addition, the results generated by comparing the differences between inactivation of protein coding genes next to non-coding RNAs have demonstrated that mutational methods utilized to inactivate protein coding genes may lead to unknown polar effects on nearby non-coding RNAs. This may lead to confusion in comparing results of studies when differing methods of mutagenesis are utilized. Further work is needed to confirm the transcription expression results presented in this study, such as RT-PCR or NanoString analysis of some of the differentially expressed genes to validate that the observed differences are real. In addition, further confirmation of the presence of CjNC110, including determining the exact length of the transcript, via methods such as northern blotting, is warranted to help add to data supporting CjNC110 as an important non-coding RNA in IA 3902 and other strains of *C. jejuni*.

Table 1. Bacterial strains utilized in this study.

Strain	Description	Source or Reference
<i>Campylobacter jejuni</i>		
W7	Wild type motile variant of NCTC 11168	Plummer <i>et al.</i> , 2012
W7 ΔCjNC110	W7 ΔCjNC110::Cm ^R	This study
Sheep Abortion (SA) IA 3902	Wild type <i>C. jejuni</i>	Sahin <i>et al.</i> , 2008
IA 3902 ΔCjNC110	IA 3902 ΔCjNC110::Cm ^R	This study
IA 3902 ΔluxS	IA 3902 ΔluxS::Kan ^R	Plummer <i>et al.</i> , 2011
IA 3902 ΔCjNC110ΔluxS	IA 3902 ΔCjNC110::Cm ^R ΔluxS::Kan ^R	This study
<i>Escherichia coli</i>		
DH5α	<i>fhuA2</i> Δ(<i>argF-lacZ</i>)U169 <i>phoA glnV44</i> Φ80 Δ(<i>lacZ</i>)M15 <i>gyrA96 recA1 relA1 endA1 thi-1</i> <i>hsdR17</i>	New England Biolabs, Ipswich, MA
DH5α pNC110::cat	DH5α containing plasmid pCjNC110::cat	This study

Kan^R = kanamycin resistance cassette
Cm^R = chloramphenicol resistance cassette

Table 2. Plasmids used in this study.

Strain	Description	Source or Reference
pGEM-T	linearized vectors with T overhang and β-galactosidase screening	Promega, Madison, WI
pCjNC110::cat	pGEM plasmid carrying CjNC110 deletion construct with Cm ^R	This study

Kan^R = kanamycin resistance cassette
Cm^R = chloramphenicol resistance cassette

Table 3. Primers used in this study.

Primers	Sequence	Target
CJnc110F2	5'-TTTGATTGCGTTTTTGCAT-3'	CjNC110
CJnc110R2	5'ATCAAGAGCTTGAGCGAAGG-3'	CjNC110
SA1356F	5'-TCCCATTGGATGTTGTTGA-3'	CjSA_1356
SA1356R	5'-CAGAACCTGGCCACAACTT-3'	CjSA_1356

Table 4A. Summary of RNAseq results following rRNA depletion and strand specific library preparation on the Illumina HiSeq 2500.

Library	Total reads	Number of successfully aligned reads			Percent mapped reads
		Chromosome	pVir	Total	
IA 3902 WT-3hr-1	4167800	4060985	27341	4088326	97.4%
IA 3902 WT-3hr-2	3785630	3686851	39278	3726129	98.4%
IA 3902 WT-3hr-3	3574775	3460965	43366	3504331	98.0%
IA 3902 WT-12hr-1	4179614	4042874	43963	4086837	97.8%
IA 3902 WT-12hr-2	4286716	4159744	45225	4204969	98.1%
IA 3902 WT-12hr-3	2968022	2103578	21429	2125007	71.6%
IA 3902 Δ CjNC110-3hr-1	3995995	3853431	61455	3914886	98.0%
IA 3902 Δ CjNC110-3hr-2	3640043	3512435	36437	3548872	97.5%
IA 3902 Δ CjNC110-3hr-3	4114232	3943639	63649	4007288	97.4%
IA 3902 Δ CjNC110-12hr-1	4646416	4488809	57391	4546200	97.8%
IA 3902 Δ CjNC110-12hr-2	4158490	4028072	60311	4088383	98.3%
IA 3902 Δ CjNC110-12hr-3	5109264	3721853	27654	3749507	73.4%
IA 3902 Δ luxS-3hr-1	3251135	3143754	51047	3194801	98.3%
IA 3902 Δ luxS-3hr-2	3026876	2939706	26144	2965850	98.0%
IA 3902 Δ luxS-3hr-3	2315385	1202081	17248	1219329	52.7%
IA 3902 Δ luxS-12hr-1	4497066	4378061	42525	4420586	98.3%
IA 3902 Δ luxS-12hr-2	3294082	3190105	36272	3226377	97.9%
IA 3902 Δ luxS-12hr-3	19473343	15405040	174495	15579535	80.0%
IA 3902 Δ CjNC110 Δ luxS-3hr-1	4480648	4339847	59374	4399221	98.2%
IA 3902 Δ CjNC110 Δ luxS-3hr-2	3117870	3013513	41098	3054611	98.0%
IA 3902 Δ CjNC110 Δ luxS-3hr-3	3680686	2866303	43328	2909631	79.1%
IA 3902 Δ CjNC110 Δ luxS-12hr-1	5329709	5181117	58908	5240025	98.3%
IA 3902 Δ CjNC110 Δ luxS-12hr-2	4179965	3853179	42962	3896141	93.2%
IA 3902 Δ CjNC110 Δ luxS-12hr-3	4018571	3875936	42462	3918398	97.5%
AVERAGE	4553847	4102162	48473	4150635	92.2%
MINIMUM	2315385	1202081	17248	1219329	52.7%
MAXIMUM	19473343	15405040	174495	15579535	98.4%
MEDIAN	4066402	3853305	43145	3905514	97.9%
TOTAL	109292333			99615240	

Table 4B. Summary of RNAseq results following rRNA depletion and strand specific library preparation on the Illumina HiSeq 2500.

Library	Percent mapped reads								
	Chromosome							pVir	
	Protein coding		Ribosomal RNA		Other known RNA		Unannotated regions	Protein coding	Unannotated regions
	Sense	Antisense	Sense	Antisense	Sense	Antisense		Sense	
IA 3902 WT-3hr-1	72	1	15	0	5	3	3	93	6
IA 3902 WT-3hr-2	85	1	4	0	5	3	2	92	8
IA 3902 WT-3hr-3	87	1	3	0	4	2	3	91	9
IA 3902 WT-12hr-1	88	1	2	0	5	2	3	91	8
IA 3902 WT-12hr-2	86	1	3	0	5	1	3	91	8
IA 3902 WT-12hr-3	74	0	17	1	4	1	2	91	9
IA 3902 Δ CjNC110-3hr-1	88	1	1	0	4	2	3	90	9
IA 3902 Δ CjNC110-3hr-2	74	0	16	0	4	2	3	94	6
IA 3902 Δ CjNC110-3hr-3	90	1	2	0	3	2	3	90	9
IA 3902 Δ CjNC110-12hr-1	87	0	2	0	6	2	3	91	8
IA 3902 Δ CjNC110-12hr-2	89	1	1	0	6	1	2	91	9
IA 3902 Δ CjNC110-12hr-3	69	0	21	1	4	1	3	92	7
IA 3902 Δ luxS-3hr-1	89	1	1	0	4	2	3	90	10
IA 3902 Δ luxS-3hr-2	78	0	11	0	4	3	3	93	7
IA 3902 Δ luxS-3hr-3	65	1	27	2	3	1	2	89	11
IA 3902 Δ luxS-12hr-1	86	1	3	0	6	2	3	91	8
IA 3902 Δ luxS-12hr-2	88	1	2	0	5	2	3	91	8
IA 3902 Δ luxS-12hr-3	79	0	11	0	5	1	2	91	9
IA 3902 Δ CjNC110 Δ luxS-3hr-1	88	1	3	0	4	2	3	91	8
IA 3902 Δ CjNC110 Δ luxS-3hr-2	88	1	3	0	3	2	3	91	9
IA 3902 Δ CjNC110 Δ luxS-3hr-3	80	1	11	0	3	1	3	90	10
IA 3902 Δ CjNC110 Δ luxS-12hr-1	88	1	2	0	5	2	3	92	8
IA 3902 Δ CjNC110 Δ luxS-12hr-2	84	1	5	0	5	2	3	90	9
IA 3902 Δ CjNC110 Δ luxS-12hr-3	82	0	5	0	6	2	3	92	8
AVERAGE	83	1	7	0	5	2	3	91	8

Table 5. Summary of differential gene expression results between mutant strains.

	Condition					
	Δ CjNC110		Δ luxS		Δ CjNC110 Δ luxS	
	3 hours	12 hours	3 hours	12 hours	3 hours	12 hours
Protein-coding genes						
Number downregulated	6	16	1	6	61	32
Number upregulated	4	7	14	6	47	29
Non-coding RNA genes						
Number downregulated	0	0	0	0	25 ^b	2
Number upregulated	1 ^a	0	1 ^a	0	1 ^a	0

^a = previously described ncRNA, CjNC140 (Dugar *et al.*, 2013)

^b = 17 tRNA genes, 3 known RNA genes (tmRNA, SRP, 6S) and 4 newly predicted ncRNA

Table 6. Differential gene expression in the IA 3902 Δ CjNC110 mutant as determined by RNAseq.

Name	Synonym	COG Code	Product	Expression (RPKM)		Significance	
				WT	ΔCjNC110	Q Value	Fold change
Exponential phase							
Genes downregulated							
hisF	CJSA_1252 ^a	E	imidazole glycerol phosphate synthase subunit HisF	84	30	1.2E-04	-2.8
pseA	CJSA_1254 ^a	D	pseudaminic acid biosynthesis PseA protein	129	50	1.1E-05	-2.6
neuB2	CJSA_1263 ^b	M	N-acetylneuraminate synthase	171	57	7.0E-09	-3.0
ptmA	CJSA_1268 ^b	QR	flagellin modification protein A	107	41	4.8E-05	-2.6
-	CJSA_1352	M	putative sugar transferase	38	17	4.3E-03	-2.2
rpsN	CJSA_1603	J	30S ribosomal protein S14	541	289	3.7E-02	-1.9
Genes upregulated							
-	CJSA_0008	S	hypothetical protein	20	62	9.0E-11	3.1
cetB	CJSA_1127 ^c	T	bipartate energy taxis response protein cetB	28	78	3.1E-03	2.8
cetA	CJSA_1128 ^c	NT	bipartate energy taxis response protein cetA	45	100	2.8E-04	2.2
-	CJSA_1261	D	hypothetical protein	34	66	1.0E-02	1.9
CjNC140	predicted RNA	-	92nt length, positive strand from 1193307 to 1193399	10	59	9.0E-17	5.9
-	predicted RNA	-	55nt length, positive strand from 1132258 to 1132313 (3' end of luxS)	36	157	1.9E-07	4.4
Stationary phase							
Genes downregulated							
panC	CJSA_0271	H	pantoate-beta-alanine ligase	173	109	4.3E-03	-1.6
-	CJSA_0559	-	putative lipoprotein	135	91	3.0E-02	-1.5
-	CJSA_0687	O	M48 family peptidase	33	22	3.2E-04	-1.5
tpx	CJSA_0735	O	thiol peroxidase	1966	1326	5.4E-03	-1.5
-	CJSA_0785	S	hypothetical protein	77	51	7.8E-03	-1.5
ciaB	CJSA_0859	-	invasion antigen B	68	43	2.9E-02	-1.6

Table 6 continued

-	CJSA_1102	S	hypothetical protein	173	105	1.2E-06	-1.6
<i>petC</i>	CJSA_1122	C	putative ubiquinol-cytochrome C reductase cytochrome C subunit	474	310	1.3E-03	-1.5
-	CJSA_1137	R	2OG-Fe(II) oxygenase	39	15	1.1E-05	-2.6
-	CJSA_1244	-	hypothetical protein	30	18	7.9E-04	-1.7
<i>hisF</i>	<u>CJSA_1252</u>	E	imidazole glycerol phosphate synthase subunit HisF	56	31	6.3E-06	-1.8
<i>neuB2</i>	<u>CJSA_1263^b</u>	M	N-acetylneuraminate synthase	58	31	5.4E-03	-1.9
-	CJSA_1266 ^b	R	hypothetical protein	43	16	5.4E-06	-2.7
<i>ptmB</i>	CJSA_1267 ^b	M	cylneuraminate cytidyltransferase (flagellin modification)	158	42	2.8E-34	-3.8
<i>ptmA</i>	<u>CJSA_1268^b</u>	QR	flagellin modification protein A	102	24	2.5E-35	-4.3
-	CJSA_t0002	-	Ile tRNA	45	28	1.1E-03	-1.6
<u>Genes upregulated</u>							
<i>hcrA</i>	CJSA_0713	K	heat-inducible transcription repressor	306	659	3.5E-04	2.2
-	CJSA_0716 ^d	R	hypothetical protein	25	68	1.8E-06	2.7
-	CJSA_0717 ^d	S	hypothetical protein	20	45	1.5E-03	2.3
-	CJSA_1107 ^e	-	hypothetical protein	50	100	2.9E-02	2.0
<i>omp50</i>	CJSA_1108 ^e	-	50 kda outer membrane protein precursor	57	118	2.9E-03	2.1
<i>luxS</i>	CJSA_1136	T	S-ribosylhomocysteinase	505	1250	5.6E-07	2.5
-	CJSA_1261	D	hypothetical protein	10	29	7.8E-11	2.9
-	predicted RNA	-	55nt length, positive strand from 1132258 to 1132313 (3' end of <i>luxS</i>)	27	699	0.0E+00	25.9

a, b, c, d, e = denotes genes within the same operon as predicted by Rockhopper

underlined = significantly different expression at both timepoints

Table 7. Differential gene expression in the IA 3902 Δ luxS mutant as determined by RNAseq.

Name	Synonym	COG Code	Product	Expression (RPKM)		Significance	
				WT	ΔluxS	Q Value	Fold change
Exponential phase							
Genes downregulated							
-	CJSA_1350	H	putative methyltransferase	2047	543	2.2E-03	-3.8
-	predicted RNA	-	55nt length, positive strand from 1132258 to 1132313 (3' end of <i>luxS</i>)	36	1	7.2E-271	-36.0
Genes upregulated							
<i>dnaN</i>	CJSA_0002	L	DNA polymerase III subunit beta	55	98	4.0E-03	1.8
-	CJSA_0008	S	hypothetical protein	20	53	1.0E-08	2.7
<i>trpF</i>	CJSA_0321 ^a	E	N-(5phosphoribosyl)anthranilate isomerase	21	59	1.2E-03	2.8
<i>trpB</i>	CJSA_0322 ^a	E	tryptophan synthase subunit beta	19	37	5.3E-02	1.9
-	CJSA_0337	-	hypothetical protein	9	24	3.1E-02	2.7
-	CJSA_0370	-	hypothetical protein	22	53	2.0E-02	2.4
-	CJSA_0732	-	hypothetical protein	88	149	3.5E-02	1.7
-	CJSA_1017	S	flagellar assembly factor FliW	163	247	4.2E-02	1.5
-	CJSA_1131	-	hypothetical protein	10	27	5.3E-02	2.7
-	CJSA_1301	O	putative nucleotidyltransferase	19	33	2.7E-02	1.7
-	CJSA_1352	M	putative sugar transferase	38	61	2.6E-02	1.6
-	CJSA_1449	R	putative helix-turn-helix containing protein	43	105	1.1E-06	2.4
-	CJSA_1549	G	hypothetical protein	31	79	4.8E-07	2.5
-	CJSA_pVir0042	-	hypothetical protein	10	29	2.2E-02	2.9
CjNC140	predicted RNA	-	92nt length, positive strand from 1193307 to 1193399	10	72	4.2E-28	7.2

Table 7 continued

Stationary phase							
Genes downregulated							
-	CJSA_0560	-	hypothetical protein	193	121	2.5E-02	-1.6
-	CJSA_0620	E	M24 family peptidase	262	147	7.4E-05	-1.8
-	CJSA_1349 ^b	G	hypothetical protein	60	24	1.1E-03	-2.5
-	<u>CJSA_1350^b</u>	H	putative methyltransferase	387	208	3.5E-09	-1.9
<i>acs</i>	CJSA_1453	I	acetyl-coenzyme A synthetase	110	65	1.7E-03	-1.7
<i>leuC</i>	CJSA_1626	E	3-isopropylmalate dehydratase large subunit	58	36	1.0E-02	-1.6
-	predicted RNA	-	55nt length, positive strand from 1132258 to 1132313 (3' end of <i>luxS</i>)	27	1	0.0E+00	-27.0
Genes upregulated							
<i>flgE</i>	CJSA_0043	N	flagellar hook protein	124	244	1.7E-03	2.0
<i>flgG2</i>	CJSA_0661 ^c	N	flagellar basal-body rod protein	308	502	5.0E-03	1.6
<i>flgG</i>	CJSA_0662 ^c	N	flagellar basal-body rod protein FlgG	292	538	1.3E-03	1.8
<i>hcrA</i>	CJSA_0713	K	heat-inducible transcription repressor	306	530	2.2E-03	1.7
-	CJSA_1107	-	hypothetical protein	50	102	3.9E-03	2.0
<i>nrfA</i>	CJSA_1292	P	putative periplasmic cytochrome C	189	324	4.1E-02	1.7

^a, ^b, ^c = denotes genes within the same operon as predicted by Rockhopper

underlined = significantly different expression at both timepoints

Table 8. Differential gene expression in the IA 3902 Δ CjNC110 Δ luxS mutant as determined by RNAseq.

				Expression (RPKM)		Significance	
Name	Synonym	COG Code	Product	WT	Δ CjNC110 Δ luxS	Q Value	Fold change
Exponential phase							
Genes downregulated							
-	CJSA_0014	S	hypothetical protein	274	166	6.8E-04	-1.7
-	<u>CJSA_0041^a</u>	-	hypothetical protein	83	51	4.8E-04	-1.6
<i>flgD</i>	<u>CJSA_0042^a</u>	N	flagellar basal body rod modification protein	159	97	1.0E-03	-1.6
<i>flgE</i>	<u>CJSA_0043^a</u>	N	flagellar hook protein	140	85	5.8E-07	-1.6
-	CJSA_0067	C	iron-sulfur cluster binding protein	737	419	1.2E-02	-1.8
<i>accD</i>	CJSA_0118	I	acetyl-CoA carboxylase subunit beta	86	48	3.7E-05	-1.8
<i>trxA</i>	CJSA_0138	O	Thioredoxin	897	548	1.2E-03	-1.6
<i>panB</i>	CJSA_0272	H	3-methyl-2-oxobutanoate	64	44	4.9E-03	-1.5
<i>motB</i>	<u>CJSA_0310</u>	N	flagellar motor protein MotB	178	94	1.7E-03	-1.9
<i>fliN</i>	CJSA_0325	NU	flagellar motor switch protein	175	119	3.4E-03	-1.5
<i>rpsU</i>	CJSA_0343	J	30S ribosomal protein S21	4581	2456	9.1E-03	-1.9
<i>frdB</i>	CJSA_0383	C	fumarate reductase iron-sulfur subunit	1352	842	3.7E-02	-1.6
<i>flaG</i>	CJSA_0514 ^b	N	flagellar protein FlaG	559	379	3.0E-05	-1.5
<i>fliS</i>	CJSA_0516 ^b	NUO	flagellar protein FliS	399	266	8.6E-04	-1.5
-	CJSA_0521	-	hypothetical protein	57	32	8.1E-04	-1.8
-	CJSA_0569	R	sodium-dependent transporter	38	24	8.9E-03	-1.6
<i>pstS</i>	CJSA_0581	P	phosphate transport system substrate-binding protein	47	25	2.0E-02	-1.9
<i>hslV</i>	CJSA_0628	O	ATP-dependent protease peptidase subunit	237	162	5.7E-03	-1.5
<i>flgH</i>	<u>CJSA_0651</u>	N	flagellar basal body L-ring protein	144	75	3.6E-02	-1.9
<i>flgG2</i>	<u>CJSA_0661^c</u>	N	flagellar basal-body rod protein	220	138	1.3E-05	-1.6
<i>flgG</i>	<u>CJSA_0662^c</u>	N	flagellar basal-body rod protein FlgG	359	213	1.3E-05	-1.7
<i>mogA</i>	CJSA_0689	H	molybdenum cofactor biosynthesis protein	198	132	3.9E-02	-1.5

Table 8 continued

<i>aspB</i>	CJSA_0718	E	aspartate transaminase	122	79	1.5E-03	-1.5
-	CJSA_0788	F	putative oxidoreductase	143	80	2.3E-02	-1.8
<i>flgL</i>	<u>CJSA_0833</u>	N	flagellar hook-associated protein FlgL	142	79	1.3E-02	-1.8
<i>rpmH</i>	CJSA_0906	-	50S ribosomal protein L34	471	288	1.2E-04	-1.6
-	CJSA_0920	Q	hypothetical protein	392	223	1.7E-08	-1.8
-	CJSA_1093	C	cytochrome c553	3846	1960	1.9E-03	-2.0
-	CJSA_1102	S	hypothetical protein	190	120	1.2E-02	-1.6
<i>dctA</i>	CJSA_1130	C	C4-dicarboxylate transport protein	147	85	9.3E-08	-1.7
<i>luxS</i>	CJSA_1136	T	S-ribosylhomocysteinase	546	330	1.5E-06	-1.7
-	CJSA_1182	C	radical SAM domain-containing protein	63	43	3.4E-03	-1.5
<i>porA</i>	CJSA_1198	-	major outer membrane protein	18344	11845	4.5E-02	-1.5
<i>hydD</i>	CJSA_1203	C	putative hydrogenase maturation protease	472	250	3.6E-10	-1.9
<i>pseB</i>	<u>CJSA_1231^d</u>	MG	UDP-GlcNAc-specific C4,6 dehydratase/C5 epimerase	205	124	3.5E-07	-1.7
<i>pseC</i>	CJSA_1232 ^d	M	C4 aminotransferase specific for PseB product	124	67	6.9E-04	-1.9
-	CJSA_1233 ^d	R	hypothetical protein	44	22	4.9E-04	-2.0
<i>neuC2</i>	<u>CJSA_1264</u>	M	putative UDP-N-acetylglucosamine 2-epimerase	38	21	4.9E-02	-1.8
-	<u>CJSA_1350^e</u>	H	putative methyltransferase	2047	519	6.2E-12	-3.9
-	CJSA_1351 ^e	H	putative methyltransferase	1163	629	1.3E-02	-1.8
<i>flgl</i>	<u>CJSA_1386^f</u>	N	lagellar basal body P-ring protein	137	61	2.2E-04	-2.2
-	CJSA_1388 ^f	-	hypothetical protein	844	513	5.4E-05	-1.6
-	CJSA_1389 ^f	-	hypothetical protein	282	173	7.2E-03	-1.6
<i>flgK</i>	<u>CJSA_1390^f</u>	N	flagellar hook-associated protein FlgK	125	75	3.5E-07	-1.7
<i>moaE</i>	CJSA_1439	H	putative molybdopterin converting factor, subunit 2	130	80	7.3E-04	-1.6
<i>nuoD</i>	CJSA_1488	C	NADH dehydrogenase I subunit D	164	93	7.7E-08	-1.8
-	<u>CJSA_1562</u>	-	hypothetical protein	138	80	9.4E-05	-1.7
-	CJSA_1568	-	hypothetical protein	4698	2214	9.9E-03	-2.1
-	CJSA_1577	R	hypothetical protein	246	168	4.0E-02	-1.5
<i>secY</i>	CJSA_1597 ^g	U	preprotein translocase subunit SecY	213	94	1.4E-15	-2.3

Table 8 continued

<i>rpIO</i>	CJSA_1598 ^g	J	50S ribosomal protein L15	335	193	2.1E-03	-1.7
<i>rpsE</i>	CJSA_1599 ^g	J	30S ribosomal protein S5	463	202	6.7E-11	-2.3
<i>rpIR</i>	CJSA_1600 ^g	J	50S ribosomal protein L18	288	161	3.9E-02	-1.8
<i>rpIF</i>	CJSA_1601 ^g	J	50S ribosomal protein L6	397	208	2.2E-09	-1.9
<i>rpsH</i>	CJSA_1602 ^g	J	30S ribosomal protein S8	371	191	2.3E-04	-1.9
<i>rpsN</i>	CJSA_1603 ^g	J	30S ribosomal protein S14	541	247	1.2E-03	-2.2
<i>rpIE</i>	CJSA_1604 ^g	J	50S ribosomal protein L5	481	252	3.6E-10	-1.9
<i>rpIX</i>	CJSA_1605 ^g	J	50S ribosomal protein L24	609	316	4.7E-04	-1.9
<i>rpIN</i>	CJSA_1606 ^g	J	50S ribosomal protein L14	554	300	1.7E-08	-1.8
<i>rpmC</i>	CJSA_1608 ^g	J	50S ribosomal protein L29	350	226	4.0E-02	-1.5
<i>rpIP</i>	CJSA_1609 ^g	J	50S ribosomal protein L16	591	407	2.1E-02	-1.5
-	CJSA_CjSRP1	-	-	4910	802	7.2E-96	-6.1
<i>ssrA</i>	CJSA_CjtmRNA1	-	-	34176	20049	1.2E-03	-1.7
-	CJSA_t0002	Ile tRNA	-	245	95	1.8E-07	-2.6
-	CJSA_t0005	Ile tRNA	-	245	96	3.1E-07	-2.6
-	CJSA_t0007	Tyr tRNA	-	661	396	1.2E-03	-1.7
-	CJSA_t0012	Met tRNA	-	24	15	1.6E-05	-1.6
-	CJSA_t0013	Gln tRNA	-	23	15	2.7E-05	-1.5
-	CJSA_t0015	Ile tRNA	-	251	103	4.1E-06	-2.4
-	CJSA_t0017	Gly tRNA	-	158	69	2.0E-03	-2.3
-	CJSA_t0018	Leu tRNA	-	50	19	1.8E-06	-2.6
-	CJSA_t0020	Val tRNA	-	93	39	1.9E-03	-2.4
-	CJSA_t0021	Arg tRNA	-	312	165	2.3E-02	-1.9
-	CJSA_t0033	Leu tRNA	-	754	318	4.3E-06	-2.4
-	CJSA_t0035	Ser tRNA	-	121	50	2.3E-03	-2.4
-	CJSA_t0036	Leu tRNA	-	213	67	2.5E-08	-3.2
-	CJSA_t0037	Arg tRNA	-	800	368	9.8E-05	-2.2
-	CJSA_t0038	Arg tRNA	-	1659	994	3.8E-03	-1.7

Table 8 continued

-	CJSA_t0039		His tRNA	850	431	1.8E-05	-2.0
-	CJSA_t0043		Ala tRNA	40	19	6.2E-11	-2.1
-	predicted RNA		16 nt length, - strand from 1577169 to 1577153 (IG CJSA 1568 / <i>nhaA1</i>)	863	186	9.8E-18	-4.6
CJNC130	predicted RNA		17 nt length, + strand from 1183929 to 1183946 (6S RNA)	693	232	1.4E-05	-3.0
-	predicted RNA		55nt length, + strand from 1132258 to 1132313 (3' end of <i>luxS</i>)	36	13	5.6E-23	-2.8
-	predicted RNA		173nt length, + strand from 198877 to 199050 (antisense: CJSA_0192)	2179	803	1.9E-25	-2.7
-	predicted RNA		37 nt length, - strand from 1358594 to 1358557 (IG CJSA_1350/CJSA_1351)	2324	919	4.6E-13	-2.5
-	predicted RNA		198 nt length, + strand from 1457497 to 1457695 (CJSA 1444 internal)	217	102	1.8E-02	-2.1
-	predicted RNA		15nt length, + strand pVir from 7643 to 7658	205	99	8.8E-08	-2.1
<u>Genes upregulated</u>							
<i>dnaN</i>	CJSA_0002	L	DNA polymerase III subunit beta	55	128	8.5E-04	2.3
-	CJSA_0008 ^h	S	hypothetical protein	20	62	1.2E-09	3.1
<i>gltd</i>	CJSA_0009 ^h	ER	glutamate synthase subunit beta	92	171	1.0E-02	1.9
<i>folk</i>	CJSA_0059	H	2-amino-4-hydroxy-6-hydroxymethyldihydropteridine pyrophosphokinase	67	108	4.9E-02	1.6
-	CJSA_0076	M	putative aspartate racemase	43	76	1.7E-02	1.8
-	CJSA_0105 ⁱ	S	hypothetical protein	156	362	1.4E-04	2.3
-	CJSA_0110 ⁱ	Q	putative pyrazinamidase/nicotinamidase	46	88	2.3E-02	1.9
<i>dgkA</i>	CJSA_0234 ^j	M	diacylglycerol kinase	29	75	1.6E-02	2.6
<i>pyrC</i>	CJSA_0236 ^j	F	Dihydroorotase	25	55	1.5E-03	2.2
<i>Tal</i>	CJSA_0257	G	Transaldolase	34	59	1.8E-02	1.7
-	CJSA_0305	-	hypothetical protein	286	606	3.0E-03	2.1
<i>trpD</i>	<u>CJSA_0320^k</u>	E	anthranilate synthase component II	72	133	2.0E-02	1.8
<i>trpF</i>	CJSA_0321 ^k	E	N-(5phosphoribosyl)anthranilate isomerase	21	83	3.4E-09	4.0
<i>trpB</i>	CJSA_0322 ^k	E	tryptophan synthase subunit beta	19	56	1.8E-06	2.9
<i>trpA</i>	CJSA_0323 ^k	E	tryptophan synthase subunit alpha	12	29	4.2E-02	2.4
-	CJSA_0337	-	hypothetical protein	9	24	2.5E-02	2.7
-	CJSA_0370	-	hypothetical protein	22	55	2.9E-02	2.5
-	<u>CJSA_0372</u>	R	colicin V production protein-like protein	90	214	1.2E-03	2.4

Table 8 continued

<i>sdhA</i>	<u>CJSA_0409^l</u>	C	succinate dehydrogenase, flavoprotein subunit	30	70	2.3E-03	2.3
<i>sdhB</i>	<u>CJSA_0410^l</u>	C	succinate dehydrogenase, iron-sulfur protein subunit	31	61	4.3E-03	2.0
<i>sdhB</i>	CJSA_0411 ^l	C	succinate dehydrogenase subunit C	33	59	2.0E-02	1.8
-	CJSA_0490 ^m	-	hypothetical protein	65	122	9.0E-03	1.9
-	CJSA_0491 ^m	P	Na/Pi-cotransporter, putative	19	34	1.2E-02	1.8
-	CJSA_0836	TK	DNA-binding response regulator	38	69	4.0E-02	1.8
<i>Cfa</i>	CJSA_1121	M	cyclopropane-fatty-acyl-phospholipid synthase	22	52	3.2E-04	2.4
<i>cetB</i>	CJSA_1127 ⁿ	T	bipartate energy taxis response protein cetB	28	97	1.8E-07	3.5
<i>cetA</i>	CJSA_1128 ⁿ	NT	bipartate energy taxis response protein cetA	45	95	1.0E-02	2.1
-	CJSA_1129	T	putative PAS domain containing signal-transduction sensor protein	57	108	8.8E-03	1.9
-	CJSA_1131	-	hypothetical protein	10	33	1.3E-03	3.3
-	CJSA_1145	OC	putative lipoprotein thioredoxin	82	159	2.8E-02	1.9
-	<u>CJSA_1164</u>	T	two-component sensor (histidine kinase)	110	173	4.5E-02	1.6
<i>cbpA</i>	CJSA_1167	O	co-chaperone protein DnaJ	22	54	4.7E-04	2.5
-	CJSA_1259 ^o	QR	methyltransferase domain-containing protein	34	74	1.4E-03	2.2
-	CJSA_1260 ^o	QR	methyltransferase domain-containing protein	26	65	1.0E-03	2.5
-	CJSA_1301	O	putative nucleotidyltransferase	19	41	4.9E-03	2.2
-	CJSA_1343	-	hypothetical protein	33	59	1.9E-02	1.8
<i>tagF</i>	CJSA_1365	M	putative CDP glycerol glycerophosphotransferase	45	74	2.0E-02	1.6
-	CJSA_1449	R	putative helix-turn-helix containing protein	43	96	2.5E-03	2.2
<i>rloH</i>	CJSA_1466	R	putative ATP/GTP-binding protein	18	34	1.2E-02	1.9
<i>nuoM</i>	CJSA_1479	C	NADH dehydrogenase I subunit M	76	144	1.8E-02	1.9
-	CJSA_1549	G	hypothetical protein	31	76	3.0E-05	2.5
<i>leuC</i>	<u>CJSA_1626^p</u>	E	3-isopropylmalate dehydratase large subunit	9	22	3.4E-02	2.4
<i>leuB</i>	<u>CJSA_1627^p</u>	CE	3-isopropylmalate dehydrogenase	11	30	1.8E-02	2.7
<i>leuA</i>	<u>CJSA_1628^p</u>	E	2-isopropylmalate synthase	25	47	1.4E-02	1.9
CjNC140	predicted RNA	-	92nt length, positive strand from 1193307 to 1193399	10	40	2.5E-06	4.0
-	<u>CJSA_pVir0042</u>	-	hypothetical protein	10	42	2.5E-06	4.2

Table 8 continued

-	CJSA_pVir0044	U	hypothetical protein	12	33	1.3E-02	2.8
-	CJSA_pVir0025	-	hypothetical protein	9	24	5.3E-02	2.7
Stationary phase							
Genes downregulated							
<i>rnhB</i>	CJSA_0010	L	ribonuclease HII	76	51	1.6E-02	-1.5
-	CJSA_0158	-	hypothetical protein	361	240	1.5E-03	-1.5
-	CJSA_0160	QR	hypothetical protein	303	207	2.7E-03	-1.5
-	CJSA_0284	P	SMR family multidrug efflux pump	41	27	1.6E-02	-1.5
<i>motB</i>	<u>CJSA_0310</u>	N	flagellar motor protein MotB	181	112	1.9E-04	-1.6
<i>trpD</i>	<u>CJSA_0320</u>	E	anthranilate synthase component II	22	11	3.1E-02	-2.0
-	CJSA_0344	-	hypothetical protein	231	149	5.0E-04	-1.6
-	<u>CJSA_0372</u>	R	colicin V production protein-like protein	190	122	6.3E-05	-1.6
-	CJSA_0389	-	hypothetical protein	474	322	2.7E-03	-1.5
-	CJSA_0396	S	putative acidic periplasmic protein	32	19	9.6E-05	-1.7
<i>sdhA</i>	<u>CJSA_0409^l</u>	C	succinate dehydrogenase, flavoprotein subunit	39	22	6.3E-05	-1.8
<i>sdhB</i>	<u>CJSA_0410^l</u>	C	succinate dehydrogenase, iron-sulfur protein subunit	38	23	4.9E-02	-1.7
<i>uxaA</i>	CJSA_0452 ^q	G	putative altronate hydrolase N-terminus	54	33	4.9E-03	-1.6
<i>uxaA</i>	CJSA_0453 ^q	G	putative altronate hydrolase C-terminus	42	28	4.6E-03	-1.5
-	CJSA_0560	-	hypothetical protein	193	111	1.1E-05	-1.7
-	CJSA_0616	S	OstA family protein	27	17	1.6E-02	-1.6
<i>trmD</i>	CJSA_0677	J	tRNA (guanine-N(1)-)-methyltransferase	32	17	5.2E-06	-1.9
<i>aroB</i>	CJSA_0951	E	3-dehydroquinate synthase	91	62	1.7E-04	-1.5
-	CJSA_1137	R	2OG-Fe(II) oxygenase	39	8	2.8E-52	-4.9
-	<u>CJSA_1164</u>	T	two-component sensor (histidine kinase)	66	42	4.5E-04	-1.6
<i>pyrH</i>	CJSA_1213	F	uridylyate kinase	250	156	5.8E-03	-1.6
-	CJSA_1349	G	hypothetical protein	60	22	5.9E-20	-2.7
-	<u>CJSA_1350</u>	H	putative methyltransferase	387	170	8.2E-04	-2.3

Table 8 continued

-	CJSA_1414	TK	putative two-component regulator	100	57	3.8E-05	-1.8
<i>Acs</i>	CJSA_1453	I	acetyl-coenzyme A synthetase	110	44	5.5E-13	-2.5
-	CJSA_1461	R	MdaB protein-like protein	66	40	3.9E-02	-1.7
<i>rnhA</i>	CJSA_1548	L	ribonuclease H	38	24	1.9E-03	-1.6
-	CJSA_1560	Q	putative ABC transport system periplasmic substrate-binding protein	25	15	3.1E-02	-1.7
<i>leuC</i>	<u>CJSA_1626^p</u>	E	3-isopropylmalate dehydratase large subunit	58	29	2.1E-07	-2.0
<i>leuB</i>	<u>CJSA_1627^p</u>	CE	3-isopropylmalate dehydrogenase	56	25	5.1E-07	-2.2
<i>leuA</i>	<u>CJSA_1628^p</u>	E	2-isopropylmalate synthase	82	46	4.2E-06	-1.8
-	CJSA_pVir0030	-	hypothetical protein	198	117	5.5E-05	-1.7
-	predicted RNA		97nt length, - strand from 907368 to 907271 (antisense: CJSA_0911)	139	86	8.1E-03	-1.6
-	predicted RNA		11nt length, + strand from 1397360 to 1397371 (IG CJSA_1387/CJSA_1388)	1543	1061	4.5E-03	-1.5
Genes upregulated							
<i>dsbI</i>	CJSA_0017	O	DsbB family disulfide bond formation protein	41	87	2.4E-02	2.1
-	CJSA_0040 ^a	-	hypothetical protein	111	330	1.6E-05	3.0
-	<u>CJSA_0041^a</u>	-	hypothetical protein	74	281	1.8E-09	3.8
<i>flgD</i>	<u>CJSA_0042^a</u>	N	flagellar basal body rod modification protein	157	481	3.8E-06	3.1
<i>flgE</i>	<u>CJSA_0043^a</u>	N	flagellar hook protein	124	390	2.4E-13	3.1
<i>flgC</i>	CJSA_0494 ^r	N	flagellar basal-body rod protein FlgC	559	911	1.2E-03	1.6
<i>flgB</i>	CJSA_0495 ^r	N	flagellar basal-body rod protein FlgB	245	644	3.3E-02	2.6
<i>flgH</i>	<u>CJSA_0651</u>	N	flagellar basal body L-ring protein	241	687	1.9E-07	2.9
<i>flgG2</i>	<u>CJSA_0661^c</u>	N	flagellar basal-body rod protein	308	829	4.1E-12	2.7
<i>flgG</i>	<u>CJSA_0662^c</u>	N	flagellar basal-body rod protein FlgG	292	886	9.2E-15	3.0
<i>hcrA</i>	CJSA_0713	K	heat-inducible transcription repressor	306	722	1.2E-08	2.4
-	CJSA_0716	R	hypothetical protein	25	51	5.1E-02	2.0
<i>flgS</i>	CJSA_0749	T	sensor histidine kinase	13	32	3.6E-03	2.5
<i>flgL</i>	<u>CJSA_0833</u>	N	flagellar hook-associated protein FlgL	176	503	2.1E-08	2.9
-	CJSA_0969	S	putative lipoprotein	820	1267	3.7E-02	1.5
-	CJSA_1107 ^s	-	hypothetical protein	50	141	1.6E-09	2.8

Table 8 continued

<i>omp50</i>	CJSA_1108 ^s	-	50 kda outer membrane protein precursor	57	148	2.4E-06	2.6
-	CJSA_1180	-	hypothetical protein	642	1553	2.1E-07	2.4
<i>pseB</i>	<u>CJSA_1231</u>	MG	UDP-GlcNAc-specific C4,6 dehydratase/C5 epimerase	208	450	8.5E-06	2.2
-	CJSA_1262 ^t	J	putative methyltransferase	18	31	3.7E-02	1.7
<i>neuB2</i>	CJSA_1263 ^t	M	N-acetylneuraminate synthase	58	157	5.7E-04	2.7
<i>neuC2</i>	<u>CJSA_1264^t</u>	M	putative UDP-N-acetylglucosamine 2-epimerase	7	25	7.9E-16	3.6
<i>flgI</i>	<u>CJSA_1386^f</u>	N	lagellar basal body P-ring protein	167	546	3.2E-11	3.3
-	CJSA_1387 ^f	-	hypothetical protein	139	354	2.4E-02	2.5
<i>flgK</i>	<u>CJSA_1390^f</u>	N	flagellar hook-associated protein FlgK	160	302	8.1E-05	1.9
-	<u>CJSA_1562</u>	-	hypothetical protein	43	126	4.3E-10	2.9
<i>p19</i>	CJSA_1570	P	periplasmic protein p19	16	44	1.5E-09	2.8
-	<u>CJSA_pVir0042</u>	-	hypothetical protein	64	110	5.1E-02	1.7
-	CJSA_pVir0013	-	hypothetical protein	35	88	1.1E-04	2.5

a, b, c, etc = denotes genes within the same operon as predicted by Rockhopper

Underlined = significantly different expression at both timepoints

Double underlined = significantly different expression at both timepoints, opposite direction

IG = intergenic

Table 9. Targets predicted for CjNC110 in *C. jejuni* IA 3902, 137nt predicted length, by TargetRNA2.

Rank	Name	Synonym	Energy	P value	Product	COG code
1	-	CJSA_1104	-17.61	0.000	hypothetical protein	S
2	<i>bioA</i>	CJSA_0281	-12.72	0.005	adenosylmethionine-8-amino-7-oxononanoate transaminase	H
3	-	CJSA_1493	-12.38	0.006	putative peptide ABC-transport system ATP-binding protein	EP
4	-	CJSA_1137^a	-11.55	0.010	2OG-Fe(II) oxygenase family oxidoreductase	R
5	<i>murD</i>	CJSA_0404	-11.20	0.012	UDP-N-acetylmuramoyl-L-alanyl-D-glutamate synthetase	M
6	-	CJSA_0015	-11.08	0.013	conserved hypothetical protein	U
7	-	CJSA_0856	-11.03	0.013	SCO1/SenC family protein	R
8	-	CJSA_0572	-10.47	0.018	putative polyphosphate kinase	S
9	<i>waaC</i>	CJSA_1075	-10.31	0.020	lipopolysaccharide heptosyltransferase I	M
10	<i>chuB</i>	CJSA_1527	-10.31	0.020	putative hemin uptake system permease protein	P
11	-	CJSA_1098	-9.54	0.029	twin-arginine translocation pathway signal	Q
12	<i>sdhA</i>	CJSA_0409	-9.44	0.030	succinate dehydrogenase, flavoprotein subunit	C
13	<i>mrdB</i>	CJSA_1220	-9.41	0.031	RodA protein-like protein	D
14	<i>kpsT</i>	CJSA_1371	-9.37	0.032	capsular polysaccharide ABC transporter, ATP-binding protein	GM
15	-	CJSA_1391	-9.22	0.034	hypothetical protein	
16	<i>cgb</i>	CJSA_1498	-9.11	0.035	single domain hemoglobin	C
17	-	CJSA_1152	-8.96	0.038	putative exporting protein	
18	-	CJSA_1455	-8.87	0.039	putativetungsten ABC-transport system permease protein	H
19	-	CJSA_0799	-8.85	0.040	YGGT family protein	
20	-	CJSA_1245	-8.67	0.043	putative amino acid activating enzyme	Q
21	<i>mraY</i>	CJSA_0405	-8.42	0.047	phospho-N-acetylmuramoyl-pentapeptide-transferase	M

^a = decreased expression observed during both logarithmic and stationary growth

Table 10. List of non-coding RNAs predicted by Rockhopper to exist using RNAseq transcriptomics.

Transcription		Strand	Length	LFG	RFG	Comments	Previously identified?
Start	Stop						
Pseudogenes with transcription							
1047422	1046663	-	759		CjSA_1052	CjSA_1052 - annotated as a pseudogene	no
1331028	1331442	+	414		CjSA_1323	CjSA_1323 - annotated as a degenerate pseudogene	no
1630614	1630418	-	196		CjSA_1630	3' region of CjSA_1630 - annotated as a pseudogene	no
1630874	1630848	-	26		CjSA_1630	5' region of CjSA_1630 - annotated as a pseudogene	no
1457497	1457695	+	198		CjSA_1444	CjSA_1444 - annotated as a pseudogene	no
1555611	1555599	-	12		CjSA_1543	CjSA_1543 - annotated as a pseudogene	no
Predicted <i>cis</i> RNA							
67249	67227	-	22	SRP	CjSA_0046	Overlaps 5' end of CjSA_0046 (pseudogene)	no
1183929	1183946	+	17	CjSA_1188	CjSA_1189	antisense to 5' UTR <i>purD</i>	Yes - CjNC130/6S
Predicted <i>trans</i> RNA							
199473	199366	-	107	CjSA_0192	CjSA_1093	intergenic <i>tetO</i> and CjSA_0192	no
71394	71379	-	15	CjSA_0049	CjSA_0050	intergenic CjSA_0049 and CjSA_0050	no
197215	197309	+	94	CjSA_0191	CjSA_0192	intergenic CjSA_0191 and CjSA_0192	no
250049	249967	-	82	CjSA_0242	CjSA_0243	intergenic CjSA_0242 and CjSA_0243	Yes - CjNC20
271319	271271	-	48	CjSA_0265	CjSA_0265	intergenic <i>peb3</i> and <i>lpxB</i>	no
441750	441796	+	46	CjSA_0444	CjSA_0445	intergenic <i>rplK</i> and <i>rplA</i> , opposite strand	no
462280	462334	+	54	CjSA_0462	CjSA_0463	intergenic <i>rpsL</i> and <i>rpsG</i>	
601205	601168	-	37	CjSA_0604	CjSA_0605	intergenic <i>ppA</i> and <i>msrA</i>	no
675392	675240	-	152	CjSA_0682	CjSA_0682	intergenic <i>dnaE</i> and CjSA_0681	Yes - CjNC60
726401	726387	-	14	CjSA_0728	CjSA_0729	Intergenic, possible 5' UTR of CjSA_0728	no
738637	738648	+	11	CjSA_0737	CjSA_0738	intergenic <i>napA</i> and <i>napG</i>	no
1112058	1112049	-	9	CjSA_1127	CjSA_1128	very small intergenic	no
1132258	1132313	+	55	CjSA_1136	CjSA_1137	intergenic <i>luxS</i> and CjSA_1137, 3' end of <i>luxS</i>	no
1153480	1153499	+	19	CjSA_1157	CjSA_1158	intergenic CjSA_1157 and <i>groEL</i>	no
1193307	1193399	+	92	CjSA_1197	CjSA_1198	intergenic CjSA_1197 and <i>porA</i>	Yes - CjNC140

Table 10 continued

1243977	1243958	-	19	CjSA_1247	CjSA_1248	intergenic CjSA_1247 and CjSA_1248	no
1358594	1358557	-	37	CjSA_1350	CjSA_1351	intergenic CjSA_1350 and CjSA_1351	no
1397360	1397371	+	11	CjSA_1387	CjSA_1388	intergenic CjSA_1387 and CjSA_1388	no
1397574	1397607	+	33	CjSA_1388	CjSA_1389	intergenic CjSA_1388 and CjSA_1389	no
1577169	1577153	-	16	CjSA_1567	CjSA_1568	Intergenic CjSA_1568 and <i>nhaA1</i>	no
1589879	1589849	-	30	CjSA_1582	CjSA_1583	intergenic CjSA_1582 and <i>eno</i>	no
1602665	1602650	-	15	CjSA_1592	CjSA_1593	intergenic CjSA_1593 and <i>gltA</i>	no
1619089	1619055	-	34	CjSA_1918	CjSA_1619	intergenic CjSA_1618 and CjSA_1619	no
Predicted antisense RNA							
180678	180760	+	82	CjSA_0173	CjSA_0174	antisense: CjSA_0174 - junction of 2 genes	no
198877	199050	+	173	CjSA_0191	CjSA_1092	antisense: CjSA_0192 - antisense to 3'end	no
907368	907271	-	97	CjSA_0910	CjSA_0911	antisense: CjSA_0911 - antisense to 5'end	no
1489555	1489543	-	12		CjSA_1476	antisense: CjSA_1476 -antisense to 5'end	no
1549038	1549028	-	10		CjSA_1535	antisense: CjSA_1535 - antisense to 3'end	no
1586230	1586134	-	96		CjSA_1576	antisense: CjSA_1576	no
1198424	1198330	-	94		CjSA_1202	antisense: <i>recR</i> - antisense to 3'end	no
Predicted pVir							
7643	7658	+	15	pVir0009	pVir0010	intergenic	no
25261	25403	+	142	pVir0033	pVir0032	intergenic	yes - Cjpv2

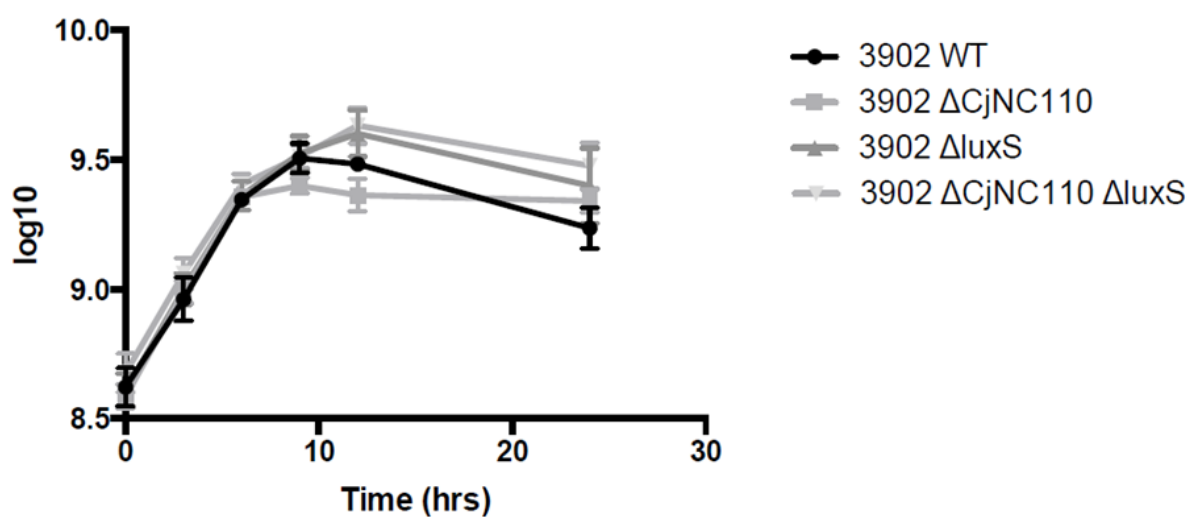
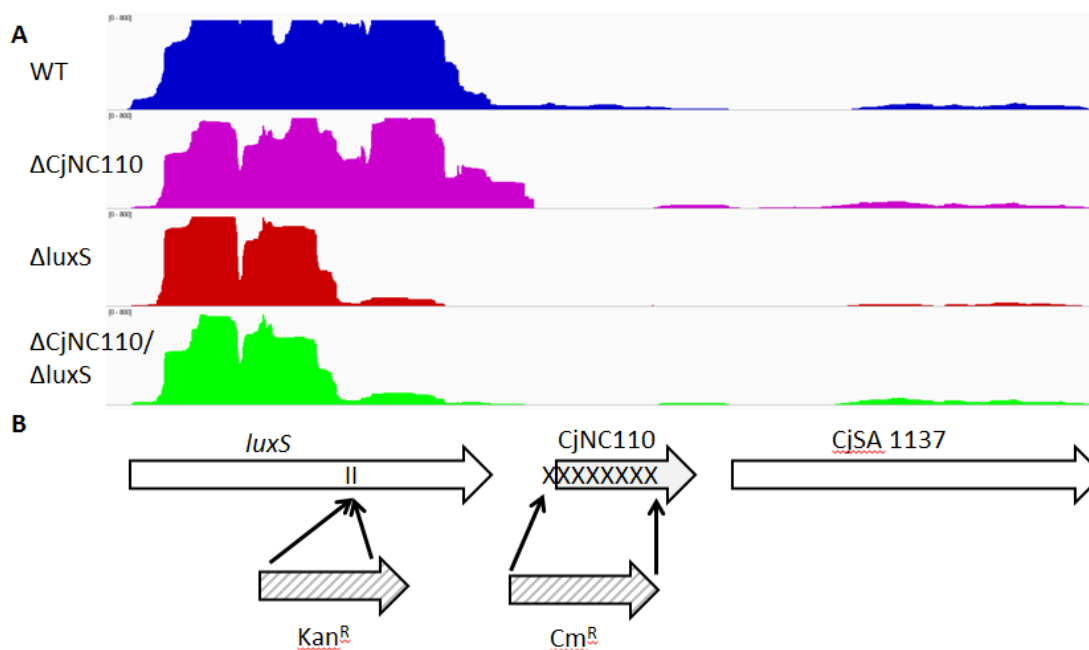
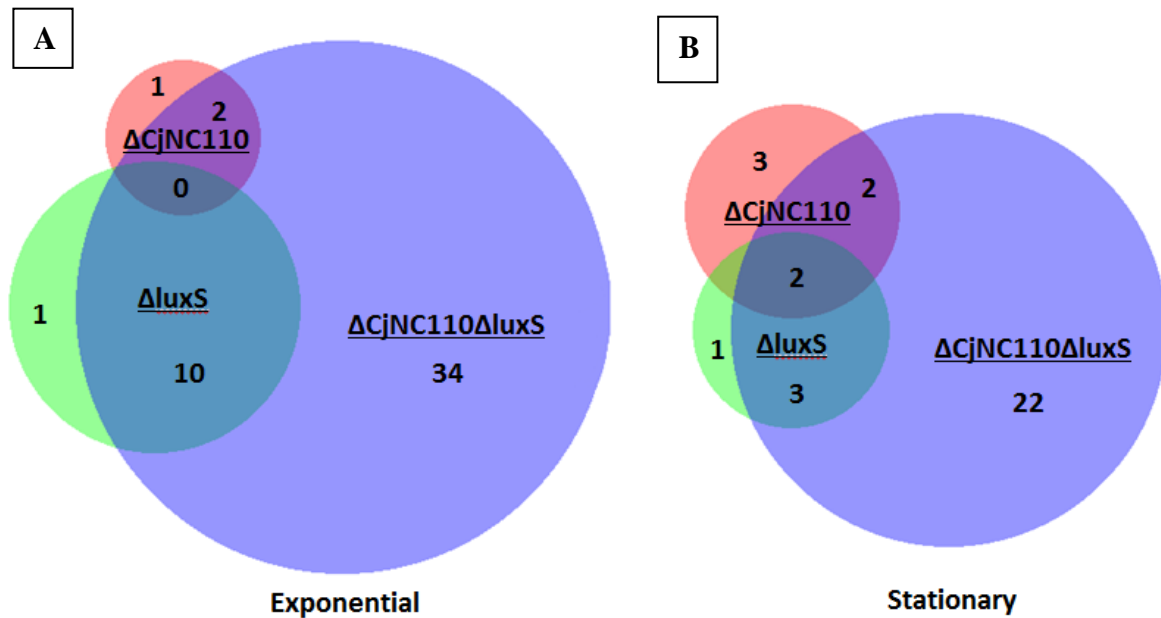


Figure 1. Growth curve of wild-type IA 3902 and isogenic mutants (mean \pm SEM). Results of four replicates (log10) of a shaking growth curve performed in 250 mL Erlenmeyer flasks under microaerophilic conditions in MH broth.



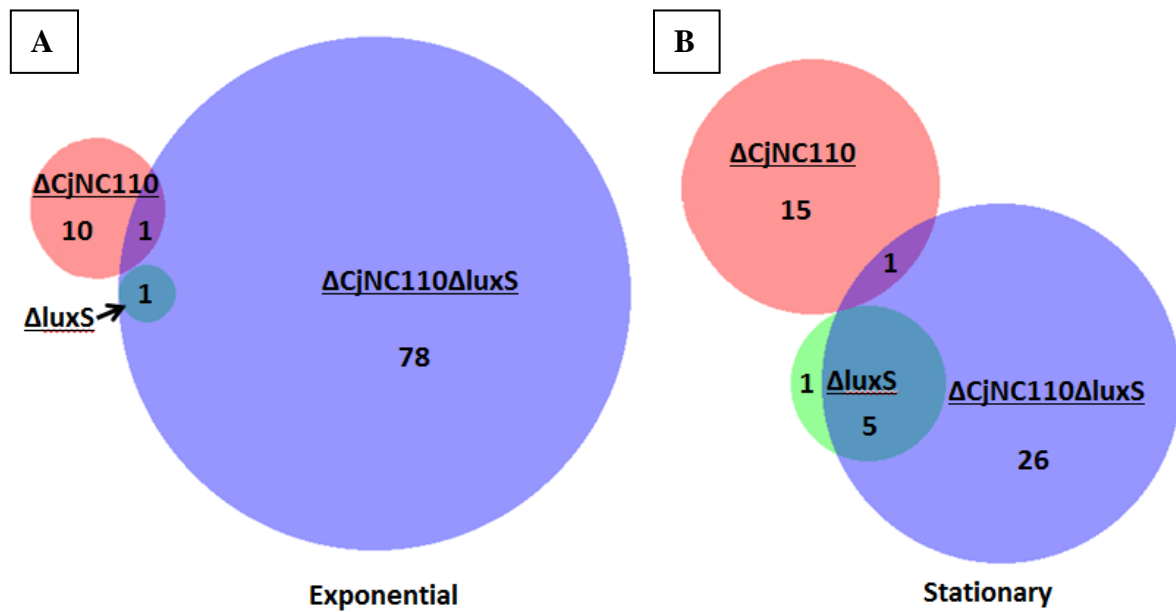
Figures 2A and 2B. Graphic view of mutations. (A) A screen capture from the IGV of the *luxS* and *CjNC110* regions of the genome, corresponding to the genome structure as depicted in (B) of all of the strains sequencing using RNAseq. (B) depicts the genome structure and mutation strategies employed to construct the mutants.

Shared upregulated genes exponential phase versus stationary phase



Figures 3A and 3B. Venn diagram depicting the overlap of shared upregulated genes during the exponential and stationary growth phases. BioVenn was used to compare the lists of known genes upregulated in all 3 mutant strains during both exponential and stationary growth.

Shared downregulated genes exponential phase versus stationary phase



Figures 4A and 4B. Venn diagram depicting the overlap of shared downregulated genes during the exponential and stationary growth phases. BioVenn was used to compare the lists of known genes downregulated in all 3 mutant strains during both exponential and stationary growth.

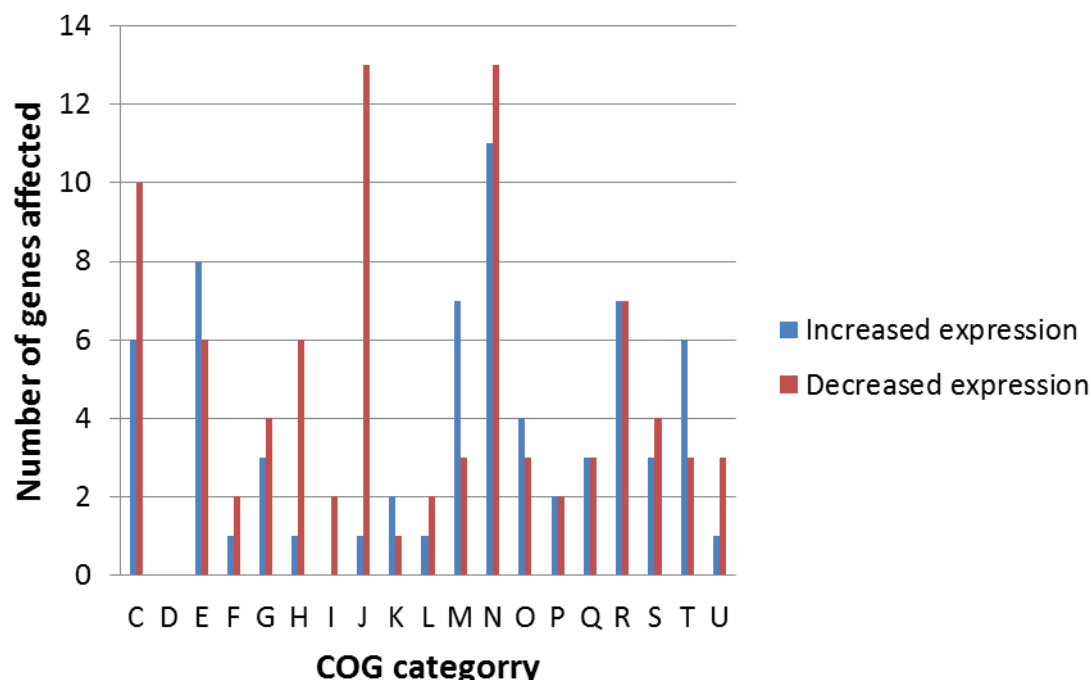
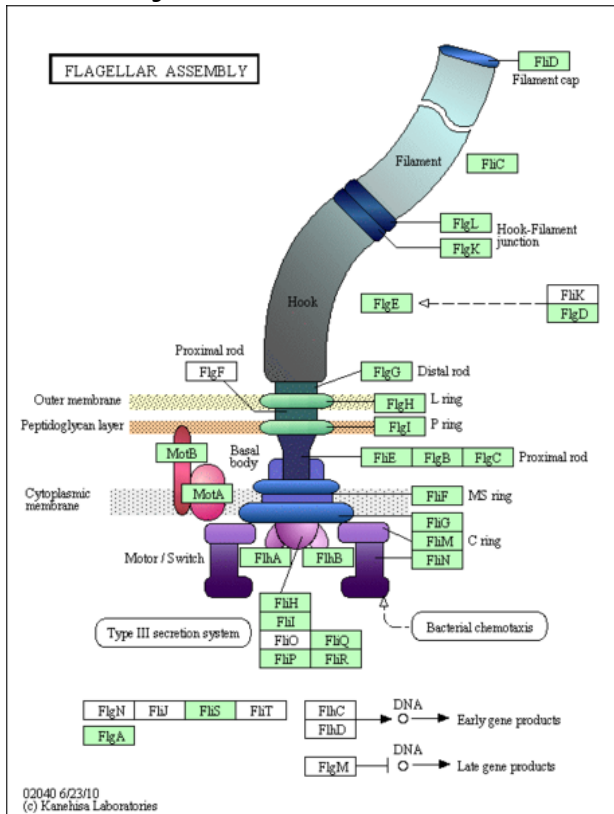
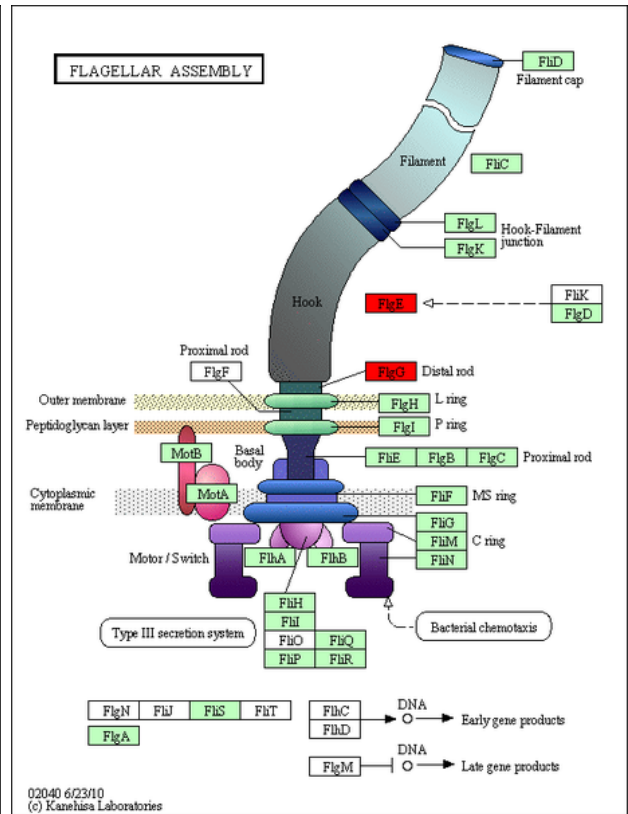
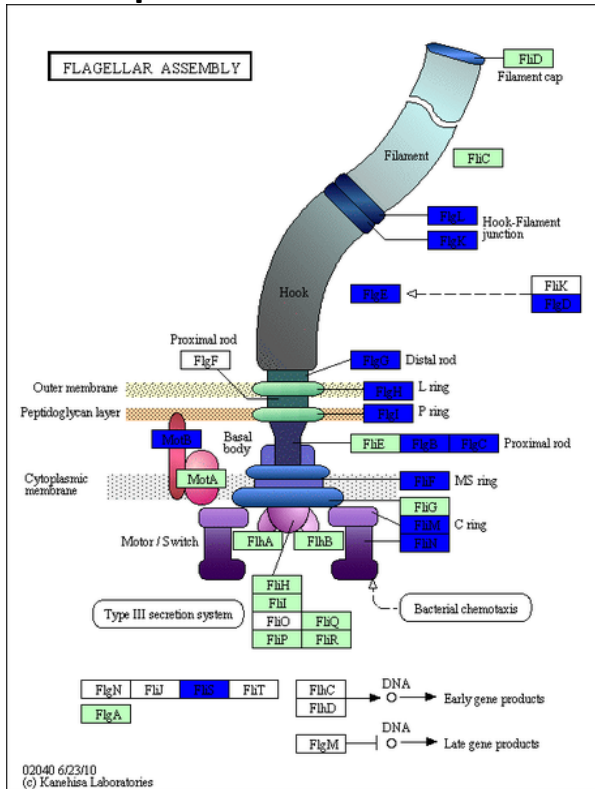


Figure 5. COG functional categories of differentially expressed genes in the $\Delta CjNC110\Delta luxS$ mutant. Clusters of Orthologous Groups (COG) categories are indicated on the x-axis, with the number of genes enriched shown on the y-axis; blue bars indicate increased expression, red bars indicate decreased expression. C - Energy production and conversion; D - Cell cycle control, mitosis and meiosis; E - Amino acid transport and metabolism; F - Nucleotide transport and metabolism; G - Carbohydrate transport and metabolism; H - Coenzyme transport and metabolism; I - Lipid transport and metabolism; J - Translation; K - Transcription; L - Replication, recombination and repair; M - Cell wall/membrane biogenesis; N - Cell motility; O - Posttranslational modification, protein turnover, chaperones; P - Inorganic ion transport and metabolism; Q - Secondary metabolites biosynthesis, transport and catabolism; R - General function prediction only; S - Function unknown; T - Signal transduction mechanisms; U - Intracellular trafficking and secretion; V - Defense mechanisms; W - Extracellular structures

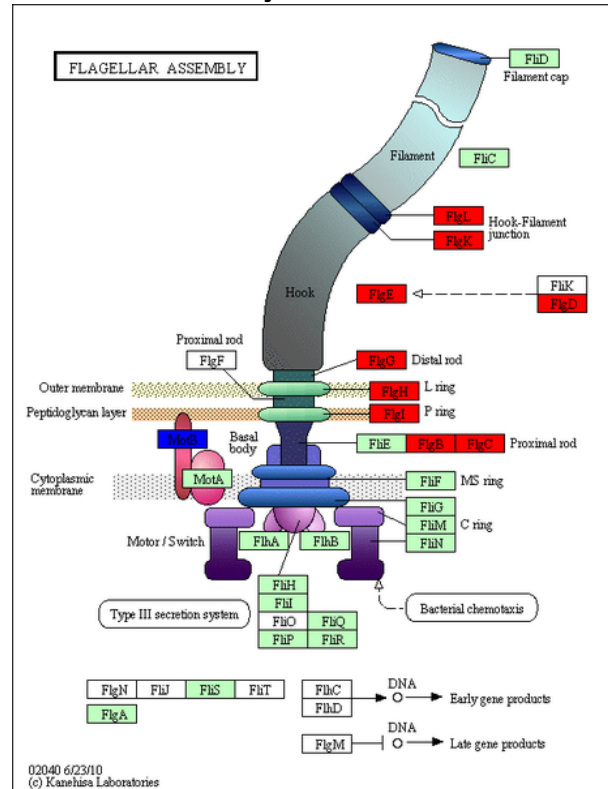
A – Δ CjNC110B – Δ luxS

Figures 6A and 6B. KEGG Pathway for flagellar assembly in *C. jejuni*: genes affected by the single mutation of either Δ CjNC110 or Δ luxS mutation during stationary growth phase. Blue color indicates downregulation of gene expression, red color indicates upregulation of gene expression, green indicates that the gene is present in *C. jejuni* IA 3902, and white indicates that the gene is not present in IA 3902.

A – Exponential



B – Stationary



Figures 7A and 7B. KEGG Pathway for flagellar assembly in *C. jejuni*: genes affected by $\Delta CjNC110\Delta luxS$ mutation during exponential (A) and stationary (B) growth phases. Blue color indicates downregulation of gene expression, red color indicates up regulation of gene expression, green indicates that the gene is present in *C. jejuni* IA 3902, and white indicates that the gene is not present in IA 3902.

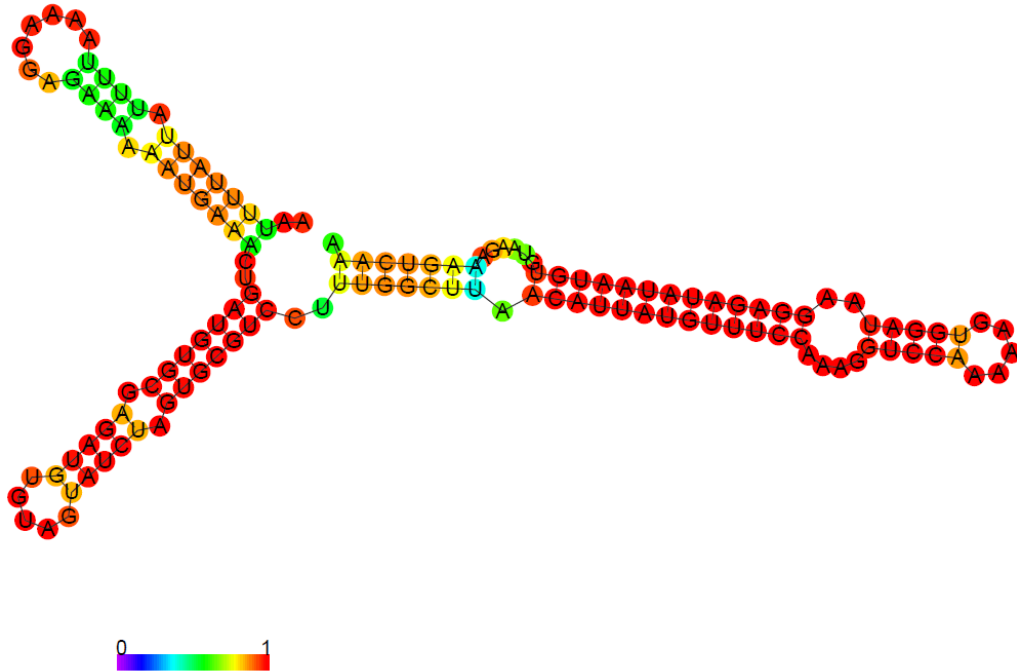
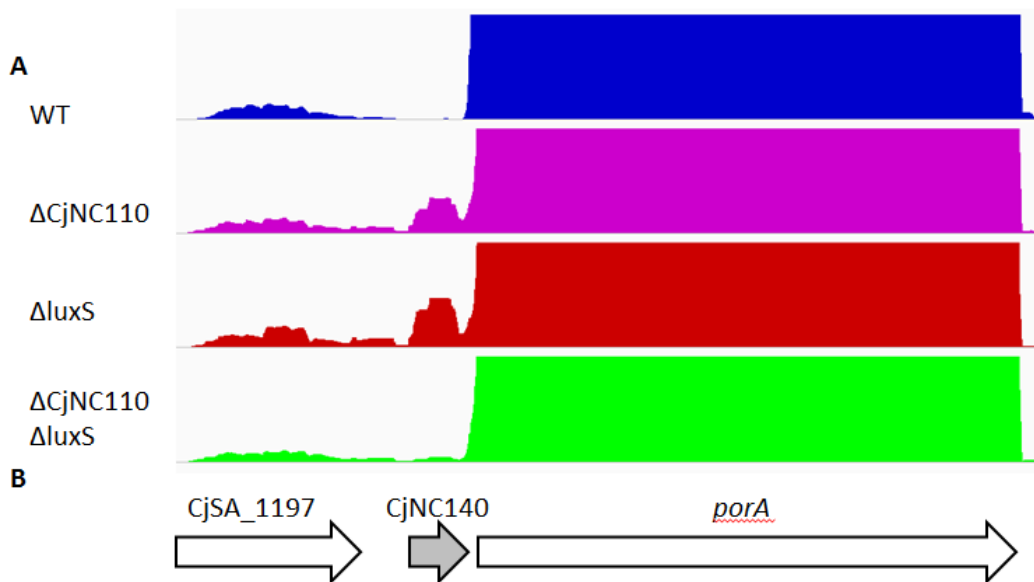


Figure 8. Structural prediction using RNAfold of the 137nt length CjNC110 RNA. The structural prediction for CjNC110 contains 3 stem loops, with the unpaired loops being the region most likely to interact with mRNAs as predicted by TargetRNA2.



Figures 9A and 9B. Graphic view of CjNC140 expression. (A) A screen capture from IGV of the *porA* and CjNC140 regions of the genome, corresponding to the genome structure as depicted in (B) of all of the strains sequencing using RNAseq.

CHAPTER 5

PHENOTYPIC CHANGES ASSOCIATED WITH INACTIVATION OF THE CjNC110

SMALL RNA IN *CAMPYLOBACTER JEJUNI* IA 3902**Abstract**

While multiple studies over the past several years have identified the presence of non-coding RNAs in the transcriptomes of various strains of the zoonotic pathogen *Campylobacter jejuni*, few have attempted to elucidate the functional role of these newly identified regulatory genes. In the previous chapter, we utilized strand specific high throughput RNA sequencing following inactivation of the CjNC110 non-coding RNA in *C. jejuni* IA 3902 to generate a list of potential mRNA regulatory targets of CjNC110 including a number of genes involved in important pathways such as energy taxis and flagellar glycosylation. Based on these observations, phenotypic assessment of growth in defined media, motility in semi-solid agar, autoagglutination ability, and autoinducer-2 (AI-2) production of the Δ CjNC110, Δ luxS, and Δ CjNC110 Δ luxS mutants compared to wild type IA 3902 was initiated. Inactivation of the CjNC110 non-coding RNA led to a statistically significant decrease in autoagglutination ability as well as AI-2 production, along with a trend towards increased motility when compared to wild type IA 3902. Mutation of the *luxS* gene led to a statistically significant decrease in motility as well as an increase in autoagglutination ability. The combined mutation of both CjNC110 and *luxS* demonstrated a further decrease in motility that was statistically significant but normal autoagglutination ability relative to wild type IA 3902. The collective results of the phenotypic and transcriptomic changes observed in our data complement each other and suggest that

CjNC110 may play an important role in regulation of energy taxis and flagellar glycosylation in *C. jejuni* IA 3902.

Introduction

Campylobacter jejuni is the leading cause of gastroenteritis due to food borne illness in humans worldwide (WHO, 2015). In addition, *C. jejuni* sheep abortion (SA) clone IA 3902 has recently emerged as an important pathogen of ovine abortion, overtaking the niche previously held by *C. fetus* subsp. *fetus* (Sahin *et al.*, 2008). Analysis of IA 3902 via a multi-omics approach revealed that IA 3902 is remarkably syntenic with the genome of *C. jejuni* type-strain 11168 (Wu *et al.*, 2013) and it does not harbor any additional known pathogenicity islands. The fact that relatively mild changes in genomic structure have led to significantly enhanced ability to cause disease by *C. jejuni* IA 3902 as described above suggests that differences in gene regulation may play a key role in regulation of virulence.

Recently, clear evidence has been published demonstrating that *C. jejuni* has the capability to produce a plethora of the important newly identified class of gene expression regulators, small non-coding RNAs (Chaudhuri *et al.*, 2011; Butcher and Stintzi, 2013; Dugar *et al.*, 2013; Porcelli *et al.*, 2013; Taveirne *et al.*, 2013). In Chapter 3, we demonstrated for the first time the expression of previously identified non-coding RNAs in *C. jejuni* IA 3902, including a number that were differentially expressed in the *in vivo* host environment. In particular, the conserved small RNA CjNC110 (Dugar *et al.*, 2013) was strongly differentially expressed during our preliminary experiments, warranting further investigation. Beyond simply establishing the existence of non-coding RNA transcripts in *Campylobacter*, there is strong need to begin to determine the functional role of these

potential regulators in this important zoonotic pathogen. The first report attempting to elucidate the role of non-coding RNA just recently published in *C. jejuni* suggests that two recently identified ncRNAs may play a role in flagellar biosynthesis; however, the authors were unable to demonstrate phenotypic changes following inactivation of these non-coding RNAs (Le *et al.*, 2015).

Regulation of cellular processes by non-coding RNAs such as CjNC110 provides a number of advantages to the bacteria when compared to the traditional model of protein-mediated regulation (Beisel and Storz, 2010). Non-coding RNAs can be rapidly produced as they do not require translation to be active, and once produced in the cell they can rapidly be recycled if necessary (Papenfort and Vogel, 2010). Non-coding RNAs can also regulate multiple different targets within a cell in a variety of ways to coordinate rapid responses to changing environments (Papenfort and Vogel, 2009). While identification of non-coding RNA has rapidly increased over the past several years, it remains challenging to assign functional roles.

In the previous chapter, we demonstrated a number of transcriptomic changes in gene expression that have the potential to lead to phenotypic changes in the Δ CjNC110 and Δ CjNC110 Δ luxS mutants. In particular, genes associated with a number of important pathways such as energy taxis and flagellar glycosylation were altered when the CjNC110 non-coding RNA was inactivated. Based on this transcriptomic data presented in Chapter 4, we hypothesized that the mutation of the small RNA CjNC110 would lead to identifiable changes in the phenotype of *C. jejuni* IA 3902. In this study, inactivation of CjNC110 was observed to affect multiple phenotypes, including motility, autoagglutination, and AI-2 activity. In addition, when combined with inactivation of the nearby *luxS* gene, unique

phenotypic differences were also observed that support the transcriptomics data already presented and indicate that some of the results generated by previous studies performed to assess the effect of mutation of the *luxS* gene may have been due to polar effects on CjNC110. When combined with the transcriptomic data presented in Chapter 4, our work suggests that differences in expression of certain genes related to autoagglutination, motility and AI-2 production may be due to a regulatory role of CjNC110 in pathways related to these important cellular functions.

Materials and Methods

Bacterial strains and culture conditions

All strains used in this study are described in **Table 1**. Mutant strains of *C. jejuni* SA (sheep abortion clone) IA 3902 Δ CjNC110 and Δ CjNC110 Δ luxS mutants were created as described in Chapter 4; the Δ luxS mutant was created previously in our lab (Plummer *et al.*, 2012). All strains were maintained in 20% glycerol stocks at -80°C and passaged from those stocks as needed for experimental procedures. *C. jejuni* IA 3902 and isogenic mutants were routinely grown in Mueller-Hinton (MH) broth or agar plates (Becton-Dickinson, Franklin Lakes, NJ) at 42°C under microaerophilic conditions with the use of compressed gas (55% O₂, 10% CO₂, 85% N₂). For strains containing a chloramphenicol resistance cassette, 5 µg/mL chloramphenicol was added to either the broth or agar plates when appropriate. For strains containing a kanamycin resistance cassette, 30 µg/mL kanamycin was added to either the broth or agar plates when appropriate. *Vibrio harveyi* strains were grown in autoinducer broth (AB) at 30°C with shaking at 175 rpm as described previously (Bassler *et al.*, 1993).

Growth curve

The A_{600} of overnight cultures was adjusted to 0.5 using sterile MH broth on a Genesys 10S VIS spectrophotometer (ThermoScientific, Waltham, MA). Cultures were then diluted 1:10 for a final targeted starting A_{600} of 0.05 in 90 mL sterile MH broth and placed in a sterile 250 mL Erlenmeyer glass flask. Cultures were incubated at 42°C under microaerophilic conditions with shaking at 125 rpm for 30 hours. Samples were removed from the flasks at designated time points (3, 6, 9, 12, 24, and 30 hours) and processed as described in Chapter 4 for RNA isolation as well as assessed for A_{600} and actual colony counts using the drop-plate method as previously described (Chen *et al.*, 2003). Samples were also collected and processed as described below for assessment of autoinducer-2 (AI-2) levels via the bioluminescence assay. All strains were assessed for growth via four independent experiments. The A_{600} of the four experiments over time were statistically analyzed using a two-way ANOVA with repeated measures and Dunnett's multiple comparison test (GraphPad Prism).

Motility and Autoagglutination

Motility was determined via inoculation of plates consisting of MH broth with 0.4% agar as previously described in our laboratory (Plummer *et al.*, 2012). Briefly, the A_{600} of overnight cultures was adjusted to 0.3 using sterile MH broth on a Genesys 10S VIS spectrophotometer (ThermoScientific). A 1 μ L volume inoculation stick was then dipped into a set volume of the standardized culture contained in the bottom of a 15 mL conical tube which was then used to make a stab inoculation into the center of the freshly made motility agar (MH broth with 0.4% Bacto agar) with a new inoculation stick for each plate. Plates

were incubated at 42°C under microaerophilic conditions as described above with the exception that the plates were incubated right-side up and in a single layer. Measurement of the outermost reach of the halo was performed at 30 hours following inoculation. All strains were assessed in quadruplicate in three independent experiments. The three experiments were statistically analyzed using a one-way ANOVA and differences between each strain assessed via Tukey's multiple comparisons test (GraphPad Prism).

Autoagglutination was assessed according to the method described previously (Misawa and Blaser, 2000) with some modifications. Briefly, the A_{600} of overnight cultures was adjusted to 1.0 in sterile Dulbecco's phosphate buffered saline (PBS) (Corning cellgro, Manassas, VA) using a Genesys 10S VIS spectrophotometer (ThermoScientific). The suspension was then aliquoted (2 mL each) into standard glass culture tubes. One subset of cultures were kept at controlled room temperature (23°C) under microaerophilic conditions; the others were incubated at 37°C microaerophilic. At 24 hours, 1 mL of the upper aqueous phase was carefully removed and A_{600} measured to determine autoagglutination activity. All strains were assessed in quadruplicate at each temperature in three independent experiments. The three experiments were statistically analyzed using a one-way ANOVA and differences between each strain assessed via Tukey's multiple comparisons test (GraphPad Prism).

***Vibrio harveyi* bioluminescence assay**

Culture samples collected from time points 3, 6, 9 and 12 hours (2 mL each timepoint) from the growth curve described above were centrifuged at 20,000 x g for 5 minutes at 4°C. The supernatant was then filter-sterilized using a 0.2 µm syringe filter to

create cell-free supernatant (CFS), which was then frozen at -80 °C until proceeding with the bioluminescence assay.

Autoinducer-2 (AI-2) levels within the collected cell-free supernatant were measured using the *Vibrio harveyi* bioluminescence assay as previously described (Surette and Bassler, 1998). Briefly, 10 µL of each sample was added to AB media containing a 1:5000 dilution of the reporter strain, *V. harveyi* strain BB170 (Bassler *et al.*, 1994) in quadruplicate. Relative light units (RLU) were measured every 15 minutes over 8 hours using the FLUOstar Omega (BMG Labtech, Ortenburg, Germany). MH broth and AB media were used as negative controls, while CFS collected from *V. harveyi* strain BB152 (Bassler *et al.*, 1993) was used as a positive control. The timepoints utilized for analysis were those occurring during the nadir of values for the negative control wells and at a standardized duration of time (3 hours 15 minutes) following initiation of increasing values for the positive wells. Following examination of the collected data, a single well from each of the four replicate wells that was located on the edge of the plate was discarded from the data analysis due to apparent systematic bias; these wells were consistently observed to have falsely increased values due to reflection from the side of the chamber. Thereafter, differences in measured RLU between strains were statistically analyzed using a two-way ANOVA with repeated measures and Sidak's multiple comparisons test (GraphPad Prism).

Results

Growth and motility

The growth of wild-type IA 3902, 3902 Δ CjNC110, 3902 Δ luxS, and 3902 Δ CjNC110 Δ luxS was evaluated over a period of 30 hours and differences tested for

statistical significance using two-way ANOVA with repeated measures of the A_{600} readings at each time point. ANOVA did identify a statistically significant difference between strains ($p < 0.05$), however, multiple comparison analysis of individual time points and strains when compared to wild type growth revealed that the only time point where the differences was considered to be statistically significant was at 30 hours for all strains. In this study, 30 hours represents the point where in most cases a decline in the A_{600} begins to occur; further examination of the actual CFU/mL over the course of the growth curve revealed that, in fact, by 30 hours cell death was beginning to occur and colony counts were decreasing (see Figure 1, Chapter 4). As further growth is assumed to be ceased at this time, there is likely very little biological significance to this finding. While there was no statistically significant difference noted in any of the strains at any other time point, there was a tendency towards decreased growth of the $\Delta CjNC110$ mutant and increased growth of the $\Delta CjNC110\Delta luxS$ mutant when compared to the wild type in all replicates of the experiment (**Figure 1**). Growth of $\Delta luxS$ closely matched that of the IA 3902 wild type throughout the course of the study as previously described for the mutation in this strain (Plummer *et al.*, 2012).

Motility of the mutant strains in semi-solid agar was compared to wild type IA 3902 at 30 hours post-inoculation for all mutant isolates, and all isolates were confirmed to be highly motile (**Figure 2A** and **2B**). Statistical analysis via one-way ANOVA indicated that there was a significant difference between strains ($p < 0.0001$). Motility for the IA 3902 $\Delta CjNC110$ strain was observed to be consistently increased above the wild type phenotype in all replicates performed. Further analysis via Tukey's multiple comparisons test did not reach statistical significance when compared to wild type, but did reach statistical significance when compared to both the $\Delta CjNC110\Delta luxS$ and $\Delta luxS$ mutants. Opposite of this, and as has

been previously suggested but not proven to be statistically significant (Plummer *et al.*, 2012), the $\Delta luxS$ mutant of IA 3902 exhibited decreased motility compared to IA 3902 wild-type which did reach statistical significance in the current study. Interestingly, analysis of the $\Delta CjNC110\Delta luxS$ revealed a decrease in motility when compared to both wild type and the $\Delta CjNC110$ strain that was again statistically significant.

Autoagglutination activity

Autoagglutination activity was measured at 23°C and 37°C following 24 hours of incubation (**Figures 3 and 4**). A statistically significant difference ($p < 0.0001$) between strains at both 23°C and 37°C was noted based on initial analysis via one-way ANOVA. At 23°C and using a cutoff for statistical significance of $p < 0.05$ when compared to wild type IA 3902, $\Delta luxS$ autoagglutination activity was noted to be increased at a statistically significant level, while $\Delta CjNC110$ exhibited statistically significant decreased autoagglutination activity. On a percentage basis, the $\Delta luxS$ mutant had 164%, and the $\Delta CjNC110$ mutant 72%, of the autoagglutination ability of the wild type at 23°C. A statistically significant difference was also noted between $\Delta CjNC110$ and both $\Delta luxS$ and $\Delta CjNC110\Delta luxS$, with $\Delta CjNC110$ exhibiting 43% and 58% of the autoagglutination activity of these mutants, respectively.

At 37°C and again using a cutoff for statistical significance of $p < 0.05$ when compared to wild type IA 3902, $\Delta luxS$ autoagglutination activity was again noted to be increased at a statistically significant level, while $\Delta CjNC110$ exhibited a statistically significant decreased autoagglutination activity. On a percentage basis, the $\Delta luxS$ mutant exhibited 115%, and the $\Delta CjNC110$ mutant 77%, of the autoagglutination ability of the wild type at 37°C. A statistically significant difference was also noted between $\Delta CjNC110$ and

both $\Delta luxS$ and $\Delta CjNC110\Delta luxS$, with $\Delta CjNC110$ exhibiting 68% and 72% of the autoagglutination activity of these mutants, respectively.

Autoagglutination activity of the $\Delta CjNC110\Delta luxS$ did not show a statistically significant difference from wild type levels at either temperature. On a percentage basis it demonstrated autoagglutination activity of 82% of wild type values at 23°C; at 37°C, the percentage was much closer to wild type at 106%. These results possibly indicate a return to mid-point between the opposing phenotypes seen within the individual mutations present.

***Vibrio harveyi* bioluminescence assay**

Bioluminescence activity was measured using the *Vibrio harveyi* assay as an approximation for autoinducer-2 (AI-2) levels generated at various time points during the growth of the wild-type and mutant strains. Both the IA 3902 $\Delta luxS$ and $\Delta CjNC110\Delta luxS$ mutant strains demonstrated no bioluminescence activity at any point during growth, indicating a complete lack of AI-2 production (**Figure 5**). This was expected as AI-2 production is dependent on a functional LuxS protein which was confirmed to be disrupted in these mutants via the transcriptomic data presented in Chapter 4. For the $\Delta CjNC110$ mutant, bioluminescence was determined to be statistically significantly decreased when compared to wild type at time points 6, 9 and 12 hours ($p < 0.05$) of the growth curve, occurring during mid to late exponential phase and early stationary phase (**Figure 6**).

Discussion

In this study we were able to demonstrate for the first time multiple phenotypic changes associated with deletional mutagenesis of the CjNC110 non-coding RNA in *C.*

jejuni IA 3902, both alone and when in combination with inactivation of the *luxS* gene. In addition, when compared to the transcriptomic changes identified in Chapter 4 of this dissertation, many of the phenotypic changes have complementary changes in genes relevant to the phenotypes observed that, when taken together, may suggest a regulatory role for CjNC110 in many important functions within *C. jejuni* IA 3902.

Motility is considered critical for the *in vivo* virulence of *C. jejuni* and requires a functional flagellar apparatus (Wassenaar *et al.*, 1991; Yao *et al.*, 1994); however, this alone is not sufficient for normal motility to be present (Golden and Acheson, 2002). In our study, while a statistically significant difference in motility was not found between the IA 3902 Δ CjNC110 mutant and wild type, there was a very consistently observed trend towards increased motility across all replicates of the motility assay that warrants further discussion. Interestingly, when assessing the transcriptomics data presented in Chapter 4, the *cetAB* operon (*Campylobacter* energy taxis proteins A and B), which is known to mediate energy taxis response in *Campylobacter*, was statistically significantly upregulated in the Δ CjNC110 mutant when compared to wild type during the exponential phase of growth; expression of *cetAB* was increased during the stationary phase as well, however, did not reach the level of statistical significance. Defects in the both the *cetA* and *cetB* genes have been shown to have altered motility phenotypes, particularly in response to migration towards critical factors in *Campylobacter* metabolism such as sodium pyruvate and fumarate, indicating that normal expression of these genes serves an important function in the ability to seek energy producing environments that allow for maximal electron transport and ATP generation (Hendrixson *et al.*, 2001; Golden and Acheson, 2002). Further elucidation of the structure of the CetA and CetB proteins revealed that CetA encodes a discrete membrane-bound MCP (methyl-

accepting chemotaxis) protein while CetB encodes a cytoplasmic PAS-domain protein, both of which are co-transcribed in a single operon (Elliott and DiRita, 2008). Investigation of expression of *cetA* and *cetB* has shown that levels of the gene products are unaffected by mutation of sigma factors σ^{54} or σ^{28} , indicating that transcription of the *cetAB* operon is likely controlled by σ^{70} or another yet unknown transcription factor. Based on this information, it seems plausible that CjNC110 might normally act as a repressor of the CetAB energy taxis system. As demonstrated in our data, removal of CjNC110 increased expression of *cetAB* and allowed for an increased motility phenotype, albeit one that did not reach statistical significance. The fact that the expression difference was most significant during log growth in our transcriptomics data is fitting considering that the highest demand for energy would likely be during the exponential phase of growth as opposed to stationary phase. Previous studies utilizing microarray data have also demonstrated that expression of *cetAB* in *C. jejuni* is growth phase dependent (Wright *et al.*, 2009; Holmes *et al.*, 2009; Stahl *et al.*, 2011). The exact effectors of CetAB that lead to increased energy taxis still remain unknown but it is suspected to be a redox sensor (Reuter and van Vliet, 2013). Additional genes have been identified to be involved in the *C. jejuni* energy taxis system, including *cetC*, which is predicted to serve as a replacement under certain circumstances for *cetB*, and *cetZ*, which is thought to regulate expression of the *cetAB* operon (Reuter and van Vliet, 2013). In *C. jejuni* IA 3902 when compared to strain 11168, *cetC* is present in the same location upstream of *cetAB*; expression of this gene is present in our transcriptomics data with no change in expression between the wild type and CjNC110 mutant. Interestingly, in IA 3902, *cetZ* is annotated as pseudogene CjSA_1052 due to a frameshift and premature stop codon when compared with 11168 (Wu *et al.*, 2013). Expression of the CjSA_1052 transcript is present in

our transcriptomic data and levels are also identical between the wild type and Δ CjNC110 mutant. Expression of a transcript in this case does not necessarily indicate the presence of a functional protein; therefore, further study of this regulatory pathway is warranted in IA 3902. It is possible that a loss of function of the CetZ regulator in IA 3902 has made regulation of the *cetAB* operon by alternative means such as via non-coding RNAs more important. The most plausible mechanism to explain how CjNC110 might normally regulate energy taxis and motility in *C. jejuni* IA 3902 is that it acts in *trans* as a repressor of translation of the *cetAB* operon. Interaction of non-coding RNAs with their target has been shown to lead to increased turnover of the mRNA message through a variety of mechanisms, including increased exposure of RNase cleavage sites, increased recruitment of some ribonucleases or increased stimulation of RNase activity (Pfeiffer *et al.*, 2009; Bandyra *et al.*, 2012). In this scenario, removal of CjNC110 might allow for a more stable mRNA message encoded by the *cetAB* operon, increasing expression of the CetA and CetB proteins and thereby allowing for an increased motility phenotype. Attempts to determine the location of the interaction between the *cetAB* operon and CjNC110 using computational prediction programs such as TargetRNA2 failed to identify an interaction region, however, computational methods of target identification are particularly unrewarding in non-model organisms such as *Campylobacter* due to a lack of conservation of small RNAs in these species (Livny *et al.*, 2008). Further work both to determine whether the observed increase in motility leads to increased ability to colonize the host as well as identification of the location of interaction between CjNC110 and the *cetAB* operon is warranted.

Minimal changes in genes associated with the flagellar apparatus were noted in the transcriptome of Δ CjNC110 which may also help to explain why an increase in energy taxis

would allow for an increase in observed motility with the assumption that normally functioning flagella are present. In contrast to the Δ CjNC110 strain, however, both the Δ luxS and Δ CjNC110 Δ luxS mutants did display altered expression of genes associated with the flagellar apparatus during at least one stage of growth (see Figures 6 and 7, Chapter 4 for review). For the Δ luxS mutant, a small number of flagellar associated genes were observed to be upregulated during stationary growth. Thus, it seems unusual that a decreased motility phenotype would be observed. No additional genes known to be related to motility in *C. jejuni* appeared to be affected by the *luxS* mutation; therefore, a reasonable explanation cannot be ascertained from this data alone. For the Δ CjNC110 Δ luxS mutant, however, there were a large number of genes involved in assembly of the flagellar apparatus that demonstrated dysregulation when both the *luxS* and CjNC110 mutations were combined. Many genes related to flagellar assembly were decreased in expression during exponential growth; however, the same genes were increased in expression during stationary growth. Our data in this study demonstrated a statistically significant decrease in motility of the Δ CjNC110 Δ luxS mutant when compared to both WT and the Δ CjNC110 mutant. This suggests that the decrease in motility is unrelated to the CjNC110 mutation when present by itself, but when both the Δ luxS and Δ CjNC110 mutations are combined, the effect of decreased motility observed in the *luxS* mutation is amplified. The observation that the deletional *luxS* mutant constructed by He *et al.* (2008) also proved to have a decrease in motility, which as discussed in Chapter 4 demonstrated similar transcriptome changes to our Δ CjNC110 Δ luxS with no shared changes to our Δ luxS mutant, corroborates these findings as well. Differences in motility observed between variations in types of mutagenesis and strain backgrounds of *luxS* mutations as described by Adler *et al.* (2014) also suggest that polar

effects of the type of mutation, which may determine whether just the *luxS* gene or the *luxS* gene and CjNC110 were affected, may play a role in these observed differences as well.

The presence of normal flagella has also been associated with autoagglutination ability and is again considered necessary but not sufficient for this important trait (Golden and Acheson, 2002). Previous studies in *C. jejuni* have demonstrated that interactions between modifications on adjacent flagellar filaments, particularly those provided by protein glycosylation, are required for normal autoagglutination (AAG) ability (Guerry *et al.*, 2006). In addition, mutants defective in autoagglutination ability have also been shown to display a decrease in adherence and invasion ability *in vitro* as well as attenuation in disease models (Guerry *et al.*, 2006). In the present study, the Δ CjNC110 mutant exhibited decreased autoagglutination when compared to wild type at both 23°C and 37°C. Interestingly, two genes that have been associated with flagellar glycosylation, *ptmA* and *neuB2*, were downregulated in our RNAseq data as presented in Chapter 4 in the Δ CjNC110 mutant when compared to wild type during both exponential and stationary growth phases. The *ptmA* and *neuB2* genes have been previously shown to be involved in production of Leg5Am7Ac and PseAm, two important structural glycans involved in flagellar glycosylation in *C. jejuni* (Logan *et al.*, 2002; McNally *et al.*, 2007). A decrease in the amount of flagellar glycosylation related to decreased production of these genes could in theory lead to decreased autoagglutination ability. The fact that we observed a decrease in autoagglutination activity in the Δ CjNC110 mutant, combined with RNAseq data indicating a decrease in the presence of the mRNA transcripts of the genes *ptmA* and *neuB2* that affect flagellar glycosylation, suggests that these findings represent a true phenotypic change in the CjNC110 mutant and an additional potential area of regulation for the CjNC110 non-coding

RNA. In this case, and in contrast to the *cetAB* operon where removal of CjNC110 led to an increase in expression, inactivation of CjNC110 led to a decrease in the expression of these two genes which were predicted to belong to the same operon in our Rockhopper analysis. In other bacterial species, small RNAs have been shown to lead to stabilization of the target mRNA (Papenfort and Vanderpool, 2015). This suggests that CjNC110 may normally serve in *trans* to prevent degradation of the *ptmA* and *neuB2* mRNA transcripts after they have been produced, leading to increased longevity of the mRNA and thus increasing levels of the translated protein. By removing CjNC110, stabilization of the mRNA message of *ptmA* and *neuB2* may not occur as normal, leading to increased turnover of the message and decreased protein production. Again, attempts to determine the location of the interaction between *ptmA*, *neuB2* and CjNC110 using computational prediction programs such as TargetRNA2 failed to identify an interaction region, however, this is not unexpected and does not decrease the possibility that a true relationship does exist. Further work both to determine whether this decrease in autoagglutination ability holds biological significance such as a decreased ability to colonize the host, as well as identification of the location of interaction between CjNC110 and these genes is warranted.

On the contrary, the Δ luxS mutant exhibited statistically significant increased autoagglutination at both 23°C and 37°C. This finding is the opposite of what was observed in a different strain of *C. jejuni*, 81-176, where the *luxS* mutation led to a decrease in autoagglutination ability (Jeon *et al.*, 2003). Mutation of the *luxS* gene by Jeon *et al.* (2003) was accomplished via inverse PCR mutagenesis which resulted in the removal of 486bp of the *luxS* gene region. As this method of mutagenesis is identical to the method used by He *et al.* (2008) that appears to have resulted in polar affects in expression of the CjNC110 non-

coding RNA, it is plausible to suggest that the results obtained in that study may also be a result of the *luxS* gene inactivation in combination with polar affects to CjNC110. While in our study, the Δ CjNC110 Δ luxS strain did not exhibit significant changes from wild type in autoagglutination ability, there are known differences between strains of *C. jejuni* in the type of flagellar glycosylation present, particularly between 11168 (which is considered syntenic to IA 3902) and 81-176, which may help to further explain the differences observed between studies (Merino and Tomas, 2014).

It is unclear at this time what mechanism allowed for increased autoagglutination ability in the Δ luxS mutant in this particular strain of *C. jejuni*. In addition, while these changes in autoagglutination are statistically significant, the biological relevance at this time is unknown. When measured in terms of percent of normal autoagglutination of the IA 3902 wild type strain, for the Δ luxS mutant, autoagglutination ability was observed to be 164% and 115% of the wild type at 23°C and 37°C, respectively. For the Δ CjNC110 mutant, autoagglutination was observed to be 72% at 23°C and 77% at 37°C of the wild type. However, when compared to the percentage of autoagglutination possible, which would be considered 100% at an A_{600} of 0.00 and 0% at an A_{600} of 1.0, both the wild type and mutant strains still exhibited a relatively high ability to autoagglutinate (**Table 2**). For comparison, mutations in the *flaA/flaB* and *flbA* genes of *C. jejuni* strain 81-176 led to a decrease from A_{600} 0.031 (96.9%) to 0.731 (24.9%) and 0.654 (35.6%), respectively (Misawa and Blaser, 2000). Differences in virulence displayed in both *in vitro* and *in vivo* models are likely to be expected with such dramatic changes in AAG activity as displayed in the *flaA/flab* and *flbA* mutations; however, as the differences displayed in our mutants were not as dramatic, it is difficult to predict how much biological significance these changes hold. As neither the *luxS*

gene nor the CjNC110 are known to be directly involved in flagellar glycosylation, it seems reasonable that inactivation of these genes could lead to a modification of autoagglutination ability without complete loss or gain of function. Further work both *in vitro* and *in vivo* assessing invasion and colonization ability are needed to determine if these changes yield significant differences in virulence. In addition, assessment for changes in the flagellar glycosylation of these mutants when compared to the wild type IA 3902 is warranted.

The final phenotype assessed in this study was the ability of the Δ CjNC110 strain to produce wild type levels of autoinducer-2 (AI-2) in the bioluminescence assay. Statistical analysis showed that for all time points except 3 hours, there was a statistically significant decrease in the ability of the Δ CjNC110 strain to induce bioluminescence via the *V. harveyi* bioassay. On initial examination, it seems counterintuitive that while the transcription of the *luxS* gene was increased in the Δ CjNC110 mutant in our RNAseq transcriptomic data as presented in Chapter 4, the relative activity of AI-2 appears decreased in the Δ CjNC110 mutant. Both the RNA used for the differential gene expression study and the cell-free supernatant used for the bioluminescence assay were obtained from the exact same set of growth curve experiments, therefore, differences between experimental conditions can be ruled out as the cause of these disparate findings. One potential explanation for the observed opposing results could be that CjNC110 may normally serve to stabilize the transcript of the *luxS* gene in IA 3902, thus allowing more transcript to be translated into the active LuxS protein and leading to what would be considered “normal” AI-2 production. In contrast, if by inactivation of CjNC110, the *luxS* gene transcript becomes less stable and its mRNA turnover is therefore increased, there would be less LuxS protein available for production of AI-2. The observed increase in gene expression of *luxS* in the Δ CjNC110 mutant may be an effort to

overcome this increased rate of turnover of the *luxS* mRNA, however, a mechanism for the increased gene expression is not readily apparent. As discussed in Chapter 4, the mutagenesis of CjCN110 in IA 3902 did lead to a single exchange in the primary structure of the protein of arginine for leucine (L161R) at amino acid 161. The mutation present is not located within either of the previously identified functional domains of the LuxS protein (Adler *et al.*, 2014), and in some species of bacteria the protein is truncated prior to this amino acid (Plummer *et al.*, 2011). Therefore it is reasonable to suggest that this substitution should result in minimal changes to the functionality of the LuxS protein in producing AI-2, however, it cannot be ruled out that this amino acid substitution is in fact responsible for the altered bioluminescence phenotype observed in the Δ CjNC110 mutant. To determine if the L161R substitution is able to affect the ability of the LuxS protein to produce AI-2, further work comparing the activity of the wild type and L161R LuxS protein via generation of recombinant protein in *E. coli*, isolation and characterization as previously described is warranted (Plummer *et al.*, 2011).

In summary, the results presented in this study demonstrate for the first time phenotypic changes associated with inactivation of the CjNC110 non-coding RNA in an important strain of *C. jejuni*, IA 3902. Growth curve analysis did not demonstrate a statistically significant difference in growth rate between strains. The Δ CjNC110 mutant was observed to demonstrate a trend towards increased motility which was suggested by upregulation of the *cetAB* energy taxis operon. Autoagglutination ability was observed to be statistically significantly decreased which may be related to decreased expression of flagellar glycosylation genes. Assessment of production of AI-2 demonstrated a statistically significant decrease in the Δ CjNC110 mutant which warrants further study. Mutation of the

$\Delta luxS$ gene demonstrated a statistically significant decrease in motility which has been previously suggested but not shown to be statistically significant, as well as an increase in autoagglutination ability. Both of these changes are in direct contrast to mutation of CjNC110. When the two independent mutations were combined in the $\Delta CjNC110\Delta luxS$ double mutant, the decreased motility phenotype of the $\Delta luxS$ mutation was amplified, however, no change in autoagglutination was seen.

Further work is needed utilizing complementation of CjNC110 into the $\Delta CjNC110$ mutant to validate that the phenotypic changes observed are in fact due solely to the deletion of the CjNC110 small RNA and not unintended polar effects to either the neighboring genes, *luxS* (upstream) or CjSA_1137 (downstream), or other unknown changes in the genome. Complementation of the CjNC110 non-coding RNA may prove to be more difficult than complementation studies performed in protein coding genes as proper length and secondary structure of the transcribed RNA is likely very important to success of complementation, whereas in protein coding genes as long as a promoter is present to initiate transcription and the coding sequence remains the same, complementation can be achieved. *In vivo* studies looking at the colonization ability of both the $\Delta CjNC110$ and $\Delta CjNC110\Delta luxS$ mutants are also warranted to determine if the phenotypic changes seen translate into changes in virulence of IA 3902. The studies we have performed thus far have focused on the role that CjNC110 plays in IA 3902 in particular, however, CjNC110 is one of the few small RNAs identified in *C. jejuni* that appear to be fairly well conserved across all of the strains tested thus far. Particularly as our data suggests that the length of CjNC110 may differ between strains of *C. jejuni*, it is possible that the effect of inactivation of this small RNA differs between strains. Some of the regulatory networks that we identified in the both the

transcriptomic and phenotypic studies also were suggested to differ between strains, therefore, studies to assess whether inactivation of CjNC110 in other strains of *C. jejuni* leads to similar phenotypic changes are warranted. Finally, determination of the location and method of interaction between CjNC110 and its target transcripts will provide yet another important piece of the puzzle which will help bring us closer to understanding gene regulation in the important human and animal pathogen, *C. jejuni* IA 3902.

Table 1. List of strains utilized in this study.

Strain	Description	Source or Reference
<i>Campylobacter jejuni</i>		
Sheep Abortion (SA) IA 3902	Wild type <i>C. jejuni</i>	Sahin <i>et al.</i> , 2008
IA 3902 Δ CjNC110	IA 3902 Δ CjNC110::Cm ^R	This dissertation
IA 3902 Δ luxS	IA 3902 luxS::Kan ^R	Plummer <i>et al.</i> , 2011
IA 3902 Δ CjNC110 Δ luxS	IA 3902 Δ CjNC110::Cm ^R luxS::Kan ^R	This dissertation
<i>Vibrio harveyi</i>		
BB170	AI-2 reporter strain with luxN::Tn5	Bassler <i>et al.</i> , 1994
BB152	AI-1 ⁻ , AI-2 ⁺ ; luxM::Tn5	Bassler <i>et al.</i> , 1993

Kan^R = kanamycin resistance cassette

Cm^R = chloramphenicol resistance cassette

Table 2. Autoagglutination activity reported as a percentage of activity possible.

Strain	23°C		37°C	
	%	A ₆₀₀ ^a	%	A ₆₀₀ ^a
IA 3902 wild type	82.3%	0.177±0.007	85.5%	0.145±0.002
IA 3902 Δ CjNC110	75.1%	0.249±0.011	81.2%	0.189±0.003
IA 3902 Δ luxS	89.3%	0.107±0.006	87.4%	0.126±0.003
IA 3902 Δ CjNC110 Δ luxS	85.5%	0.145±0.017	86.4%	0.136±0.005

^a = autoagglutination activity measured by A₆₀₀, with standard error of the mean

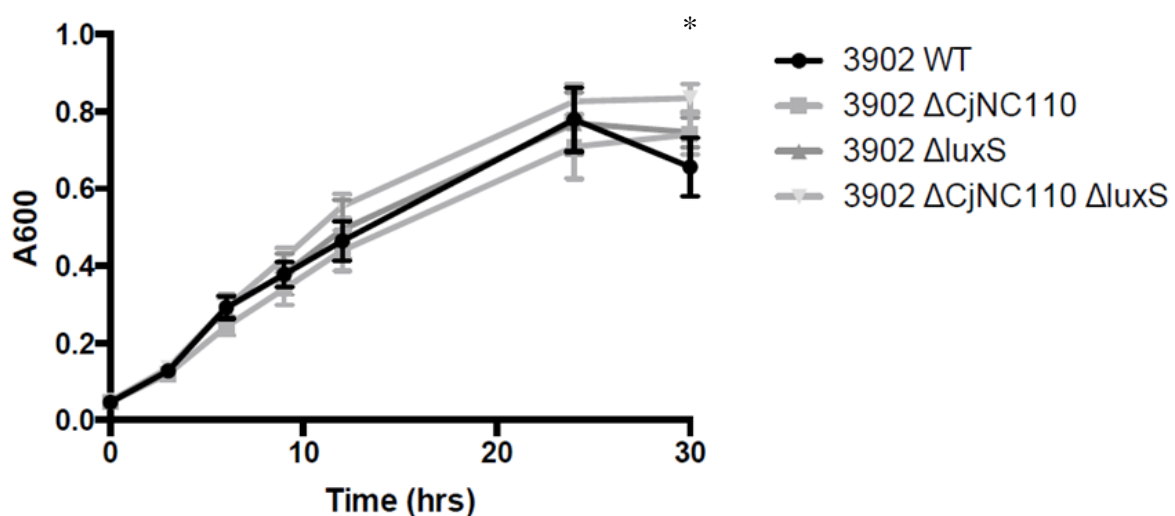


Figure 1. Shaking Growth curve of wild-type IA 3902 and isogenic mutants (mean \pm SEM). Results of four replicates (A_{600}) of a shaking growth curve performed in 250 mL Erlenmeyer flasks under microaerophilic conditions in MH broth. Analysis via two-way ANOVA revealed a statistically significant difference between strains ($p < 0.05$), however, multiple comparison analysis of individual time points and strains when compared to wild type growth revealed that the only time point where the differences was considered to be statistically significant was at 30 hours for all strains (denoted by *).

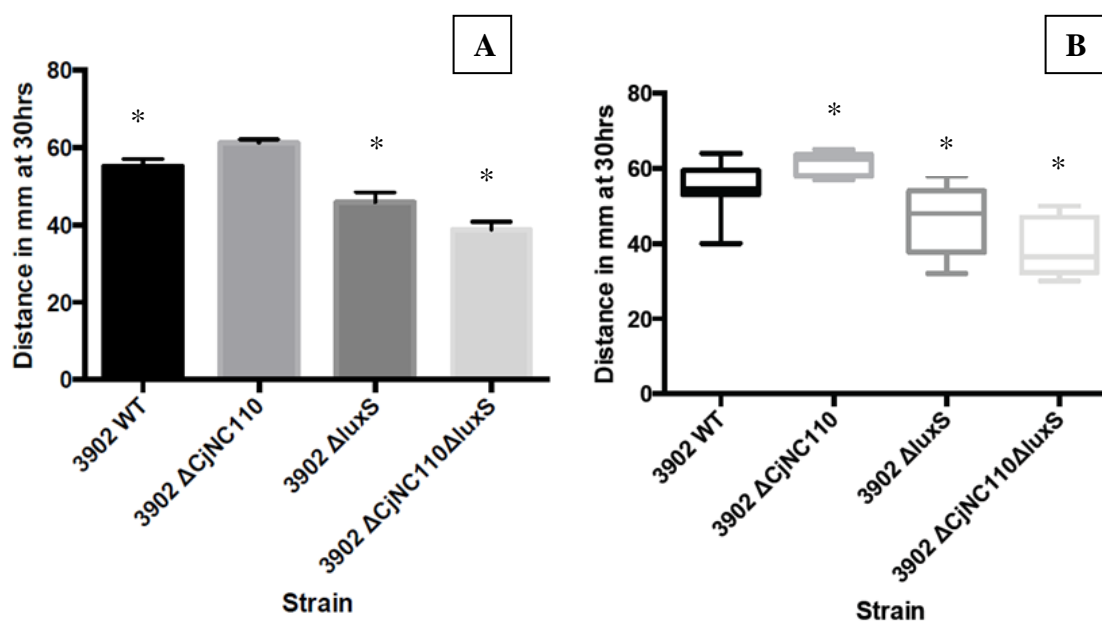


Figure 2A and 2B. Motility assay of wild-type IA 3902 and isogenic mutants (A - mean \pm SEM; B – box and whisker plot of min, median, and max). Results of motility assay performed in semi-solid agar and measured at 30 hours post inoculation. Statistical analysis via one-way ANOVA indicated that there was a significant difference between strains ($p < 0.0001$). In (A), * denotes a statistically significant difference from the wild type strain. In figure (B), * denotes a statistically significant difference from the Δ CjNC110 mutant.

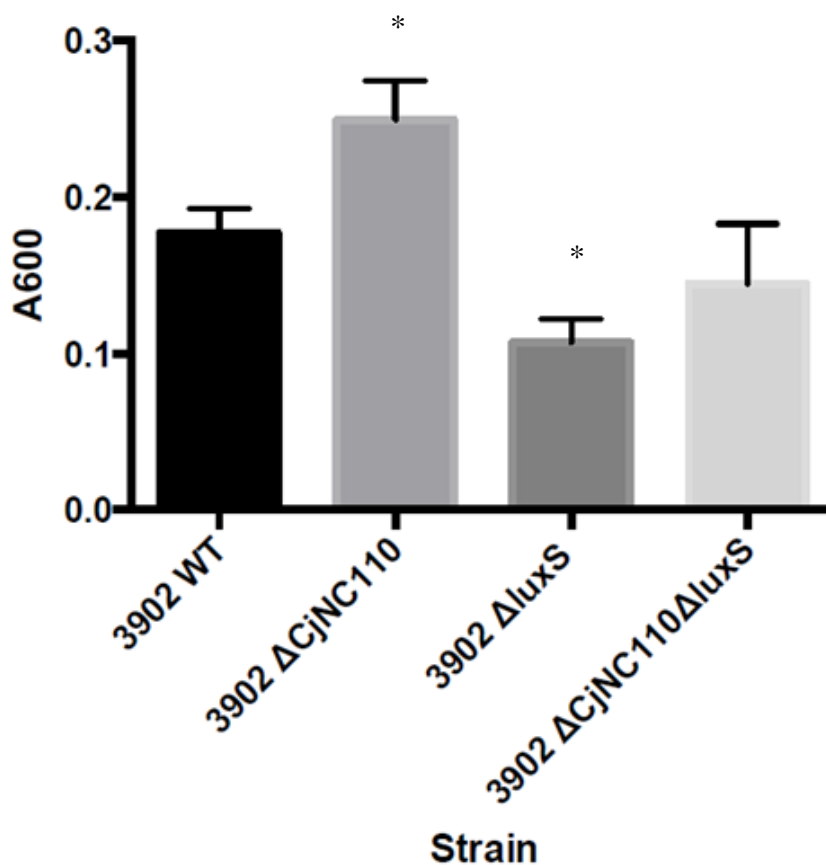


Figure 3. Autoagglutination activity after 24 hours incubation at 23°C (mean ± SEM).

A statistically significant difference ($p < 0.0001$) between strains at 23°C was noted based on initial analysis via one-way ANOVA. At 23°C and using a cutoff for statistical significance of $p < 0.05$ when compared to wild type IA 3902, $\Delta luxS$ autoagglutination activity was noted to be increased at a statistically significant level, while $\Delta CjNC110$ exhibited statistically significant decreased autoagglutination activity (denoted by *).

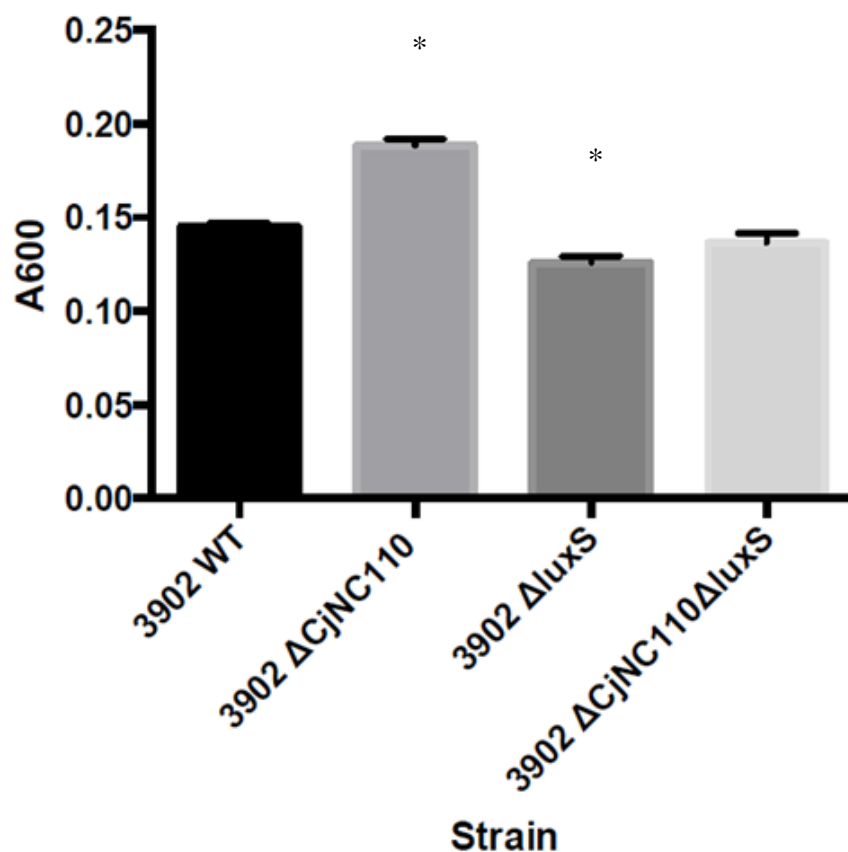


Figure 4. Autoagglutination activity after 24 hours incubation at 37°C (mean ± SEM).

A statistically significant difference ($p < 0.0001$) between strains at 37°C was noted based on initial analysis via one-way ANOVA. At 37°C and using a cutoff for statistical significance of $p < 0.05$ when compared to wild type IA 3902, $\Delta luxS$ autoagglutination activity was noted to be increased at a statistically significant level, while $\Delta CjNC110$ exhibited statistically significant decreased autoagglutination activity (denoted by *).

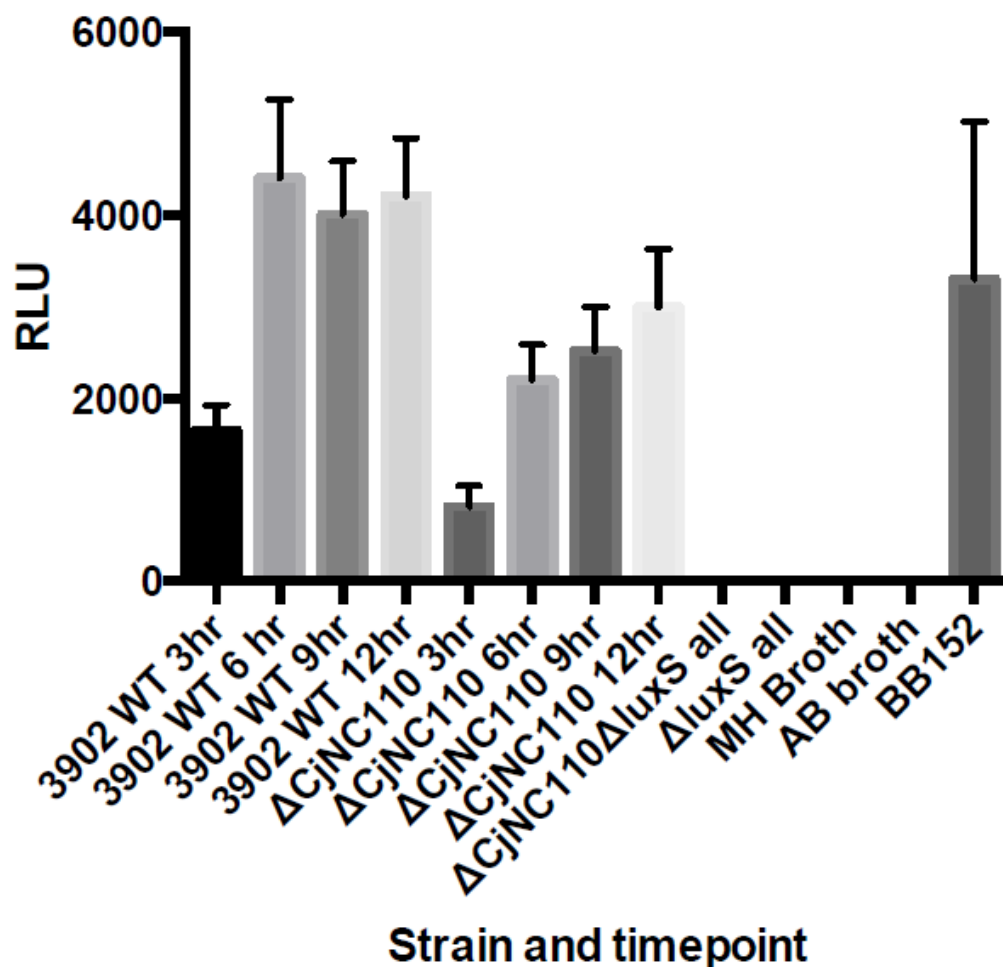


Figure 5. Bioluminescence as measured via the *Vibrio harveyi* bioassay (mean \pm SEM). Bioluminescence activity of 3902 Δ CjNC110 compared to the positive control strains *Vibrio harveyi* BB152 and 3902 wild type. Each bar represents the average of four replicates with standard error. BB152 is the positive control. MH and AB broth are shown as negative controls. Both the IA 3902 Δ luxS and Δ CjNC110 Δ luxS mutant strains demonstrated no bioluminescence activity at any point during growth, indicating a complete lack of AI-2 production as expected. Production of AI-2 increased over time during the course of the growth curve for both wild type and Δ CjNC110 strains.

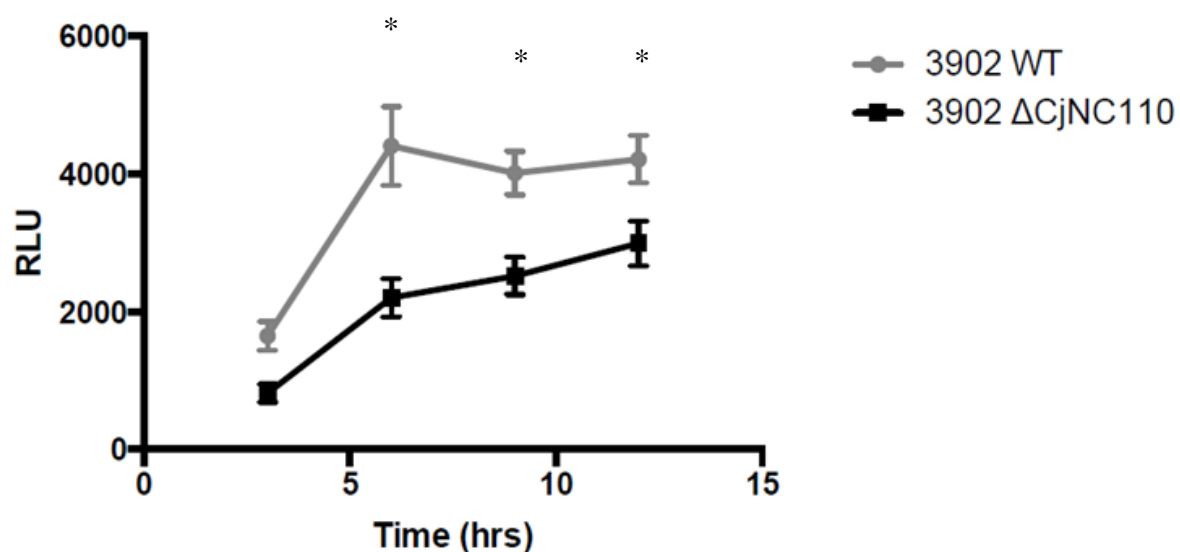


Figure 6. Bioluminescence as measured via the *Vibrio harveyi* bioassay over the course of growth (mean \pm SEM). Bioluminescence activity of 3902 Δ CjNC110 compared to the 3902 wild type over the course of growth. The bioluminescence of the Δ CjNC110 mutant was determined to be statistically significantly decreased when compared to wild type at time points 6, 9 and 12 hours ($p < 0.05$) of the growth curve, occurring during mid to late exponential phase and early stationary phase (denoted by *).

CHAPTER 6

SUMMARY AND FUTURE DIRECTIONS

Summary

Campylobacter jejuni is the leading cause of foodborne bacterial gastroenteritis worldwide and is an important cause of ovine abortion particularly in the United States. Colonization of the gallbladder by *C. jejuni* is thought to play a key role in transmission and persistence of this important zoonotic agent; however, there is a fundamental knowledge gap in our understanding of the molecular mechanisms utilized to establish infection in such a harsh environment. The objective for this dissertation was to determine the molecular mechanisms responsible for *C. jejuni* colonization of the gallbladder as well as localize the site of colonization within the gallbladder. Our central hypothesis was that changes in expression of the *C. jejuni* transcriptome including both protein coding genes and non-coding RNAs allow it to adapt to the bile-rich environment and colonize the protective mucous lining of the gallbladder where it acts as a chronic nidus of pathogen shedding. To test this hypothesis, the following specific aims were developed: 1) identify the location of gallbladder colonization by *C. jejuni* 2) identify specific bacterial elements responsible for adaptation of *C. jejuni* for survival in bile and 3) select specific non-coding RNAs that are differentially expressed in the gallbladder environment for further study.

First, we utilized a unique model of direct inoculation of *C. jejuni* IA 3902 into the ovine gallbladder to demonstrate the preferred location of IA 3902 within the gallbladder environment using immunohistochemistry staining of the major outer membrane protein (MOMP). We observed high levels of MOMP staining deep with the glands of the

gallbladder mucosa as well as in free-floating luminal debris. We were then able to demonstrate that *C. jejuni* IA 3902 appears to have an affinity for neutral mucin, acid mucin and L-fucose in the ovine gallbladder based on observation of the organism localized in higher numbers to areas with increased staining for PAS, Alcian blue and lectin. These data suggest that to survive within the harsh environment of the gallbladder, colonization of the deep mucosal glands of the gallbladder occurs to allow avoidance of the constant flushing action of bile release and the detergent activities of bile salts in the lumen. Once established, this site of colonization can then serve as a nidus of chronic infection and shedding into the environment where the infection can then be maintained in the herd or lead to human exposure and zoonotic disease.

Second, we utilized the bacteria collected from the *in vivo* sheep gallbladder inoculation model and *in vitro* inoculated bile to harvest total RNA for assessment of the complete transcriptome of *C. jejuni* IA 3902 via RNAseq during exposure to this important host environment, the sheep gallbladder. We demonstrated that the transcriptional environment during direct interaction within the host, as displayed by utilizing *in vivo* inoculation of and RNA recovery from the sheep gallbladder environment, provides a more robust picture of the complexity of gene regulation required for survival when compared to *in vitro* exposure to ovine bile alone. Using these data, we confirmed the role of the multi-drug efflux pumps *cmeABC* and *cmeDEF* for survival within bile and the host gallbladder. We identified a subset of 67 genes that were upregulated during all conditions and timepoints, suggesting a key role in survival within bile, including two highly expressed hypothetical proteins that warrant further study. We also identified a subset of 77 genes upregulated only under the *in vivo* conditions which suggests that they may be important in responding to

environmental cues only found in the host. In addition to identification of important protein coding genes, seven previously identified non-coding RNAs were confirmed to be differentially expressed within our data. Small non-coding RNAs have been shown in other species of bacteria to play a key role in regulating gene expression, suggesting that they may play an important role in rapid regulation of gene expression upon exposure to bile and the host environment.

Following our preliminary *in vivo* gallbladder transcriptome analysis, we identified a previously validated ncRNA, CjNC110, which appeared to be differentially regulated in the host environment. A mutant was constructed to inactivate this small RNA, and this mutation was also transferred into the previously constructed $\Delta luxS$ mutant in IA 3902 to generate a double knockout of these neighboring genes. By again utilizing RNAseq technology, we were able to perform transcriptional analysis of the effects of inactivation of both the CjNC110 and *luxS* genes, individually and in combination, in *C. jejuni* IA 3902. The results of this study have allowed us to identify for the first time potential regulatory roles in a number of important pathways such as energy taxis and flagellar glycosylation for the CjNC110 non-coding RNA in *C. jejuni*. The results reported here establish that differential RNAseq can be used to help determine functional roles of non-coding RNAs within bacteria to help direct future studies of phenotypic changes. In addition, the results generated by comparing the differences between inactivation of protein coding genes next to non-coding RNAs have demonstrated that mutational methods utilized to inactivate protein coding genes may lead to unknown polar effects on nearby non-coding RNAs which may cause confusion in comparing results of studies when differing methods are utilized.

Finally, we utilized the transcriptional changes observed within the RNAseq data to design experiments to assess for potential phenotypic changes in the IA 3902 Δ CjNC110 mutant and Δ CjNC110 Δ luxS double mutant and compared those to the phenotype of the Δ luxS mutant. Growth curve analysis did not demonstrate a statistically significant difference in growth rate between strains. The Δ CjNC110 mutant was observed to demonstrate a trend towards increased motility and statistically significant decreased autoagglutination ability, both phenotypes which were suggested by the RNAseq data. Mutation of the Δ luxS gene demonstrated a statistically significant decrease in motility as well as an increase in autoagglutination ability, both of which were in direct contrast to mutation of CjNC110. When the two independent mutations were combined in the Δ CjNC110 Δ luxS double mutant, the decreased motility phenotype of the Δ luxS mutation was amplified; however, no change in autoagglutination was seen. This data represents the first report of phenotypically identifiable changes associated with inactivation of a small non-coding RNA in any strain of *C. jejuni*.

Collectively, these findings provide new insights into several levels of the *C. jejuni* pathobiology of the emerging zoonotic pathogen sheep abortion clone IA 3902. The results along each step of the process complement the findings of the previous work and provide a strong foundation for future research focusing on the role of the gallbladder environment in maintaining *C. jejuni* within animal populations as well as the molecular mechanisms such as non-coding small RNAs that allow it to survive in this harsh environment.

Future directions

The sheep gallbladder inoculation model developed for this study provides many additional opportunities to further study the molecular mechanisms of survival utilized by *C. jejuni* to persist within this harsh host environment; however, additional work utilizing a more natural model of inoculation is also warranted. Oral inoculation of *C. jejuni* IA 3902 to confirm that colonization of the deep mucosal glands of the gallbladder occurs under conditions similar to natural exposure is an important next step in proving that gallbladder colonization is a key component to maintaining *C. jejuni* within a susceptible population. In addition, future work combining oral inoculation with prior placement of a Hemoclip® over the common bile duct should prove useful in determining whether the route of infection of the gallbladder is septicemia via the bloodstream, liver, and secretion into the bile, or retrograde through the common bile duct into the gallbladder directly from the intestinal tract.

The results obtained in the transcriptomic study of the response of *C. jejuni* to exposure to the ovine gallbladder provided a wealth of potential areas of further research. First, additional work to validate the differential expression of a subset of the genes and non-coding RNAs identified in this study via RT-PCR or other modalities such as the NanoString nCounter is warranted. Following validation, a number of key targets including the two highly expressed hypothetical proteins warrant further study, in particular the putative outer membrane protein CjSA_1528. In addition to identification of important protein coding genes, seven previously identified non-coding RNAs were confirmed to be differentially expressed within our data; as these represent potential regulators with the ability to have far reaching impact on global gene expression, further study of these should be a primary focus

of future work. In particular, the CjNC140, which demonstrated differential expression both in all four conditions of exposure to bile, as well as during exponential growth in the CjN110 mutant transcriptomic study, is a small RNA that may work together with CjNC110 to mediate gene expression in IA 3902 and warrants further study.

Additional work is also needed to confirm the results presented in the RNAseq transcriptomic study of the CjNC110 mutant, again utilizing such technology as RT-PCR for individual genes or NanoString nCounter to screen a large number of genes at once. Northern blot analysis of some of the differentially expressed small non-coding RNAs to validate both their existence and length is also warranted, particularly of CjNC110 itself, as the apparent length of CjNC110 in IA 3902 as determined via RNAseq appears to be longer than the length observed in other strains of *C. jejuni*. Further work is needed utilizing complementation of CjNC110 into the Δ CjNC110 mutant to validate that the phenotypic changes observed are in fact due solely to the deletion of the CjNC110 small RNA and not unintended polar effects to either the neighboring genes, *luxS* (upstream) or CjSA_1137 (downstream), or other unknown changes in the genome. Complementation of the CjNC110 non-coding RNA may prove to be more difficult than complementation studies performed in protein coding genes as proper length and secondary structure of the transcribed RNA is likely very important to success of complementation, whereas in protein coding genes as long as a promoter is present to initiate transcription and the coding sequence remains the same, complementation can be achieved. *In vivo* studies looking at the colonization ability of both the Δ CjNC110 and Δ CjNC110 Δ luxS mutants are also warranted to determine if the phenotypic changes seen translate into changes in virulence of IA 3902. The studies we have performed thus far have focused on the role that CjNC110 plays in IA 3902 in particular,

however, CjNC110 is one of the few small RNAs identified in *C. jejuni* that appear to be fairly well conserved across all of the strains tested thus far. Particularly as our data suggests that the length of CjNC110 may differ between strains of *C. jejuni*, it is possible that the effect of inactivation of this small RNA differs between strains. Some of the regulatory networks that we identified in both the transcriptomic and phenotypic studies also were suggested to differ between strains, therefore, studies to assess whether inactivation of CjNC110 in other strains of *C. jejuni* leads to similar phenotypic changes are warranted. Finally, determination of the location and method of interaction between CjNC110 and its target transcripts will provide yet another important piece of the puzzle which will help bring us closer to understanding gene regulation in the important human and animal pathogen, *C. jejuni* IA 3902.

REFERENCES

1. Acik, M. N. and B. Cetinkaya (2006). "Heterogeneity of *Campylobacter jejuni* and *Campylobacter coli* strains from healthy sheep." Vet Microbiol **115**(4): 370-375.
2. Adler, L., T. Alter, S. Sharbati and G. Golz (2014). "Phenotypes of *Campylobacter jejuni* luxS mutants are depending on strain background, kind of mutation and experimental conditions." PLoS One **9**(8): e104399.
3. Aiba, H. (2007). "Mechanism of RNA silencing by Hfq-binding small RNAs." Curr Opin Microbiol **10**(2): 134-139.
4. Akiba, M., J. Lin, Y. W. Barton and Q. Zhang (2006). "Interaction of CmeABC and CmeDEF in conferring antimicrobial resistance and maintaining cell viability in *Campylobacter jejuni*." J Antimicrob Chemother **57**(1): 52-60.
5. Allen, K. J. and M. W. Griffiths (2001). "Effect of environmental and chemotactic stimuli on the activity of the *Campylobacter jejuni* flaA sigma(28) promoter." FEMS Microbiol Lett **205**(1): 43-48.
6. Alm, R. A., P. Guerry and T. J. Trust (1993). "The *Campylobacter* sigma 54 flaB flagellin promoter is subject to environmental regulation." J Bacteriol **175**(14): 4448-4455.
7. Alvaro, D., A. Cantafora, A. F. Attili, S. Ginanni Corradini, C. De Luca, G. Minervini, A. Di Biase and M. Angelico (1986). "Relationships between bile salts hydrophilicity and phospholipid composition in bile of various animal species." Comp Biochem Physiol B **83**(3): 551-554.
8. Attack, J. M., P. Harvey, M. A. Jones and D. J. Kelly (2008). "The *Campylobacter jejuni* thiol peroxidases Tpx and Bcp both contribute to aerotolerance and peroxide-mediated stress resistance but have distinct substrate specificities." J Bacteriol **190**(15): 5279-5290.
9. Babakhani, F. K. and L. A. Joens (1993). "Primary swine intestinal cells as a model for studying *Campylobacter jejuni* invasiveness." Infect Immun **61**(6): 2723-2726.
10. Bandyra, K. J., N. Said, V. Pfeiffer, M. W. Gorna, J. Vogel and B. F. Luisi (2012). "The seed region of a small RNA drives the controlled destruction of the target mRNA by the endoribonuclease RNase E." Mol Cell **47**(6): 943-953.
11. Baptissart, M., A. Vega, S. Maqdasy, F. Caira, S. Baron, J. M. Lobaccaro and D. H. Volle (2013). "Bile acids: from digestion to cancers." Biochimie **95**(3): 504-517.

12. Barnhart, J. L. and D. W. Upson (1979). "Bile flow and electrolyte composition of bile associated with maximum bilirubin excretion in sheep." Can J Physiol Pharmacol **57**(7): 710-716.
13. Barrick, J. E., N. Sudarsan, Z. Weinberg, W. L. Ruzzo and R. R. Breaker (2005). "6S RNA is a widespread regulator of eubacterial RNA polymerase that resembles an open promoter." RNA **11**(5): 774-784.
14. Bassler, B. L., M. Wright, R. E. Showalter and M. R. Silverman (1993). "Intercellular signalling in *Vibrio harveyi*: sequence and function of genes regulating expression of luminescence." Mol Microbiol **9**(4): 773-786.
15. Bassler, B. L., M. Wright and M. R. Silverman (1994). "Multiple signalling systems controlling expression of luminescence in *Vibrio harveyi*: sequence and function of genes encoding a second sensory pathway." Mol Microbiol **13**(2): 273-286.
16. Begley, M., C. G. Gahan and C. Hill (2005). "The interaction between bacteria and bile." FEMS Microbiol Rev **29**(4): 625-651.
17. Beisel, C. L. and G. Storz (2010). "Base pairing small RNAs and their roles in global regulatory networks." FEMS Microbiol Rev **34**(5): 866-882.
18. Berks, B. C., F. Sargent and T. Palmer (2000). "The Tat protein export pathway." Mol Microbiol **35**(2): 260-274.
19. Bischler, T., H. S. Tan, K. Nieselt and C. M. Sharma (2015). "Differential RNA-seq (dRNA-seq) for annotation of transcriptional start sites and small RNAs in *Helicobacter pylori*." Methods **86**: 89-101.
20. Blaser, M. J. (1993). "Role of the S-layer proteins of *Campylobacter fetus* in serum-resistance and antigenic variation: a model of bacterial pathogenesis." Am J Med Sci **306**(5): 325-329.
21. Blaser, M. J., P. F. Smith, J. E. Repine and K. A. Joiner (1988). "Pathogenesis of *Campylobacter fetus* infections. Failure of encapsulated *Campylobacter fetus* to bind C3b explains serum and phagocytosis resistance." J Clin Invest **81**(5): 1434-1444.
22. Brantl, S. (2007). "Regulatory mechanisms employed by cis-encoded antisense RNAs." Curr Opin Microbiol **10**(2): 102-109.
23. Brantl, S. and N. Jahn (2015). "sRNAs in bacterial type I and type III toxin-antitoxin systems." FEMS Microbiol Rev **39**(3): 413-427.
24. Breaker, R. R. (2012). "Riboswitches and the RNA world." Cold Spring Harb Perspect Biol **4**(2).

25. Bryner, J. H., P. C. Estes, J. W. Foley and P. A. O'Berry (1971). "Infectivity of three *Vibrio fetus* biotypes for gallbladder and intestines of cattle, sheep, rabbits, guinea pigs, and mice." Am J Vet Res **32**(3): 465-470.
26. Burrough, E. R., O. Sahin, P. J. Plummer, Q. Zhang and M. J. Yaeger (2009). "Pathogenicity of an emergent, ovine abortifacient *Campylobacter jejuni* clone orally inoculated into pregnant guinea pigs." Am J Vet Res **70**(10): 1269-1276.
27. Burrough, E. R., Z. Wu, O. Sahin, Q. Zhang and M. J. Yaeger (2012). "Spatial distribution of putative growth factors in the guinea pig placenta and the effects of these factors, plasma, and bile on the growth and chemotaxis of *Campylobacter jejuni*." Vet Pathol **49**(3): 470-481.
28. Burrough, E., S. Terhorst, O. Sahin and Q. Zhang (2013). "Prevalence of *Campylobacter* spp. relative to other enteric pathogens in grow-finish pigs with diarrhea." Anaerobe **22**: 111-114.
29. Butcher, J., R. A. Handley, A. H. van Vliet and A. Stintzi (2015). "Refined analysis of the *Campylobacter jejuni* iron-dependent/independent Fur- and PerR-transcriptomes." BMC Genomics **16**: 498.
30. Butcher, J. and A. Stintzi (2013). "The transcriptional landscape of *Campylobacter jejuni* under iron replete and iron limited growth conditions." PLoS One **8**(11): e79475.
31. Caldelari, I., Y. Chao, P. Romby and J. Vogel (2013). "RNA-mediated regulation in pathogenic bacteria." Cold Spring Harb Perspect Med **3**(9): a010298.
32. Chandrashekhar, K., Kassem, II, C. Nislow, D. Gangaiah, R. A. Candelero-Rueda and G. Rajashekara (2015). "Transcriptome analysis of *Campylobacter jejuni* polyphosphate kinase (ppk1 and ppk2) mutants." Virulence **6**(8): 814-818.
33. Chaudhuri, R. R., L. Yu, A. Kanji, T. T. Perkins, P. P. Gardner, J. Choudhary, D. J. Maskell and A. J. Grant (2011). "Quantitative RNA-seq analysis of the *Campylobacter jejuni* transcriptome." Microbiology **157**(10): 2922-2932.
34. Chen, C. Y., G. W. Nace and P. L. Irwin (2003). "A 6 x 6 drop plate method for simultaneous colony counting and MPN enumeration of *Campylobacter jejuni*, *Listeria monocytogenes*, and *Escherichia coli*." J Microbiol Methods **55**(2): 475-479.
35. Clark, B. L. and M. J. Monsbrough (1979). "The prevalence of *Campylobacter fetus* in the gall bladder of sheep." Aust Vet J **55**(1): 42-43.
36. Coleman, R., S. Iqbal, P. P. Godfrey and D. Billington (1979). "Membranes and bile formation. Composition of several mammalian biles and their membrane-damaging properties." Biochem J **178**(1): 201-208.

37. CDC (Centers for Disease Control) (2013). "*Campylobacter jejuni* " Retrieved December 22, 2015 from <http://www.cdc.gov/pulsenet/pathogens/Campylobacter.html>.
38. Conway, T., J. P. Creecy, S. M. Maddox, J. E. Grissom, T. L. Conkle, T. M. Shadid, J. Teramoto, P. San Miguel, T. Shimada, A. Ishihama, H. Mori and B. L. Wanner (2014). "Unprecedented high-resolution view of bacterial operon architecture revealed by RNA sequencing." *MBio* **5**(4): e01442-01414.
39. Corcionivoschi, N., M. Clyne, A. Lyons, A. Elmi, O. Gundogdu, B. W. Wren, N. Dorrell, A. V. Karlyshev and B. Bourke (2009). "*Campylobacter jejuni* cocultured with epithelial cells reduces surface capsular polysaccharide expression." *Infect Immun* **77**(5): 1959-1967.
40. Croucher, N. J. and N. R. Thomson (2010). "Studying bacterial transcriptomes using RNA-seq." *Curr Opin Microbiol* **13**(5): 619-624.
41. Dakdouki, G. K., G. F. Araj and M. Hussein (2003). "*Campylobacter jejuni*: unusual cause of cholecystitis with lithiasis. Case report and literature review." *Clin Microbiol Infect* **9**(9): 970-972.
42. Darfeuille, F., C. Unoson, J. Vogel and E. G. Wagner (2007). "An antisense RNA inhibits translation by competing with standby ribosomes." *Mol Cell* **26**(3): 381-392.
43. de Sa, P. H., A. A. Veras, A. R. Carneiro, K. C. Pinheiro, A. C. Pinto, S. C. Soares, M. P. Schneider, V. Azevedo, A. Silva and R. T. Ramos (2015). "The impact of quality filter for RNA-Seq." *Gene* **563**(2): 165-171.
44. Debruyne, L., D. Gevers and P. VanDamme (2008). Taxonomy of the family *Campylobacteraceae*. *Campylobacter*. I. Nachamkin, C. M. Syzmanski and M. J. Blaser. Washington, D.C., ASM Press: 3-25.
45. Delong, W. J., M. D. Jaworski and A. C. Ward (1996). "Antigenic and restriction enzyme analysis of *Campylobacter* spp associated with abortion in sheep." *Am J Vet Res* **57**(2): 163-167.
46. Diker, K. S. and E. Istanbuluoglu (1986). "Ovine abortion associated with *Campylobacter jejuni*." *Vet Rec* **118**(11): 307.
47. Diker, K. S., M. Sahal and N. Aydin (1988). "Ovine abortion associated with *Campylobacter coli*." *Vet Rec* **122**(4): 87.
48. Dowd, G. C., S. A. Joyce, C. Hill and C. G. Gahan (2011). "Investigation of the mechanisms by which *Listeria monocytogenes* grows in porcine gallbladder bile." *Infect Immun* **79**(1): 369-379.

49. Dugar, G., A. Herbig, K. U. Forstner, N. Heidrich, R. Reinhardt, K. Nieselt and C. M. Sharma (2013). "High-resolution transcriptome maps reveal strain-specific regulatory features of multiple *Campylobacter jejuni* isolates." PLoS Genet **9**(5): e1003495.
50. Dzieciol, M., M. Wagner and I. Hein (2011). "CmeR-dependent gene Cj0561c is induced more effectively by bile salts than the CmeABC efflux pump in both human and poultry *Campylobacter jejuni* strains." Res Microbiol **162**(10): 991-998.
51. Elliott, K. T. and V. J. DiRita (2008). "Characterization of CetA and CetB, a bipartite energy taxis system in *Campylobacter jejuni*." Mol Microbiol **69**(5): 1091-1103.
52. Elvers, K. T. and S. F. Park (2002). "Quorum sensing in *Campylobacter jejuni*: detection of a luxS encoded signalling molecule." Microbiology **148**(Pt 5): 1475-1481.
53. Enocksson, A., J. Lundberg, E. Weitzberg, A. Norrby-Teglund and B. Svenungsson (2004). "Rectal nitric oxide gas and stool cytokine levels during the course of infectious gastroenteritis." Clin Diagn Lab Immunol **11**(2): 250-254.
54. ERS (Economic Research Service), USDA (United States Department of Agriculture) (2014). "Cost Estimates of Foodborne Illnesses " Retrieved December 22, 2015, from <http://www.ers.usda.gov/data-products/cost-estimates-of-foodborne-illnesses.aspx>.
55. Ertas, H. B., G. Ozbey, A. Kilic and A. Muz (2003). "Isolation of *Campylobacter jejuni* and *Campylobacter coli* from the gall bladder samples of sheep and identification by polymerase chain reaction." J Vet Med B Infect Dis Vet Public Health **50**(6): 294-297.
56. Firehammer, B. D., S. A. Lovelace and W. W. Hawkins, Jr. (1962). "The isolation of *Vibrio fetus* from the ovine gallbladder." Cornell Vet **52**: 21-35.
57. Fortina, P. and S. Surrey (2008). "Digital mRNA profiling." Nat Biotechnol **26**(3): 293-294.
58. Fox, E. M., M. Raftery, A. Goodchild and G. L. Mendz (2007). "*Campylobacter jejuni* response to ox-bile stress." FEMS Immunol Med Microbiol **49**(1): 165-172.
59. Galperin, M. Y., K. S. Makarova, Y. I. Wolf and E. V. Koonin (2015). "Expanded microbial genome coverage and improved protein family annotation in the COG database." Nucleic Acids Res **43**(Database issue): D261-269.
60. Gaynor, E. C., N. Ghori and S. Falkow (2001). "Bile-induced 'pili' in *Campylobacter jejuni* are bacteria-independent artifacts of the culture medium." Mol Microbiol **39**(6): 1546-1549.
61. Geiss, G. K., R. E. Bumgarner, B. Birditt, T. Dahl, N. Dowidar, D. L. Dunaway, H. P. Fell, S. Ferree, R. D. George, T. Grogan, J. J. James, M. Maysuria, J. D. Mitton, P. Oliveri, J. L. Osborn, T. Peng, A. L. Ratcliffe, P. J. Webster, E. H. Davidson, L. Hood

- and K. Dimitrov (2008). "Direct multiplexed measurement of gene expression with color-coded probe pairs." Nat Biotechnol **26**(3): 317-325.
62. Georg, J. and W. R. Hess (2011). "cis-antisense RNA, another level of gene regulation in bacteria." Microbiol Mol Biol Rev **75**(2): 286-300.
 63. Gibreel, A., D. M. Tracz, L. Nonaka, T. M. Ngo, S. R. Connell and D. E. Taylor (2004). "Incidence of antibiotic resistance in *Campylobacter jejuni* isolated in Alberta, Canada, from 1999 to 2002, with special reference to tet(O)-mediated tetracycline resistance." Antimicrob Agents Chemother **48**(9): 3442-3450.
 64. Gibson, D. G., L. Young, R. Y. Chuang, J. C. Venter, C. A. Hutchison, 3rd and H. O. Smith (2009). "Enzymatic assembly of DNA molecules up to several hundred kilobases." Nat Methods **6**(5): 343-345.
 65. Giguere, S., J. F. Prescott and P. M. Dowling (2013). Antimicrobial therapy in veterinary medicine. Ames, IA, Wiley-Blackwell.
 66. Golden, N. J. and D. W. Acheson (2002). "Identification of motility and autoagglutination *Campylobacter jejuni* mutants by random transposon mutagenesis." Infect Immun **70**(4): 1761-1771.
 67. Gonzalez-Escobedo, G., J. M. Marshall and J. S. Gunn (2011). "Chronic and acute infection of the gall bladder by *Salmonella Typhi*: understanding the carrier state." Nat Rev Microbiol **9**(1): 9-14.
 68. Gottesman, S. (2005). "Micros for microbes: non-coding regulatory RNAs in bacteria." Trends Genet **21**(7): 399-404.
 69. Grogono-Thomas, R., M. J. Blaser, M. Ahmadi and D. G. Newell (2003). "Role of S-layer protein antigenic diversity in the immune responses of sheep experimentally challenged with *Campylobacter fetus* subsp. *fetus*." Infect Immun **71**(1): 147-154.
 70. Grogono-Thomas, R., J. Dworkin, M. J. Blaser and D. G. Newell (2000). "Roles of the surface layer proteins of *Campylobacter fetus* subsp. *fetus* in ovine abortion." Infect Immun **68**(3): 1687-1691.
 71. Gruber, A. R., R. Lorenz, S. H. Bernhart, R. Neubock and I. L. Hofacker (2008). "The Vienna RNA websuite." Nucleic Acids Res **36**(Web Server issue): W70-74.
 72. Guccione, E., A. Hitchcock, S. J. Hall, F. Mulholland, N. Shearer, A. H. van Vliet and D. J. Kelly (2010). "Reduction of fumarate, mesaconate and crotonate by Mfr, a novel oxygen-regulated periplasmic reductase in *Campylobacter jejuni*." Environ Microbiol **12**(3): 576-591.

73. Guerry, P. (2007). "*Campylobacter* flagella: not just for motility." Trends Microbiol **15**(10): 456-461.
74. Guerry, P., C. P. Ewing, M. Schirm, M. Lorenzo, J. Kelly, D. Pattarini, G. Majam, P. Thibault and S. Logan (2006). "Changes in flagellin glycosylation affect *Campylobacter* autoagglutination and virulence." Mol Microbiol **60**(2): 299-311.
75. Gunn, J. S. (2000). "Mechanisms of bacterial resistance and response to bile." Microbes Infect **2**(8): 907-913.
76. Guraya, S. Y., A. A. Ahmad, S. M. El-Ageery, H. A. Hemeg, H. A. Ozbak, K. Yousef and N. A. Abdel-Aziz (2015). "The correlation of *Helicobacter pylori* with the development of cholelithiasis and cholecystitis: the results of a prospective clinical study in Saudi Arabia." Eur Rev Med Pharmacol Sci **19**(20): 3873-3880.
77. Haas, B. J., M. Chin, C. Nusbaum, B. W. Birren and J. Livny (2012). "How deep is deep enough for RNA-Seq profiling of bacterial transcriptomes?" BMC Genomics **13**: 734.
78. He, Y., J. G. Frye, T. P. Strobaugh and C. Y. Chen (2008). "Analysis of AI-2/LuxS-dependent transcription in *Campylobacter jejuni* strain 81-176." Foodborne Pathog Dis **5**(4): 399-415.
79. Hedstrom, O. R., R. J. Sonn, E. D. Lassen, B. D. Hultgren, R. O. Crisman, B. B. Smith and S. P. Snyder (1987). "Pathology of *Campylobacter jejuni* abortion in sheep." Vet Pathol **24**(5): 419-426.
80. Hendrixson, D. R., B. J. Akerley and V. J. DiRita (2001). "Transposon mutagenesis of *Campylobacter jejuni* identifies a bipartite energy taxis system required for motility." Mol Microbiol **40**(1): 214-224.
81. Hendrixson, D. R. and V. J. DiRita (2003). "Transcription of sigma54-dependent but not sigma28-dependent flagellar genes in *Campylobacter jejuni* is associated with formation of the flagellar secretory apparatus." Mol Microbiol **50**(2): 687-702.
82. Hitchcock, A., S. J. Hall, J. D. Myers, F. Mulholland, M. A. Jones and D. J. Kelly (2010). "Roles of the twin-arginine translocase and associated chaperones in the biogenesis of the electron transport chains of the human pathogen *Campylobacter jejuni*." Microbiology **156**(Pt 10): 2994-3010.
83. Holmes, K., T. J. Tavender, K. Winzer, J. M. Wells and K. R. Hardie (2009). "AI-2 does not function as a quorum sensing molecule in *Campylobacter jejuni* during exponential growth in vitro." BMC Microbiol **9**: 214.
84. Hugdahl, M. B., J. T. Beery and M. P. Doyle (1988). "Chemotactic behavior of *Campylobacter jejuni*." Infect Immun **56**(6): 1560-1566.

85. Hulsen, T., J. de Vlieg and W. Alkema (2008). "BioVenn - a web application for the comparison and visualization of biological lists using area-proportional Venn diagrams." BMC Genomics **9**: 488.
86. Jahn, N. and S. Brantl (2013). "One antitoxin--two functions: SR4 controls toxin mRNA decay and translation." Nucleic Acids Res **41**(21): 9870-9880.
87. Jayarao, B. M., S. C. Donaldson, B. A. Straley, A. A. Sawant, N. V. Hegde and J. L. Brown (2006). "A survey of foodborne pathogens in bulk tank milk and raw milk consumption among farm families in pennsylvania." J Dairy Sci **89**(7): 2451-2458.
88. Jayarao, B. M. and D. R. Henning (2001). "Prevalence of foodborne pathogens in bulk tank milk." J Dairy Sci **84**(10): 2157-2162.
89. Jeon, B., K. Itoh, N. Misawa and S. Ryu (2003). "Effects of quorum sensing on flaA transcription and autoagglutination in *Campylobacter jejuni*." Microbiol Immunol **47**(11): 833-839.
90. Jimenez, E., B. Sanchez, A. Farina, A. Margolles and J. M. Rodriguez (2014). "Characterization of the bile and gall bladder microbiota of healthy pigs." Microbiologyopen **3**(6): 937-949.
91. Jolley, K. A. and M. C. Maiden (2010). "BIGSdb: Scalable analysis of bacterial genome variation at the population level." BMC Bioinformatics **11**: 595.
92. Joslin, S. N. and D. R. Hendrixson (2009). "Activation of the *Campylobacter jejuni* FlgSR two-component system is linked to the flagellar export apparatus." J Bacteriol **191**(8): 2656-2667.
93. Kanehisa, M., Y. Sato, M. Kawashima, M. Furumichi and M. Tanabe (2015). "KEGG as a reference resource for gene and protein annotation." Nucleic Acids Res.
94. Kelly, D. J. (2001). "The physiology and metabolism of *Campylobacter jejuni* and *Helicobacter pylori*." Symp Ser Soc Appl Microbiol(30): 16S-24S.
95. Keo, T., J. Collins, P. Kunwar, M. J. Blaser and N. M. Iovine (2011). "*Campylobacter* capsule and lipooligosaccharide confer resistance to serum and cationic antimicrobials." Virulence **2**(1): 30-40.
96. Kery, M. B., M. Feldman, J. Livny and B. Tjaden (2014). "TargetRNA2: identifying targets of small regulatory RNAs in bacteria." Nucleic Acids Res **42**(Web Server issue): W124-129.
97. Kirkbride, C. A. (1993). "Diagnoses in 1,784 ovine abortions and stillbirths." J Vet Diagn Invest **5**(3): 398-402.

98. Konkel, M. E., S. G. Garvis, S. L. Tipton, D. E. Anderson, Jr. and W. Cieplak, Jr. (1997). "Identification and molecular cloning of a gene encoding a fibronectin-binding protein (CadF) from *Campylobacter jejuni*." Mol Microbiol **24**(5): 953-963.
99. Konkel, M. E., B. J. Kim, V. Rivera-Amill and S. G. Garvis (1999). "Bacterial secreted proteins are required for the internalization of *Campylobacter jejuni* into cultured mammalian cells." Mol Microbiol **32**(4): 691-701.
100. Konkel, M. E., J. D. Klena, V. Rivera-Amill, M. R. Monteville, D. Biswas, B. Raphael and J. Mickelson (2004). "Secretion of virulence proteins from *Campylobacter jejuni* is dependent on a functional flagellar export apparatus." J Bacteriol **186**(11): 3296-3303.
101. Kortmann, J. and F. Narberhaus (2012). "Bacterial RNA thermometers: molecular zippers and switches." Nat Rev Microbiol **10**(4): 255-265.
102. Lacal, J., C. Garcia-Fontana, F. Munoz-Martinez, J. L. Ramos and T. Krell (2010). "Sensing of environmental signals: classification of chemoreceptors according to the size of their ligand binding regions." Environ Microbiol **12**(11): 2873-2884.
103. Lamendella, R., J. W. Domingo, S. Ghosh, J. Martinson and D. B. Oerther (2011). "Comparative fecal metagenomics unveils unique functional capacity of the swine gut." BMC Microbiol **11**: 103.
104. Le, M. T., M. van Veldhuizen, I. Porcelli, R. J. Bongaerts, D. J. Gaskin, B. M. Pearson and A. H. van Vliet (2015). "Conservation of sigma28-Dependent Non-Coding RNA Paralogs and Predicted sigma54-Dependent Targets in Thermophilic *Campylobacter* Species." PLoS One **10**(10): e0141627.
105. Lee, A., J. L. O'Rourke, P. J. Barrington and T. J. Trust (1986). "Mucus colonization as a determinant of pathogenicity in intestinal infection by *Campylobacter jejuni*: a mouse cecal model." Infect Immun **51**(2): 536-546.
106. Lertsethtakarn, P., K. M. Ottemann and D. R. Hendrixson (2011). "Motility and chemotaxis in *Campylobacter* and *Helicobacter*." Annu Rev Microbiol **65**: 389-410.
107. Lin, J., M. Akiba, O. Sahin and Q. Zhang (2005b). "CmeR functions as a transcriptional repressor for the multidrug efflux pump CmeABC in *Campylobacter jejuni*." Antimicrob Agents Chemother **49**(3): 1067-1075.
108. Lin, J., C. Cagliero, B. Guo, Y. W. Barton, M. C. Maurel, S. Payot and Q. Zhang (2005a). "Bile salts modulate expression of the CmeABC multidrug efflux pump in *Campylobacter jejuni*." J Bacteriol **187**(21): 7417-7424.

109. Lin, J., L. O. Michel and Q. Zhang (2002). "CmeABC functions as a multidrug efflux system in *Campylobacter jejuni*." Antimicrob Agents Chemother **46**(7): 2124-2131.
110. Lin, J., O. Sahin, L. O. Michel and Q. Zhang (2003). "Critical role of multidrug efflux pump CmeABC in bile resistance and in vivo colonization of *Campylobacter jejuni*." Infect Immun **71**(8): 4250-4259.
111. Livny, J., H. Teonadi, M. Livny and M. K. Waldor (2008). "High-throughput, kingdom-wide prediction and annotation of bacterial non-coding RNAs." PLoS One **3**(9): e3197.
112. Logan, S. M., J. F. Kelly, P. Thibault, C. P. Ewing and P. Guerry (2002). "Structural heterogeneity of carbohydrate modifications affects serospecificity of *Campylobacter* flagellins." Mol Microbiol **46**(2): 587-597.
113. Lorenz, R., S. H. Bernhart, C. Honer Zu Siederdissen, H. Tafer, C. Flamm, P. F. Stadler and I. L. Hofacker (2011). "ViennaRNA Package 2.0." Algorithms Mol Biol **6**: 26.
114. Lund, S. P., D. Nettleton, D. J. McCarthy and G. K. Smyth (2012). "Detecting differential expression in RNA-sequence data using quasi-likelihood with shrunken dispersion estimates." Stat Appl Genet Mol Biol **11**(5).
115. Luo, Y., O. Sahin, L. Dai, R. Sippy, Z. Wu and Q. Zhang (2012). "Development of a loop-mediated isothermal amplification assay for rapid, sensitive and specific detection of a *Campylobacter jejuni* clone." J Vet Med Sci **74**(5): 591-596.
116. MacKichan, J. K., E. C. Gaynor, C. Chang, S. Cawthraw, D. G. Newell, J. F. Miller and S. Falkow (2004). "The *Campylobacter jejuni* dccRS two-component system is required for optimal in vivo colonization but is dispensable for in vitro growth." Mol Microbiol **54**(5): 1269-1286.
117. Malik-Kale, P., C. T. Parker and M. E. Konkel (2008). "Culture of *Campylobacter jejuni* with sodium deoxycholate induces virulence gene expression." J Bacteriol **190**(7): 2286-2297.
118. Mannering, S. A., D. M. West, S. G. Fenwick, R. M. Marchant and K. O'Connell (2006). "Pulsed-field gel electrophoresis of *Campylobacter jejuni* sheep abortion isolates." Vet Microbiol **115**(1-3): 237-242.
119. Marchler-Bauer, A., M. K. Derbyshire, N. R. Gonzales, S. Lu, F. Chitsaz, L. Y. Geer, R. C. Geer, J. He, M. Gwadz, D. I. Hurwitz, C. J. Lanczycki, F. Lu, G. H. Marchler, J. S. Song, N. Thanki, Z. Wang, R. A. Yamashita, D. Zhang, C. Zheng and S. H. Bryant (2015). "CDD: NCBI's conserved domain database." Nucleic Acids Res **43**(Database issue): D222-226.

120. Martino, M. C., R. A. Stabler, Z. W. Zhang, M. J. Farthing, B. W. Wren and N. Dorrell (2001). "*Helicobacter pylori* pore-forming cytolysin orthologue TlyA possesses in vitro hemolytic activity and has a role in colonization of the gastric mucosa." Infect Immun **69**(3): 1697-1703.
121. McClure, R., D. Balasubramanian, Y. Sun, M. Bobrovskyy, P. Sumby, C. A. Genco, C. K. Vanderpool and B. Tjaden (2013). "Computational analysis of bacterial RNA-Seq data." Nucleic Acids Res **41**(14): e140.
122. McNally, D. J., A. J. Aubry, J. P. Hui, N. H. Khieu, D. Whitfield, C. P. Ewing, P. Guerry, J. R. Brisson, S. M. Logan and E. C. Soo (2007). "Targeted metabolomics analysis of *Campylobacter coli* VC167 reveals legionaminic acid derivatives as novel flagellar glycans." J Biol Chem **282**(19): 14463-14475.
123. McSweeney, E. and R. I. Walker (1986). "Identification and characterization of two *Campylobacter jejuni* adhesins for cellular and mucous substrates." Infect Immun **53**(1): 141-148.
124. Mearns, R. (2007). "Abortion in sheep: Investigation and principal causes." In practice **29**: 40-46.
125. Mellin, J. R. and P. Cossart (2015). "Unexpected versatility in bacterial riboswitches." Trends Genet **31**(3): 150-156.
126. Merino, S. and J. M. Tomas (2014). "Gram-negative flagella glycosylation." Int J Mol Sci **15**(2): 2840-2857.
127. Milnes, A. S., I. Stewart, F. A. Clifton-Hadley, R. H. Davies, D. G. Newell, A. R. Sayers, T. Cheasty, C. Cassar, A. Ridley, A. J. Cook, S. J. Evans, C. J. Teale, R. P. Smith, A. McNally, M. Toszeghy, R. Fitter, A. Kay and G. A. Paiba (2008). "Intestinal carriage of verocytotoxigenic *Escherichia coli* O157, *Salmonella*, thermophilic *Campylobacter* and *Yersinia enterocolitica*, in cattle, sheep and pigs at slaughter in Great Britain during 2003." Epidemiol Infect **136**(6): 739-751.
128. Misawa, N. and M. J. Blaser (2000). "Detection and characterization of autoagglutination activity by *Campylobacter jejuni*." Infect Immun **68**(11): 6168-6175.
129. Mou, K. T. (2015). Mechanisms and roles of the LuxS system, methyl recycling, and DNA methylation on the physiology of *Campylobacter jejuni*. PhD, Iowa State University.
130. Muraoka, W. T. and Q. Zhang (2011). "Phenotypic and genotypic evidence for L-fucose utilization by *Campylobacter jejuni*." J Bacteriol **193**(5): 1065-1075.
131. Ogden, I. D., J. F. Dallas, M. MacRae, O. Rotariu, K. W. Reay, M. Leitch, A. P. Thomson, S. K. Sheppard, M. Maiden, K. J. Forbes and N. J. Strachan (2009).

- "*Campylobacter* excreted into the environment by animal sources: prevalence, concentration shed, and host association." Foodborne Pathog Dis **6**(10): 1161-1170.
132. Oliver, S. P., K. J. Boor, S. C. Murphy and S. E. Murinda (2009). "Food safety hazards associated with consumption of raw milk." Foodborne Pathog Dis **6**(7): 793-806.
 133. Oliveros, J. C. (2007-2015). "Venny. An interactive tool for comparing lists with Venn's diagrams. ." Retrieved December 3, 2015, from <http://bioinfogp.cnb.csic.es/tools/venny/index.html>.
 134. Oporto, B., J. I. Esteban, G. Aduriz, R. A. Juste and A. Hurtado (2007). "Prevalence and strain diversity of thermophilic *Campylobacter* in cattle, sheep and swine farms." J Appl Microbiol **103**(4): 977-984.
 135. Papenfort, K. and C. K. Vanderpool (2015). "Target activation by regulatory RNAs in bacteria." FEMS Microbiol Rev **39**(3): 362-378.
 136. Papenfort, K. and J. Vogel (2009). "Multiple target regulation by small noncoding RNAs rewires gene expression at the post-transcriptional level." Res Microbiol **160**(4): 278-287.
 137. Papenfort, K. and J. Vogel (2010). "Regulatory RNA in bacterial pathogens." Cell Host Microbe **8**(1): 116-127.
 138. Parkhill, J., B. W. Wren, K. Mungall, J. M. Ketley, C. Churcher, D. Basham, T. Chillingworth, R. M. Davies, T. Feltwell, S. Holroyd, K. Jagels, A. V. Karlyshev, S. Moule, M. J. Pallen, C. W. Penn, M. A. Quail, M. A. Rajandream, K. M. Rutherford, A. H. van Vliet, S. Whitehead and B. G. Barrell (2000). "The genome sequence of the food-borne pathogen *Campylobacter jejuni* reveals hypervariable sequences." Nature **403**(6770): 665-668.
 139. Parveen, N. and K. A. Cornell (2011). "Methylthioadenosine/S-adenosylhomocysteine nucleosidase, a critical enzyme for bacterial metabolism." Mol Microbiol **79**(1): 7-20.
 140. Passalacqua, K. D., A. Varadarajan, C. Weist, B. D. Ondov, B. Byrd, T. D. Read and N. H. Bergman (2012). "Strand-specific RNA-seq reveals ordered patterns of sense and antisense transcription in *Bacillus anthracis*." PLoS One **7**(8): e43350.
 141. Pearson, B. M., D. J. Gaskin, R. P. Segers, J. M. Wells, P. J. Nuijten and A. H. van Vliet (2007). "The complete genome sequence of *Campylobacter jejuni* strain 81116 (NCTC11828)." J Bacteriol **189**(22): 8402-8403.
 142. Pei, Z. and M. J. Blaser (1993). "PEB1, the major cell-binding factor of *Campylobacter jejuni*, is a homolog of the binding component in gram-negative nutrient transport systems." J Biol Chem **268**(25): 18717-18725.

143. Pernitzsch, S. R., S. M. Tirier, D. Beier and C. M. Sharma (2014). "A variable homopolymeric G-repeat defines small RNA-mediated posttranscriptional regulation of a chemotaxis receptor in *Helicobacter pylori*." Proc Natl Acad Sci U S A **111**(4): E501-510.
144. Pfeiffer, V., K. Papenfort, S. Lucchini, J. C. Hinton and J. Vogel (2009). "Coding sequence targeting by MicC RNA reveals bacterial mRNA silencing downstream of translational initiation." Nat Struct Mol Biol **16**(8): 840-846.
145. Pittman, M. S., K. T. Elvers, L. Lee, M. A. Jones, R. K. Poole, S. F. Park and D. J. Kelly (2007). "Growth of *Campylobacter jejuni* on nitrate and nitrite: electron transport to NapA and NrfA via NrfH and distinct roles for NrfA and the globin Cgb in protection against nitrosative stress." Mol Microbiol **63**(2): 575-590.
146. Pittman, M. S. and D. J. Kelly (2005). "Electron transport through nitrate and nitrite reductases in *Campylobacter jejuni*." Biochem Soc Trans **33**(Pt 1): 190-192.
147. Plummer, P., O. Sahin, E. Burrough, R. Sippy, K. Mou, J. Rabenold, M. Yaeger and Q. Zhang (2012). "Critical role of LuxS in the virulence of *Campylobacter jejuni* in a guinea pig model of abortion." Infect Immun **80**(2): 585-593.
148. Plummer, P., J. Zhu, M. Akiba, D. Pei and Q. Zhang (2011). "Identification of a key amino acid of LuxS involved in AI-2 production in *Campylobacter jejuni*." PLoS One **6**(1): e15876.
149. Plummer, P. J. (2009). The mechanisms and roles of quorum sensing in the pathobiology of *Campylobacter jejuni*. PhD, Iowa State University.
150. Poly, F., T. D. Read, Y. H. Chen, M. A. Monteiro, O. Serichantalergs, P. Pootong, L. Bodhidatta, C. J. Mason, D. Rockabrand, S. Baqar, C. K. Porter, D. Tribble, M. Darsley and P. Guerry (2008). "Characterization of two *Campylobacter jejuni* strains for use in volunteer experimental-infection studies." Infect Immun **76**(12): 5655-5667.
151. Porcelli, I., M. Reuter, B. M. Pearson, T. Wilhelm and A. H. van Vliet (2013). "Parallel evolution of genome structure and transcriptional landscape in the Epsilonproteobacteria." BMC Genomics **14**(1): 616.
152. Rajashekara, G., M. Drozd, D. Gangaiah, B. Jeon, Z. Liu and Q. Zhang (2009). "Functional characterization of the twin-arginine translocation system in *Campylobacter jejuni*." Foodborne Pathog Dis **6**(8): 935-945.
153. Raphael, B. H., S. Pereira, G. A. Flom, Q. Zhang, J. M. Ketley and M. E. Konkel (2005). "The *Campylobacter jejuni* response regulator, CbrR, modulates sodium deoxycholate resistance and chicken colonization." J Bacteriol **187**(11): 3662-3670.

154. Reuter, M. and A. H. van Vliet (2013). "Signal balancing by the CetABC and CetZ chemoreceptors controls energy taxis in *Campylobacter jejuni*." PLoS One **8**(1): e54390.
155. Rivera-Amill, V., B. J. Kim, J. Seshu and M. E. Konkel (2001). "Secretion of the virulence-associated *Campylobacter* invasion antigens from *Campylobacter jejuni* requires a stimulatory signal." J Infect Dis **183**(11): 1607-1616.
156. Robinson, J. T., H. Thorvaldsdottir, W. Winckler, M. Guttman, E. S. Lander, G. Getz and J. P. Mesirov (2011). "Integrative genomics viewer." Nat Biotechnol **29**(1): 24-26.
157. Roth, A. and R. R. Breaker (2009). "The structural and functional diversity of metabolite-binding riboswitches." Annu Rev Biochem **78**: 305-334.
158. RUMA (Responsible Use of Medicines in Agriculture) Alliance. (2005). "Responsible use of antimicrobials in sheep production." Retrieved December 19, 2015, from <http://www.ruma.org.uk/wp-content/uploads/2014/09/sheep-antimicrobials-long.pdf>
159. Russell, R. G., M. O'Donnoghue, D. C. Blake, Jr., J. Zulty and L. J. DeTolla (1993). "Early colonic damage and invasion of *Campylobacter jejuni* in experimentally challenged infant *Macaca mulatta*." J Infect Dis **168**(1): 210-215.
160. Sahin, O., C. Fitzgerald, S. Stroika, S. Zhao, R. J. Sippy, P. Kwan, P. J. Plummer, J. Han, M. J. Yaeger and Q. Zhang (2012). "Molecular evidence for zoonotic transmission of an emergent, highly pathogenic *Campylobacter jejuni* clone in the United States." J Clin Microbiol **50**(3): 680-687.
161. Sahin, O., Kassem, II, Z. Shen, J. Lin, G. Rajashekara and Q. Zhang (2015). "*Campylobacter* in Poultry: Ecology and Potential Interventions." Avian Dis **59**(2): 185-200.
162. Sahin, O., P. J. Plummer, D. M. Jordan, K. Sulaj, S. Pereira, S. Robbe-Austerman, L. Wang, M. J. Yaeger, L. J. Hoffman and Q. Zhang (2008). "Emergence of a tetracycline-resistant *Campylobacter jejuni* clone associated with outbreaks of ovine abortion in the United States." J Clin Microbiol **46**(5): 1663-1671.
163. Sanad, Y. M., K. Jung, I. Kashoma, X. Zhang, Kassem, II, Y. M. Saif and G. Rajashekara (2014). "Insights into potential pathogenesis mechanisms associated with *Campylobacter jejuni*-induced abortion in ewes." BMC Vet Res **10**: 274.
164. Sanchez, B., C. G. de los Reyes-Gavilan and A. Margolles (2006). "The F1F0-ATPase of *Bifidobacterium animalis* is involved in bile tolerance." Environ Microbiol **8**(10): 1825-1833.
165. Schlafer, D. H. and R. B. Miller (2007). Female genital system Pathology of Domestic Animals. M. G. Maxie. New York, Elsevier-Saunders: 429-564.

166. Shao, Y. and B. L. Bassler (2012). "Quorum-sensing non-coding small RNAs use unique pairing regions to differentially control mRNA targets." Mol Microbiol **83**(3): 599-611.
167. Shao, Y. and B. L. Bassler (2014). "Quorum regulatory small RNAs repress type VI secretion in *Vibrio cholerae*." Mol Microbiol **92**(5): 921-930.
168. Sharma, C. M., S. Hoffmann, F. Darfeuille, J. Reignier, S. Findeiss, A. Sittka, S. Chabas, K. Reiche, J. Hackermuller, R. Reinhardt, P. F. Stadler and J. Vogel (2010). "The primary transcriptome of the major human pathogen *Helicobacter pylori*." Nature **464**(7286): 250-255.
169. Sharma, C. M. and J. Vogel (2009). "Experimental approaches for the discovery and characterization of regulatory small RNA." Curr Opin Microbiol **12**(5): 536-546.
170. Shigematsu, M., A. Umeda, S. Fujimoto and K. Amako (1998). "Spirochaete-like swimming mode of *Campylobacter jejuni* in a viscous environment." J Med Microbiol **47**(6): 521-526.
171. Skirrow, M. B. (1994). "Diseases due to *Campylobacter*, *Helicobacter* and related bacteria." J Comp Pathol **111**(2): 113-149.
172. Smyth, G. K. (2004). "Linear models and empirical bayes methods for assessing differential expression in microarray experiments." Stat Appl Genet Mol Biol **3**:3.
173. Stahl, M., J. Butcher and A. Stintzi (2012). "Nutrient acquisition and metabolism by *Campylobacter jejuni*." Front Cell Infect Microbiol **2**: 5.
174. Stahl, M., L. M. Friis, H. Nothaft, X. Liu, J. Li, C. M. Szymanski and A. Stintzi (2011). "L-fucose utilization provides *Campylobacter jejuni* with a competitive advantage." Proc Natl Acad Sci U S A **108**(17): 7194-7199.
175. Stanley, K. N., J. S. Wallace, J. E. Currie, P. J. Diggle and K. Jones (1998). "Seasonal variation of thermophilic *Campylobacters* in lambs at slaughter." J Appl Microbiol **84**(6): 1111-1116.
176. Stintzi, A., D. Marlow, K. Palyada, H. Naikare, R. Panciera, L. Whitworth and C. Clarke (2005). "Use of genome-wide expression profiling and mutagenesis to study the intestinal lifestyle of *Campylobacter jejuni*." Infect Immun **73**(3): 1797-1810.
177. Storz, G., J. Vogel and K. M. Wassarman (2011). "Regulation by small RNAs in bacteria: expanding frontiers." Mol Cell **43**(6): 880-891.

178. Storz, J., M. L. Miner and M. E. Marriott (1964). "Early events in *Vibrio fetus* infection of ewes." Zentralblatt für Veterinärmedizin Reihe B (Zoonoses and Public Health) **11**(6): 475-486.
179. Surette, M. G. and B. L. Bassler (1998). "Quorum sensing in *Escherichia coli* and *Salmonella typhimurium*." Proc Natl Acad Sci U S A **95**(12): 7046-7050.
180. Taveirne, M. E., C. M. Theriot, J. Livny and V. J. Dirita (2013). "The Complete *Campylobacter jejuni* Transcriptome during Colonization of a Natural Host Determined by RNAseq." PLoS One **8**(8): e73586.
181. Thomason, M. K. and G. Storz (2010). "Bacterial antisense RNAs: how many are there, and what are they doing?" Annu Rev Genet **44**: 167-188.
182. Thorvaldsdottir, H., J. T. Robinson and J. P. Mesirov (2013). "Integrative Genomics Viewer (IGV): high-performance genomics data visualization and exploration." Brief Bioinform **14**(2): 178-192.
183. Valentin-Hansen, P., M. Eriksen and C. Udesen (2004). "The bacterial Sm-like protein Hfq: a key player in RNA transactions." Mol Microbiol **51**(6): 1525-1533.
184. Van Deun, K., F. Pasmans, R. Ducatelle, B. Flahou, K. Vissenberg, A. Martel, W. Van den Broeck, F. Van Immerseel and F. Haesebrouck (2008). "Colonization strategy of *Campylobacter jejuni* results in persistent infection of the chicken gut." Vet Microbiol **130**(3-4): 285-297.
185. van Opijnen, T. and A. Camilli (2013). "Transposon insertion sequencing: a new tool for systems-level analysis of microorganisms." Nat Rev Microbiol **11**(7): 435-442.
186. van Putten, J. P., L. B. van Alphen, M. M. Wosten and M. R. de Zoete (2009). "Molecular mechanisms of *Campylobacter* infection." Curr Top Microbiol Immunol **337**: 197-229.
187. van Spreeuwel, J. P., G. C. Duursma, C. J. Meijer, R. Bax, P. C. Rosekrans and J. Lindeman (1985). "*Campylobacter* colitis: histological immunohistochemical and ultrastructural findings." Gut **26**(9): 945-951.
188. van Vliet, A. H. (2010). "Next generation sequencing of microbial transcriptomes: challenges and opportunities." FEMS Microbiol Lett **302**(1): 1-7.
189. Vanderpool, C. K., D. Balasubramanian and C. R. Lloyd (2011). "Dual-function RNA regulators in bacteria." Biochimie **93**(11): 1943-1949.
190. Vaughan-Shaw, P. G., J. R. Rees, D. White and P. Burgess (2010). "*Campylobacter jejuni* cholecystitis: a rare but significant clinical entity." BMJ Case Rep **2010**: bcr1020092365.

191. Vorwerk, H., C. Huber, J. Mohr, B. Bunk, S. Bhuj, O. Wensel, C. Sproer, A. Fruth, A. Flieger, K. Schmidt-Hohagen, D. Schomburg, W. Eisenreich and D. Hofreuter (2015). "A transferable plasticity region in *Campylobacter coli* allows isolates of an otherwise non-glycolytic food-borne pathogen to catabolize glucose." Mol Microbiol.
192. Wade, J. T. and D. C. Grainger (2014). "Pervasive transcription: illuminating the dark matter of bacterial transcriptomes." Nat Rev Microbiol **12**(9): 647-653.
193. Wagenaar, J. A., N. P. French and A. H. Havelaar (2013). "Preventing *Campylobacter* at the source: why is it so difficult?" Clin Infect Dis **57**(11): 1600-1606.
194. Wagner, E. G., S. Altuvia and P. Romby (2002). "Antisense RNAs in bacteria and their genetic elements." Adv Genet **46**: 361-398.
195. Wang, Y. and D. E. Taylor (1990a). "Chloramphenicol resistance in *Campylobacter coli*: nucleotide sequence, expression, and cloning vector construction." Gene **94**(1): 23-28.
196. Wang, Y. and D. E. Taylor (1990b). "Natural transformation in *Campylobacter* species." J Bacteriol **172**(2): 949-955.
197. Wassarman, K. M. and G. Storz (2000). "6S RNA regulates *E. coli* RNA polymerase activity." Cell **101**(6): 613-623.
198. Wassenaar, T. M., N. M. Bleumink-Pluym and B. A. van der Zeijst (1991). "Inactivation of *Campylobacter jejuni* flagellin genes by homologous recombination demonstrates that flaA but not flaB is required for invasion." EMBO J **10**(8): 2055-2061.
199. Waters, L. S. and G. Storz (2009). "Regulatory RNAs in bacteria." Cell **136**(4): 615-628.
200. Wehner, S., K. Damm, R. K. Hartmann and M. Marz (2014). "Dissemination of 6S RNA among bacteria." RNA Biol **11**(11): 1467-1478.
201. Wen, Y., J. Feng and G. Sachs (2013). "*Helicobacter pylori* 5'ureB-sRNA, a cis-encoded antisense small RNA, negatively regulates ureAB expression by transcription termination." J Bacteriol **195**(3): 444-452.
202. WHO. (2015). "WHO estimates of the global burden of foodborne diseases: foodborne disease burden epidemiology reference group 2007-2015." Retrieved December 3, 2015 from http://apps.who.int/iris/bitstream/10665/199350/1/9789241565165_eng.pdf.

203. Wong, T. L., L. Hollis, A. Cornelius, C. Nicol, R. Cook and J. A. Hudson (2007). "Prevalence, numbers, and subtypes of *Campylobacter jejuni* and *Campylobacter coli* in uncooked retail meat samples." J Food Prot **70**(3): 566-573.
204. Woodall, C. A., M. A. Jones, P. A. Barrow, J. Hinds, G. L. Marsden, D. J. Kelly, N. Dorrell, B. W. Wren and D. J. Maskell (2005). "*Campylobacter jejuni* gene expression in the chick cecum: evidence for adaptation to a low-oxygen environment." Infect Immun **73**(8): 5278-5285.
205. Wosten, M. M., J. A. Wagenaar and J. P. van Putten (2004). "The FlgS/FlgR two-component signal transduction system regulates the fla regulon in *Campylobacter jejuni*." J Biol Chem **279**(16): 16214-16222.
206. Wright, J. A., A. J. Grant, D. Hurd, M. Harrison, E. J. Guccione, D. J. Kelly and D. J. Maskell (2009). "Metabolite and transcriptome analysis of *Campylobacter jejuni* in vitro growth reveals a stationary-phase physiological switch." Microbiology **155**(Pt 1): 80-94.
207. Wu, Z., O. Sahin, Z. Shen, P. Liu, W. G. Miller and Q. Zhang (2013). "Multi-omics approaches to deciphering a hypervirulent strain of *Campylobacter jejuni*." Genome Biol Evol **5**(11): 2217-2230.
208. Wu, Z., R. Sippy, O. Sahin, P. Plummer, A. Vidal, D. Newell and Q. Zhang (2014). "Genetic diversity and antimicrobial susceptibility of *Campylobacter jejuni* isolates associated with sheep abortion in the United States and Great Britain." J Clin Microbiol **52**(6): 1853-1861.
209. Wurtzel, O., N. Sesto, J. R. Mellin, I. Karunker, S. Edelheit, C. Becavin, C. Archambaud, P. Cossart and R. Sorek (2012). "Comparative transcriptomics of pathogenic and non-pathogenic *Listeria* species." Mol Syst Biol **8**: 583.
210. Yang, I., S. Nell and S. Suerbaum (2013). "Survival in hostile territory: the microbiota of the stomach." FEMS Microbiol Rev **37**(5): 736-761.
211. Yao, R., D. H. Burr, P. Doig, T. J. Trust, H. Niu and P. Guerry (1994). "Isolation of motile and non-motile insertional mutants of *Campylobacter jejuni*: the role of motility in adherence and invasion of eukaryotic cells." Mol Microbiol **14**(5): 883-893.
212. Yao, R., D. H. Burr and P. Guerry (1997). "CheY-mediated modulation of *Campylobacter jejuni* virulence." Mol Microbiol **23**(5): 1021-1031.
213. Zhang, Q., J. C. Meitzler, S. Huang and T. Morishita (2000). "Sequence polymorphism, predicted secondary structures, and surface-exposed conformational epitopes of *Campylobacter* major outer membrane protein." Infect Immun **68**(10): 5679-5689.

214. Ziprin, R. L., C. R. Young, J. A. Byrd, L. H. Stanker, M. E. Hume, S. A. Gray, B. J. Kim and M. E. Konkel (2001). "Role of *Campylobacter jejuni* potential virulence genes in cecal colonization." Avian Dis **45**(3): 549-557.